STUDIES ON UPTAKE OF ARSENIC BY METAL OXIDES

By

NICY AJITH
CHEM01201404005

Analytical Chemistry Division
Bhabha Atomic Research Centre

A Thesis submitted to the
Board of Studies in Chemical Sciences
in Partial fulfillment of requirements
for the degree of

DOCTOR OF PHILOSOPHY
of
HOMI BHABHA NATIONAL INSTITUTE

December, 2019

Homi Bhabha National Institute

Recommendations of the Viva Voce Committee

As members of the Viva Voce Committee, we certify that we have read the dissertation prepared by Mrs. Nicy Ajith entitled "Studies on uptake of arsenic by metal oxides" and recommend that it may be accepted as fulfilling the thesis requirement for the award of Degree of Doctor of Philosophy.

Chairman - Prof. P. D. Naik — Date: 18/07/2020

Guide / Convener - Prof. K. K. Swain — Date: 18.07.2020

Examiner - Prof. N. Rajesh — Date: 18.07.2020

Member 1 - Prof. A. K. Tripathi — Date: 18.07.2020

Member 2 - Prof. A. K. Pandey — Pandey — Date: July 18, 2020

Member 3 - Prof. S Mishra — Date: 18. July. 2020

Technology adviser - Dr. Remya Devi P. S. — Date: 18 July 2020

Final approval and acceptance of this thesis is contingent upon the candidate's submission of the final copies of the thesis to HBNI.

I hereby certify that I have read this thesis prepared under my direction and recommend that it may be accepted as fulfilling the thesis requirement.

Date: 18.07.2020

Place: MUMBAI

Dr. K K Swain

(Guide)

---

[1] This page is to be included only for final submission after successful completion of viva voce.

STATEMENT BY AUTHOR

This dissertation has been submitted in partial fulfillment of requirements for an advanced degree at Homi Bhabha National Institute (HBNI) and is deposited in the Library to be made available to borrowers under rules of the HBNI.

Brief quotations from this dissertation are allowable without special permission, provided that accurate acknowledgement of source is made. Requests for permission for extended quotation from or reproduction of this manuscript in whole or in part may be granted by the Competent Authority of HBNI when in his or her judgment the proposed use of the material is in the interests of scholarship. In all other instances, however, permission must be obtained from the author.

(Nicy Ajith)

DECLARATION

I, hereby declare that the investigation presented in the thesis has been carried out by me. The work is original and has not been submitted earlier as a whole or in part for a degree / diploma at this or any other Institution / University.

(Nicy Ajith)

List of Publications arising from the thesis

Journal

1. “An ultrasound assisted reductive method for preparation of MnO_2: Modification of XAD and application in removal of arsenic”, **Nicy Ajith** and K. K. Swain, *Separation Science and Technology*, **2020**, 55(9), 1715-1723.

2. “Study on the performance and interaction of different synthetic iron oxides for arsenic uptake using ^{76}As radiotracer”, **Nicy Ajith** and K. K. Swain, *Applied Radiation and Isotope*, **2019**, 153, 108807.

3. “Interaction of As(III) and As(V) on manganese dioxide: XPS and electrochemical investigations”, **Nicy Ajith**, K. Bhattacharyya, Priyanka R. Ipte, A. K. Satpati, A. K. Tripathi, R. Verma and Kallola K. Swain, *Journal of Environmental Science and Health, Part-A*, **2019**, 54(4), 277-285.

4. “Sorption of arsenic on manganese dioxide synthesized by solid state reaction”, A. A. Dalvi, **Nicy Ajith**, K.K. Swain and R. Verma, *Journal of Environmental Science and Health, Part-A*, **2015**, 50(8), 866-873.

5. “Sorption of As(III) and As(V) on chemically synthesized manganese dioxide”, **Nicy Ajith**, A. A. Dalvi, K. K. Swain, P. S. Remya Devi, B. B. Kalekar, R. Verma and A.V.R. Reddy, *Journal of Environmental Science and Health, Part-A*, **2013**, 48(4), 422-428.

Conference/Symposium

1. **“**Preparation of MnO_2 coated XAD resin by sonochemical method for removal of arsenic from groundwater”, **Nicy Ajith**, Kallola K. Swain and R. Verma, *Proceedings of symposium on Emerging Trends in Analytical Chemistry (ETAC-2016)*, 21-23 September **2016**, Bangalore.

2. "Study on sorption of arsenic(III) and (V) on magnetite", **Nicy Ajith**, Kallola K. Swain, M. Ghosh and Rakesh Verma, *Proceedings of biennial symposium on Emerging Trends in Separation Science and Technology (SESTEC-2016)*, 17-20 May **2016**, Guwahati.
3. "Removal of arsenic from groundwater samples collected from arsenic contaminated areas of West Bengal", **Nicy Ajith**, K. K. Swain, Aditi A. Dalvi and R. Verma, *Proceedings of symposium on Current Trends in Analytical Chemistry (CTAC-2015)*, 26-29 April **2015**, Mumbai.
4. "Effect of ions present in groundwater on sorption of arsenic on manganese dioxide", **Nicy Ajith**, Aditi A. Dalvi, K. K. Swain, R. Verma and A. V. R. Reddy, Proceedings of *biennial symposium on Emerging Trends in Separation Science and Technology (SESTEC-2014)*, 25-28 February **2014**, Mumbai.

(Nicy Ajith)

Dedicated to

My Grandparents

ACKNOWLEDGEMENTS

First and foremost, I thank Almighty for all the blessings till date and forthcoming.

I must give my high, respectful gratitude to my guide Dr. K. K. Swain, Head, Nuclear Analytical Methods Section, Analytical Chemistry Division (ACD), Bhabha Atomic Research Centre (BARC) for the continuous support, valuable guidance and ever-friendly nature throughout my research work in a respectable manner. I am very much grateful to him for being with me from the day one of my career till date.

I sincerely acknowledge the support and guidance of Dr. H. Pal, Associate Director (A), Chemistry Group and Head, Analytical Chemistry Division for sparing his busy schedule and improving the quality of the thesis.

I take this opportunity to thank Dr. R. Verma, Former Head, Nuclear Analytical Methods Section, ACD, BARC, for his guidance throughout my research. I am greatly thankful to Dr. A. V. R. Reddy, Former Head, ACD, BARC, for his encouragement, critical suggestions and posing challenging questions throughout my work. The scientific discussions with him had helped me a lot to improve the quality of the work. My special thanks to Dr. B. Venkataramani, Former Head, ACD, BARC and late Dr. S.R. Kayasth, for their inspiration, support and care during the early stages of my research career.

It is with immense gratitude that I acknowledge the insightful comments, suggestions and encouragement rendered by my Doctoral Committee consisting of eminent scientists Dr. P. D. Naik (Chairman), Dr. A. K. Tripathi, Dr. A. K. Pandey, Dr. S Mishra along with my mentor and dear friend Dr. Remya Devi P. S.

My sincere thanks to Dr. A. K. Tyagi, Dr. R. K. Singhal, Dr. Sanjukta A Kumar, Dr. A. K. Satpati, Dr. K. Bhattacharya, Dr. Rakesh Shukla, Dr. A. K. Debnath, Dr. R. Tewari for the scientific discussions and experimental help during the work.

I am privileged for having Aditi A. Dalvi, Madhusudan Ghosh, Trupti A. Chavan, Jagannath Datta, Sandipan, Mehzabin, Sudeshna, Harshala, Srikant, as my colleagues and friends, who had provided great company during all these years. I thank Dr. Sangita D. Kumar, Dr. Naina Raje, Shri. K. C. Thomas and all other colleagues of ACD, BARC, for facilitating a healthy and cheerful working environment. I thank all my batch-mates and friends in BARC, who helped me, at the times of requirement.

I am thankful to operation crew members of Dhruva and Critical Facility reactors for their co-operation during neutron irradiations.

There is no need for formal word of thanks for my entire family for their love and continuous support and who have stood beside me throughout the journey. I am thankful to my beloved husband Ajith, for the immense care, advices and motivations, I’ve been getting all this while. I express my everlasting love to my son, Robin and daughter, Neha, for giving colors to my life. My parents (Usha and Rajan), in-laws (Leela and John), sisters (Bency and Ringle) and brothers (Arun, Nike and Nijo) are the pillars of mental strength in my life, who have always been there for me no matter where I am. The memorable moments spent with my dear cousins helped me a lot in enjoying every moment of my life.

I express my sincere gratitude to all my teachers. Their blessings have helped me in reaching this goal.

Finally, I thank all my friends who have helped me directly or indirectly in the successful completion of my thesis. Anyone, whose contribution is not mentioned in the above list, is also acknowledged.

(Nicy Ajith)

CONTENTS

Page No.

Chapter - I

Chapter - II

Chapter - IV

Arsenic Uptake on Manganese Dioxides 101 - 131

Chapter - V

Chapter - VI

Abstract

1.	**Name of Candidate:**	Ms. Nicy Ajith
2.	**Name of the Constituent Institution:**	Bhabha Atomic Research Centre, Mumbai
3.	**Enrolment Number:**	CHEM01201404005
4.	**Title of the Thesis:**	Studies on uptake of arsenic by metal oxides
5.	**Board of Studies:**	Chemical Sciences

The arsenic contamination in groundwater is currently a major problem in many parts of the world, which needs to be addressed adequately to meet the demand of the safe potable water. This thesis explores synthesis, characterization and efficacy of different synthesized metal oxides (iron and manganese oxides) as sorbents, for arsenic uptake and possible arsenic remediation from water. The studies have been carried out using ^{76}As radiotracer in batch equilibration mode. The experimental includes the preparation of ^{76}As radiotracer, conversion of it to As(III) and As(V) species and confirming the species by solvent extraction. The studies include the effect of pH, kinetics, isotherm evaluation, effect of co-occurring ions on the sorption behavior of iron oxides (goethite, hematite and magnetite) / manganese dioxide (MnO_2) for arsenic uptake and evaluation of applicability of these sorbents in removing arsenic from real groundwater samples. The sorbents have been studied for the leaching property in groundwater pH and also for their regeneration and reusability. To understand the sorption mechanism, she elaborated the XPS and electrochemical measurements of the As(III) and As(V) species by iron oxides and MnO_2. Based on the experimental findings the sorption mechanism has been figured out as complexation involving change in the oxidation state of arsenic species during sorption. With the knowledge gained, a sorbent, MnO_2, has been identified successfully, which has also been modified in the form of coating on resin beads (MX-4 beads) and applied for arsenic removal studies.

The main objective of this work has been to study the changes occurring to the oxidation states of both the adsorbent and adsorbate during their interaction. This may help in development of efficient and economic arsenic removal method from groundwater.

LIST OF FIGURES

Figure Caption **Page**

No.

Chapter - I

Chapter - II

Chapter - III

Chapter - IV

Chapter - V

LIST OF TABLES

Title of the Table **Page**

No.

Chapter - I

Chapter - II

Chapter - III

Chapter - IV

Chapter - V

Chapter - VI

Thesis Highlight

Name of the student: NICY AJITH

Name of the CI/OCC: Bhabha Atomic Research Centre, Mumbai

Enrolment no.: CHEM01201404005

Thesis title: Studies on uptake of arsenic by metal oxides

Discipline: Chemical Sciences; **Date of viva voce:** July 18, 2020

Studies on uptake of arsenic by different naturally occurring metal oxides are important for understanding the sorption mechanism, which helps in development of efficient arsenic removal method from water. The main objective of this work has been to study the changes occurring to the oxidation states of both the adsorbent and adsorbate during their interaction. In this thesis, arsenic uptake by laboratory synthesized oxides of iron and manganese were studied elaborately using ^{76}As radiotracer in batch equilibration mode.

The preliminary investigation of interaction of arsenic and metal oxides was carried out by solvent extraction for elucidation of the oxidation state of arsenic after sorption. The mechanism of sorption of arsenic by the sorbents was studied via electrochemical investigations. The results showed that in magnetite, i.e. mixed iron oxide, the As(III) and As(V) were taken up as such. For hematite and goethite, the mechanism of uptake of As(III) and As(V) were found to be partially redox type of interaction. For manganese dioxide (MnO_2), mechanism of uptake for As(III) is oxidative adsorption process and As(V) undergo adsorption without any redox modification. Observed results were confirmed using X-ray photoelectron spectroscopy. Based on the data, detailed mechanisms of sorption of arsenic onto oxides of iron and manganese were proposed.

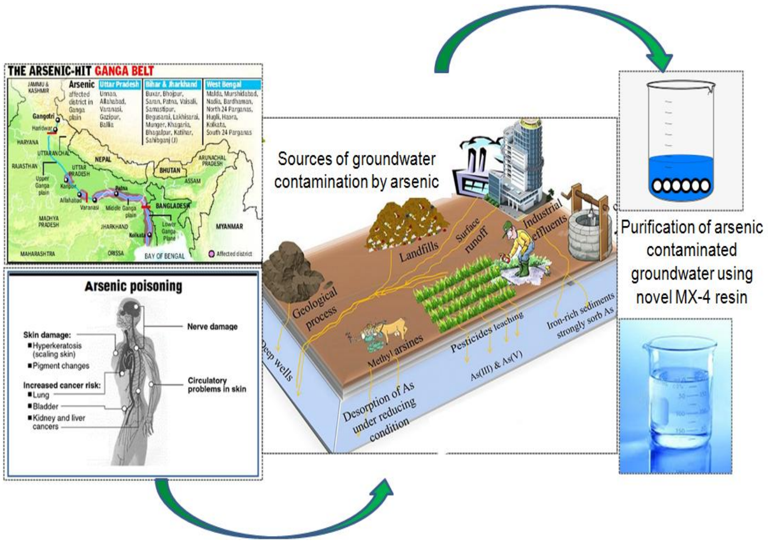

MnO_2 was found to be the most promising adsorbent for arsenic; therefore a modified material was synthesized for easy arsenic removal. A novel, sonochemical reduction of permanganate was used to prepare MnO_2 nanoparticles coated XAD-4 resin and the modified resin was successfully applied for quantitative removal of arsenic from groundwater samples, collected from arsenic contaminated regions of North 24 Parganas, West Bengal, India.

Chapter - I

Introduction

1.1. Water: Availability in nature

The entire life on earth depends on one major factor, “WATER”. Water is essential for the survival of living creations. Access to safe drinking water is a basic human right. Nearly 70 % of earth is covered with water: 97.5 % is saline/sea water and remaining only 2.5 % is fresh water. The major source of fresh water is glaciers, where about two third of the fresh water is trapped in the form of ice. The rest is present as surface water (ponds, lakes, rivers, streams) and underground water (groundwater), of which only about 0.007 % is available for daily use [1]. Even though the percentage of groundwater is very small compared to the total water on earth, its importance cannot be ignored. Globally, over two billion people depend on groundwater as the source of drinking water. Notably, India is the largest consumer of groundwater in the world.

1.2. Toxic elements in drinking water

For humans, nineteen elements are listed as necessary for daily intake. These elements are categorized into three groups: (1) essential (2) probably essential and (3) potentially toxic. Water, is considered as the universal solvent, and it inherently contains some of the essential elements as well as few toxic elements (contaminants). The US Environmental Protection Agency (EPA) enforces certain drinking water standards. The contaminants in water are categorized as primary and secondary contaminants. Primary contaminants are those which may cause a direct health risk to humans. These include inorganic and organic chemicals, radionuclides and microorganisms. The secondary contaminants are those which cause, cosmetic effects like, skin or tooth discoloration and aesthetic effects such as taste, odour and color, to water. The primary contaminants can bind strongly to cellular molecules and interfere with the biological functioning of these components and hence are termed as toxic. Thus, water needs to be critically evaluated for these elements.

The list of fifteen primary inorganic contaminants along with the associated health hazards are listed in the Table 1. 1 for a quick reference.

Table 1.1: List of primary inorganic contaminants [2-3]

Sl. No.	Contaminant	Maximum contaminant level (MCL; mg/L)	Health effects
1	Antimony	0.006	Increase in blood cholesterol, decrease in blood sugar
2	Arsenic	0.010	Skin damage, problems with circulatory systems, increased risk of getting cancer
3	Asbestos (fiber >10 μm)	7 (Maximum Fibre Level)	Increased risk of developing benign intestinal polyps
4	Barium	2	Increase in blood pressure
5	Beryllium	0.004	Intestinal lesions
6	Cadmium	0.005	Kidney damage
7	Chromium	0.1	Allergic dermatitis
8	Copper	1.3	Gastrointestinal distress, Liver or kidney damage
9	Cyanide (as free cyanide)	0.2	Nerve damage, thyroid problems
10	Fluoride	4.0	Bone disease
11	Lead	0.015	Kidney problems, high blood pressure
12	Mercury (inorganic)	0.002	Kidney damage
13	Nitrate, Nitrite	10 1	Infants: could become seriously ill and, if untreated, may die. Symptoms include shortness of breath and blue-baby syndrome.
14	Selenium	0.05	Hair or fingernail loss, numbness in fingers or toes, circulatory problems
15	Thallium	0.0005	Hair loss, kidney, intestine or liver problems

Among the fifteen inorganic contaminants listed, arsenic is one of the highly toxic element. It is the oldest poison known to man and called as “the king of poisons”. The agency for toxic substances and disease registry (ATSDR), ranked arsenic as number 1 in the 2001 list of hazardous substances at superfund sites [4]. It is also designated as Group 1: carcinogenic to human, by International Agency for Research on Cancer (IARC) [5]. Therefore many researchers are working on various aspects of arsenic toxicity and remediation.

1.3. Sources of arsenic in nature

Arsenic is a metalloid and found to be the 20th most abundant element in the earth’s crust. The element was discovered by Albertus Magnus way back in 1200. Arsenic can be found in soil and minerals in small concentrations. The major arsenic bearing minerals are listed in the Table 1.2. Among the list, the most abundant arsenic bearing mineral is arsenopyrite, FeAsS [6]. Arsenic is also present in nature as adsorbed form, onto Fe(III) and Mn(IV) oxide/hydroxide materials, as a result of weathering of sulfide bearing minerals [7].

The rapid growth of population, industrialization and agriculture activities have caused the surface water sources to either dried up or rather contaminated. As a result, groundwater has become the main source of drinking water in many developing countries. Thus, installing tubewells, for providing presumably the safe drinking water to the population are very common. In the recent decades, the problem of arsenic contamination in groundwater, occurring from the naturally occurring arsenic sources, has received a tremendous attention, considering very high toxicity of arsenic on human health.

The risk of arsenic contamination of surface and groundwater arises through natural processes as well as from human (anthropogenic) activities. The natural processes include weathering, volcanic eruptions, forest fires and various biological activities. The different anthropogenic activities are mining, combustion of fossil fuels, wood preservation and the use of arsenic containing pesticides and herbicides in farming [6].

Table 1.2: Major arsenic bearing minerals occurring in nature [6]

Mineral	**Chemical formulae**
Native arsenic	As
Orpiment	As_2S_3
Realgar	As_4S_4
Arsenopyrite	$FeAsS$
Arsenolite	As_2O_3
Olivenite	Cu_2OHAsO_4
Cobaltite	$CoAsS$
Proustite	Ag_3AsS_3
Scorodite	$FeAsO_4.2H_2O$
Niccolite	$NiAs$
Tennantite	$(Cu,Fe)_{12}\ As_4S_{13}$
Enargite	Cu_3AsS_4

1.4. Arsenic contamination in groundwater

As per the literature reports, presently more than 140 million population spreading in more than 70 countries are affected by arsenic contaminated groundwater (Fig. 1.1) [6, 8-11]. Bangladesh and India (West Bengal) are the most affected among the countries [8, 12-13]. In India, seven states are reported with groundwater arsenic contamination problem, namely, West Bengal, Jharkhand, Bihar, Uttar Pradesh, Assam, Manipur and Chhattisgarh [14-15]. In recent reports, 96 districts in 12 states in India as well as over 10 million population spread only in nine districts of West Bengal are still using arsenic contaminated groundwater [16-17].

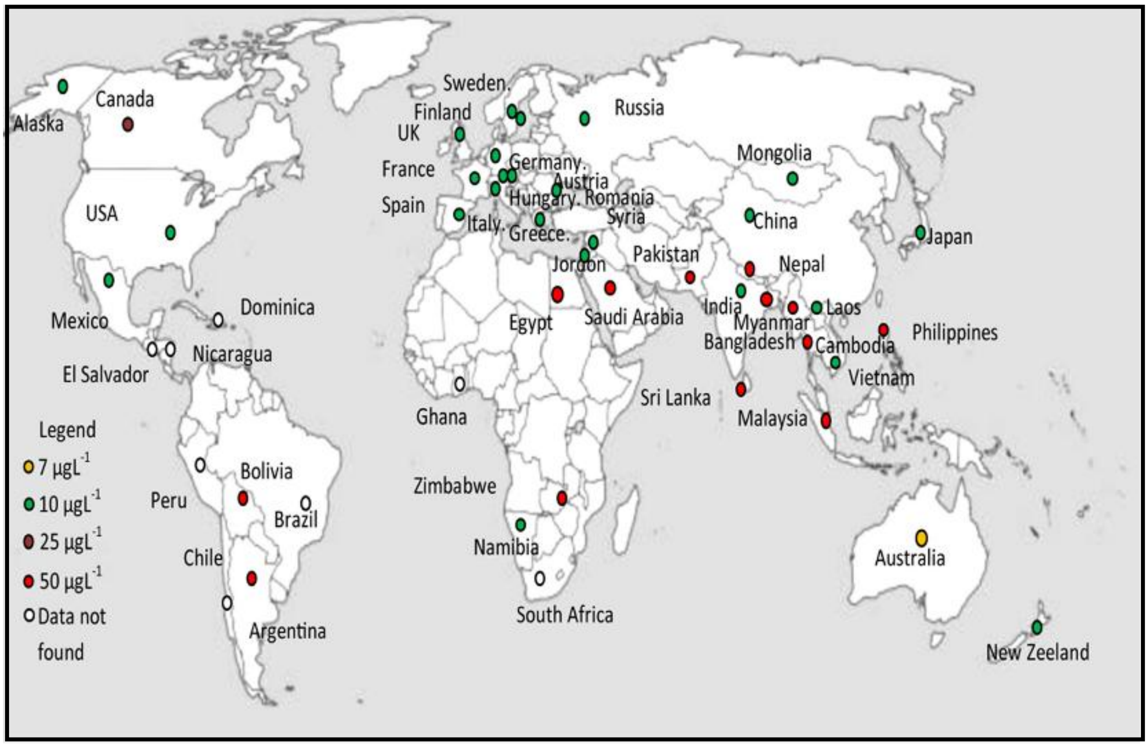

Figure 1.1: Arsenic affected countries and the contaminant levels [18]

1.5. Mechanisms of Arsenic mobilization

The natural process of leaching of arsenic from its sources has been explained mainly by two theories.

1.5.1. Pyrite oxidation hypothesis

Arsenopyrite (FeAsS) is the most abundant sulphide mineral in earth's crust. Arsenic exists both as +3 and -1 oxidation states in this mineral. The deposits are found to be present underground. Due to the increase in the use of tubewells, the water table goes down the iron pyrite layer. Thus, the atmospheric oxygen comes in contact with the pyrite layer and it undergoes oxidation. During oxidation, the arsenic becomes As(V). This negative species, gets adsorbed on to the iron oxide. When the water gets recharged, due to the prevailing reducing conditions, the As(V) gets reduced and released to water as As(III) [14]. Due to the microbial action, the released Fe(II) and As(III) get oxidized to

Fe(III) and As(V), respectively. The chemical reaction involving dissolution of arsenopyrite involving microbial oxidation is given in equation 1.1 [19].

$$\underset{\text{(Arsenopyrite)}}{4FeAsS_{(s)}} + 13O_2 + 6H_2O \xrightarrow{\text{Microbial oxidation}} 4Fe(III) + 4SO_4^{2-} + 12H^+ + 4AsO_4^{3-}{}_{(aq.)} \quad (1.1)$$

1.5.2. Hydroxide reduction hypothesis

The high concentration of arsenic is present in the alluvial sediments as a coating on iron hydroxides. These are found as deposits on valleys. When the water level gets lowered, a microbial reductive dissolution of the organic matter, deposited on the sediments, takes place in anaerobic environment. This results in the reduction of iron hydroxide and releases the arsenic (both in As(III) and As(V) oxidation states) to groundwater [14]. The chemical reaction of the above mechanism is given in equation 1.2 [13, 19].

$$4\ FeOOH(As)_{(s)} + CH_2O + 7\ H_2CO_3 \longrightarrow 4\ Fe^{2+} + As_{(d)} + 8\ HCO_3^- + 6H_2O \qquad (1.2)$$

Where, $As_{(d)}$ means dissolved As(III) and As(V).

1.6. Chemistry of arsenic

Arsenic can exist in -3, 0, +3 and +5 oxidation states, but -3 and 0 are rarely occurred in nature. Thus arsenic chemistry focuses mainly on the As(III) and As(V) species. Arsenic forms different inorganic and organic species involving As(III) and As(V) oxidation states (Fig.1.2). The inorganic oxyanion species include: arsenous acid [As(III)] and arsenic acid [As(V)]. The general organic forms of arsenic in water are: (1) mono-methylated arsenic species - methylarsenite [monomethylarsonous acid; MMA(III)] and methylarsenate [monomethylarsonic acid; MMA(V)] and (2) di-methylated arsenic species - dimethylarsenite [dimethylarsonous acid; DMA(III)] and dimethylarsenate [dimethylarsonic acid; DMA(V)] [20-21]. As(V) is more prevalent in surface water, whereas As(III) occurs mostly in anaerobic ground waters. Pourbaix (Eh-pH) diagram (Fig.1.3), is used to explain the speciation of arsenic. In groundwater, depending on the pH as well as the redox conditions prevailing, arsenic exists as protonated/deprotonated inorganic oxyanions involving As(III) and As(V) (Fig. 1.2) [22-23]. Under reducing conditions, As(III) species are predominant whereas in neutral and oxidizing conditions As(V) species are more stable [24].

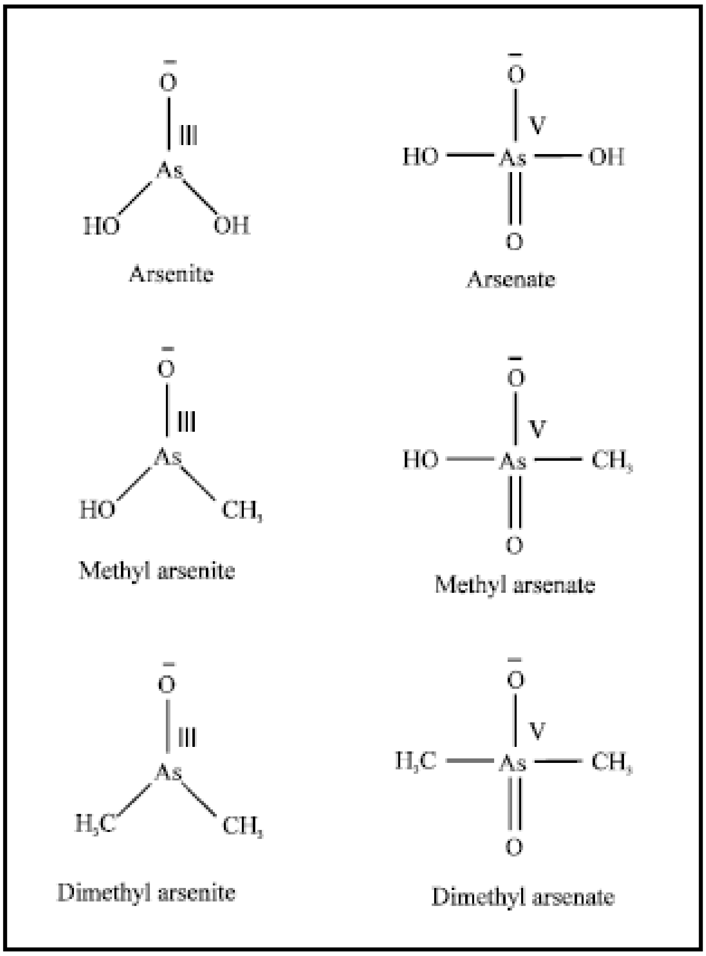

Figure 1.2: Structures of arsenic species [20]

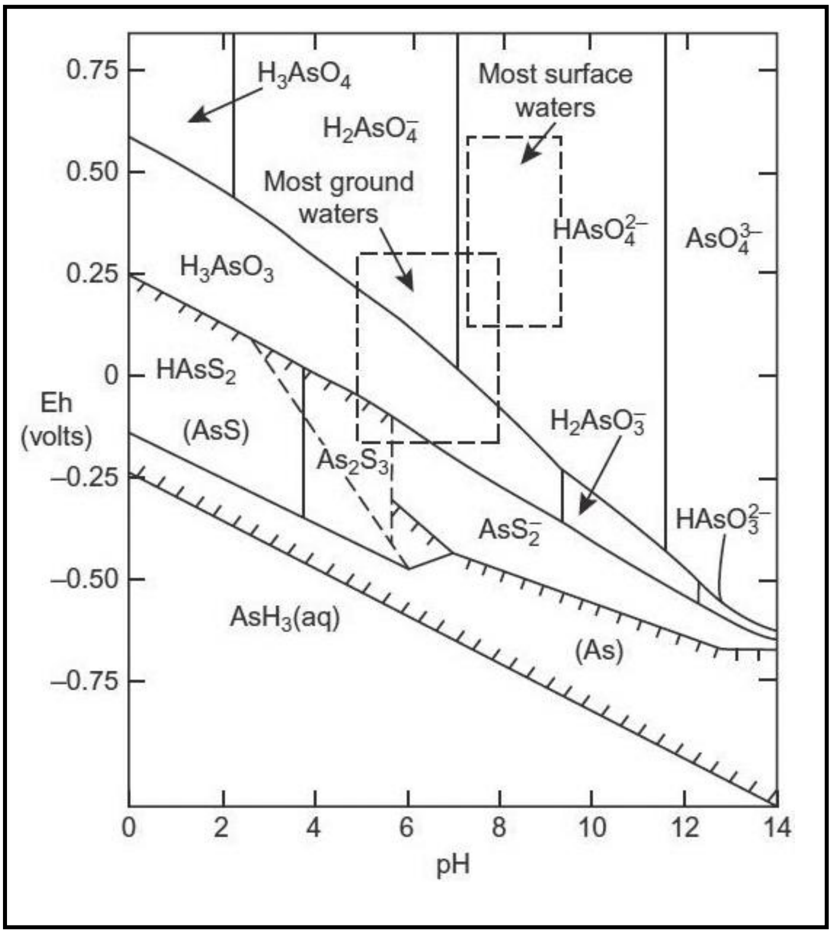

Figure 1.3: Eh-pH diagram for arsenic at 25 °C and 1 bar [23]

According to the speciation plots, Fig. 1.4 and 1.5, the As(III) exists mostly as neutral species ($H_3AsO_3^0$; pH < 9.2), whereas, As(V) is mostly negatively charged ($H_2AsO_4^-$, $HAsO_4^{2-}$ and AsO_4^{3-}) in entire pH range [6, 25]. In natural aqueous medium, the arsenic mobility depends on the interaction with heavy metal oxides. In this condition, the neutral As(III) species is less strongly absorbed on to the majority of the metal oxides than the negatively charged As(V). Accordingly, As(III) species in general display more mobility as compared to the As(V) species.

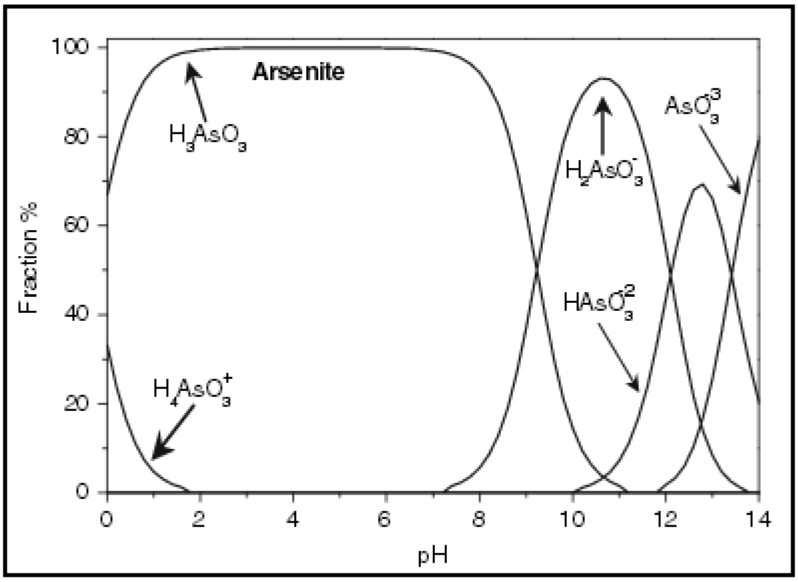

Figure 1.4: Speciation plot for As(III) as a function of pH [26]

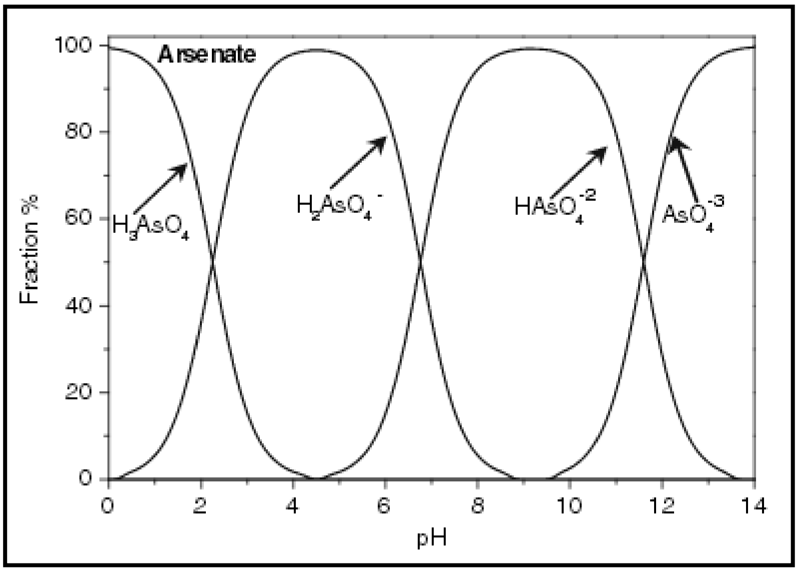

Figure 1.5: Speciation plot for As(V) as a function of pH [26]

1.7. Arsenic in the human body and related health effects

The toxic effects of arsenic in human body have been explained in the literatures [27-28]. The absorbed arsenic species - whether organic or inorganic, As(III) or As(V), are transported to different parts of the body through blood, mainly in the form of mono-methylated arsenic (MMA) species. The metabolism of arsenic in the body takes place in the following way.

Once, ingested, the inorganic As(III) and As(V) interacts differently. The toxicity of As(III), is a result of strong binding of As(III) species with the thiol (-SH) groups in proteins, present in the body enzymes, causing inactivation of the enzymes. As(V) species behave similarly as phosphate, hence substitute the phosphate groups in important biomolecules like adenosine triphosphate (ATP) and adenosine diphosphate (ADP). This disrupts the ATP production and thus normal cell functioning gets highly affected. These effects may often be very severe, leading to death due to multi-organ failure [29-30].

After entering a cell, reduction of arsenate to arsenite occurs. In liver, arsenite is converted into the methylated forms producing the MMA and DMA [31-32]. Incontrast to the inorganic species of arsenic, in humans, there is no strong binding observed for the organic species of arsenic - MMA and DMA species. The inorganic species of arsenic are more toxic and carcinogenic, compared to the organic arsenic compounds [30].

The toxicity of different arsenic species are in the order as mentioned below:

Inorganic arsenic species > organic arsenic species

Inorganic arsenic species: As(III) > As(V)

Organic arsenic species: MMA(III) > MMA(V) > DMA (III) > DMA (V)

From the extent of chromosomal aberrations induced by the exposure of As(III) and As(V), it has been indicated that the As(III) is more potent and genotoxic than the As(V) species [28, 33]. The chronic exposure of arsenic has caused to induce carcinogenesis and cardiovascular disorders in large population in Bangladesh and West Bengal, India. The studies carried out in the populations exposed to arsenic in West Bengal, exhibited severe skin lesions (melanosis, keratosis, hyperkeratosis, dorsal keratosis), non-pitting oedema to gangrene and cancer (skin, internal organs) [34-36]. The arsenic exposure also leads to weakness, anaemia, chronic lung disease, cardiovascular disease, gastrointestinal disease, hearing loss, cataract, and diabetes mellitus [35]. The biomethylation is the pathway for the detoxication of arsenic. After formation of MMA and DMA, it gets excreted primarily via urine [29, 36].

1.8. Toxic limits of arsenic in drinking water

Treatment of arsenic becomes a difficult task to accomplish, due to the ability of arsenic to change its valence states and the formation of multiple species having different toxicity and mobility. Depending on the adverse health effects of arsenic on humans, the World Health Organization (WHO) had kept the maximum permissible limit (MPL) for arsenic in drinking water as 50 μg L^{-1}. The MPL of arsenic in drinking water was, however, reduced by the United States Environmental Protection Agency (USEPA) and WHO, in 1993, from 50 μg L^{-1} to 10 μg L^{-1} [37]. Depending on the situations, the MPL for As in drinking water, is still kept as 50 μg L^{-1} in few countries, where an alternate source of arsenic free water is not available. In India, the Bureau of Indian Standards (BIS) has reduced the MPL value of arsenic to 10 μg L^{-1} in the year 2009 [38-39].

1.9. Remediation methods for arsenic

Since the arsenic contamination in drinking water originates mainly from natural sources, the complete remediation of arsenic is extremely difficult. Attempts are being made to develop methods to minimize the effect of arsenic contamination. At present many treatment methods are in use (Fig. 1.6), mainly,

(1) Coagulation - flocculation

(2) Oxidation

(3) Adsorption

(4) Ion-exchange

(5) Membrane technologies

(6) Bio-remediation

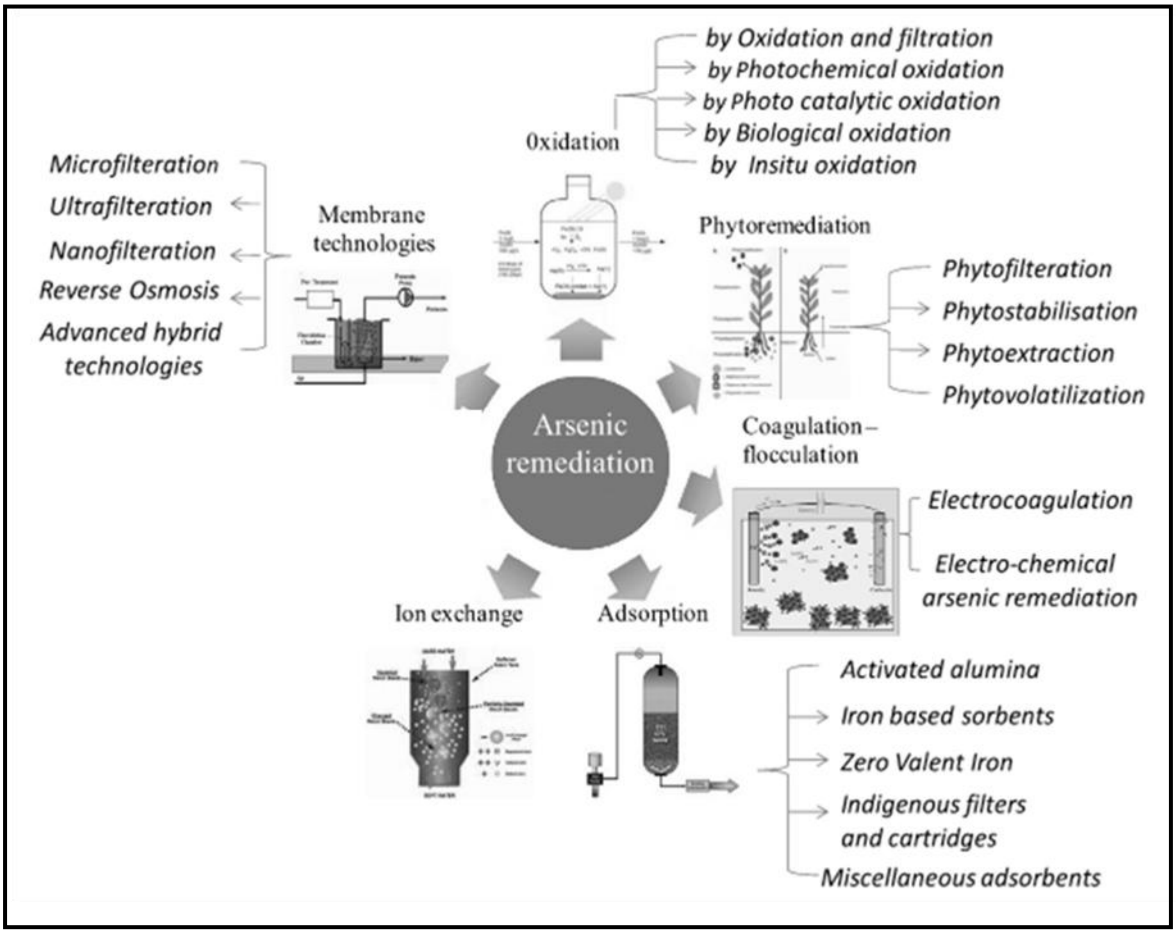

Figure 1.6: Schematic showing the various arsenic removal techniques [40]

1.9.1. Coagulation - flocculation methods

A positively charged coagulant is added in large excess to the arsenic contaminated water. This coagulant reduces the negative charge on the colloids (colloids are extremely small particles having high surface charge) and thus starts to agglomerate and form larger particles. These particles are flocs and the process is termed as flocculation. The soluble arsenic present in the system is incorporated into the flocs, co-precipitated and consequently, gets removed. Consequently, these coagulates are removed either by sedimentation or by filtration. Commonly used coagulants are aluminum sulfate [$Al_2(SO_4)_3 \cdot 18H_2O$] and ferric salts like ferric chloride ($FeCl_3$) or ferric sulfate [$Fe_2(SO_4)_3 \cdot 7H_2O$] [18, 41-44].

As(V) is negatively charged in the normal groundwater pH range, whereas As(III) is neutral species. So before coagulation process is applied, a pre-oxidation step is needed to be carried out for complete conversion of As(III) to As(V). Another major problem associated with this method is the production of large amount of sludge containing significant amount of arsenic. This sludge containing arsenic needs to be properly disposed off, to prevent secondary pollution. Also, after the treatment, the water needs to be thoroughly checked for its potability. These limitations have restrained the large scale applicability of this method.

1.9.2. Oxidation methods

Oxidation alone cannot remove arsenic, it needs to be done followed by coagulation, adsorption or ion-exchange. In oxidation method, the soluble As(III) is completely converted to As(V) form, which can be precipitated and removed. The different oxidants are chlorine, chlorine dioxide, ozone, hydrogen peroxide, chloroamine, permanganate, air and pure oxygen. For arsenic oxidation, advanced phyto-processes like, ultraviolet (UV) irradiation and solar energy irradiation are also widely used. In these processes, hydroxyl radicals are generated through photolysis and helps in the fast oxidation of As(III) to As(V) [18, 41-44].

Similar to coagulation process, the sludge generation and disposal is also one of the major problems faced during oxidation process. The water to be treated needs to be studied thoroughly prior to treatment, and then selected oxidant has to be added. Presence of some competing anions can interfere with the kinetics of oxidation of arsenic and make the process to slow down. pH adjustment prior to oxidation, again is a prerequisite for maximum effectiveness. Also, while using certain oxidants, there are chances of toxic by-product formation making the treated water not suitable for its consumption.

1.9.3. Adsorption methods

In the contaminant removal, sorption is the general term used, which includes both adsorption (occurs on the surface mainly) and absorption (occurs on the entire volume) processes. The process of adsorption is the preferential accumulation of the adsorbate present in the gaseous or solution phase on to the adsorbent present as the solid phase. When the adsorbate is accumulated on to the adsorbent in two dimensional way, it is termed as “adsorption”, whereas, the accumulation of adsorbate into the adsorbent in three dimensional mode is called “surface precipitation”.

The surface functional groups on the sorbent are often responsible for efficient sorption. These groups are defined precisely as “a chemically reactive molecular unit bound on to the surface of a solid at its periphery such that the reactive components of the unit can be bathed by a fluid” [45]. When an active sorbent surface comes in contact with water, initially the water molecules adhere on the surface and subsequently hydroxyl groups are formed. These groups are responsible in imparting a surface charge to the sorbent. As a result, the sorbent can attract the ions of opposite charge (counter ions) efficiently and repel ions of same charge (co-ions).

Sorption process can be classified into two categories:

(1) non-specific (electrostatic/physical) sorption, resulting in the outer sphere complex formation and

(2) specific (chemical) sorption, resulting in the bond formation and inner sphere complexation.

Sorbents commonly used in water treatment are: activated carbons, alumina, silica, iron oxides, manganese oxide and zeolites [18, 41-44, 46]. Adsorption efficiency in general depends on number of factors, like, pH, adsorbate concentration, nature of the sorbent and the presence of the co-occurring ions.

The major advantages of the adsorption process are: easy operation, low cost, high removal efficiency, no by-product formation and easy regeneration. The major drawback here is that the sorbent gets exhausted after few cycles of operation and consequently it needs to be replaced. So periodic monitoring and replacement of the sorbent bed, is a must in this process.

1.9.4. Ion-exchange processes

Anion exchange is used as a technique for removal of negative arsenic oxyanion species. In this process, an anion on the solid phase is exchanged with the arsenic oxyanion in the aqueous phase. The resins are three-dimensional hydrocarbon network having large number of exchangeable groups, which are electrostatically bound to the resin beads. Strong base anion exchange resin in chloride or hydroxide form are commonly used for the removal of negatively charged As(V) species [18, 41-44, 46]. The efficiency of this process can be improved by using a pre-oxidation step, to convert As (III) to As (V).

The excess of oxidant needs to be removed in order to avoid the damage of sensitive resins. The efficiency of the ion-exchange process strongly depends on the pH, total dissolved solids (TDS) and the concentration of co-occurring ions like, sulfates and nitrates. The main problem in this process is the release of chemicals used in the resin into the environment.

1.9.5. Membrane technologies

Membrane acts as barriers for some constituents, which are bigger than the pore size of membrane, whereas, it allows water to simply pass through. Membrane based techniques are often driven by an external force. Here the force applied is pressure. Depending upon the amount of pressure applied, the techniques are categorized as - (i) Low pressure membrane process - microfiltration (MF) and ultrafiltration (UF) and (ii) High pressure membrane process - nanofiltration (NF) and reverse osmosis (RO) [18, 41-44, 46]. The separation in these processes depends upon the pore size of the membrane used. The details are listed in Table 1.3. The limitations of this method are the need for adjustment of pH before treatment, high cost of operation, high water rejection, long conditioning time and treatment time needed.

Table 1.3: The parameters and applications of various membrane technologies

Processes	**Pore size (nm)**	**Pressure required (bar)**	**Application**
Microfiltration (MF)	100 - 10,000	0.1 - 2	Pretreatment
Ultrafiltration (UF)	2 - 100	0.1 - 5	Removal of macromolecules, bacteria and viruses
Nanofiltration (NF)	0.5 - 2	3 - 20	Desalination, removal of organic compounds
Reverse osmosis (RO)	< 0.5	5 - 120	Removal of dissolved salts

1.9.6. Bio-remediation

The bio-remediation is the process of arsenic removal with the help of plants and microbes. These are environment friendly technology. The process of removal involves mainly three steps - phytoextraction, phytostabilization and phytovolatilization. The plants like Chinese brake fern, water hyacinth and lesser duckweed were used for arsenic phyto-remediation. The microbes like sulfate reducing bacteria and other species of chemoautotrophic arsenite-oxidizing bacteria (CAOs) such as Paenibacillus, Pseudomonas, Haemophilus, Micrococcus and Bacillus have been investigated extensively for the removal of arsenic from water [47-51].

The advantages and disadvantages of all the arsenic removal techniques discussed in this section are summarized in Table 1.4.

Table 1.4: Summary of advantages and disadvantages of arsenic removal technologies

Technology	Advantages	Disadvantages
Coagulation-flocculation	(i) Simple and low capital cost (ii) High removal efficiency (iii) Applicable for large water volume (iv) Removal for As(V) is high	(i) High coagulant dose is required (ii) Interferences from co-occurring ions (iii) Pre-oxidation required for As(III), which can produce harmful by-products (iv) Produces toxic sludge, could lead to environmental contamination (v) Additional separation step necessary
Oxidation	(i) Simple process and low cost operation (ii) Applicable for large volume of water	(i) Formation of harmful by-products (ii) Low removal efficiency (iii) Slow process (iv) Additional removal process is necessary
Adsorption	(i) High removal efficiency (ii) Simple process and low cost operation (iii) Commercially available chemicals (iv) No harmful by-products (v) Easy regeneration	(i) Periodic replacement of adsorbent material (ii) Adsorption bed gets exhausted (iii) Produces toxic solid waste (iv) Yet to be standardized
Ion exchange	(i) Well-defined medium and capacity (ii) Removal is moderately effective	(i) Expensive (ii) Requires high-tech operation and maintenance (iii) Regeneration creates a sludge disposal problem (iv) As(III) is difficult to remove, needs pre-oxidation (v) Interferences from other anions (vi) Can causes clogging
Membrane techniques	(i) High removal efficiency (ii) No toxic solid waste is produced (iii) Capable of removal of other contaminants and microorganisms	(i) Very high capital cost (ii) Pre-conditioning is needed (iii) Removal efficiency is very low for As(III), pre-treatment is needed (iv) High water rejection (v) Toxic wastewater is produced
Bio-remediation	(i) Environmental friendly (ii) Chemicals free (iii) Long-term remediation	(i) Yet to be standardized

1.10. Adsorption: A promising technology for arsenic uptake

Among the different arsenic removal processes, adsorption is considered to be the most promising and clean technology. The major advantages of this technique are listed in Table 1.4. In this process, the material used for removing a particular constituent from the bulk is termed as ‘adsorbent’, whereas, the constituent which is removed from bulk is termed as ‘adsorbate’. The interaction mechanisms involved between an adsorbent and adsorbate can be: (i) physical (Van der Waal’s/electrostatic force) sorption and (ii) chemical (bond formation) sorption. The maximum removal efficiency for any adsorbent-adsorbate combination can be achieved by studying the detailed interaction mechanisms that occur on the sorbent surface. There are wide varieties of sorbents, both natural and synthetic, which are in use for arsenic removal from groundwater. The most promising among them are the oxides of iron and manganese.

While considering the water treatment, a sorbent which is environmental friendly attracts the most attention, since we are not adding any extra harmful chemical to the system. Both the iron and manganese oxides are present abundantly in soils and minerals. Report by Kumar et al, observed that the iron oxides present in soils and sediments have strong affinity for negative oxyanion species of arsenic [52]. As we have seen in Section 1.5, these oxides plays important role in the arsenic adsorption and mobilization processes. This can be explained in terms of the high affinity that exists between inorganic arsenic species and iron/manganese oxides. They can remove arsenic by acting as a sorbent, co-precipitant or by behaving as a reductant/oxidant.

1.10.1. Arsenic uptake on iron oxides

Iron oxides can exists in various forms and among them - goethite (α-FeOOH), hematite (α-Fe_2O_3) and magnetite (Fe_3O_4) are most abundant in nature and widely applied for water treatment applications. There are reports on the use of iron oxides for As(III)/As(V) removal [53-59]. Most of these reports realizes mostly the As(V) removal by iron oxide, because the kinetics of As(III) oxidation to As(V) is found to be very slow (> 72 h). The main factor discussed by the researchers on arsenic sorption by iron oxide is pH. The maximum arsenic adsorption takes place at pH < 5. Another important factor highlighted in the literature is the crystallinity of the sorbent. The more is the crystallinity, lesser the surface area and less will be sorption efficiency. Hence, among iron oxides, highly amorphous ferrihydrite is reported to display better sorption property. Another form of iron, i.e. zero valent iron, is also used widely for water treatment applications. The major problem faced, while using iron oxide for water treatment, is the iron leaching/dissolution.

The mechanism of arsenic and iron oxide interactions are discussed in few reports [60-63]. Most of these reports suggests that the mechanism of interaction of arsenic with different iron oxides is mostly complexation and surface precipitation. Gimenez et al and Mamindy et al reported that there is no effect of ionic strength on the arsenic uptake by the iron oxides [55, 64]. The studies found that the presence of competitive ions can reduce the arsenic removal capacity significantly. Researchers had studied the oxidation state of arsenic, after sorption on iron oxides, using techniques like extended X-ray absorption fine-structure (EXAFS), fourier transform infrared (FTIR) spectroscopy, scanning electronic microscopy-energy dispersive (SEM-EDAX) spectroscopy. Inspite of all the studies, no conclusive evidence could be found regarding the changes occurring to the oxidation states of arsenic and iron during the sorption process.

1.10.2. Arsenic uptake on manganese dioxide

Manganese dioxide (MnO_2) is well known as a strong oxidant. There are literatures which suggest that MnO_2 is also a good sorbent for arsenic, since it oxidizes As(III) completely and converts to less toxic As(V) form, and removes arsenic through sorption. It is reported that the oxidation reaction of As(III) to As(V) in the presence of MnO_2 is thermodynamically feasible over a wide range of pH. Reports suggest that the kinetics of oxidation of As(III) to As(V) by MnO_2 is very fast and occurs within few minutes [65-66]. In a study by Contreras et al, MnO_2 is realized to be following an ion exchange type of interaction mechanism, wherein the adsorbate ions get trapped by the MnO_2 structure and stoichiometric proportion of hydrogen ions are released in to solution [67].

Most of the mechanism studies in the literature have been carried out utilizing birnessite (δ-MnO_2) [68-72], the main MnO_2 component found in sediments. The studies done by Foster et al, using extended X-ray absorption fine structure (EXAFS) and X-ray absorption near edge structure (XANES), could suggest a bidendate binuclear complex formation between As(V) species and birnessite [72]. According to a study utilizing SEM-EDS, the above complex formation was again observed by Tournassat et al [69]. The study by Manning et al. reported that after the sorption of As(III)/As(V) by MnO2, the complex formed in both the cases are similar, which indicated that the complexation occurs with As(V) and MnO_2. There is also evidence for the formation of an intermediate, Mn(III), in the sorption process of As(III)/As(V) by MnO_2 [68]. The reactions involved in the present cases are given in equations 1.3 - 1.5.

At low pH:

$$MnO_2 + H_3AsO_3 + 2\ H^+ \longrightarrow Mn^{2+} + H_3AsO_4 + H_2O \qquad (1.3)$$

At neutral pH:

$$2\ MnO_2 + H_3AsO_3 \longrightarrow 2\ MnOOH^* + H_3AsO_4 \qquad (1.4)$$

$$H_3AsO_3 + 2\ MnOOH^* + 2\ H^+ \longrightarrow 2\ Mn^{2+} + HAsO_4^{2-} + 3\ H_2O \qquad (1.5)$$

*MnOOH is an intermediate with Mn(III) oxidation state formed during the reaction.

The sorption of arsenic on iron and manganese oxides depends on many factors like: pH, initial concentration of arsenic, surface area and capacity of the sorbent. The comparison of these factors for different forms of iron oxides and manganese dioxides are tabulated in Table 1.5. Even though there are number of reports, from the table we can see that the practical applicability is limited because many of the studies concentrate only on As(V) species alone, which again needs to be addressed thoroughly to see the applicability in real groundwater.

Table 1.5: Comparison of arsenic sorption capacity of iron oxides and manganese dioxide

Adsorbent	**pH**	**Surface area (m^2 g^{-1})**	**Initial As concentration (mg L^{-1})**	**Adsorption capacity (mg g^{-1})**		**Reference**
				As(III)	**As(V)**	
Hematite	-	-	0.975	-	0.204	[73]
Hematite	4.2	14.4	1.01	-	0.20	[74]
Natural hematite	7.3	0.38	0.075, 75	0.271	0.830	[53]
Commercial hematite	2-10	1.66	0.5	-	0.41	[64]
Goethite	1.5-2.5	29	2.25	-	15	[75]
Natural goethite	7.5	2	0.075, 75	0.374	0.449	[53]
Commercial goethite	2-10	11.61	0.5	-	1.2	[64]
Natural magnetite	6.5	0.89	0.075, 75	0.206	0.253	[53]
Commercial magnetite	2-10	1.6	0.5	-	0.85	[64]
MnO_2	7.9	17	1	-	0.172	[76]
MnO_2 containing ore	6.5	-	-	0.53	15.38	[77]

1.11. Motivation for the work

The extensive literature review on the adsorptive removal of arsenic from groundwater by oxides/hydroxides of iron and manganese, suggests that the effect of several factors, mainly pH of the medium, nature of sorbent, surface area, needs to be studied thoroughly. Comprehensive work is required for comparing the abilities and shortcomings of both the sorbents. More investigation is required on the arsenic-sorbent interactions and the determination of the changes occurring to the oxidation states of arsenic and the metal oxides. Also the main challenge is to modify the promising sorbent, among them with good sorption properties, so as to apply for field applications with ease of operation. These motivated us to choose iron and manganese oxides for arsenic removal application in a detailed manner, giving more importance for the mechanistic evaluation of their interactions.

1.12. Objectives of the study

The main objectives of the present work are:

(i) Preparation and characterization of different iron oxides like goethite, hematite and magnetite. The sorption study of arsenic on these iron oxides using radiotracer technique in batch equilibration mode and understanding the effects of pH, kinetics and interference from co-occurring ions on sorption of arsenic. A comparative study on the properties of these sorbents including their leaching, regeneration and reusability. Evaluation of the sorption mechanism using appropriate analytical techniques.

(ii) Preparation of manganese dioxide (MnO_2) via different methods of preparation viz. wet chemical method and solid state mixing method and their characterization using suitable techniques. The sorption study of arsenic on MnO_2 using ^{76}As radiotracer.

Understanding the effects of pH, kinetics and interference from co-occurring ions on sorption of arsenic on MnO_2. Comparative study on various properties of the MnO_2 prepared by different methods. Evaluation of the sorption mechanism using solvent extraction, spectroscopic and electrochemical investigation.

(iii) Evaluation of practical applicability, by using the sorbents for arsenic removal from real arsenic contaminated groundwater samples collected from arsenic contaminated region in India.

(iv) Preparation of modified sorbent using the sorbent with good sorption properties, its characterization, evaluation of different sorption parameters and application to real arsenic contaminated groundwater.

Chapter - II

Synthesis of adsorbents and characterization

2.1. Introduction

Among the various removal processes for arsenic from groundwater, adsorption is considered as superior due to the high removal efficiency, high capacity and reusability. Studies on uptake of arsenic by different naturally occurring metal oxides are important for understanding the sorption mechanism, which helps in the development of efficient arsenic removal method from water. In nature, arsenic is generally found to be adsorbed onto iron, manganese and aluminum hydroxides as As(III) or As(V) oxyanions. When there is a reducing environment, these metal hydroxides partially reduce and solubilize, resulting in the release of arsenic to groundwater [6]. Several methods including adsorption on inorganic oxides/hydroxides have been reported for the removal of arsenic from water [78-82]. The promising sorption properties are attributed by high surface area, reusability and ease of operation.

In this work, oxides of iron and manganese were chosen for the uptake studies. The interaction of arsenic with iron oxide and manganese dioxide was studied using the sorbents synthesized in our laboratory. Criteria for selecting various synthesis routes were: (i) the simple steps, (ii) no high temperature and high pressure operations involved and (iii) no addition of harmful chemical which affects the final application. Different iron oxides, namely magnetite, goethite and hematite, were synthesized by chemical methods [83]. Manganese dioxide (MnO_2) was prepared by two solution routes and a solid state mixing route [84-85]. A modified sorbent, XAD-4 resin coated with MnO_2 (MX-4 resin), was also prepared [86].

The structures of the synthesized oxides were identified by X-ray powder diffraction (XRD) analysis. The particle size, surface area and point of zero charge (PZC) of the synthesized sorbents were measured. Along with these, transmission electron microscopic

(TEM) and thermo-gravimetric measurement (TG) were carried out for the characterization of the prepared MnO_2. Characterization of the MX-4 resin was done by attenuated total reflection Fourier transform infrared spectrometry (ATR-FTIR), scanning electron microscopy (SEM) and neutron activation analysis (NAA). The results were compared with those reported in the literature.

The characterization techniques, their working principles and the optimized parameters for these measurements have been described briefly in this chapter. Methods of preparation of the arsenic tracer solutions and the solvent extraction study for the determination of oxidation state of arsenic in the tracer solutions are also described in this chapter.

2.2. Materials and methods

2.2.1. Reagents and chemicals

The chemicals viz., ferric nitrate [$Fe(NO_3)_3 \cdot 9H_2O$; molecular weight (MW) - 404.00 g mol^{-1}], ammonium ferric sulphate [Mohr's salt; $(NH_4)_2SO_4.FeSO_4.6H_2O$; MW - 392.13 g mol^{-1}], ferric chloride ($FeCl_3.6H_2O$; MW - 270.30 g mol^{-1}), potassium permanganate ($KMnO_4$; MW - 158.03 g mol^{-1}), manganese sulphate ($MnSO_4.4H_2O$; MW - 223.07 g mol^{-1}), manganese acetate [$Mn(CH_3CO_2)_2.4H_2O$; MW - 245.09 g mol^{-1}], arsenious oxide (As_2O_3; MW - 197.84 g mol^{-1}), sodium hydroxide pellets (NaOH; MW - 40.00 g mol^{-1}) and sodium chloride (NaCl; MW - 58.44 g mol^{-1}) were used for the preparation of sorbents. These chemicals are of analytical reagent (AR) grade and used without further purification. For the preparation of modified sorbent, XAD-4 resin (Amberlite; surface area - 750 m^2 g^{-1} and bead size 20 - 60 mesh) purchased from Fluka, Germany, was used as an inert support material. Before use, these resin beads were washed 3-4 times with deionised (DI) water, for removing surface impurities. The reagents concentrated hydrochloric acid (HCl), concentrated nitric acid (HNO_3), ammonia solution (NH_4OH)

and benzene (C_6H_6) were of AR grade and used without further purification. All the necessary dilutions were done using deionised (DI) water (resistivity 18.2 MΩ cm^{-1} and total organic carbon < 10 μg L^{-1}) from Milli-Q water purification system.

2.2.2. Equipments

All the weighing was done using a high precision analytical semimicro balance (Mettler - Toledo, dual range, readability - 0.01 mg). pH measurement was carried out in Oakton pH meter employing glass electrode (pH700, USA), with digital display having precision of ± 0.01 unit. A mechanical shaker was utilized for the equilibrations at room temperature. Radioactivity measurement was done using a high purity germanium (HPGe) detector (Canberra, Australia, relative efficiency: 30 %, resolution: 1.9 keV at 1332 keV) coupled to 8k channel analyzer.

2.3. Preparation of iron oxides

2.3.1. Method-1: Preparation of goethite

Synthesis of goethite was done via the method described in literature [87-88] as per the reactions 2.1 and 2.2. Ferric nitrate solution (1 M) was prepared by dissolving 80 g of the salt in 200 mL DI water. Sodium hydroxide solution (2.5 M) was made by dissolving 10 g of NaOH pellets in 100 mL DI water. The NaOH solution was added dropwise with constant stirring at 50 rotations per minute (rpm) to ferric nitrate solution. A dark red coloured ferrihydrite (Fig. 2.1 (a)) started precipitating. This suspension was kept under constant stirring on a hot plate for 2 h at 90 ^{o}C. The structural rearrangement occurred and yellow coloured precipitate appeared. This colour change was a visual confirmation of the formation of goethite (Fig. 2.1 (b)). The suspension was left overnight. Goethite precipitate was washed several times with DI water till the supernatant became neutral. The yellow precipitate was air dried and kept in air tight polypropylene container for further use.

$$Fe(NO_3)_3.9H_2O + 3NaOH \longrightarrow Fe(OH)_3 + 3NaNO_3 + 9H_2O \qquad (2.1)$$

$$Fe(OH)_3 \xrightarrow{\text{2 h stirring, @ 90 }^{o}\text{C}} \alpha\text{-FeOOH (Goethite)} + H_2O \qquad (2.2)$$

2.3.2. Method-2: Preparation of hematite

The initial preparation step of hematite was same as that for goethite. A solution of 2.5 M NaOH was added drop-wise to 1 M ferric nitrate solution and dark red coloured ferrihydrite was precipitated (equation 2.1). The suspension was stirred for 2 h at 50 rpm in room temperature. The dark red coloured ferrihydrite got coagulated and precipitated completely. As done for goethite, this suspension was also left overnight. The precipitate was washed several times with DI water till the supernatant becomes neutral. For the conversion of ferrihydrite to hematite, dehydroxylation of the dark red precipitate was done by heating at 300 ^{o}C for 36 h in a muffle furnace [87-88] as per the reaction 2.3. A reddish brown powder, typical colour of hematite (Fig. 2.1 (c)) was obtained after heating. This powder was stored in polypropylene container for further use.

$$2\ \alpha\text{-FeOOH} \xrightarrow{\text{36 h heating, @ 300 }^{o}\text{C}} \alpha\text{-}Fe_2O_3\text{ (Hematite)} + H_2O \qquad (2.3)$$

2.3.3. Method-3: Preparation of magnetite

100 mL of ammonium ferrous sulphate and ferric nitrate solutions were prepared by dissolving 50 g of the corresponding salt in separate beakers. These solutions were mixed slowly and ammonia solution was added till solution becomes alkaline. The chemical reactions followed the steps as given in equations 2.4 - 2.7 [89]. Obtained suspension was kept at 50 rpm on a magnetic stirrer with hot plate at 80 ^{o}C for 2 h [87-88]. The precipitate was then filtered and washed many times with DI water till supernatant was neutral. For the complete conversion of hydroxides to oxides, the dark brown precipitate

was heated in an oven at 100 °C for 12 h. The final powder was black, indicating the color of magnetite (Fig. 2.1 (d)).

$$Fe^{2+} + 2OH^{-} \longrightarrow Fe(OH)_2 \qquad (2.4)$$

$$Fe^{3+} + 3OH^{-} \longrightarrow Fe(OH)_3 \qquad (2.5)$$

$$Fe(OH)_3 \longrightarrow \alpha\text{-}FeOOH + H_2O \qquad (2.6)$$

$$Fe(OH)_2 + 2\alpha\text{-}FeOOH \longrightarrow Fe_3O_4\ \text{(Magnetite)} + 2H_2O \qquad (2.7)$$

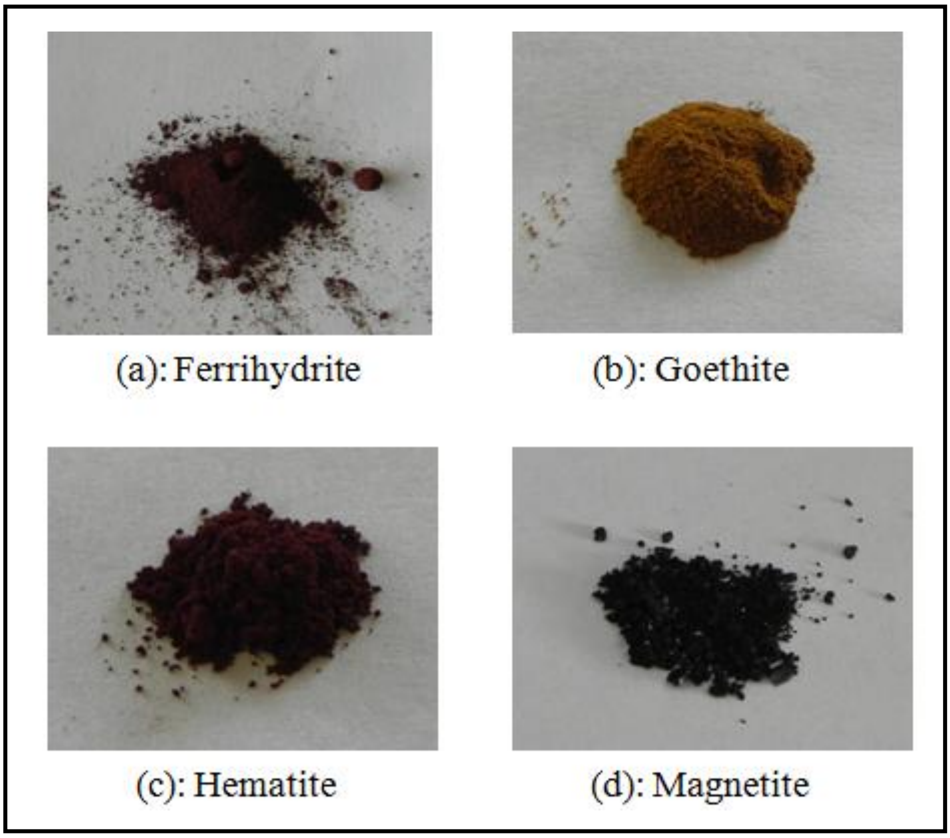

Figure 2.1: Images of synthesized ferrihydrite and various iron oxide samples.

2.4. Preparation of manganese dioxides

2.4.1. Method-1

250 mL of $KMnO_4$ (21.3 g L^{-1}) and $MnSO_4$ (71.4 g L^{-1}) solutions were prepared separately in two beakers by dissolving the appropriate amounts of salt in DI water. The $MnSO_4$ solution was heated on a hot plate to 90 °C. The $KMnO_4$ solution was added dropwise to hot manganese sulphate solution with constant stirring. Manganese dioxide (MnO_2) got precipitated [90] as per the chemical reaction given in equation 2.8. Obtained

suspension was kept under stirring and heating at 90 °C for 15 min. Then the suspension was allowed to cool to room temperature. The MnO_2 formed was washed till the supernatant was neutral. The black coloured MnO_2 [Fig. 2.2] was filtered, air dried and stored in polypropylene bottles.

$$2KMnO_4 + 3MnSO_4 + 2H_2O \longrightarrow 5MnO_2 + K_2SO_4 + 2H_2SO_4 \qquad (2.8)$$

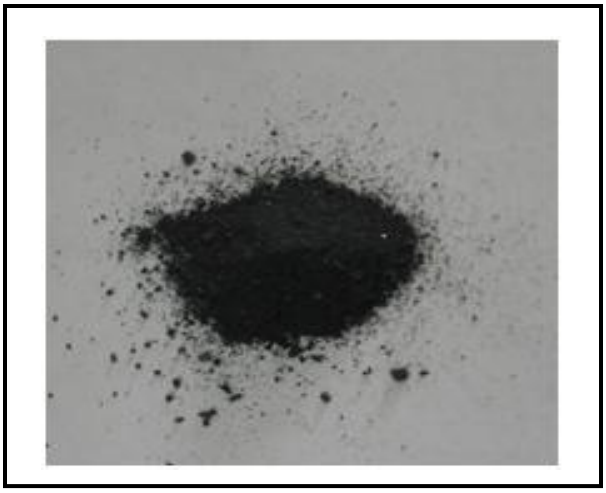

Figure 2.2: Image of synthesized manganese dioxide sample.

2.4.2. Method-2

Manganese dioxide (MnO_2) was prepared by reduction of Mn^{7+} to Mn^{4+} by the addition of concentrated HCl following the reaction 2.9. A 250 mL of 0.4 M $KMnO_4$ solution was prepared in DI water and heated to 60 °C. Concentrated HCl (~ 65 mL) was also heated at 60 °C in another beaker. Both the solutions were mixed slowly and the resultant solution was heated to 90 °C under constant stirring [68]. The solution was cooled to room temperature. The precipitated MnO_2 was washed till neutralization using DI water. MnO_2 was filtered, air dried and stored in polypropylene bottles.

$$2KMnO_4 + 8HCl \longrightarrow 2MnO_2 + 2KCl + 4H_2O + 3Cl_2 \qquad (2.9)$$

2.4.3. Method-3

A solid state reaction method was adopted for the preparation of MnO_2 [91]. $KMnO_4$ (12 g) and manganese acetate (28 g) salts were mixed together in an agate mortar for 1 h. The colour of the salt changes from purple to black. The chemical reaction occurring during the mixing is given in equation 2.10. The mixture was put in DI water and heated at 90 °C for 6 h under stirring condition. The cooled suspension was neutralized by repeated cycles of DI water washing. The filtered MnO_2 was air dried and stored in polypropylene bottles.

$$2MnO_4^- + 3Mn^{2+} + 2H_2O \longrightarrow 5MnO_2 + 4H^+ \qquad (2.10)$$

2.5. Preparation of modified sorbent

A simple reduction method of permanganate (MnO_4^-) with the assistance of ultrasound [92] was used for coating MnO_2 on XAD-4 resin. The structure of XAD-4 is given in Fig. 2.3 [93]. The entire procedure of preparation of MnO_2 coated XAD-4 resin, designated as MX-4, was optimized. The $KMnO_4$ concentration, ultrasonic frequency and time of sonication were optimized to be 0.1 M, 35 kHz and 10 min, respectively. The reaction vessel used was 100 mL stoppered conical flask sealed with parafilm. The experiments were done in room temperature. The procedure adopted was as follows: 20 g of XAD-4 beads were soaked in 0.1 M $KMnO_4$ solution for 15 min, followed by 10 min of ultrasound irradiation using Retsch UR-1 ultrasonic bath (35 kHz, 240 W) (Fig. 2.4).

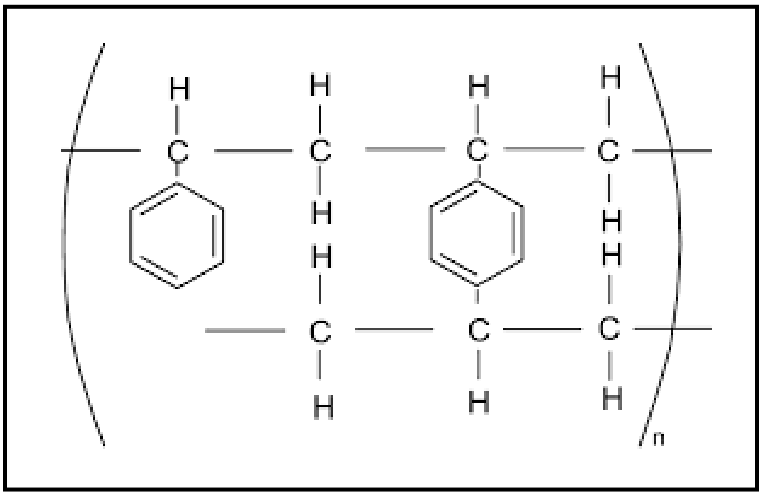

Figure 2.3: General structure of XAD-4 [93].

The mechanism of formation of MnO_2 during sonication is represented by the reactions 2.11 - 2.15 [94-96].

$$H_2O +))) \longrightarrow H^{\bullet} + {}^{\bullet}OH \qquad (2.11)$$

$$2H^{\bullet} \longrightarrow H_2 \qquad (2.12)$$

$$H^{\bullet} + OH^{\bullet} \longrightarrow H_2O \qquad (2.13)$$

$$2OH^{\bullet} \longrightarrow H_2O_2 \qquad (2.14)$$

$$MnO_4^{-} + 3H^{\bullet} \longrightarrow MnO_2 + OH^{-} + H_2O \qquad (2.15)$$

where,))) indicates sonication.

The sonication renders the formation of $H^{\cdot}$, $OH^{\cdot}$, H_2O, H_2 and H_2O_2, among them, two are reducing species, namely $H^{\cdot}$ and H_2. The experimental observation by Abulizi et al [95] explains that the permanganate reduction occurs by $H^{\cdot}$. Similarly Baral et al [96] explained that the oxidation of the MnO_2 or Mn(II) can occur by H_2O_2, but this requires higher alkaline medium and high H_2O_2 concentration. Since our experiments were conducted in neutral medium and for only 10 minutes sonication, this route was not expected to occur. Thus, we propose an $H^{\cdot}$ assisted formation of the coating of MnO_2 on XAD-4.

The MX-4 beads obtained were washed with DI water and air dried till use. XAD-4 resin beads and MX-4 beads are shown in Fig. 2.5.

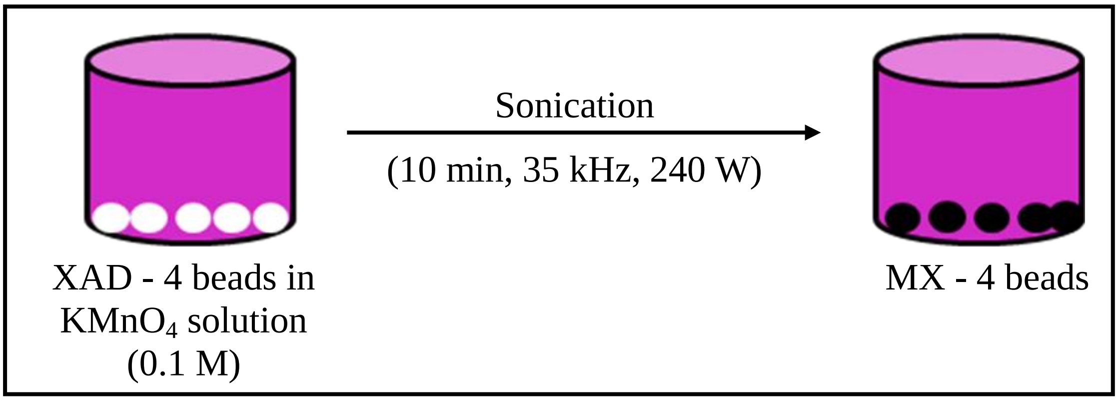

Figure 2.4: Schematic of the preparation of MX-4 beads.

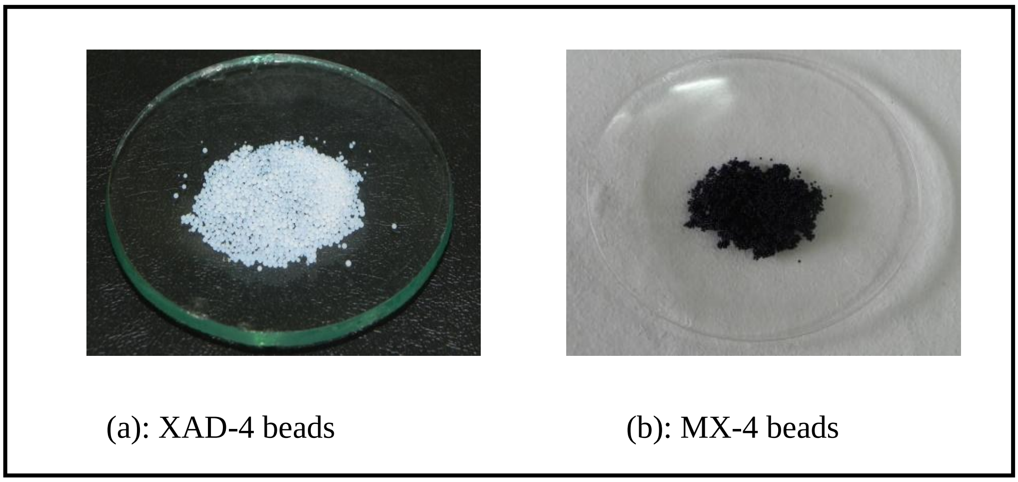
(a): XAD-4 beads

(b): MX-4 beads

Figure 2.5: Images of XAD-4 and MX-4 beads.

2.6. Characterization of iron oxides

2.6.1. X-ray diffraction (XRD) measurement

X-ray diffraction (XRD) is a non-destructive technique, used mainly for the characterization of crystallinity of solid materials. XRD is governed by Bragg's law (equation 2.16). The general principle is depicted in Fig. 2.6. For crystalline compounds, there always exists a long range order and we get diffraction peaks at particular diffraction angles. The compound is identified by conversion of these observed diffraction peaks to d-spacings, as the d-values are the characteristics of the compound. The identification of compound is done by comparing the d-values obtained with those of the standard patterns in JCPDS file. For amorphous materials, since there is no periodicity in the material, no diffraction peaks will be observed from the X-ray diffraction studies.

$$n \times \lambda = 2d \sin\theta \qquad (2.16)$$

Where n is an integer called the order of reflection, λ is the wavelength of the incident X-ray beam, d is the distance between atomic layers in a crystal (d-spacing) which is characteristic of a compound and θ is the angle of incidence.

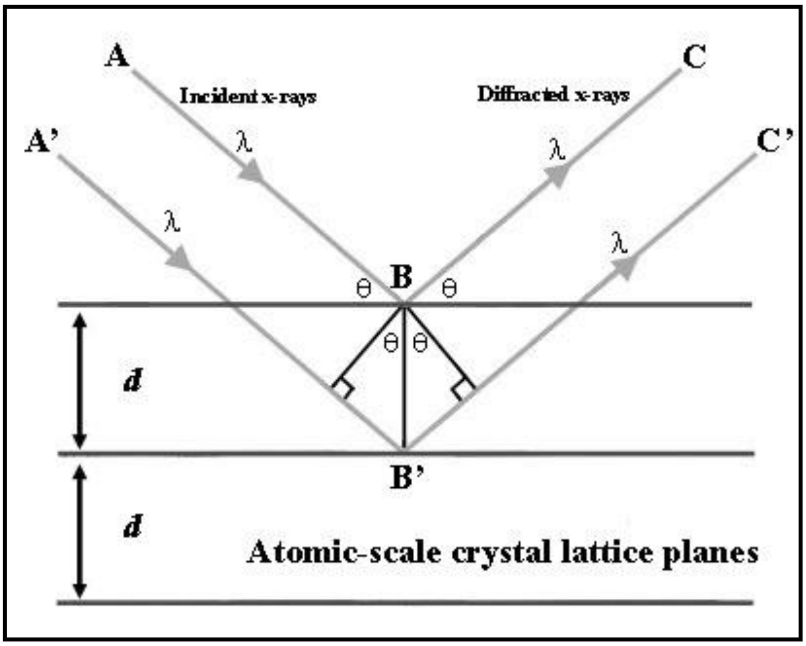

Figure 2.6: Schematic of X-ray diffraction and basis of Bragg's law [97].

The synthesized iron oxides were characterized by XRD analysis using PANalytical powder X-ray diffractometer (Xpert-Pro, Almelo, Netherlands) at room temperature. A Cu K_α radiation (λ = 1.540 Å) operating at 40 kV voltage and 40 mA current was used as X-ray source. An argon filled proportional counter was used as the detector. The XRD pattern was recorded in 2θ angular range between 10 and 70° with a step width of 0.02° and step time of 4 s. The XRD analysis revealed the crystallographic structure as well as the phases of the synthesized iron oxides as goethite (α-FeOOH; Fig. 2.7), hematite (α-Fe_2O_3; Fig. 2.8) and magnetite (Fe_3O_4; Fig. 2.9).

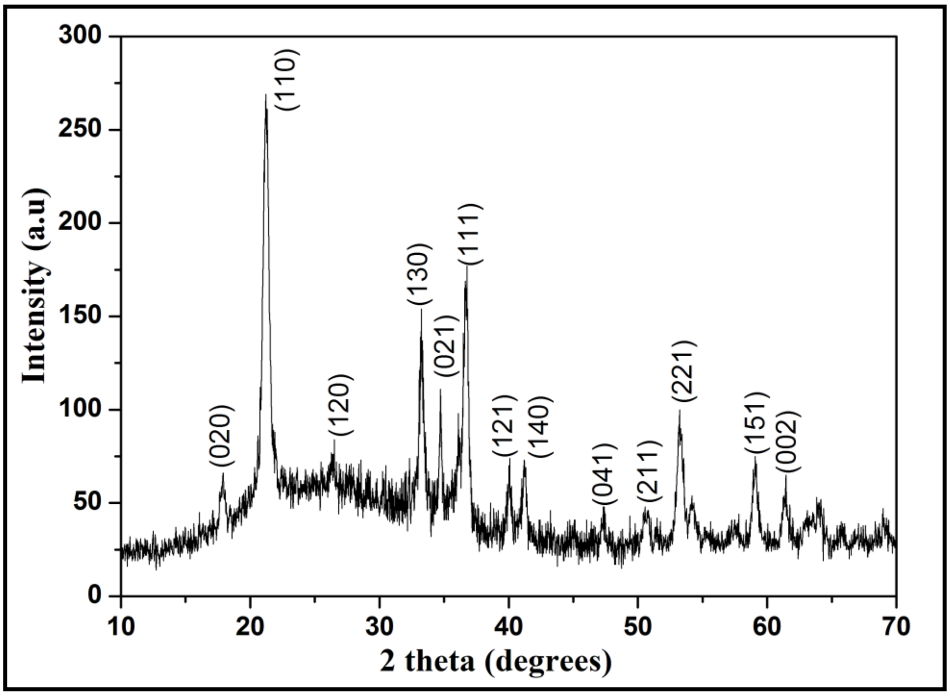

Figure 2.7: XRD spectra of goethite (α-FeOOH), JCPDS Code: 81-0464.

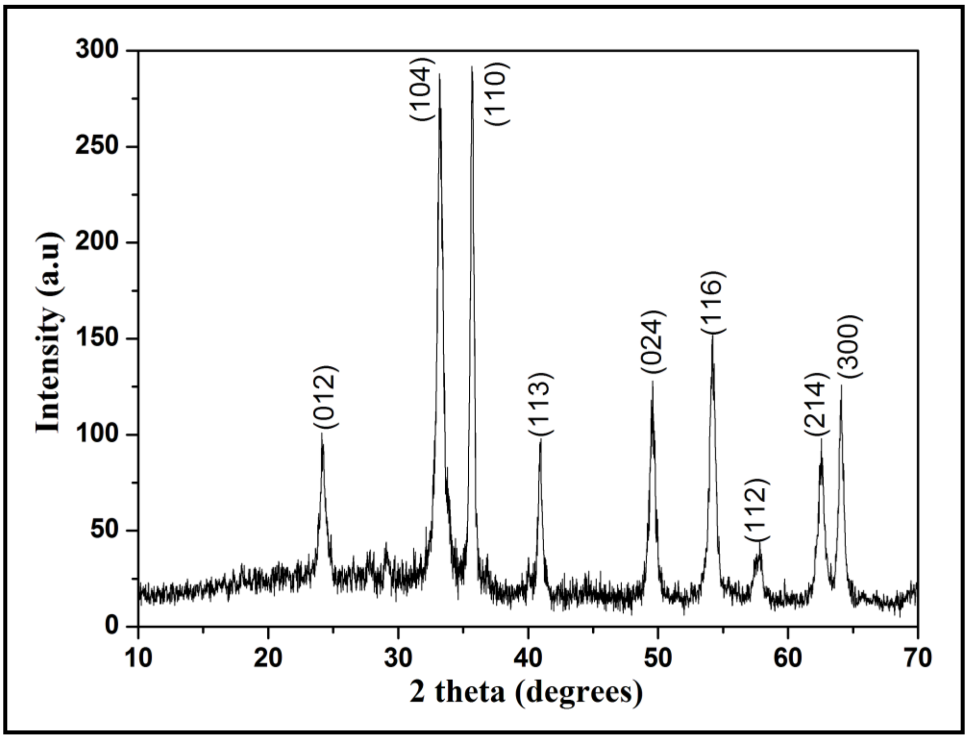

Figure 2.8: XRD spectra of hematite (α-Fe_2O_3), JCPDS Code: 86-055.

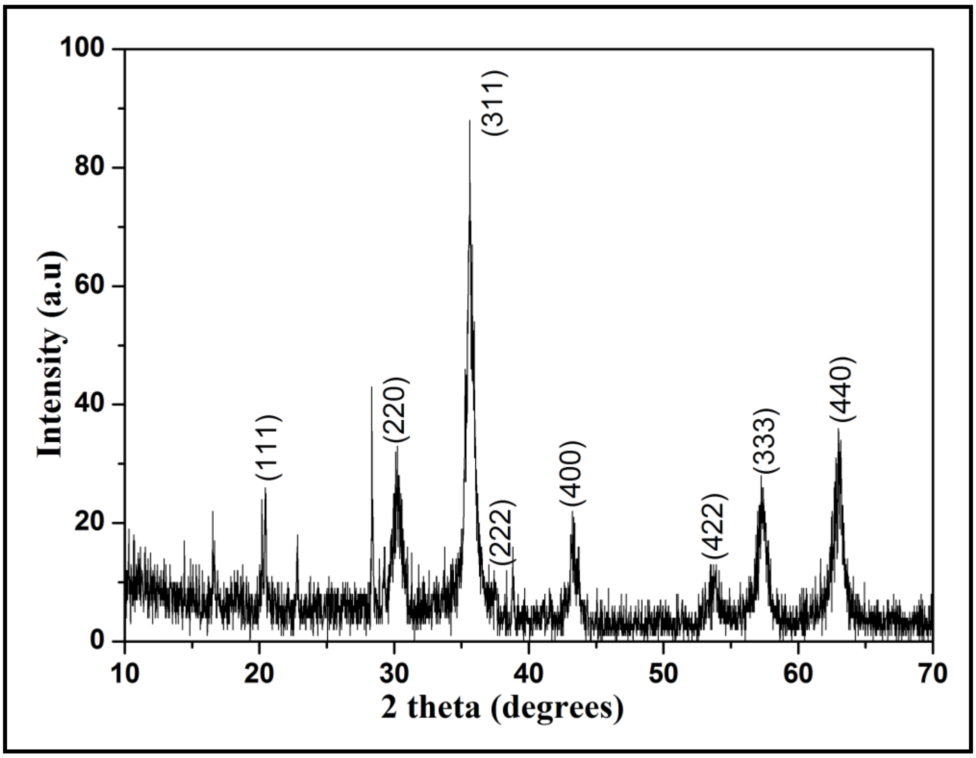

Figure 2.9: XRD spectra of magnetite (Fe_3O_4), JCPDS Code: 19-0629.

2.6.2. Surface area measurement

The measurement of surface area is based on Brunauer, Emmett and Teller (BET) theory [98]. The weighed material is taken in the sample holder and degassing is done by heating to 110 °C in continuous flow of nitrogen. The nitrogen is allowed to form an adsorbed layer, in the pattern of a monolayer, on the material by cooling it to liquid nitrogen temperature. The desorption of nitrogen is done by bringing the sample to room temperature. The thermal conductivity bridge is used as the detector, which measures the change in the nitrogen concentration during the adsorption and desorption. From this, the surface area of the sample is calculated.

In this study, the measurement of BET surface area of the adsorbent was done using an indigenously developed surface area analyzer (make: BARC). The surface area obtained for goethite, hematite and magnetite are listed in Table 2.1.

2.6.3. Point of zero charge (PZC) measurement

Point of zero charge (PZC) of the suspended particles is an important property associated with their adsorption characteristics. The stability of colloidal particles is often understand through zeta potential measurements. Zeta potential is the difference in potential between the surface of the particle and the dispersion medium. Higher the magnitude of zeta potential, higher the repulsive forces between the particles and hence higher is the stability for the suspension. But when the zeta potential is less, the attractive forces between the particles are stronger and the particles get agglomerated. At PZC, the zeta potential is zero, and this is a very characteristic parameter for the suspended particles.

In suspensions, a colloidal particle is always associated with surface charge (Fig. 2.10). Accordingly, when an electric field is applied, the charged particles gain velocity because of the interaction with the applied field, which in turn is proportional to the zeta potential of the concerned particles. This motion of the particles in an electric field is termed as electrophoresis. During the application of an electric field, the suspension is irradiated with a laser light to monitor the electrophoresis process. Understandably, there will be a Doppler frequency shift observed in the scattered light compared to the incident light due to the change in the velocity of particles in the medium by the applied electric field. This frequency shift ($\Delta\nu$) of scattered light is measured which can be converted to electrophoretic mobility, μ [99]. From that, the zeta potential is calculated using the following equations 2.17 - 2.19. When the zeta potential is zero, indicating that the net charge on the particles is zero, particles remain stationary in an electric field. The pH at which the net charge on the surface of the particles becomes zero is characterized as the PZC of the concerned particles.

$$\Delta\nu = \frac{2\ V\ n\ \sin\frac{\theta}{2}}{\lambda} \qquad (2.17)$$

$$V = \mu \times E \qquad (2.18)$$

$$Z = \frac{4\,\pi\,\mu\,\eta}{\xi} \qquad (2.19)$$

Where Δv is the shift in frequency (Doppler shift), V is the velocity of the particle, n is the refractive index of the medium, θ the angle at which scattered light is detected, λ is the wavelength of the laser light, μ the mobility of particle, E is the electric field applied, η is the viscosity of the medium, ξ is the dielectric constant of the medium and Z is the zeta potential.

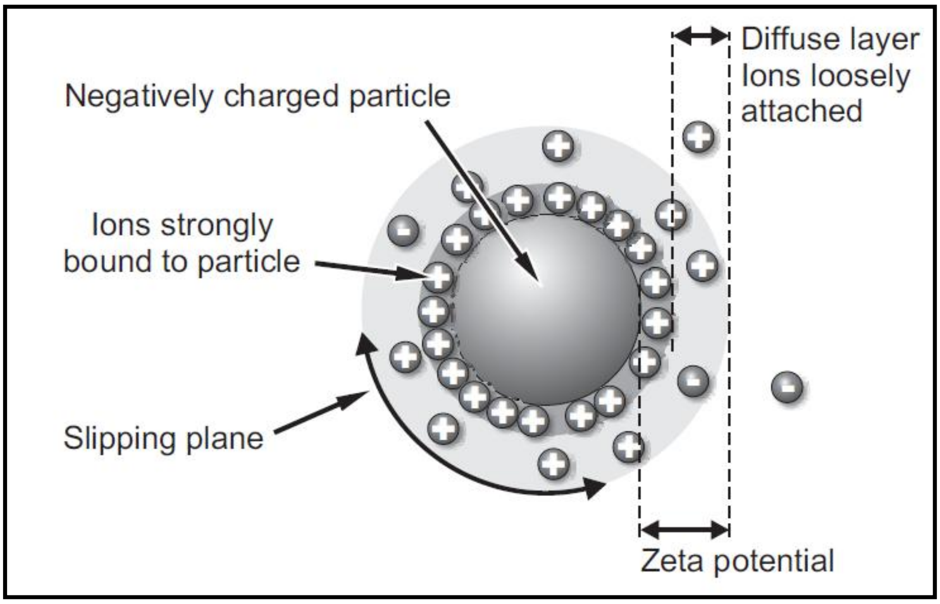

Figure 2.10: Schematic of a charged suspended particle in a medium and the conceptual presentation of its zeta potential [100].

PZC of synthesized iron oxides was measured using Malvern Zetasizer nano-Z instruments, UK. The light source used was He-Ne laser (632.8 nm) operated at 4 mW. The measurement was carried out using a quartz cell with 10 mm path length. All the measurements were conducted at room temperature. The iron oxides were taken in DI water, pH was adjusted between 1 - 12 using dilute NaOH and HNO_3 solutions. The ultrasonication was done for 1 min using UR-1, Retsch GmbH, Germany (35 kHz, 240

W) to avoid agglomeration of the particles. The PZC values obtained are listed in Table 2.1.

2.6.4. Particle size measurement

The principle of particle size determination is based on dynamic light scattering (DLS) method [101]. In a suspension, all the suspended particles are in continuous Brownian motion. When the particles are irradiated with a laser light (He - Ne laser operated at 632.8 nm at maximum power), as the larger particles move slowly, they scatter the light at smaller angles, while the smaller particles that move at higher speed, scatter the light at larger angles. The velocity of the particle (translational diffusion coefficient, D) and the particle size (r) is related by Stokes-Einstein equation (equation 2.20). The basic criterion for applying the equation is that the particle needs to be on Brownian motion. The angular scattering intensity data is measured with respect to time and utilized to calculate the size distribution of the particles.

The Stokes-Einstein equation is given as:

$$D = k_B \times \frac{T}{(6 \pi \eta r)} \qquad (2.20)$$

Where D is the translational diffusion constant ($m^2 s^{-1}$), k_B is the Boltzmann constant, T is the absolute temperature, η is the viscosity and r is the hydrodynamic radius of the particle.

The particle size measurements were done using Malvern 4800 Autosizer with a He-Ne laser source of wavelength 632.8 nm. The particle size range obtained from the measurement is given in Table 2.1.

Table 2.1: Characteristics of the synthesized iron oxide samples.

Characterization techniques	**Goethite**	**Hematite**	**Magnetite**
XRD	α-FeOOH	α-Fe_2O_3	Fe_3O_4
Surface area ($m^2\ g^{-1}$)	51 ± 8	18 ± 3	35 ± 2
PZC (pH)	8.0 ± 0.3	7.2 ± 0.4	6.8 ± 0.3
Particle size (nm)	164 - 295	190 - 342	320 - 340

2.7. Characterization of manganese dioxides

2.7.1. X-ray diffraction (XRD) measurement

The prepared manganese dioxides (MnO_2) were characterized by XRD measurements by PANalytical Powder X-ray diffractometer (Xpert-Pro, Almelo, Netherlands) using the monochromatized Cu - K_α source ($\lambda = 1.540$ Å) and measuring the diffraction from 10 - 70° (2θ angle) with step width of 0.02° and step time of 4 s, at room temperature. The XRD analysis revealed the structures of MnO_2 formed as ramsdellite (method-1; Fig. 2.11) and α-MnO_2 (method-2 and method-3; Figs. 2.12 and 2.13, respectively). For the solid state mixing method, it was reported that the MnO_2 obtained was a mixture of δ-MnO_2 and α-MnO_2 [91]. For our synthesized sample, however, the XRD measurement showed the MnO_2 is formed with α-MnO_2 structure only. This deviation possibly occurred due to the differences in the proportion of manganese acetate tetra hydrate and potassium permanganate used in the present work (3:2) as compared to that reported by Li et al. (2:3) [91].

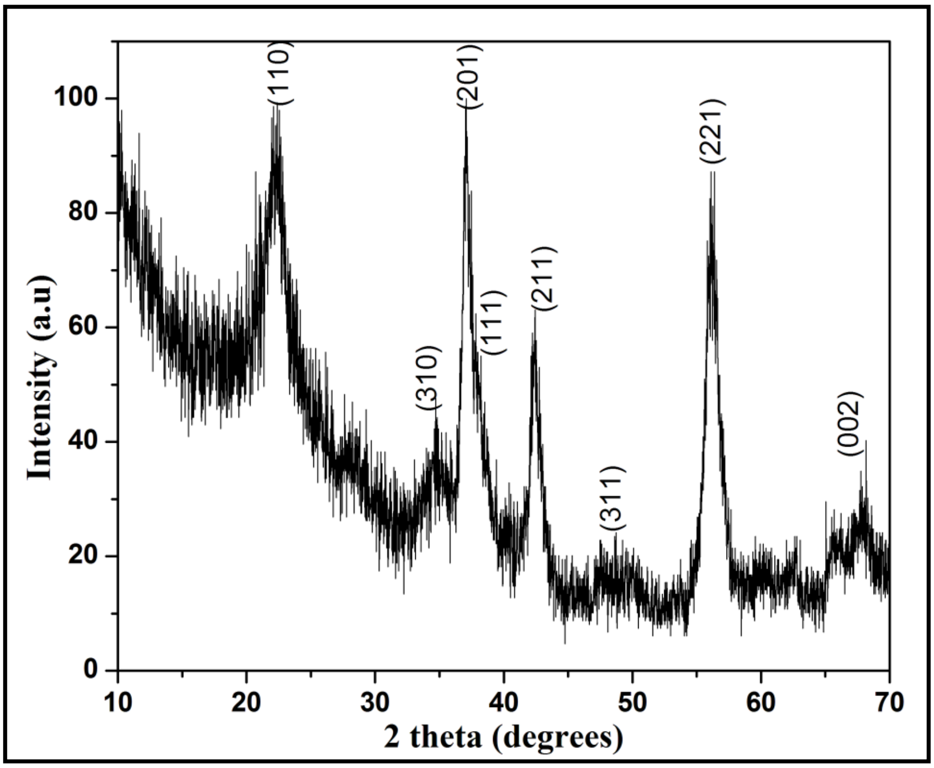

Figure 2.11: XRD spectra of MnO_2 (ramsdellite) prepared from method-1, JCPDS Code: 44-0142.

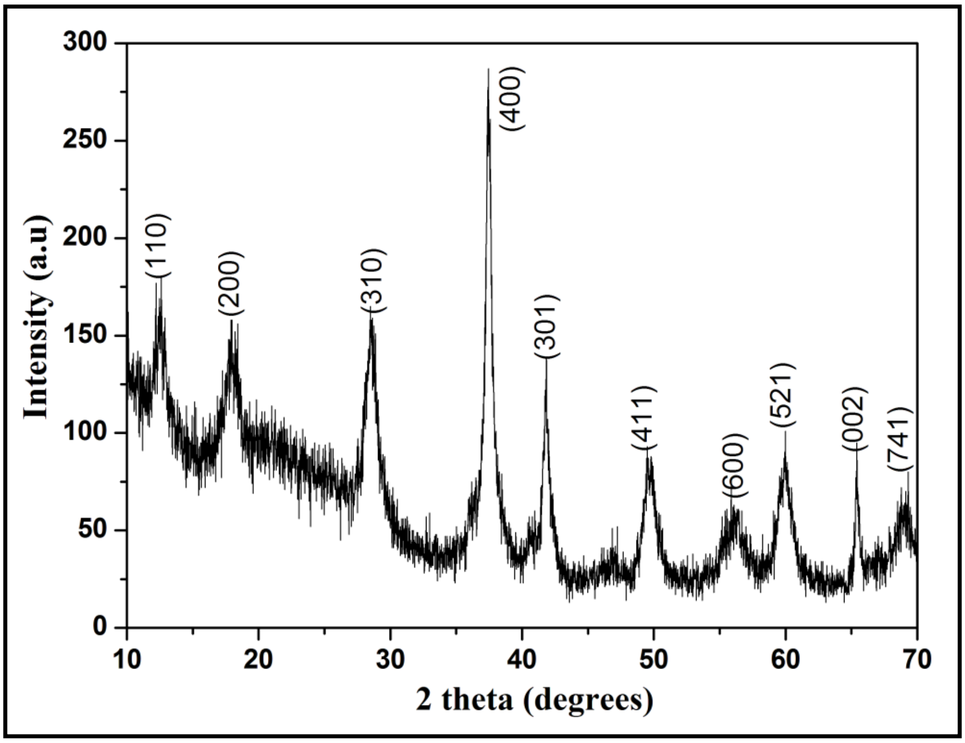

Figure 2.12: XRD spectra of MnO_2 (α-MnO_2) prepared from method-2, JCPDS Code: 44-0141.

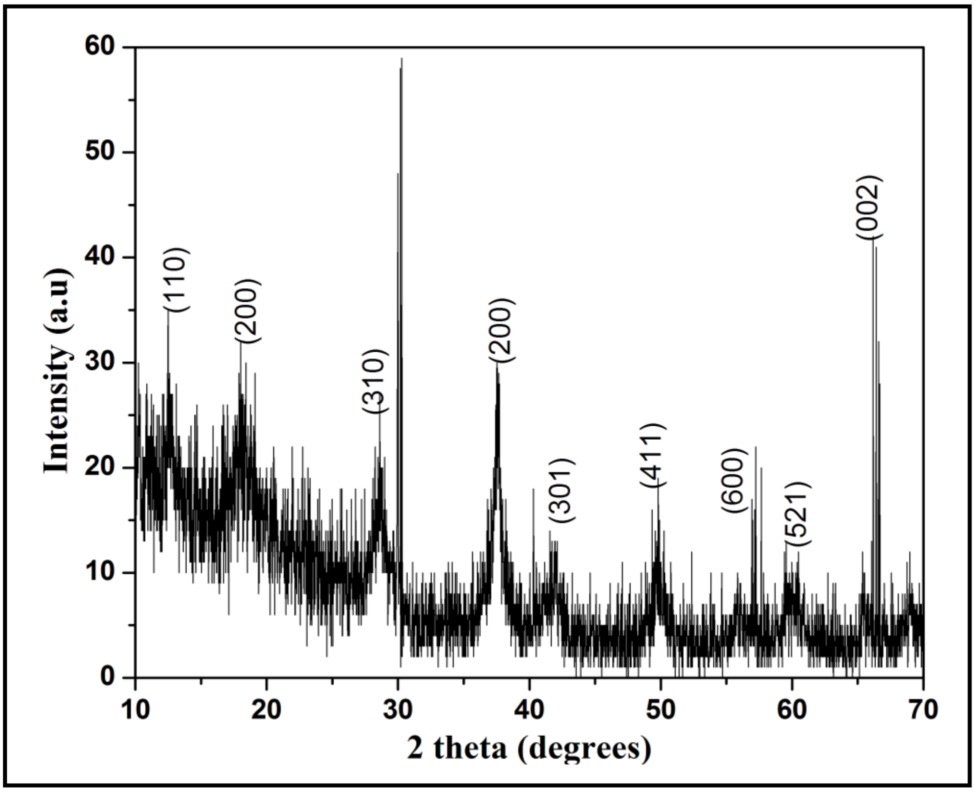

Figure 2.13: XRD spectra of MnO_2 (α-MnO_2) prepared from solid state mixing method, JCPDS Code: 44-0141.

2.7.2. Surface area measurement

The surface area measurement of MnO_2, prepared in this study, was done based on BET single point method. The surface area obtained for MnO_2 prepared by method-1, method-2 and method-3 were shown in Table 2.2. Surface area of MnO_2 synthesized by solid state mixing method was higher compared to the surface areas of MnO_2 synthesized by two solution methods.

2.7.3. Point of zero charge (PZC) measurement

The PZC of MnO_2 was measured following the procedure discussed in Section 2.6.3. The PZC values obtained are listed in Table 2.2. The zeta potential values indicate that the surface of MnO_2 is positively charged below PZC and negatively charged above PZC.

2.7.4. Thermogravimetric (TG) measurement

Thermogravimetric (TG) analysis is done in controlled atmosphere, where the changes in the mass of the sample are continuously monitored with respect to the changes in the temperature. TG is applied for studying the thermal decomposition of the compounds. From TG plots, the water contents in the compounds can be easily determined. A TG set up consists of a furnace in which a sample holder, connected to a highly precise thermobalance, is attached. The sample is heated at a constant rate. Any chemical reaction resulting in the increase or decrease in the weight of the sample is recorded through the thermobalance. A TG plot is obtained by plotting the mass change / percentage of loss or gain of the initial mass on the y axis versus either temperature / time on the x-axis.

For MnO_2 characterization, TG measurements were carried out in dynamic argon atmosphere using Netzsch thermal analyzer (Model STA-409, GmBH, Germany). The heating rate of 10 K min^{-1} was maintained for all the measurements. The TG curves of MnO_2 prepared by method-1 and method-2 Figs. 2.14 and that of MnO_2 prepared by method-3 is shown in Fig. 2.15. The net water loss of 8.7 %, 6.5 % and 3.9 % were occurred in the temperature range of 25 - 300 °C for the manganese dioxide samples prepared via methods 1, 2 and 3, respectively. The physisorbed water was removed first at temperature <130 °C, whereas water of crystallization was lost in the temperature range of 130 - 300 °C for different samples. TG studies suggest that manganese dioxide prepared by method-1 has a higher physisorbed water content (6.0 %) than that of method-2 (3.3 %) and method-3 (1.2 %). But the water of crystallization for MnO_2 prepared by all the methods was quite comparable (Table 2.2). At >300 °C, MnO_2 decomposes to Mn_2O_3, as indicated from all the TG plots [102].

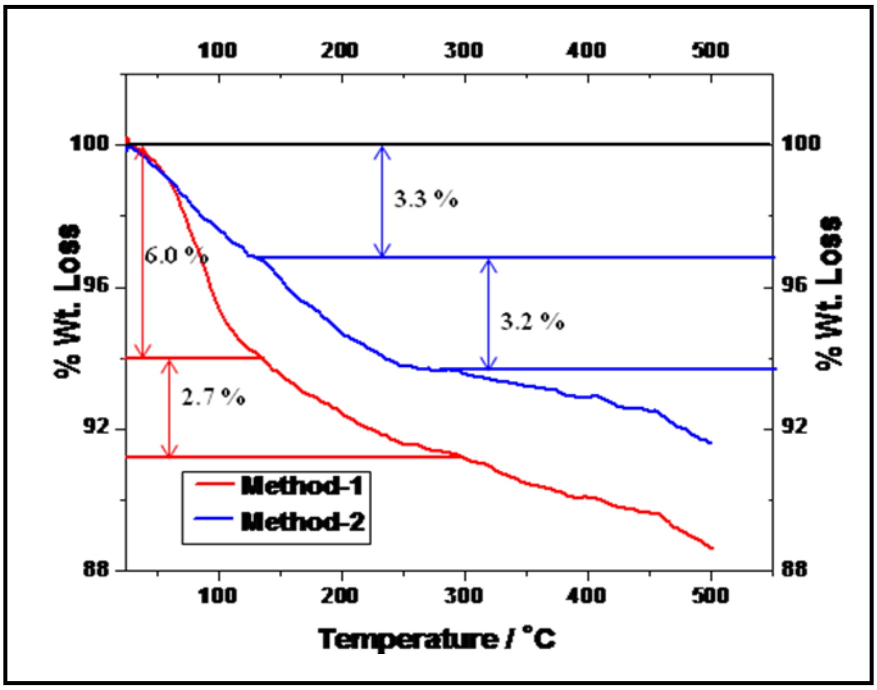

Figure 2.14: TG plots of MnO_2 samples prepared from method-1 (ramsdellite) and method-2 (α-MnO_2).

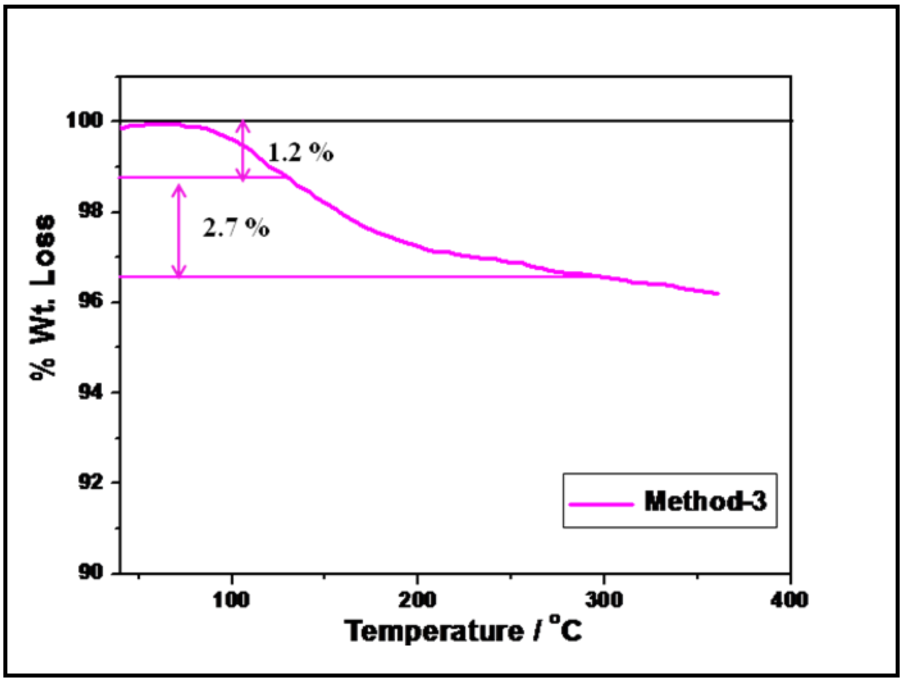

Figure 2.15: TG plot of MnO_2 (α-MnO_2) sample prepared from solid state mixing method.

Table 2.2: Characteristics of the synthesized manganese dioxide samples

Characterization techniques	**Method – 1**	**Method – 2**	**Method – 3**
XRD	Ramsdellite (1 X 2 tunnel)	α-MnO_2 (2 X 2 tunnel)	α-MnO_2 (2 X 2 tunnel)
Surface area ($m^2\ g^{-1}$)	77 ± 5	67 ± 5	131 ± 12
PZC (pH)	3.8 ± 0.4	3.9 ± 0.4	4.1 ± 0.3
TG (Water content, %)	6.0% (<130°C) 2.7% (<300°C)	3.3% (<130°C) 3.2% (<300°C)	1.2% (<130°C) 2.7% (<300°C)

2.7.5. Transmission electron microscopy (TEM) imaging

Transmission electron microscope (TEM) is an important technique used for high resolution imaging purposes. In broad sense, TEM is similar to normal microscope, but difference is that it uses electrons instead of light. Since electrons are used, the resolution is better compared to normal microscope that uses light for imaging. In TEM, a beam of electrons is transmitted through the sample. Due to the interactions of these electrons with the sample, an image is formed. The image thus formed is then magnified and transferred onto an imaging device, like a fluorescent screen, a photographic film, or a sensor such as scintillator attached to charge-coupled device (CCD). The lighter and darker areas in the image represent, the areas with maximum and minimum transmission of electrons respectively.

TEM measurement, (magnification: 50 k) carried out on MnO_2 prepared by solid state mixing method, showed that most of the MnO_2 particles were needle - shaped (100-200 nm) (Fig. 2.16).

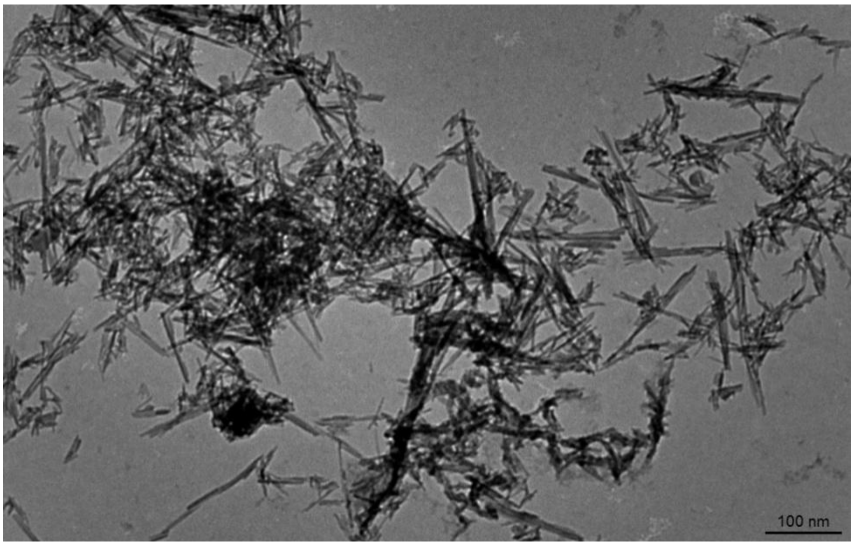

Figure 2.16: TEM image of MnO_2 prepared by solid state mixing method.

2.8. Characterization of modified sorbent

2.8.1. Fourier-transform infrared spectroscopy (FTIR) analysis

FTIR is a vital tool for identifying the functional groups in a molecule, by producing an absorption spectrum for various functional groups in the system that acts like a molecular "fingerprint". The instrumentation consists of an IR light source, an interferometer and a detector which collects the radiation that comes out of the sample. The sample absorbs the light with specific frequencies that are the characteristics of the sample spectrum. Detector records the change in energy with respect to time for all wavelengths/frequencies simultaneously. The Fourier transform function converts the intensity versus time spectrum into intensity versus frequency spectrum. Thus, the Fourier transform converts the detector output to an interpretable frequency spectrum that provides the structural insights of the sample.

FT-IR spectra of both the XAD-4 and MX-4 beads were measured using ATR-FTIR, Bruker, Model ALPHA-P instrument and are shown in Fig. 2.17. Infra red spectrum of the MX-4 resin indicated the presence of MnO_2 in the coated resin [103]. The MnO_2 characteristic bands, 567 and 630 cm^{-1}, corresponds to the Mn - O stretching vibrations.

The bands 1600 and 3368 cm^{-1} corresponds to the bending and stretching vibrations of -OH group in the adsorbed water.

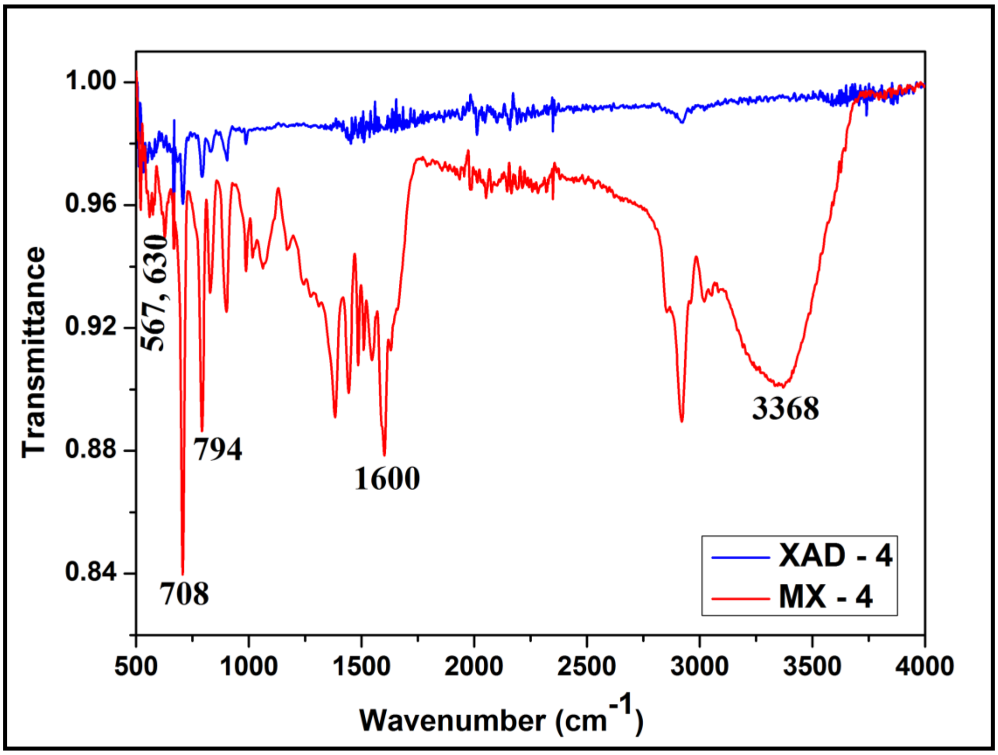

Figure 2.17: FTIR spectra of the XAD-4 beads and MnO_2 coated beads (MX-4).

2.8.2. Scanning electron microscopy (SEM) imaging

A scanning electron microscope (SEM) is an electron microscope that generates images of a material surface by scanning with a focused beam of electrons. This is a widely used technique to know the surface morphology as well as composition (semi quantitative) of the materials. In this technique secondary electron, emitted by the excited atoms upon bombardment of the accelerated electrons, are detected. Since the wavelength of electrons is much smaller than the wavelength of light, the resolution of SEM is much superior than that of a light microscope (better than 1 nm).

The surface morphology of the XAD-4 and MX-4 resin beads was studied by scanning electron microscopy (SEM) imaging. The images were taken by a TESCAN VEGA-3 SEM, having tungsten cathode. The samples were mounted using carbon tape. To prevent the charging of the surface, a 15 nm thick Au layer was sputter coated on to the sample surface. This coating helped in the improvement of the signal to noise ratio. SEM images of XAD-4 and MX-4 beads are shown in Fig. 2.18.

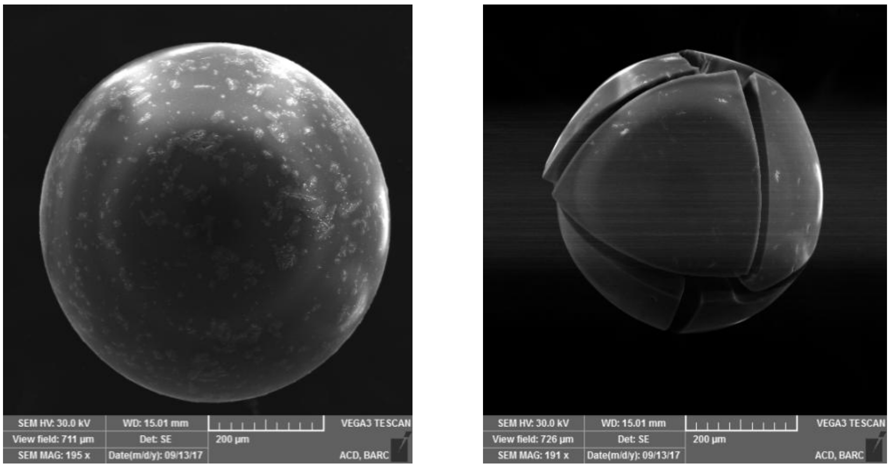

(a): XAD-4 (b): MX-4

Figure 2.18: SEM images of XAD-4 and MX-4 beads

Figure 2.18 (a) is the image of XAD-4 after sonication in DI water, whereas Figure 2.18 (b) is the coated bead. The images show the surface morphology of the beads, having spherical shape of almost the same diameter. The image of MX-4 beads has uniform layers of MnO_2 coating.

2.8.3. Neutron activation analysis (NAA)

Neutron activation analysis (NAA) is a nuclear analytical technique utilized for the quantification of analytes. In this technique, the sample is exposed to neutrons to produce radionuclides of the concerned elements and the radiations emitted by the radionuclides so formed are measured using suitable detectors for their quantification. The energy of radiation emitted is characteristic of the radioisotope formed whereas intensity of the radiation is proportional to the mass of the analyte. For the quantification of analyte in the sample, a matrix matched standard is also irradiated along with sample for a comparison.

Relative method of NAA was utilized for the quantification (equation 2.21).

$$\frac{A_{std}}{A_{sam}} = \frac{W_{std}}{W_{sam}} \quad (2.21)$$

Here A_{std} and A_{sam} are the activities (cps) of standard and sample, whereas, W_{std} and W_{sam} are the weight of the analyte in standard and sample, respectively.

The manganese concentration in the MX-4 resins was determined by NAA using a low flux AHWR critical facility (CF) reactor, BARC (irradiation time, t_i = 4 h). About 100 mg of samples were packed in cleaned polythene packets. The details of Mn nuclear data was given in Table 2.3. The Mn ICP Merck standard solution (1 g L^{-1}) was used as standard. The standard solution was evaporated on filter paper under IR lamp and sealed in polythene. These polythene packets were triply sealed and irradiated in CF reactor. After irradiation, the activity of ^{56}Mn ($t_{1/2}$= 2.58 h, Eγ = 846.76 and 1810.73 keV) was measured using an HPGe detector (Canberra), coupled to 8k channel analyzer having relative efficiency of 30 % and resolution of 1.9 keV at 1332 keV. The results obtained for manganese contents in the MX-4 beads (four independent batches) were given in Table 2.4. The average concentration of manganese dioxide was calculated to be (2.65 ± 0.21) %.

Table 2.3: Relevant nuclear data for ^{56}Mn radionuclide [104].

Natural abundance (%) of ^{55}Mn	**(n,γ) cross-section (barns)**	**Product**	**Mode of decay**	**Half-life (h)**	**γ-ray energy (keV)**	**γ-ray abundance (%)**
100	13.3	^{56}Mn	β^- (100 %)	2.58	846.76	98.9
					1810.73	26.9

Table 2.4: NAA results of MnO_2 content on MX-4 resin prepared in the present work.

Synthesis Batch	**MnO_2 (%)**
Batch - 1	2.67 ± 0.14
Batch - 2	2.73 ± 0.17
Batch - 3	2.47 ± 0.14
Batch - 4	2.71 ± 0.12

2.8.4. Point of zero charge (PZC) measurement

A pH drift method [105] was used for the PZC measurements of XAD-4 and MX-4 resins. In this method, 25 mL of 0.01 M NaCl solution was taken in number of 50 mL stoppered polypropylene bottles. The initial pH (pH_{ini}) values of the solutions in these bottles were adjusted from 1 to 12 with an interval of about 1, using 0.01 M HCl and 0.01 M NaOH. To these pH adjusted solutions, about 50 mg of XAD-4/MX-4 beads were added. After 48 h of agitation at 25 rpm, the suspensions were filtered and the final pH (pH_{fin}) filtrate solutions were measured. The pH_{fin} values were plotted against the respective pH_{ini} values. The PZC is the pH at which both the pH_{ini} and pH_{fin} are estimated to be the same. The PZC values for XAD-4 and MX-4 resins were thus estimated to be 7.6 ± 0.3 and 8.7 ± 0.2, respectively, as shown in Fig. 2.19.

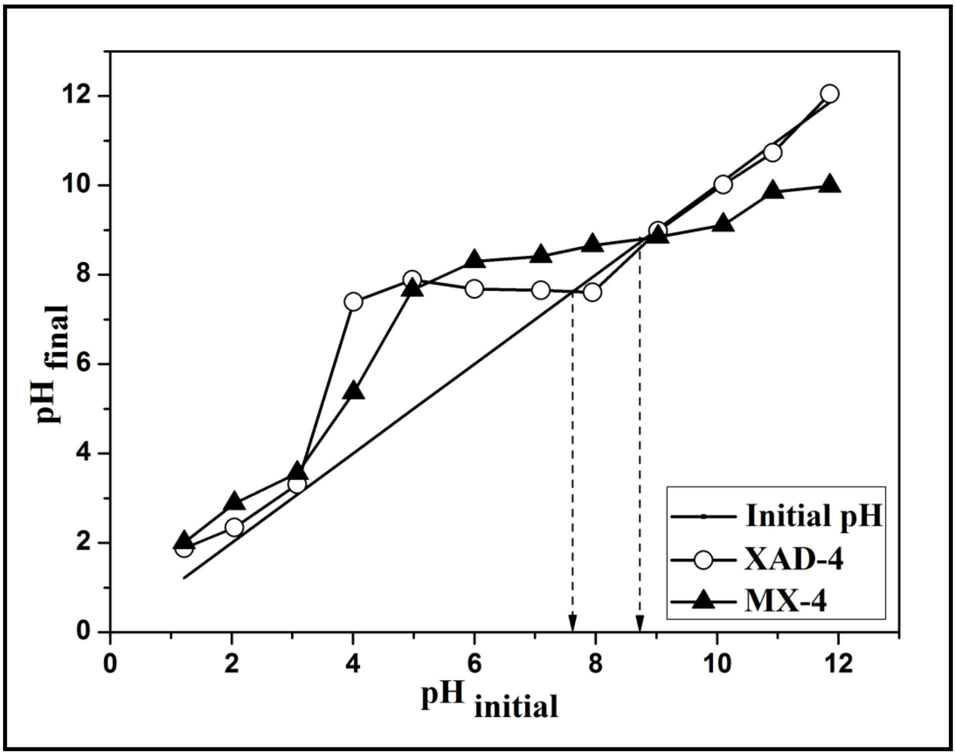

Figure 2.19: PZC plot of XAD-4 and MX-4 beads

2.9. Preparation of radiotracer solutions - As(III) and As(V)

All the studies were done using radioactive tracer solutions of arsenic (^{76}As). Arsenious oxide (As_2O_3) powder, about 1-2 mg was packed in clean polyethylene and irradiated in the pneumatic carrier facility (PCF), Dhruva reactor, BARC, Mumbai at a thermal neutron flux of ~ 10^{13} cm^{-2} s^{-1}. The irradiation time was 1 min. The nuclear data of arsenic are given in Table 2.4.

Table 2.5: Relevant nuclear data for ^{76}As radionuclide [104].

Natural abundance (%) of ^{75}As	**(n,γ) cross-section (barns)**	**Product**	**Mode of decay**	**Half-life (h)**	**γ-ray energy (keV)**	**γ-ray abundance (%)**
100	4.5	^{76}As	β^- (100 %)	26.24	559.10	45.0
					657.05	6.2

For the preparation of As(III) tracer solution, the irradiated powder was dissolved directly in 0.1 M NaOH solution. The As(V) tracer solution was prepared by dissolving the irradiated As_2O_3 in concentrated HNO_3 followed by heating. The required concentration of 2 mg L^{-1} solution was made by diluting with DI water. The scheme for preparation of the tracer solutions are given in Fig. 2.20. The oxidation state of arsenic in the radiotracer solution was confirmed by solvent extraction method using benzene as the extractant [106].

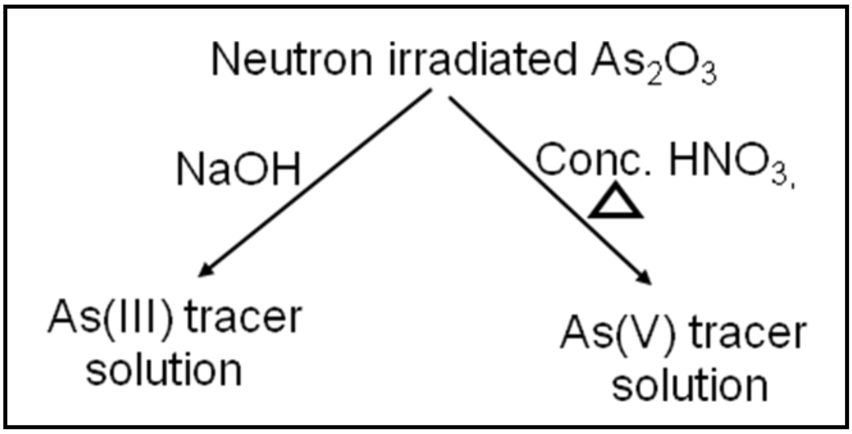

Figure 2.20: Scheme for preparation of arsenic radiotracer solution.

2.10. Solvent extraction method: Determination of oxidation state of arsenic in radiotracer solution

1 mL of the above prepared radiotracer solutions were taken in separate glass beakers and carefully evaporated to near dryness by heating on hot plate. About 10 mL of concentrated HCl was added to each beaker and heated to get clear solution. The solution was taken in a stoppered glass tube sealed with parafilm and the initial count rate of ^{76}As (C_{ini}) ($t_{1/2}$ - 26.24 h, $E\gamma$ - 559.10 & 657.05 keV) was measured using HPGe detector. Then 10 mL of benzene, pre-equilibrated with concentrated HCl was added and equilibrated for 10 min in a separating funnel. Both the phases were allowed to separate. The final count rate of ^{76}As in the HCl phase was measured using HPGe (C_{fin}) and compared with the initial count rate of ^{76}As. The percentage of As(V) was determined by equation 2.22. The

detailed scheme is given in Fig. 2.21. The solvent extraction method using benzene as a solvent for the separation of As(III) and As(V) species is well reported in the literature [106]. This method was utilized for the determination of oxidation state of arsenic species before as well as after the sorption also. As given in the literature, the As(III) forms neutral $AsCl_3$ in strong HCl medium. These neutral species are easily extracted into the non-polar solvent benzene, whereas As(V), which forms negatively charged species, is not extracted [106].

$$As(V)\ (\%) = \frac{C_{fin}}{C_{ini}} \times 100 \qquad (2.22)$$

Where, C_{ini} and C_{fin} represent the initial and final count rates of ^{76}As in the solutions, respectively.

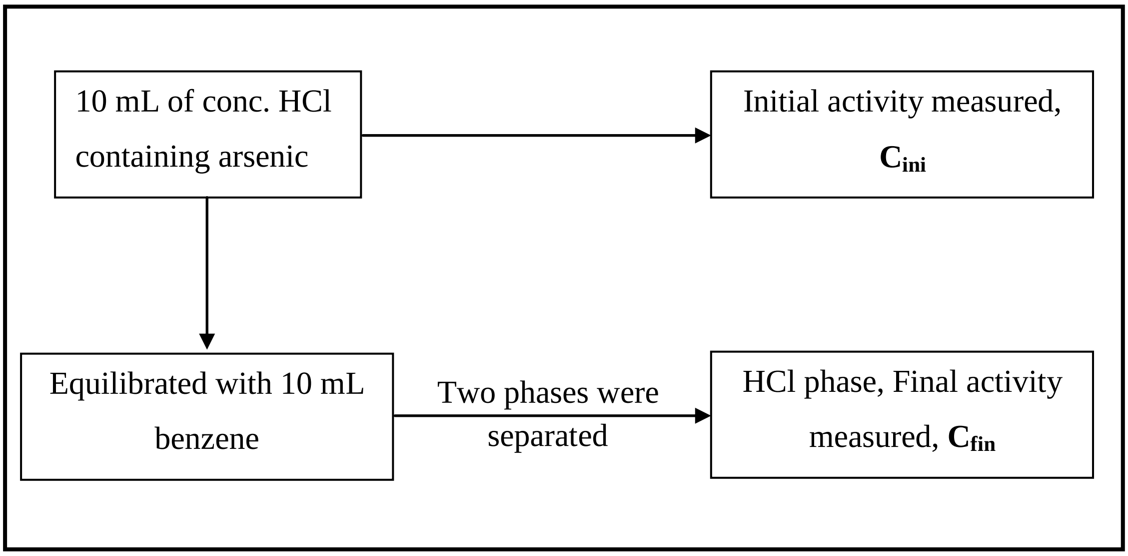

Figure 2.21: Scheme of solvent extraction method for separation of As(III) and As(V) from solution.

Chapter - III

Arsenic uptake on iron oxides

3.1. Introduction

Arsenic contamination in groundwater is a major problem in the world. Among the various methods, which could be applied for the removal of arsenic, adsorption plays an important role. Adsorption is considered to be a superior technique due to the high arsenic removal efficiency and ease of operation. The review literatures related to arsenic removal give an overall picture of the adsorption procedures utilizing charcoal, sand, zeolites, polymeric materials and naturally occurring metal oxides/hydroxides as the adsorbents [107-111].

The natural iron oxides/hydroxides play an important role in the mobilization of arsenic in water by adsorption on to the surfaces of these materials in natural environments [6, 9, 25, 112]. The same mechanism can suitably be applied for the removal of arsenic from groundwater also. In this context, many literatures are available which reported iron oxide as one of the promising sorbent for total arsenic removal [53-55, 113-114] due to the strong adsorption properties. But when the adsorption mechanism of As(III) and As(V) on iron oxides are considered, the literature on the differential adsorption mechanisms are scanty [59-60, 115].

Thus a detailed study comprising of the different parameters like, the effect of pH, adsorbent dose, regeneration method and the elucidation of interaction mechanism of arsenic with different iron oxides is not available in the literature. This chapter elaborates the study of all the necessary parameters like pH, kinetics, capacity, leaching study, interference from co-occurring ions, regeneration and reusability, which affects the sorption of arsenic using different iron oxides, viz. goethite, hematite and magnetite as sorbents [83]. Present chapter also focuses on the mechanistic study of arsenic - iron oxide interaction using appropriate analytical techniques.

3.2. Materials and methods

3.2.1. Reagents and chemicals

The chemicals used for the studies are of analytical reagent (AR) grade and used without further purification. The inorganic salts like, ferric nitrate [$Fe(NO_3)_3\cdot 9H_2O$; molecular weight (MW) - 404.00 g mol^{-1}], ammonium ferric sulphate [Mohr's salt; $(NH_4)_2SO_4.FeSO_4.6H_2O$; MW - 392.13 g mol^{-1}], ferric chloride [$FeCl_3.6H_2O$; MW - 270.30 g mol^{-1}], arsenic trioxide [As_2O_3; MW - 197.84 g mol^{-1}], arsenic pentoxide [As_2O_5; MW - 229.84 g mol^{-1}], sodium chloride [NaCl; MW - 58.44 g mol^{-1}], calcium chloride [$CaCl_2$; MW - 110.98 g mol^{-1}], magnesium chloride [$MgCl_2$; MW - 95.21 g mol^{-1}], sodium bicarbonate [$NaHCO_3$; MW - 84.01 g mol^{-1}] and sodium dihydrogen phosphate [NaH_2PO_4; MW - 119.98 g mol^{-1}] were used during this work. The AR grade reagents used are concentrated hydrochloric acid (HCl), concentrated nitric acid (HNO_3), ammonia solution (NH_4OH) and dilute sodium hydroxide (NaOH). All the necessary dilutions and dissolution of salts were done using deionised (DI) water (resistivity 18.2 MΩ cm^{-1} and total organic carbon < 10 μg L^{-1}) from Milli-Q water purification system.

3.2.2. Equipments

All the weighing was done using a high precision analytical semimicro balance (Mettler - Toledo, dual range, readability - 0.01 mg). pH measurements were carried out in Oakton pH meter employing glass electrode (pH700, USA), with digital display having precision of ± 0.01 unit. A mechanical shaker was utilized for the equilibrations at room temperature. Radioactivity measurements were done using a high purity germanium detector (HPGe) (Canberra, Australia, relative efficiency: 30 %, resolution: 1.9 keV at 1332 keV) coupled to 8k channel analyzer. The characterization of the sorbents were done using X-ray diffraction (XRD), surface area, point of zero charge (PZC) and particle size measurements (Section 2.6).

3.2.2.1. Inductively coupled plasma-optical emission spectrometric (ICPOES) measurement

Inductively coupled plasma optical emission spectrometry (ICPOES) is one of the versatile spectroscopic techniques for determination of trace elements in various matrices. In ICPOES, the sample solution is aspirated into the plasma. The high temperature of the plasma (~10000 K) causes dissociation of the sample into atoms and ions, and excites them to higher energy levels. The excited atoms/ions de-excite through thermal or radiative (emission) transitions to the lower energy states. The light emitted in the radiative transition corresponds to specific wavelengths, characteristics to the analytes, which are measured using suitable detectors (PMT/CCD). In these cases, the emission intensity is proportional to the concerned analyte concentration. For quantification of the analyte, initially standards of known concentration are passed and the corresponding intensities are measured and these data are used to obtain a calibration plot. Then the sample is passed to get the intensity for the analyte of interest and accordingly the concentration of analyte is calculated from the calibration plot. This technique is very advantageous due to its multi element capability, sensitivity and high sample throughput.

3.2.2.2. Inductively coupled plasma mass spectrometric (ICPMS) measurement

ICPMS is a highly sensitive technique, used for the quantification of elements at trace or ultra-trace levels. The plasma provides very high temperature so that the elements present in the sample gets ionized. The ions are extracted in to quadrupole mass analyzer. The ions get sorted out depending on the mass to charge ratio and detected using electron multiplier tube detector. Observed signal is proportional to the concentration of the element present in the sample. Similar to ICPOES, in ICPMS also the concentration of the element in a sample is calculated through construction of a calibration plot, using single or multi-element reference standards.

3.3. Experimental

3.3.1. Preparation of iron oxides

The iron oxides, viz., goethite (α-FeOOH), hematite (α-Fe_2O_3) and magnetite (Fe_3O_4), were synthesized following the literature reports [87-89] and the details are elaborated in Chapter 2, Section 2.3.1. Briefly, NaOH solution (2.5 M) was added dropwise to 1 M ferric nitrate solution, resulting in the formation of ferrihydrite. This is the base material for the preparation of goethite and hematite. For goethite preparation, the suspension was heated on a hot plate for 2 h at 90 ^{o}C and subsequently, for the complete conversion of hydroxides to oxides, the precipitate was heated in a oven at 100 ^{o}C for 12 h. For preparation of hematite, the ferrihydrite suspension was stirred for 2 h at room temperature, followed by heating at 300 ^{o}C for 36 h in a muffle furnace. The magnetite was prepared by mixing of ammonium ferrous sulphate and ferric nitrate solutions and adding ammonia solution dropwise till solution becomes alkaline. The resulting suspension was heated on a hot plate at 80 ^{o}C for 2 h. All the iron oxides prepared were washed with DI water till they become neutral which was then followed by air-drying. For further use these dried iron oxides were stored in air tight polypropylene containers. These synthesized sorbents were characterized using X-ray diffraction (XRD), surface area, point of zero charge (PZC) and particle size measurements. The details of these measurements have been discussed in the earlier chapter, Section 2.6.

3.3.2. Sorption studies of arsenic by iron oxides

Three iron oxides e.g. (1) goethite (2) hematite and (3) magnetite, synthesized as mentioned in Section 2.3 were used during the present study. The sorption experiments were carried out in batch equilibration mode at room temperature using ^{76}As radiotracer technique. The tracer solutions were prepared following the procedure given in Section 2.9. The oxidation state of the arsenic in the prepared solution was confirmed by solvent extraction procedure (Section 2.10). The As(III) and As(V) sorption studies were done separately using ^{76}As radiotracer ($t_{1/2}$ = 26.4 h, E_γ = 559 and 657 keV) solutions (2 mg L^{-1}) taken in 50 mL stoppered glass bottles. The pH was adjusted to 3 - 11, using 0.1 M HCl and 0.1 M NaOH solutions. The initial count rate (C_{ini}) in the solutions was measured using high purity germanium (HPGe) detector. These solutions were equilibrated with ~ 0.1 g of sorbent for the optimized time, i.e., 2 h at 100 rotations per minute (rpm) in a mechanical shaker. After equilibration, the suspensions were centrifuged and filtered using Whatman 42 filter papers. The final count rate of ^{76}As in the supernatant (C_{fin}), was measured. The sorption of arsenic (%) was calculated using equation 3.1.

$$Sorption\ of\ arsenic\ (\%) = \frac{(C_{ini} - C_{fin})}{C_{ini}} \times 100 \qquad (3.1)$$

Where, C_{ini} and C_{fin} represent the initial and final count rate (counts per second, cps) of ^{76}As in solutions.

For the confirmation that the oxidation states of arsenic in solutions were not changed during equilibrations, an independent set of arsenic tracer solutions [2 mg L^{-1} As(III)/As(V); pH 3 - 11] was kept for 2 h equilibration, without addition of sorbent. The oxidation state of arsenic in these solutions was determined prior to experiments, by solvent extraction studies (Section 2.10).

3.3.3. Kinetic studies for arsenic sorption by iron oxides

The kinetic studies for arsenic sorption were performed on all the three synthesized iron oxides. The method adopted was similar to that explained in Section 3.3.2. All the experiments were done at pH 7 and the time of equilibration was varied from 30 min to 24 h. The percentage sorption of arsenic was evaluated using equation 3.1.

3.3.4. Isotherm studies for arsenic sorption by iron oxides

For the adsorption isotherm, the method adopted was similar as mentioned in Section 3.3.2. The studies were done at neutral pH and arsenic concentrations were varied from 2 to 400 mg L^{-1}. The arsenic in solutions was taken as a combination of fixed concentration of radioactive arsenic (2 mg L^{-1}) plus varying amounts of inactive arsenic. The tracer solutions and inactive arsenic was mixed thoroughly to maintain homogeneity. The count rates of arsenic were measured, before and after equilibration with the sorbents, and the percentage sorption was calculated using equation 3.1.

3.3.5. Leaching studies on iron oxides

Release of iron during arsenic sorption was studied for all the three iron oxides. In this context, three independent sets of experiments were done at pH 7. (i) 100 mg of each iron oxides was added to different stoppered flasks and equilibrated in 25 mL of DI water for 2 h, (ii) 100 mg of iron oxides were added to separate flasks having 2 mg L^{-1} inactive As(III) solution at pH 7 and shaken for 2 h and (iii) the above experiment was repeated with 2 mg L^{-1} inactive As(V) solution. After the equilibration, the sorbents were filtered using Whatman 42 filter paper and the iron concentrations were analyzed using ICPOES technique following the procedure below.

The aqueous solutions were analyzed for Fe using an ICPOES (JobinVyon, Model ACTIVA-500) equipped with a photo multiplier tube (PMT) as a detector. The parameters used for measurement are given in Table 3.1. The standards were prepared by using Fe Merck ICP standard solution (1 g L^{-1}). Working standards were prepared by serial dilutions of the 1 g L^{-1} stock solution of Fe. The standards were maintained in 2 % HNO_3 medium to prevent hydrolysis. The calibration of the instrument was done using the standards of Fe concentrations 1 - 10 mg L^{-1}. 2 % HNO_3 solution was taken as calibration blank. The Fe contents in the experimental solutions were then quantified using the calibration plot.

Table 3.1: Instrumental parameters for iron determination by ICP-OES.

Parameter	**Value**
Power reference (RF) incident power (kW)	1.0
Plasma argon flow rate (L min^{-1})	12
Sheath argon flow rate (L min^{-1})	0.2
Nebulizer argon flow rate (L min^{-1})	0.9
Pump (mL min^{-1})	1.00
Mist chamber	Glass cyclone spray chamber
Nebulizer	Concentric glass nebuliser
Wavelength of Fe (nm)	259.94

3.3.6. Regeneration studies on iron oxides

For regeneration studies, different concentrations of NaOH solutions, 0.1 M, 0.5 M and 1 M, were used. The arsenic sorption was done on three iron oxides following the procedure given in Section 3.3.2. The arsenic sorbed sorbents were separated from the suspensions by centrifugation. The count rates of ^{76}As on the sorbent were measured, C_{ini}. For desorption of arsenic, the sorbents were equilibrated with NaOH solutions for time 30 min - 4 h. After the equilibration, the suspensions were centrifuged and the separated sorbent was again measured for the ^{76}As count rate, C_{fin}. The counts were substituted in equation 3.1 and the results obtained were for the percentage of regeneration achieved.

3.3.7. Reusability studies on iron oxides

To study the potential of iron oxides as sorbent for arsenic removal, the reusability study is important. The iron oxides once used for arsenic sorption were reused, without regeneration, upto 5 cycles for arsenic uptake from fresh solutions (Section 3.3.2) without any significant reduction in sorption efficiency.

3.3.8. Effect of common ions on arsenic sorption by iron oxides

The effect of presence of common ions in ground water, like Na^+, Ca^{2+}, Mg^{2+}, Cl^-, HCO_3^- and PO_4^{3-}, on the arsenic sorption properties of the studied iron oxide sorbents are also investigated in the present work. The sorption experiments were done as per the procedure given in Section 3.3.2, on the solutions containing the concentrations of ions in the range of 5 - 5000 mg L^{-1}. The solutions were at neutral pH, with time of equilibration as 2 h.

3.3.9. Application of iron oxides to arsenic contaminated groundwater

Two arsenic contaminated groundwater, collected from tube wells of North 24 Parganas district, West Bengal, India, are investigated to understand the applications of iron oxides to arsenic contaminated groundwater. The arsenic sorption experiments were done without any pre-treatment. 25 mL of groundwater was equilibrated with 0.1 g each of synthesized iron oxides. The equilibration time was kept as 2 h at 100 rpm. After sorption, the sorbents were separated by filtration. The solutions, before and after sorption, were analyzed using ICPMS (Model VG PQ ExCell, VG Elemental, UK) for arsenic concentration.

3.3.10. Study of arsenic sorption mechanism on iron oxides

3.3.10.1. X-ray photoelectron spectroscopy (XPS) measurements

For XPS, the sample pellets were made as follows:

(1) About 100 mg of each iron oxide (goethite, hematite and magnetite) was equilibrated with 25 mL of DI water for 2 h. The sorbents were filtered, air dried and made pellets of 10 mm diameter using hydraulic press by applying 7 tonne pressure. These were the blank pellets.

(2) About 100 mg of sorbents were equilibrated with 25 mL of 2 mg L^{-1} As(III) solutions at pH 7 for 2 h. The pellets were made after air drying. These were the As(III) sorbed iron oxide pellets.

(3) The above method was repeated by using As(V) solution. The pellets so made were the As(V) sorbed iron oxide pellets.

(4) For preparation of As(III) and As(V) standards, pellets of As_2O_3 and As_2O_5 salts were prepared.

The XPS measurements were performed using Mg-K_α (1253.6 eV) X-ray source and DESA-150 electron analyzer (M/s. Staib Instruments, Germany) as detector. The sample was placed on double sided carbon tape for analysis. The binding energy scale was calibrated using Au-$4f_{7/2}$ peak (83.95 eV) as an internal reference. The peak fitting was done using XPSPEAK41 software. The binding energies obtained for the sorbents were matched with the binding energies of the standards stored in the XPS library. The area under the peak was determined by the least-squares fitting of the Gaussian line shape.

3.3.10.2. Electrochemical studies

Electrochemical methods are nowadays been widely applied for qualitative and quantitative determinations, due to the fast analysis and portability. There is report on the arsenic determination by electrochemical technique by using electrodes with necessary modifications [116]. To elucidate the mechanism of interaction of iron oxide with As(III)/As(V), an electrochemical investigation was carried out. Electrochemical measurements were conducted using the potentiostat/galvanostat (CHI 760E; from CH Instruments) with three electrode system. A modified glassy carbon electrode (GCE), standard calomel electrode (SCE) and platinum (Pt) electrode were adopted as working, reference and counter electrodes, respectively. The experiments were done at room temperature and in inert atmosphere. For the experiments, the GCE was modified following the procedure below: GCE surface was cleaned by rubbing with 1 μm alumina powder, followed by sonication for 10 min. An iron oxide suspension was made by sonicating 10 mg iron oxide in 1 mL of DI water containing 0.05 % nafion solution, for

15 minutes. This helps in achieving homogeneity of the solution. GCE modification was done by drop-casting 10 µL of the solution onto the GCE surface and air-drying. The modified GCE was used in the solutions of pH 7. The supporting electrolyte used was 0.5 M KNO_3. The cyclic voltammetry (CV) and differential pulse voltammetry (DPV) experiments were carried out using the modified GCE.

3.4. Results and discussion

3.4.1. Sorption studies of arsenic by iron oxides

For sorption studies, the arsenic concentration was fixed as 2 mg L^{-1}, based on the arsenic concentration reported [6] from arsenic contaminated region in India. For sorption studies, pH range chosen was 3 - 11. pH < 3 was avoided, due to the high solubility of iron oxide at acidic pH.

In Figs. 3.1 and 3.2, the sorption plots, for As(III) and As(V) on three iron oxides, show almost quantitative sorption by all the three sorbents up to pH 9. For goethite and magnetite, higher sorptions were observed at alkaline pH also, but for hematite, the sorption decreases in alkaline pH. The sorption on these iron oxides can be explained using the PZC values of the iron oxides. From the arsenic speciation plot given in Figs. 1.4 and 1.5, the As(III) exists as neutral species ($H_3AsO_3^0$) upto pH 9 whereas for As(V) the species in this pH is mostly negatively charged ($H_2AsO_4^-$, $HAsO_4^{2-}$) [54]. The –OH group present on the sorbent surface undergoes exchange/ionization depending on the pH, resulting in a surface charge on the sorbent. Thus complex formation happens between the –OH group on the sorbent surface as well as the –OH group on the arsenic species (the structure of both the arsenic oxyhydroxide species are given in Fig. 1.2). At pH < PZC, the surface of the sorbents are positive, thus a clear electrostatic interaction, in addition to complexation plays a vital role in sorption.

For pH > PZC, i.e. at alkaline pH, the surface of the sorbents are negatively charged due to the deprotonation of the surface –OH groups. The arsenic compounds also exist as the negatively charged species under these pH conditions. Therefore, due to the electrostatic repulsive force, the sorption efficiency decreased for hematite at the alkaline pH conditions. But the same consideration of pH > PZC cannot explain the high sorption of arsenic on magnetite and goethite at pH >9. According to Guo et al [73], efficient arsenic removal by magnetite and goethite at higher pH involves a complex mechanism of electrostatic as well as complex formation. The results obtained in the present study are also in accordance with the mechanism suggested in the literature.

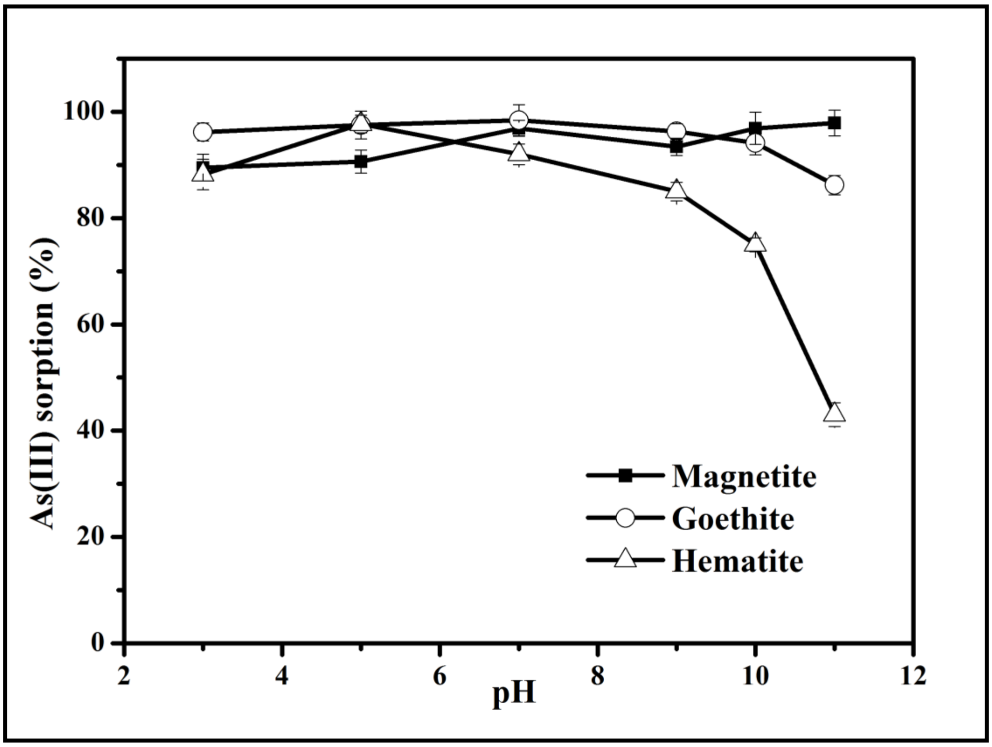

Figure 3.1: Sorption plot of As(III) on different iron oxide sorbents.

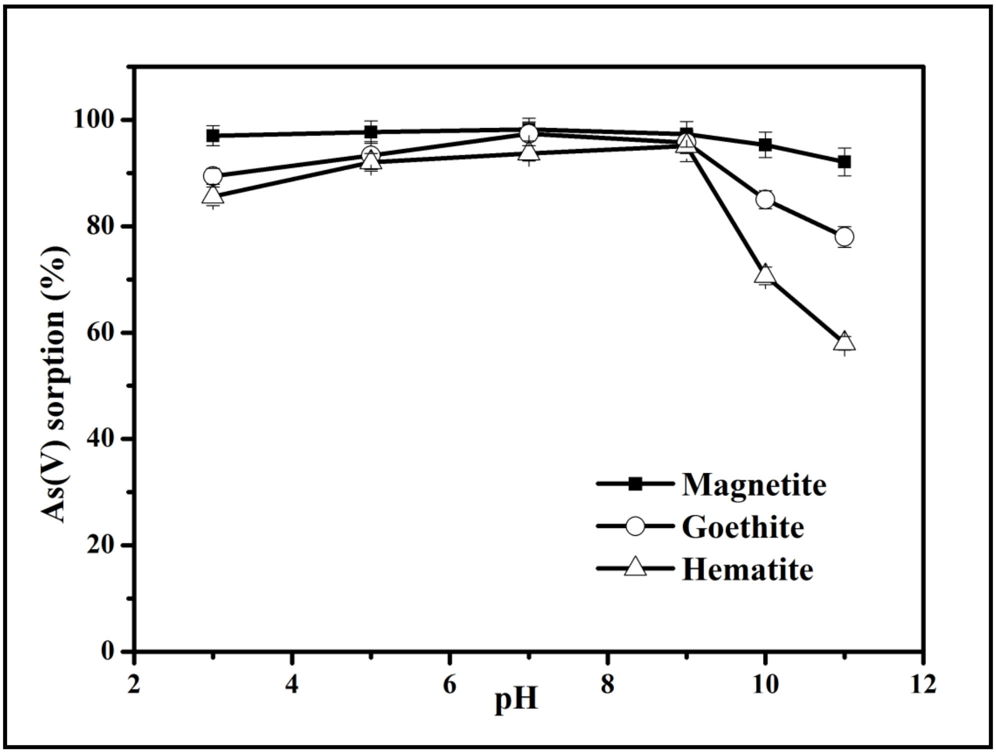

Figure 3.2: Sorption plot of As(V) on different iron oxide sorbents.

In the present context, it was essential to follow the oxidation state of arsenic during the course of sorption process. For this, the solvent extraction procedure was adopted. Details of the procedure are given in Section 2.10. Solvent extraction study was done on the arsenic solutions after equilibrating the same without iron oxide sorbents. The activity of ^{76}As in the case of As(III) experiment remained solely in the organic phase, whereas activity was observed quantitatively in the aqueous HCl phase in the case of As(V) experiment. The results confirmed that the oxidation state of arsenic in the tracer solutions was not changing during the equilibration time (2 h).

3.4.2. Kinetic studies for arsenic sorption by iron oxides

The kinetic studies for sorption of As(III) and As(V) on the three iron oxides at neutral pH are plotted in Fig. 3.3 and 3.4, respectively. From the plots, it is observed that the sorption is faster for goethite and slower in the case of hematite. Thus, kinetics for arsenic sorption on iron oxides followed the order: goethite > magnetite > hematite. The pattern remained exactly the same for both As(III) and As(V) uptake. For goethite, sorption was >98 % in 2 h, but for magnetite and hematite it was about 90 % and about 78 %, respectively, for the same time of equilibration. On further increase in the time of equilibration, only marginal increase in sorption was observed. As a result, the time of equilibration in all the other experiments using iron oxides was fixed to be 2 h.

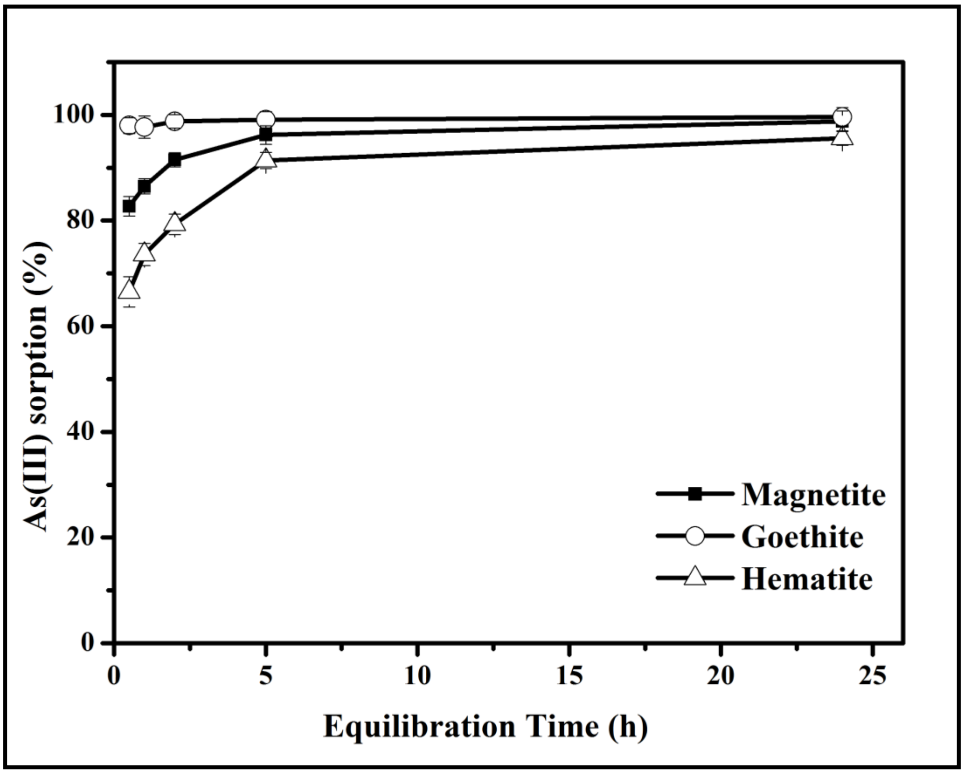

Figure 3.3: Kinetic plots for As(III) sorption on different iron oxides.

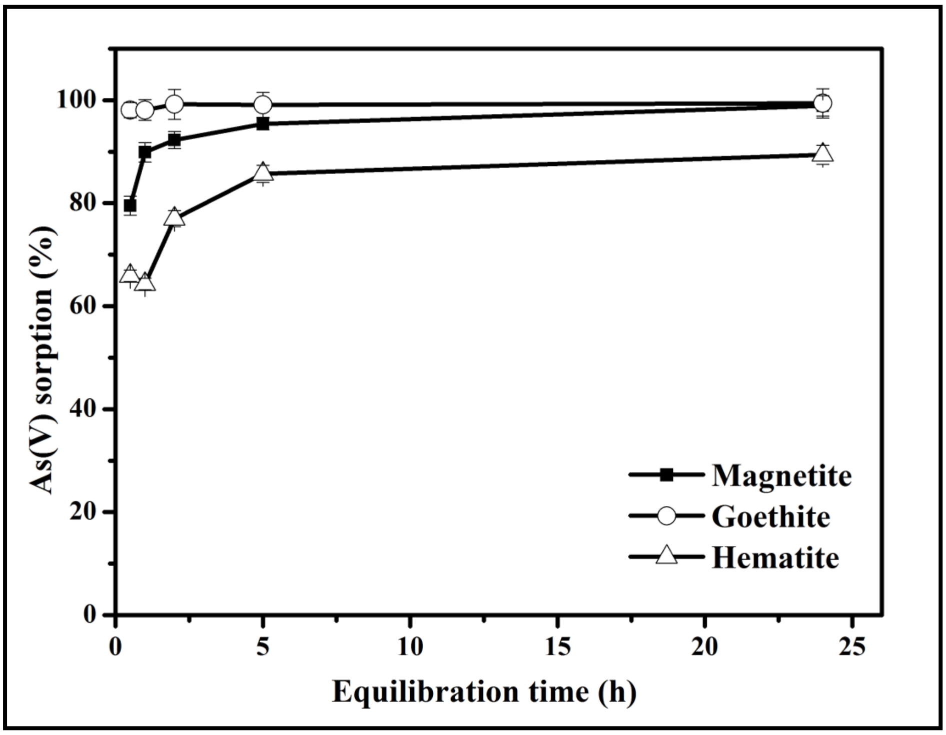

Figure 3.4: Kinetic plots for As(V) sorption on different iron oxides.

For the investigation of sorption mechanism, study of kinetics is important. The kinetics experimental data were evaluated by both pseudo first order (PFO) and pseudo second order (PSO) kinetic models [113]. The linearized equations for PFO and PSO are given in equations 3.2 and 3.3 respectively.

$$\log(Q_e - Q_t) = \log(Q_e) - \frac{k_1 t}{2.303} \qquad (3.2)$$

$$\frac{t}{Q_t} = \frac{1}{h} + \frac{t}{Q_e} \qquad (3.3)$$

Where Q_t and Q_e represents the amount of arsenic adsorbed per gram of the iron oxide at time, t and at equilibrium (mg g^{-1}) respectively, k_1 = rate constant for PFO reaction, ‘h’ represents the rate constant for PSO reaction, ie., $h = k_2 Q_e^2$, and k_2 = the rate constant for PSO reaction.

For all three iron oxides, the data fitted well with pseudo second order (PSO) kinetic equation, given in equation 3.3. This infers that chemisorption is the predominant mechanism of sorption of As(III) and As(V) on iron oxide sorbent. The plots are given in Figs. 3.5 - 3.7. The kinetic parameters obtained from the plots are listed in Table 3.2.

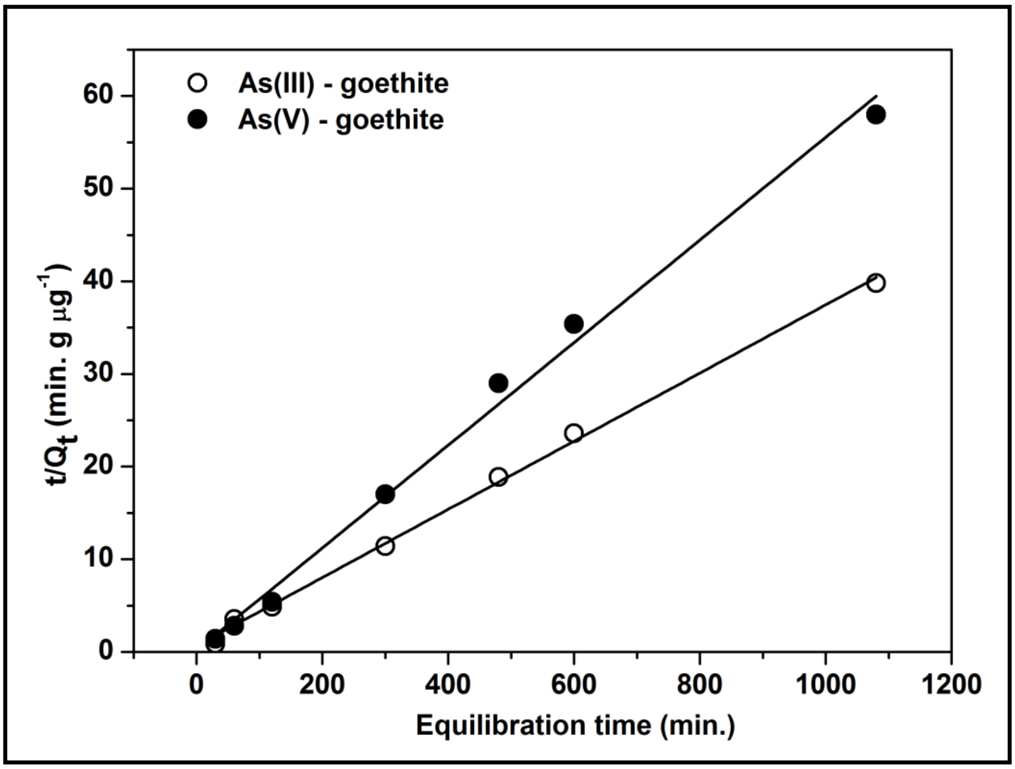

Figure 3.5: Pseudo second order kinetic plot for sorption of As(III) and As(V) on goethite. (Circles are the experimental data and the straight lines are the linear fits following equation 3.3).

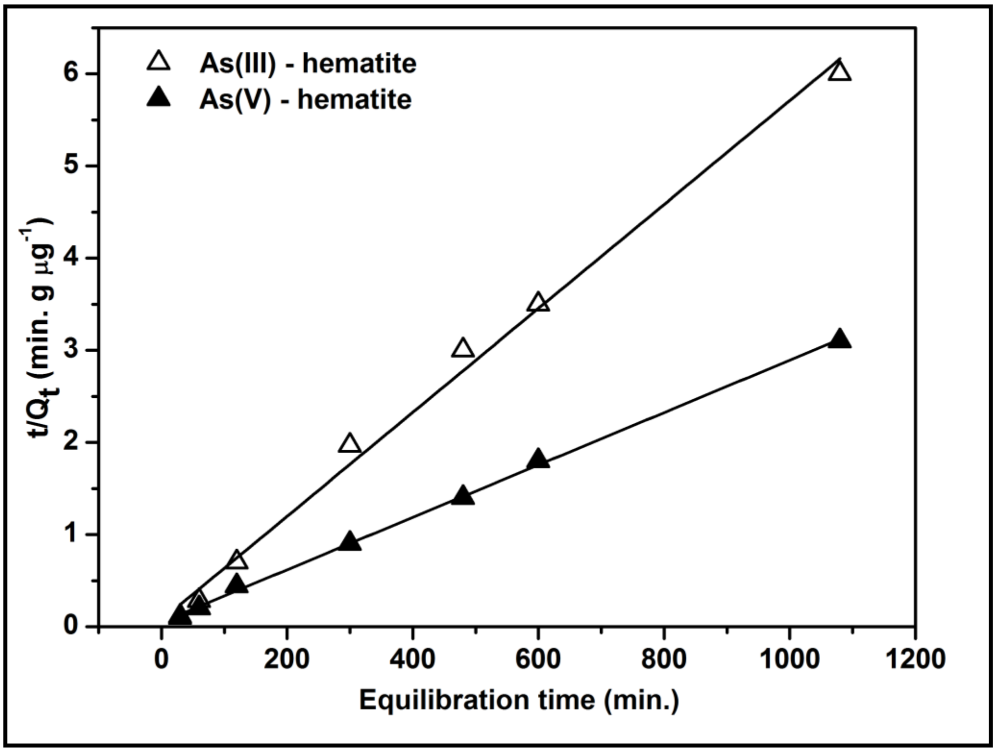

Figure 3.6: Pseudo second order kinetic plot for sorption of As(III) and As(V) on hematite. (Triangles are the experimental data and the straight lines are the linear fits following equation 3.3).

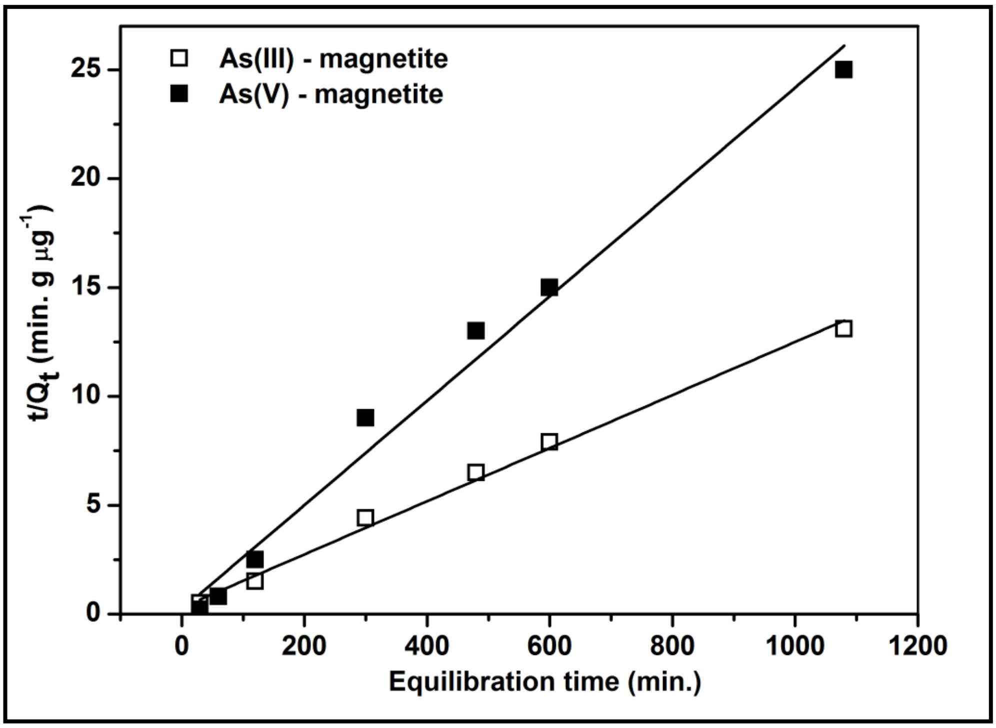

Figure 3.7: Pseudo second order kinetic plot for sorption of As(III) and As(V) on magnetite. (Squares are the experimental data and the straight lines are the linear fits following equation 3.3).

Table 3.2: Kinetic fitting parameters for PSO reaction for As(III) and As(V) adsorption by iron oxide sorbents

Sorbent	**Arsenic species**	**Q_e (calculated) mg g^{-1}**	**K_2**	**R^2**
Goethite	As(III)	0.027	9.2×10^{-4}	0.997
	As(V)	0.018	5.0×10^{-4}	0.993
Hematite	As(III)	0.177	2.2×10^{-6}	0.993
	As(V)	0.352	4.0×10^{-7}	0.999
Magnetite	As(III)	0.082	4.5×10^{-5}	0.994
	As(V)	0.042	1.2×10^{-4}	0.983

3.4.3. Isotherm studies for arsenic sorption by iron oxides

For environmental applications, Langmuir and Freundlich isotherms are commonly used for describing sorption equilibrium [117]. The adsorption isotherms for arsenic uptake by iron oxides followed the Freundlich adsorption isotherm [Figs. 3.8 - 3.10]. These results thus suggest a multilayer sorption of arsenic on the heterogeneous surface sites of iron oxides [118].

Freundlich isotherm is represented by the following equation:

$$Q_e = K_f \, C_e^{\frac{1}{n}} \tag{3.4}$$

Where K_f = Freundlich constant related to adsorption capacity (mg g^{-1}), n = Freundlich constant related to adsorption intensity, C_e =the equilibrium arsenic concentration (mg L^{-1}) and Q_e=the amount of arsenic adsorbed per gram of the iron oxide at equilibrium (mg g^{-1}).

The above equation 3.4, can be written in the linearized form as,

$$\ln Q_e = \ln K_f + \frac{1}{n} \ln C_e \tag{3.5}$$

Observed fitting of the experimental data following equation 3.5 are shown in Figs. 3.8 - 3.10 and the fitting parameters thus obtained are listed in Table 3.3. From the Table 3.3, we observe that n > 1 in all the cases, which indicate that (1) all the three iron oxides are having large heterogeneity and (2) the sorption of arsenic by iron oxides is a favorable process [119].

The Freundlich adsorption capacities (K_f) as listed in Table 3.3 suggest that, the adsorption capacity for goethite is the highest among the three iron oxide sorbents. The arsenic sorption capacity obtained is in the order, goethite > magnetite > hematite. This order is similar to the order obtained following the kinetics of the sorption process. For goethite and magnetite, we found that the capacity for As(V) uptake is double than that for As(III). This is presumably due to two different sorption mechanisms involved for the uptake of As(III) and As(V) by the iron oxide sorbents.

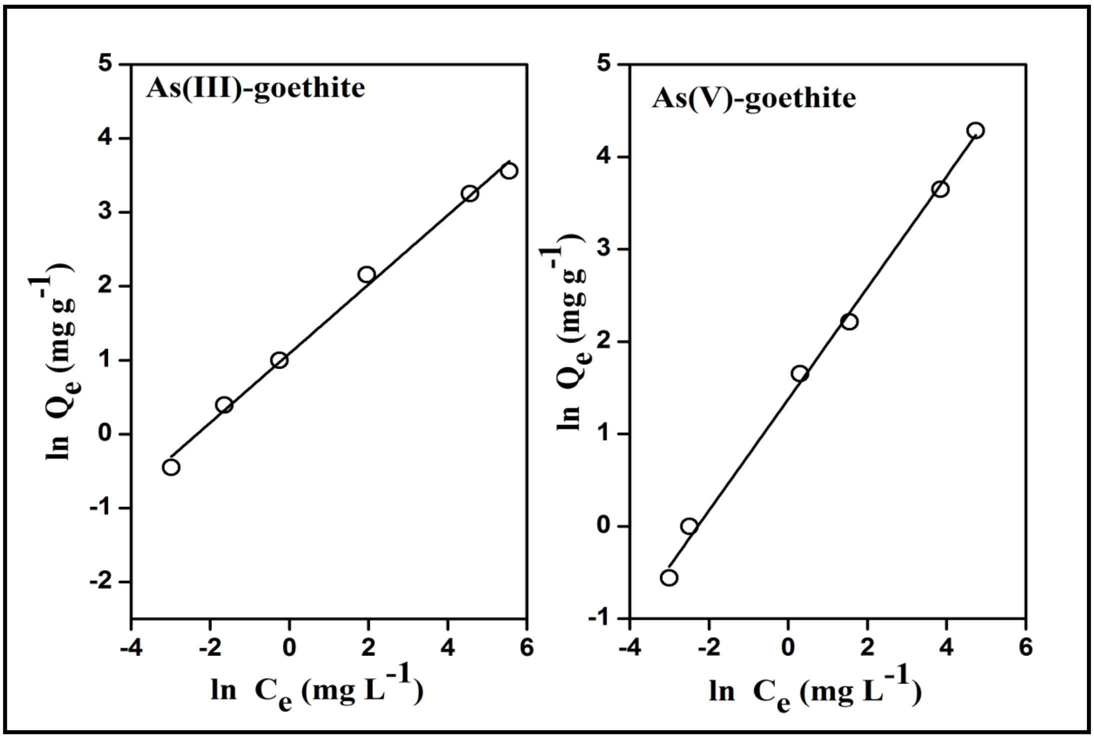

Figure 3.8: Freundlich isotherm for sorption of As(III) and As(V) on goethite. (Circles are the experimental data and the straight lines are the linear fits following equation 3.3).

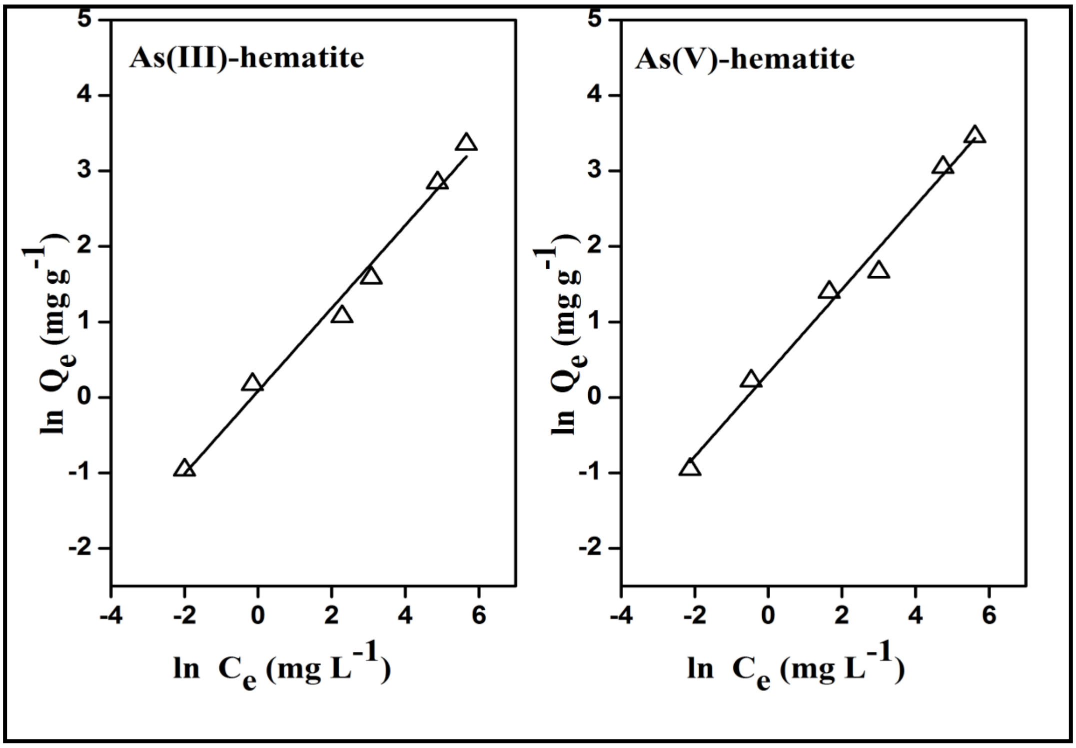

Figure 3.9: Freundlich isotherm for sorption of As(III) and As(V) on hematite. (Triangles are the experimental data and the straight lines are the linear fits following equation 3.3).

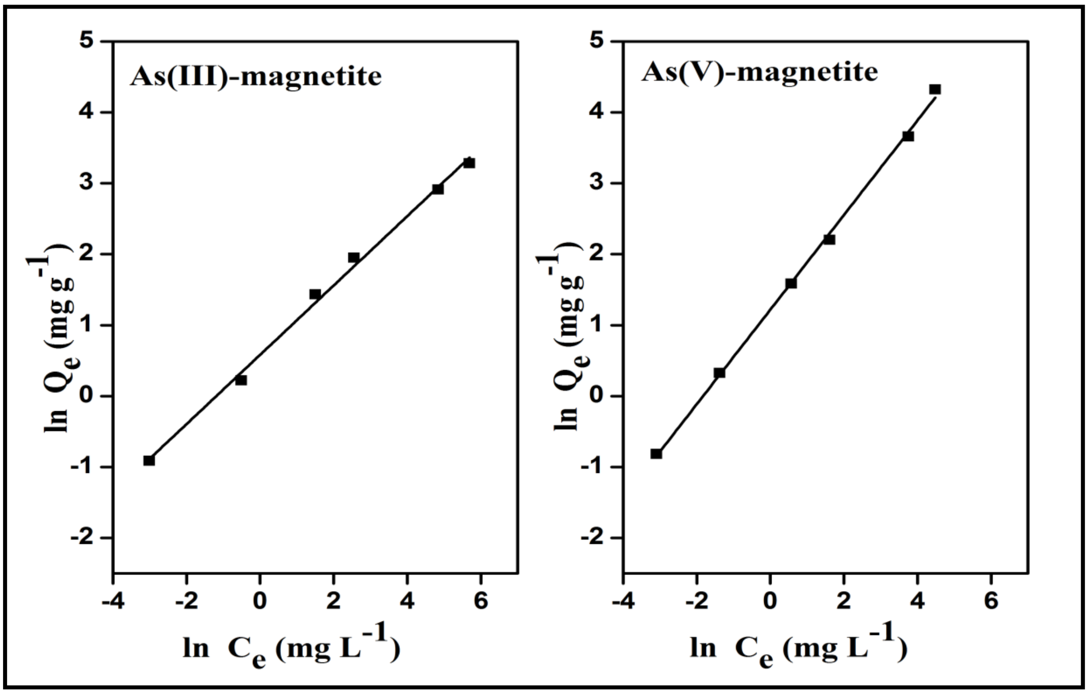

Figure 3.10:Freundlich isotherm for sorption of As(III) and As(V) on magnetite. (Squares are the experimental data and the straight lines are the linear fits following equation 3.3).

Table 3.3: Fitting parameters for the Freundlich isotherms for As(III) and As(V) adsorption on the iron oxide sorbents

Sorbent	**Arsenic species**	**R^2**	**K_f (mg g^{-1})**	**n**
Goethite	As(III)	0.993	2.97	2.14
	As(V)	0.996	3.96	1.66
Hematite	As(III)	0.983	1.09	1.82
	As(V)	0.984	1.38	1.81
Magnetite	As(III)	0.995	1.79	2.04
	As(V)	0.998	3.38	1.50

3.4.4. Leaching studies on iron oxides

The leaching study of iron oxide during sorption of arsenic from groundwater is very important. There are guidelines [3] for maximum iron leaching during water treatment. The iron is categorized as secondary contaminant [120], i.e. no direct impact on health but imparts aesthetic effects (includes change in odour, taste etc) to water.

In the present study, the iron release was determined by ICPOES measurements. The procedure for Fe determination using ICPOES technique has been given in Section 3.2.2.1. The results obtained for the dissolution of different iron oxides at pH 7 are given in Table 3.4.

The maximum acceptable limit of iron in drinking water is 0.3 mg L^{-1}, where as, in the case of no alternate source of water available without Fe content, the limit is relaxed to 1 mg L^{-1} [3]. From the table, it is seen that except for magnetite, the iron release was within the acceplable limit. For magnetite, iron release increased in the presence of both the arsenic species. But for goethite, the Fe leaching reduced drastically after the uptake of arsenic.

Table 3.4: Results obtained for iron leaching from iron oxides

Sorbents	**Fe conc. (mg L^{-1})**		
	Without As	**Presence of As(III)**	**Presence of As(V)**
Goethite	5.6 ± 0.3	1.0 ± 0.2	1.4 ± 0.4
Hematite	0.2 ± 0.1	0.8 ± 0.3	0.2 ± 0.1
Magnetite	2.5 ± 0.1	8.9 ± 0.5	7.2 ± 0.2

3.4.5. Regeneration studies on iron oxides

The results of the regeneration studies obtained in the present study were not encouraging. The regeneration obtained through desorption measurement of arsenic was maximum for goethite, i.e. 35 - 40 %, using 1 M NaOH solution and 4 h equilibration. For magnetite only 25 % desorption was achieved. No regeneration was possible for hematite. These results are in confirmation with the proposition that the iron oxide - arsenic interaction is not simply an electrostatic interaction but involve some bond formation, i.e. chemisorption.

3.4.6. Reusability studies on iron oxides

Even though the results of the regeneration studies were not promising, the studied iron oxide sorbents were still tested for their reusability. The sorbents (without regeneration), were reused in fresh arsenic [As(III) and As(V)] solutions (2 mg L^{-1}) consecutively for 5 cycles (one cycle comprising of uptake of arsenic from 2 mg L^{-1} solution using 0.1 g of sorbent) and the results are given in the Fig. 3.11. The results showed that the sorption efficiency was > 90 % for both magnetite and goethite, but for hematite the efficiency decreased in 2 cycles.

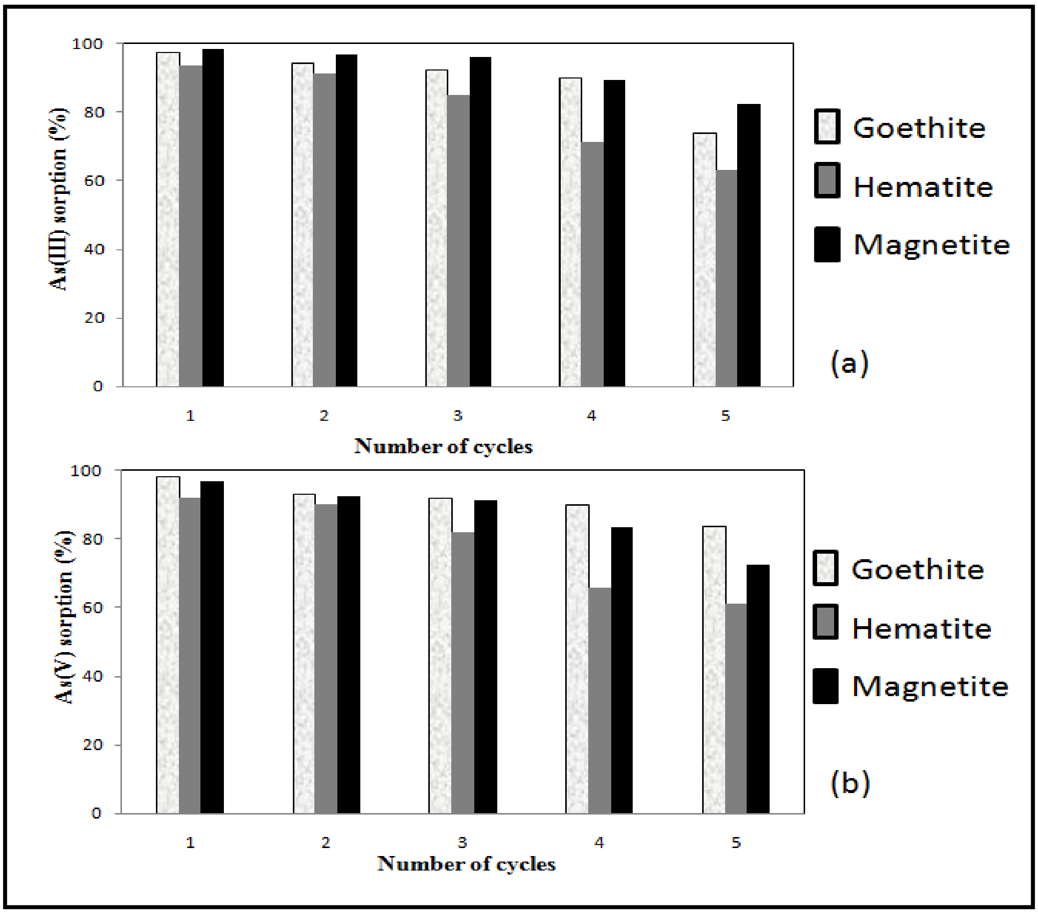

Figure 3.11: Reusability study of iron oxides for (a) As(III) and (b) As(V).

3.4.7. Effect of common ions on arsenic sorption by iron oxides

The effect of common ions on arsenic sorption was studied using goethite as the representative sorbent. Na^+, Ca^{2+}, Mg^{2+}, Cl^-, HCO_3^- and PO_4^{3-} ions are in general, listed as the commonly occurring ions in ground water [121]. The typical concentration range of these ions in groundwater is listed in Table 3.5 below. The concentrations of these ions were chosen in three different ranges in the current study:

(i) lower range, i.e. ten times lower than the typical concentration in the groundwater,

(ii) in the range of the typical concentration in the groundwater and

(iii) higher range, i.e. ten times more than the typical concentration in the groundwater (Table 3.6).

The presence of phosphate ions has a small retarding effect on the arsenic sorption, but it was only about 10 % decrease in sorption for a 50 mg L^{-1} of phosphate in the solution.

This is understandably due to the structural similarity of phosphate and arsenate groups. The effect of phosphate is not a concern for arsenic removal, because, such a high level of phosphate is in general not found in common groundwater samples.

Table 3.5: Typical concentration range of the common ions in groundwater [121].

Common ions	**Concentration found in groundwater (mg L^{-1})**
Na^+	210 - 1000
Ca^{2+}	36 - 51
Mg^{2+}	22 - 39
Cl^-	8.5 – 21.0
HCO_3^-	771 - 3134
PO_4^{3-}	0.1 - 0.49

Table 3.6: Effect of interfering ions on sorption of arsenic by the studied goethite sorbent.

Ion	**Amount taken (mg L^{-1})**	**As(III) sorption (%)**	**As(V) sorption (%)**
Ca^{2+}	5	93.1	97.0
	50	93.3	96.7
	500	94.2	96.6
Mg^{2+}	15	93.1	97.0
	150	93.3	96.7
	1500	94.2	96.6
Na^+	50	94.8	97.5
	500	93.1	96.3
	5000	90.1	94.3
Cl^-	50	93.1	97.0
	500	93.3	96.7
	5000	94.2	96.6
HCO_3^-	60	94.8	97.5
	600	93.1	96.3
	6000	90.1	94.3
PO_4^{3-}	5	93.5	94.8
	50	84.8	95.9
	500	81.5	83.4

3.4.8. Application of iron oxides to arsenic contaminated groundwater

Since the sorption efficiency was not affected by the presence of common ions, goethite, hematite and magnetite sorbents were applied for the arsenic remediation from the real groundwater samples. For this study, two groundwater samples were collected from North 24 Parganas, West Bengal, India. The characterizations of the collected groundwater samples were independently done and the results are shown in Table 3.7. Sorption studies reveal that the removal of arsenic is achieved to take it easily below 10 μg L^{-1} (WHO limit) in one cycle by using magnetite, whereas for goethite, it took two equilibrations. The results obtained for the arsenic concentration in groundwater after equilibration with iron oxides are given in Table 3.8.

Table 3.7: Characterization of the groundwater samples obtained from North 24 Parganas, West Bengal.

Parameters	**GW-1**	**GW-2**
pH	7.3 ± 0.2	7.7 ± 0.2
Conductance (μS)	352 ± 4	536 ± 18
Na^+ (mg L^{-1})	18.4 ± 2.2	36.2 ± 3.6
Ca^{2+} (mg L^{-1})	39.1 ± 1.2	360 ± 11
Mg^{2+} (mg L^{-1})	7.3 ± 0.5	16.5 ± 1.2
Fe^{2+} (mg L^{-1})	0.52 ± 0.12	2.91 ± 0.36
Cl^- (mg L^{-1})	18.9 ± 2.1	556 ± 24
HCO_3^- (mg L^{-1})	79 ± 6	137 ± 19
PO_4^{3-} (mg L^{-1})	0.25 ± 0.10	0.66 ± 0.21
As (μg L^{-1})	163 ± 8	710 ± 35

Table 3.8: Concentration of arsenic in groundwater before and after sorption using iron oxides.

Sample	**Initial arsenic conc. (µg L^{-1})**	**Conc. after filtration and sorption by goethite (µg L^{-1})**	**Conc. after filtration and sorption by hematite (µg L^{-1})**	**Conc. after filtration and sorption by magnetite (µg L^{-1})**
GW-1	163 ± 8	2.2 ± 0.1	9.6 ± 0.3**	5.2 ± 0.2
GW-2	710 ± 35	8.5 ± 0.3**	35 ± 6#	9.4 ± 0.5

**Arsenic removal achieved in 2 cycles; # Arsenic removal achieved in 3 cycles

3.4.9. Study of arsenic sorption mechanism on iron oxides

3.4.9.1. XPS measurements

The XPS measurements were done to study the oxidation state of arsenic after the uptake by the iron oxides, viz. goethite, hematite and magnetite. The survey scans (Figs. 3.12 - 3.14) showed the presence of Fe, O, and C in blank iron oxides. Presence of carbon is due to the carbon tape used to hold the sample pellets. The XPS plots for arsenic standards were given in Fig. 3.15. The As *3d* peaks can be de-convoluted into $3d_{5/2}$ and $3d_{3/2}$. In the observed results, more emphasis is given to the $3d_{5/2}$ peak, as this peak is of higher intensity.

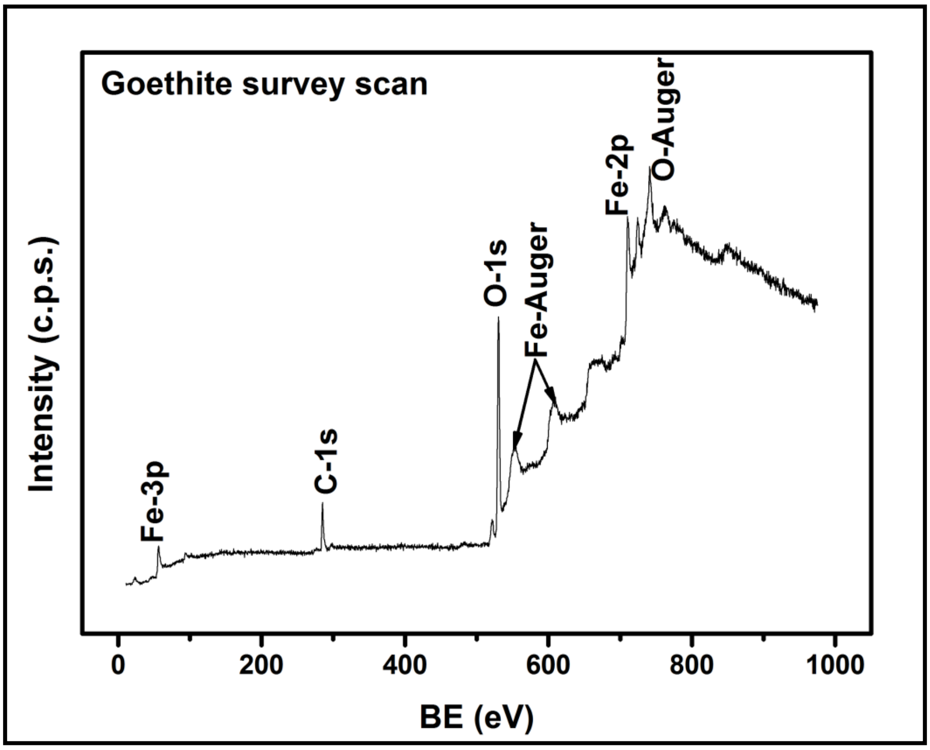

Figure 3.12: XPS survey scan of goethite.

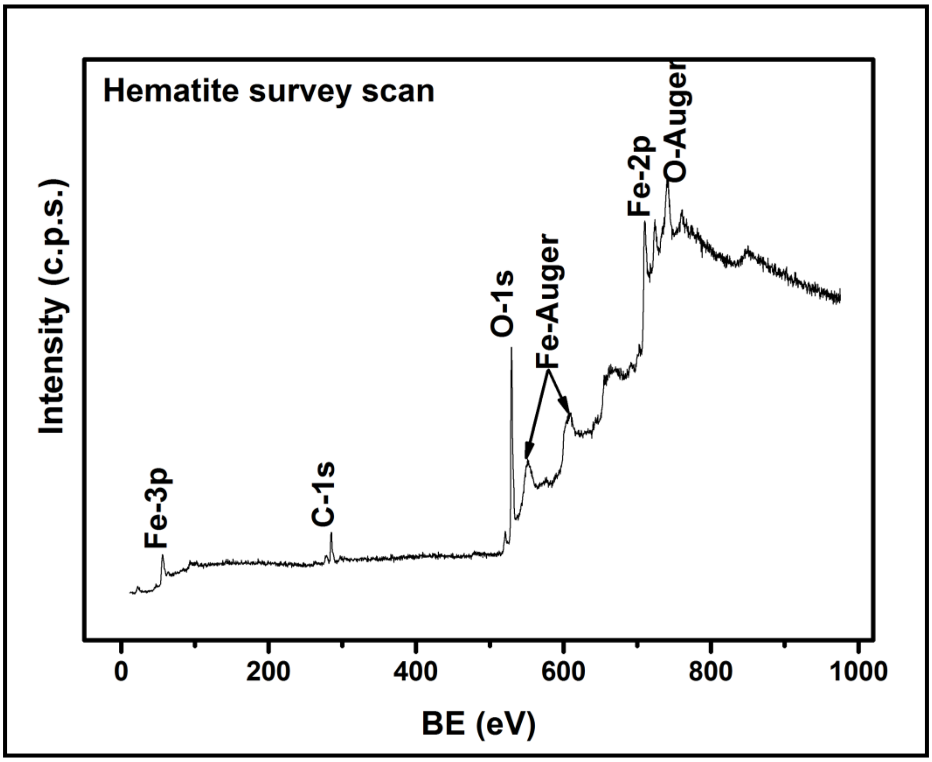

Figure 3.13: XPS survey scan of hematite.

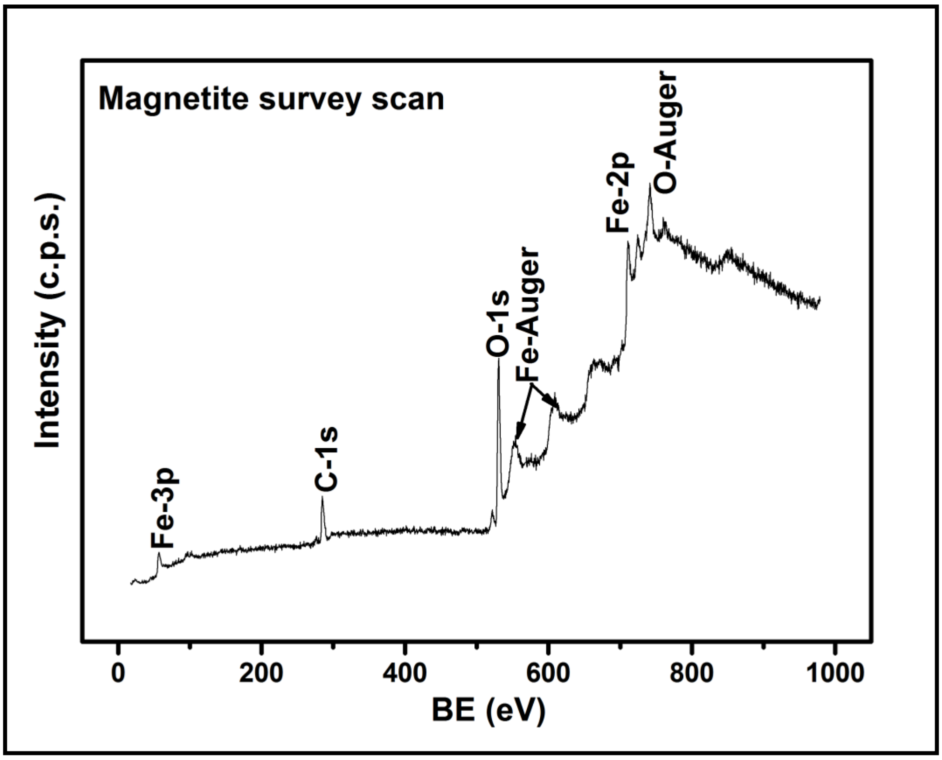

Figure 3.14: XPS survey scan of magnetite.

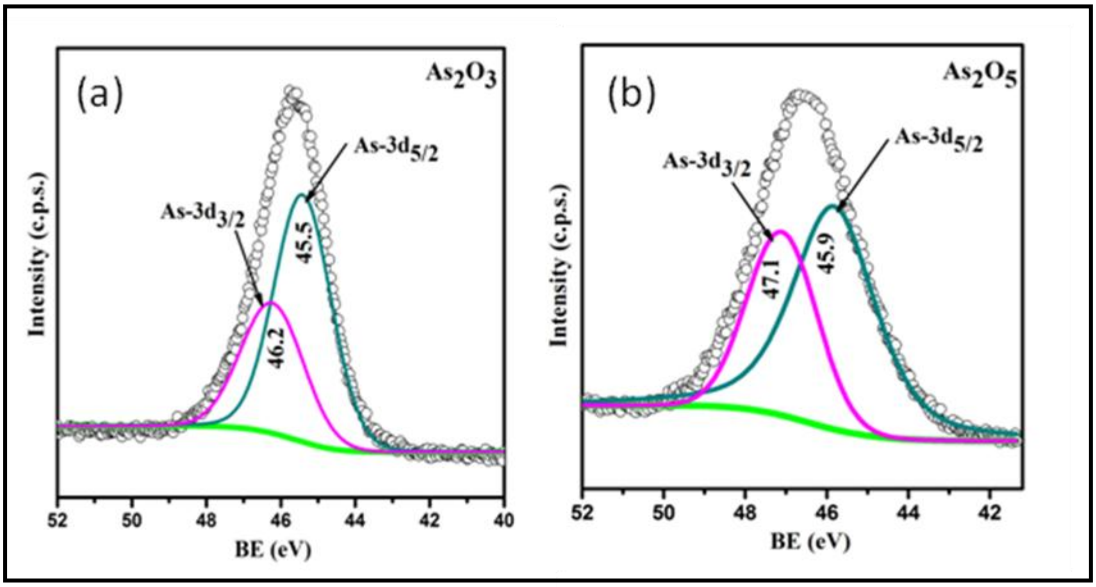

Figure 3.15: XPS plots of arsenic (As *3d*) [As(III) and As(V) standards].

(A) XPS study of goethite system

The Fe *2p* spectrum observed was a doublet (due to spin orbital coupling) which corresponds to Fe $2p_{3/2}$ [binding energy (B. E.) = 710.3 eV] and Fe $2p_{1/2}$ (B.E. = 723.9 eV). The Fe $2p_{3/2}$ peak was de-convoluted to two peaks [Fig. 3.16 (a)] which indicated the presence of both Fe(II) (B.E. = 709.9 eV) and Fe(III) (B.E. = 712.0 eV) in the sample. The presence of the Fe(II) was due to the partial reductive dissolution occurring to goethite (Table 3.4), when the goethite was equilibrated with DI water. The XPS results are listed in Table 3.9.

Table 3.9: XPS study of goethite - arsenic system (Binding energies in eV)

Sample	**As *3d*$_{5/2}$**	**Fe *2p*$_{3/2}$**	**O *1s***	**Species**
Goethite	-	709.9	529.7	O^{2-} (Fe - O)
		712.0	530.8	OH^-
As_2O_3: As(III) standard	45.5	-	531.3	O^{2-} (As - O)
As_2O_5: As(V) standard	45.9	-	530.6	O^{2-} (H_2O)
			531.9	O^{2-}
As(III)-goethite	45.2	709.9	529.1	O^{2-} (Fe - O)
	47.2	712.4	530.5	O^{2-} (H_2O)
			531.9	O^{2-} (As - O)
As(V)-goethite	45.3	710.0	529.4	O^{2-} (Fe - O)
	47.0	711.6	530.6	O^{2-} (H_2O)
		713.1 (new)	531.9	O^{2-} (As - O)

As(III)-goethite system

The spectrum corresponding to arsenic (As *3d*$_{5/2}$) of As(III) sorbed on goethite is shown in Fig. 3.17 (a). The As *3d*$_{5/2}$ peak, on de-convolution shows two components: As(III) (B.E. 45.2 eV) and As(V) (B.E. 47.2 eV). This observation suggests that As(III) on interaction with goethite gets oxidized partially to As(V). The Fe *2p*$_{3/2}$ spectrum of As(III)-goethite is shown in Fig. 3.16 (b). De-convolution of Fe *2p*$_{3/2}$ peak, leads to two peaks [Fig. 3.16 (b)] similar to those present in goethite blank. The 0.4 eV shift of the Fe(III) peak is because of the interactions occurred during arsenic sorption.

From the B.E. of arsenic, it is clear that oxidation occurred for As(III). Due to the presence of oxygen along with Fe(III) oxide, there occurs an oxidation to the arsenic species [122]. During the arsenic oxidation, the Fe(III) gets reduced, and since oxygen is also present there, iron gets oxidized again and remains attached with the iron oxide surface as Fe(III). The B.E. of Fe(II) is not getting changed, because there is no role of Fe(II), during the sorption process of As(III).

As(V)-goethite system

The spectrum corresponding to arsenic (As $3d_{5/2}$) of As(V)-goethite system is shown in Fig. 3.17 (b). The As $3d_{5/2}$ spectrum is similar to the spectrum of As(III)-goethite, having two components: As(III) (B.E. 45.3 eV) and As(V) (B.E. 47.0 eV). The initial arsenic species was As(V), which underwent partial reduction with the action of the hydroxide groups present on the surface of goethite. As a result, the arsenic uptake by goethite was a result of redox reaction and the As(III):As(V) ratio remained similar for both As(III) and As(V) sorption. The Fe $2p_{3/2}$ spectrum of As(V)-goethite is shown in Fig. 3.16 (c). The Fe $2p_{3/2}$ peak is de-convoluted into three components with B.E. values of 710.0, 711.6 and 713.1 eV, respectively. The first peak of lower B.E. is for the Fe bonded to oxide and the second peak is for the Fe-hydroxide linkage. The 713.1 eV peak could be attributed to the formation of a new Fe compound due to the reduction and sorption of arsenic on the goethite surface.

Due to the presence of oxygen in the reaction system, the Fe(II) gets oxidized to Fe(III). The excess electrons expelled is taken up by As(V) and it undergoes reduction. Accordingly, the As(III) gets adsorbed on to the goethite surface. Observed results suggest that As(V) is sorbed on to goethite after disproportionation. The arsenic uptake by goethite is thus apparently through both Fe(II) and Fe(III), which is supported by a significant change in the B.E. of Fe (Table 3.9). The remaining unreacted Fe(II) on the goethite shows almost similar B.E. as that in blank goethite, where as for the Fe(III), the B.E. peak is splitted into two as follows: (i) 711.6 eV for uncomplexed Fe(III) and (ii) 713.1 eV for the arsenic complexed Fe(III).

O 1s spectra

The deconvoluted O 1s XPS spectra for blank goethite, As(III)-goethite and As(V)-goethite are given in the Fig. 3.18. The blank goethite [Fig. 3.18 (a)] has two deconvoluted O *1s* peaks at: 529.7 and 530.8 eV. The peak at 529.7 eV corresponds to lattice oxygen (O^{2-}) which is bonded with Fe(III) in goethite. The peak at 530.8 eV is attributed to the oxygen associated to the chemically or physically adsorbed water. The O *1s* peaks for both the As(III)-goethite [Fig. 3.18 (b)] and As(V)-goethite [Fig. 3.18 (c)] are very similar. The three peaks obtained in both the cases are (i) O^{2-} in the iron oxide, (ii) oxygen associated to the adsorbed water layer and (iii) oxygen in the arsenic oxide. The B.E. 531.9 eV, suggests that there exists a clear bonding between Fe and As through oxygen. This was further confirmed from the oxygen B.E. observed for the arsenic oxide standard.

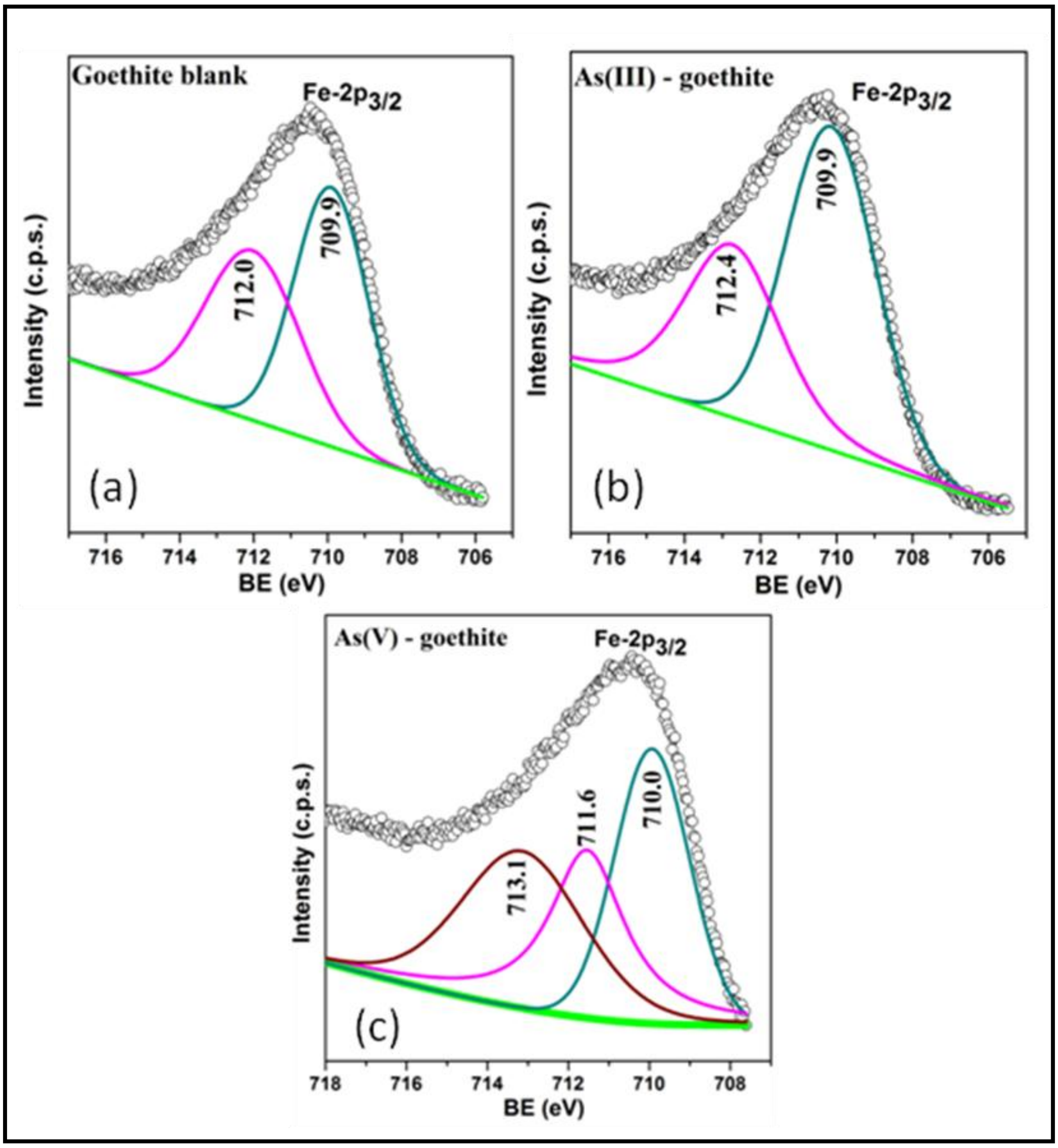

Figure 3.16: Goethite Fe $2p_{3/2}$ XPS plot

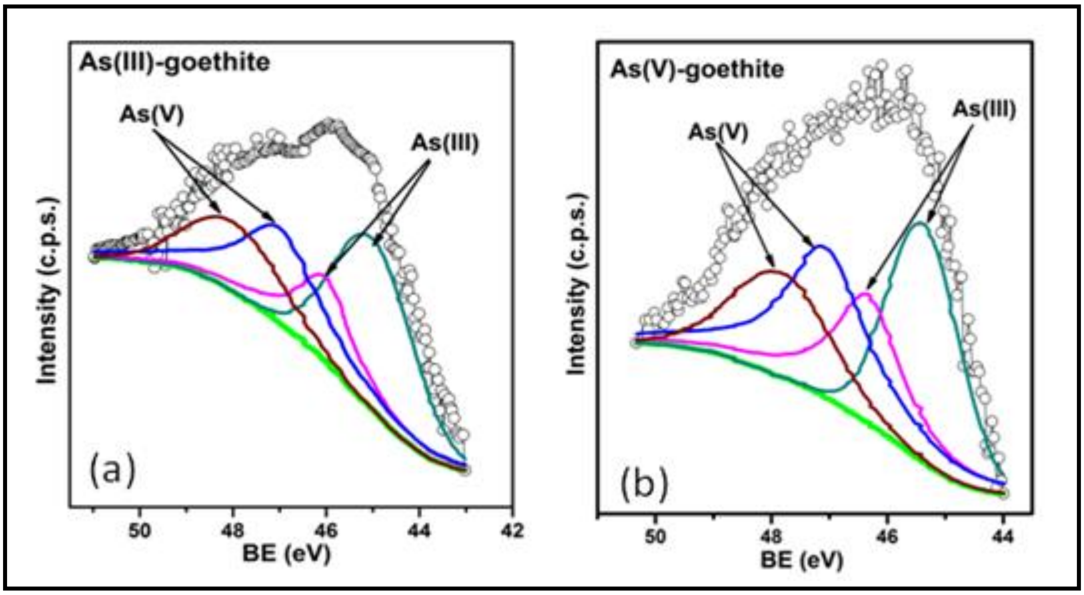

Figure 3.17: Goethite As $3d_{5/2}$ XPS plot

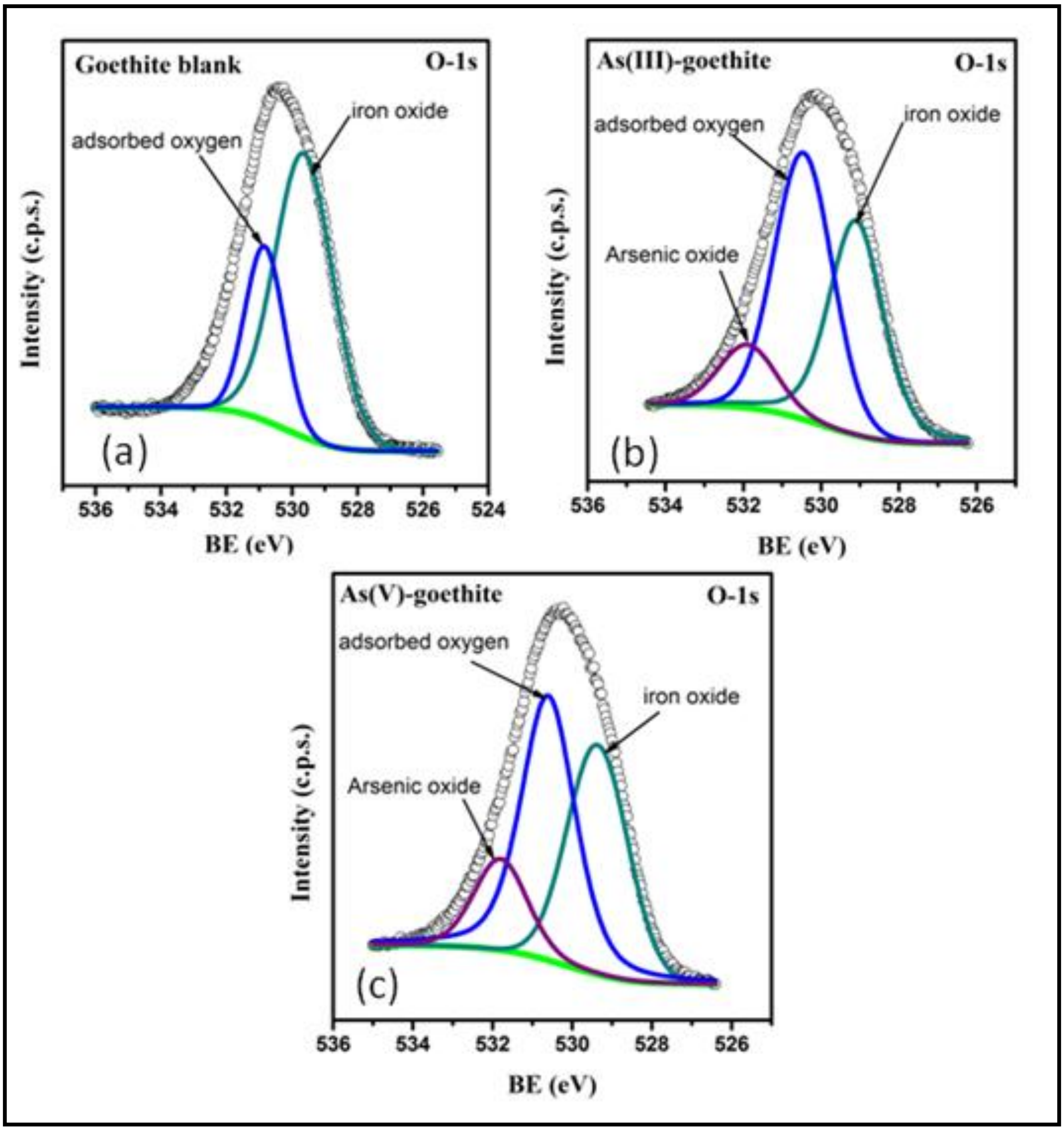

Figure 3.18: Goethite O *1s* XPS plot

(B) XPS study of hematite system

The Fe $2p_{3/2}$ spectrum of hematite blank is deconvoluted into 709.5 eV and 711.9 eV peaks [Fig. 3.19 (a)], which are attributed to Fe(II) and Fe(III), as explained before, in the case of goethite system. The binding energies observed for Fe, As and O are given in Table 3.10.

Table 3.10: XPS study of hematite - arsenic system (Binding energies in eV)

Sample	**As $3d_{5/2}$**	**Fe $2p_{3/2}$**	**O $1s$**	**Species**
Hematite	-	709.5	529.1	O^{2-} (Fe - O)
		711.9	531.1	O^{2-} (H_2O)
As_2O_3: As(III) standard	45.5	-	531.3	O^{2-} (As - O)
As_2O_5: As(V) standard	45.9	-	530.6	O^{2-} (H_2O)
			531.9	O^{2-} (As - O)
As(III) - hematite	44.8	709.4	529.3	O^{2-} (Fe - O)
	46.7	711.8	530.6	O^{2-} (H_2O)
			532.0	O^{2-} (As - O)
As(V) - hematite	44.7	709.3	529.0	O^{2-} (Fe - O)
	47.0	710.9	530.5	O^{2-} (H_2O)
		712.8 (new)	532.0	O^{2-} (As - O)

As(III)-hematite system

The arsenic $3d_{5/2}$ spectrum of As(III)-hematite is given in Fig. 3.20 (a). The As $3d_{5/2}$, has two components: As(III) and As(V). The Fe $2p_{3/2}$ spectrum of As(III)-hematite is shown in Figure 3.19 (b). On de-convolution, this band gives two peaks with B.E. values as 709.4 and 711.8 eV, respectively [Fig. 3.19 (b) and Table 3.10].

The mechanism of As(III) sorption by hematite is apparently similar to that of goethite. In this case also two arsenic species are observed after sorption on to hematite. These results confirm the proposition that a redox reaction occurrs between As(III) (oxidation) and Fe(III) (reduction) during the uptake of arsenic by hematite.

As(V)-hematite system

The As $3d_{5/2}$ spectrum of As(V)-hematite system is shown in Figure 3.20 (b). The As $3d_{5/2}$ spectrum is similar to the spectrum of As(III)-hematite, having two components: As(III) (B.E. 44.7 eV) and As(V) (B.E. 47.0 eV). The uptake of arsenic by hematite is similar to that by goethite. The Fe $2p_{3/2}$ spectrum of As(V)-hematite is shown in Fig. 3.19 (c). The Fe $2p_{3/2}$ peak is de-convoluted into three components, two of them matches with the peaks of blank hematite. The additional 712.8 eV peak corresponds to a new Fe compound formed after the sorption of As(V) species. Observed results suggest that both As(III) and As(V) are sorbed on to hematite after their disproportionation. It is suggested that the electrons released during the oxidation of Fe(II), due to the oxygen present in the system, are involved in the reduction of As(V).

O 1s spectra

The deconvoluted O *1s* XPS spectra for blank hematite, As(III)-hematite and As(V)-hematite are given in Fig. 3.21. The blank hematite [Fig. 3.21 (a)] has two deconvoluted O *1s* peaks at: 529.1 eV and 531.1 eV, respectively. The peak at 529.7 eV corresponds to lattice oxygen (O^{2-}) and is bonded with Fe(III)/Fe(II) in hematite. The peak at 531.1 eV is attributed to the surface hydroxide group. The O *1s* peak for both the As(III)-hematite and As(V)-hematite are similar. The three peaks obtained in both the cases are (i) O^{2-} in the iron oxide, (ii) oxygen in adsorbed water layer and (iii) oxygen bonded to arsenic species. The O *1s* (B. E. 532.0 eV) obtained for both the arsenic species sorbed on hematite, confirmed that the adsorbed arsenic species was a mixture of As(III) and As(V).

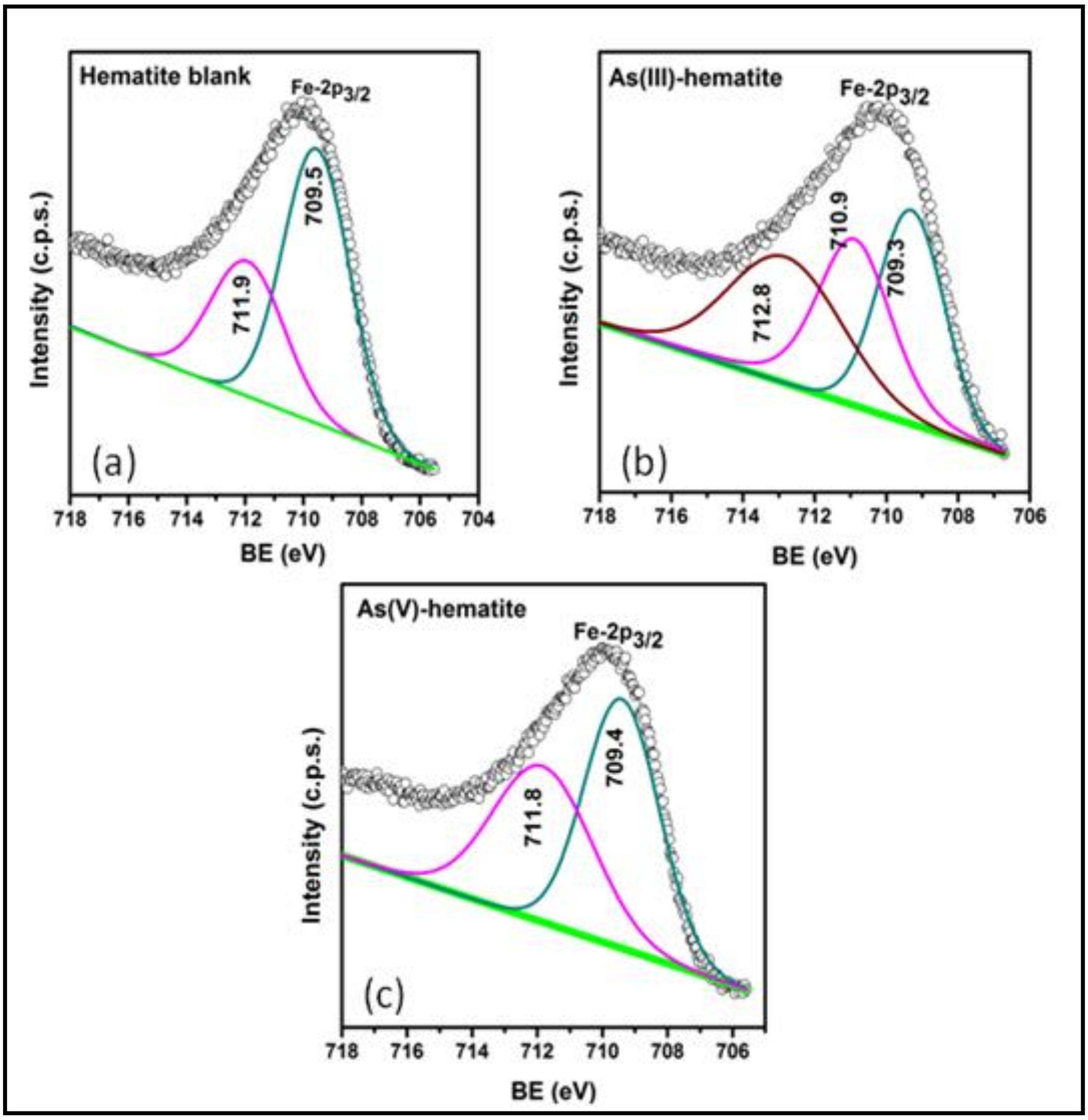

Figure 3.19: Hematite Fe $2p_{3/2}$ XPS plot

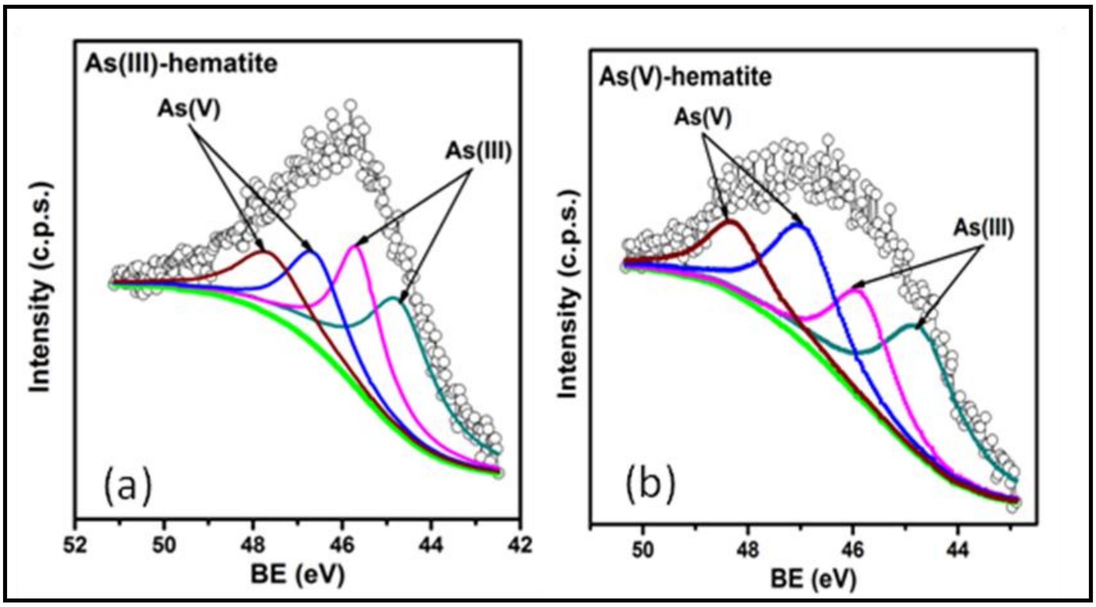

Figure 3.20: Hematite As $3d_{5/2}$ XPS plot

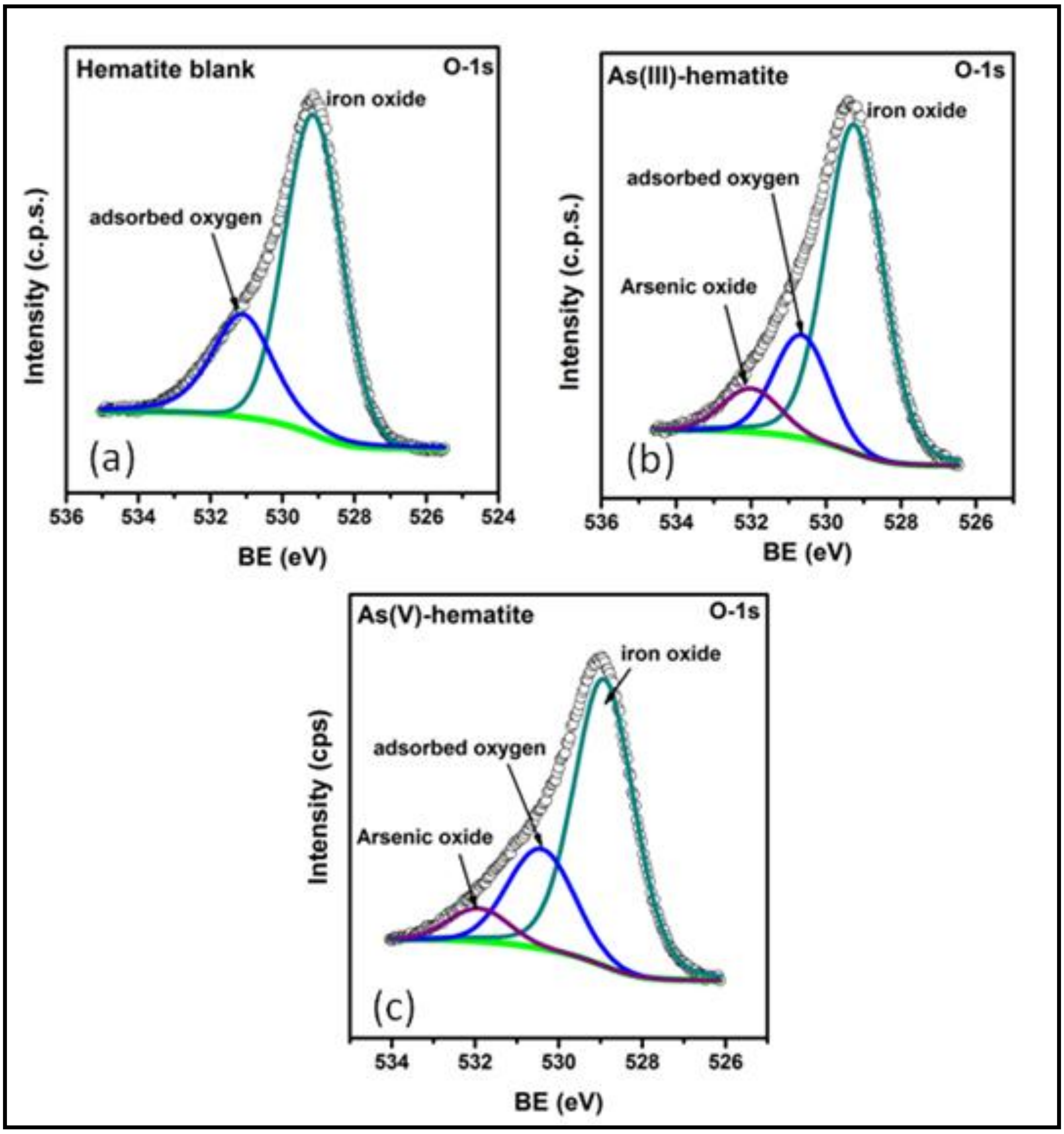

Figure 3.21: Hematite O *1s* XPS plot

(C) XPS study of magnetite system

Magnetite is a mixed oxide, having Fe(II) and Fe(III) oxides. For magnetite, the Fe $2p_{3/2}$ spectrum is deconvoluted into two peaks of B.E. 710.0 eV and 712.2 eV, respectively [Fig. 3.22 (a)], which are attributed to Fe(II) and Fe(III). The binding energies observed for Fe, As and O are given in Table 3.11.

Table 3.11: XPS study of magnetite - arsenic system (Binding energies in eV)

Sample	**As $3d_{5/2}$**	**Fe $2p_{3/2}$**	**O 1s**	**Species**
Magnetite	-	710.0	529.5	O^{2-} (Fe - O)
		712.2	531.0	OH^-
			532.8	O^{2-} (H_2O)
As_2O_3: As(III) standard	45.5	-	531.3	O^{2-} (As - O)
As_2O_5: As(V) standard	45.9	-	530.6	O^{2-} (H_2O)
			531.9	O^{2-} (Fe - O)
As(III)-magnetite	44.5	708.3	525.9	O^- (partial negative charge)
		710.5	528.2	O^- (partial negative charge)
			530.3	O^{2-} (Fe - O)
As(V)-magnetite	45.6	707.0	526.5	O^- (partial negative charge)
		709.7	529.5	O^{2-} (Fe - O)
		712.0	531.3	O^{2-} (H_2O)

As(III)-magnetite system

The arsenic $3d_{5/2}$ spectrum of As(III)-magnetite is given in Fig. 3.23 (a). The As $3d_{5/2}$, has got only single component [As(III)] having B.E. of 44.5 eV (1 eV shift to the lower side is observed). The Fe $2p_{3/2}$ spectrum of As(III)-magnetite is shown in Figure 3.22 (b); on de-convolution it gives two peaks with B.E. values as 708.3 eV and 710.5 eV, respectively, which correspond to Fe(II) and Fe(III) of the magnetite system [Figure 3.22 (b) and Table 3.11]. Observed results suggests that the As(III) in contact with magnetite remains in the same oxidation state. Similarly, for Fe(II) and Fe(III), there is no redox reaction indicated. The B.E. for both Fe species however experiences about 1.7 eV shift towards lower energies.

As(V)-magnetite system

The As $3d_{5/2}$ spectrum of As(V)-magnetite system is shown in Figure 3.23 (b). The As $3d_{5/2}$ spectrum is similar to the spectrum of As(III)-magnetite, having only one component with B.E. 45.6 eV, matching with As(V). The Fe $2p_{3/2}$ spectrum of As(V)-magnetite is shown in Figure 3.22 (c). The Fe $2p_{3/2}$ peak is de-convoluted into three components of B.E. 707.0, 709.7 eV and 712.0 eV, respectively. Observed results suggest that As(III) and As(V) are sorbed onto the magnetite directly without involving any redox reaction. Thus, during the uptake of As(V) by magnetite, the arsenic species remained as As(V). The B.E. of iron [Fe(II) and Fe(III)] observed a uniform shift of about 0.3 eV towards lower energies. However, a new peak is observed in this case at 707.0 eV, which could be due to the formation of fresh Fe(II) during the course of reductive dissolution of Fe(III) from magnetite.

O 1s spectra

The deconvoluted O *1s* XPS spectra for blank magnetite, As(III)-magnetite and As(V)-magnetite are given in Fig. 3.24. The blank magnetite [Fig. 3.24 (a)] has three deconvoluted O 1s peaks at: 529.5, 531.0 and 532.8 eV, respectively. The peak at 529.5 eV corresponds to the lattice oxygen (O^{2-}) and is bonded with Fe(III)/Fe(II) in magnetite. The peak at 531.0 and 532.8 eV are attributed to the surface hydroxide group and adsorbed water. The O *1s* peaks for both the As(III)-magnetite and As(V)-magnetite are very similar. The three peaks obtained in both the cases are due to (i) O^{2-} in iron oxide, (ii) oxygen in adsorbed water layer and (iii) oxygen bonded to arsenic species.

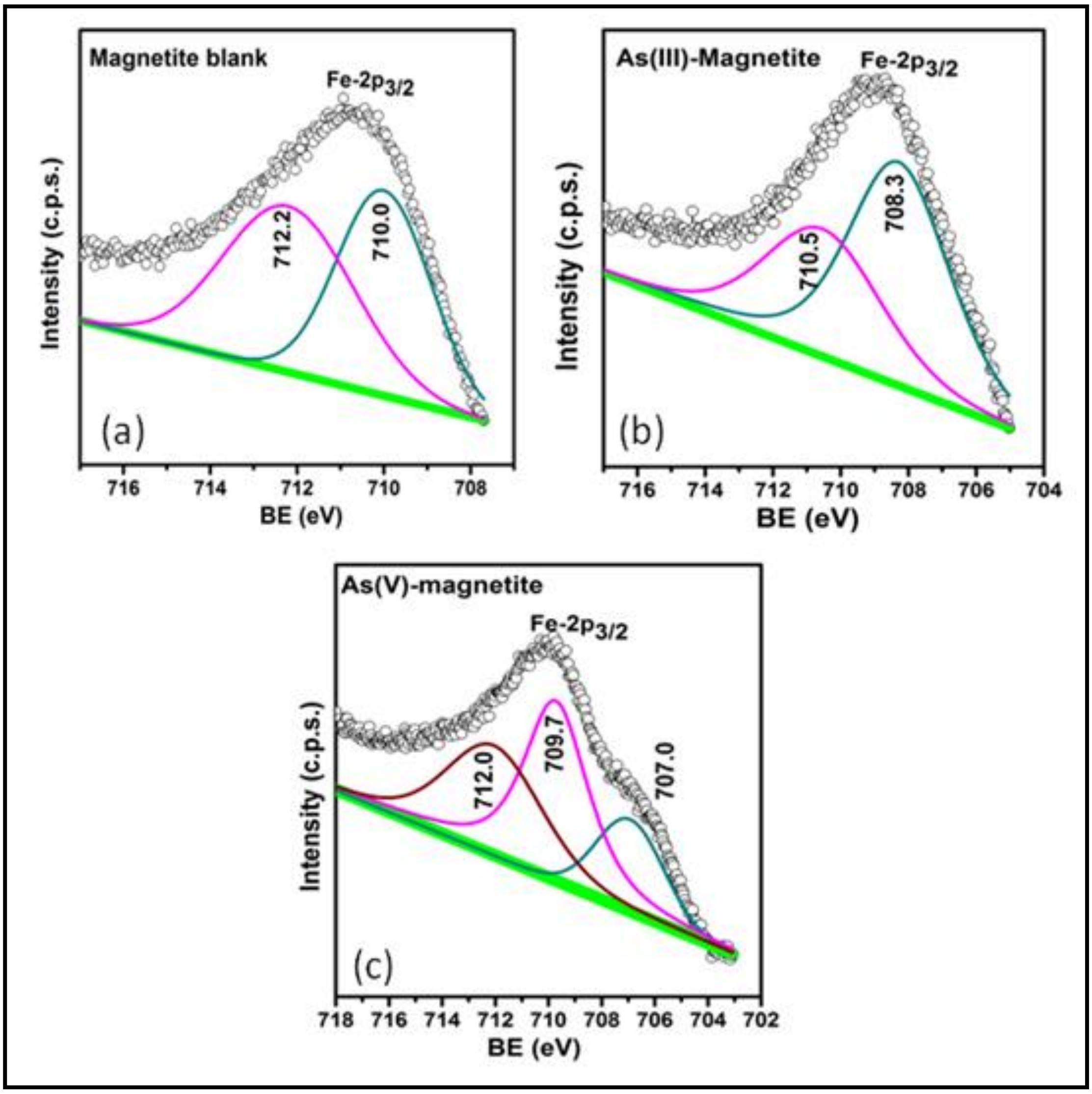

Figure 3.22: Magnetite Fe $2p_{3/2}$ XPS plot

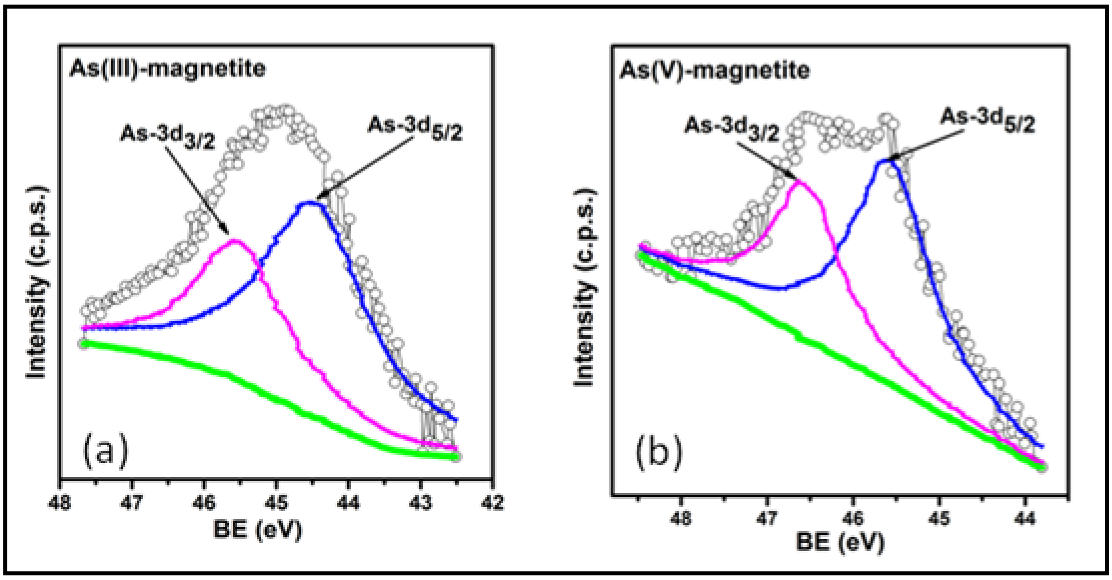

Figure 3.23: Magnetite As $3d_{5/2}$ XPS plot

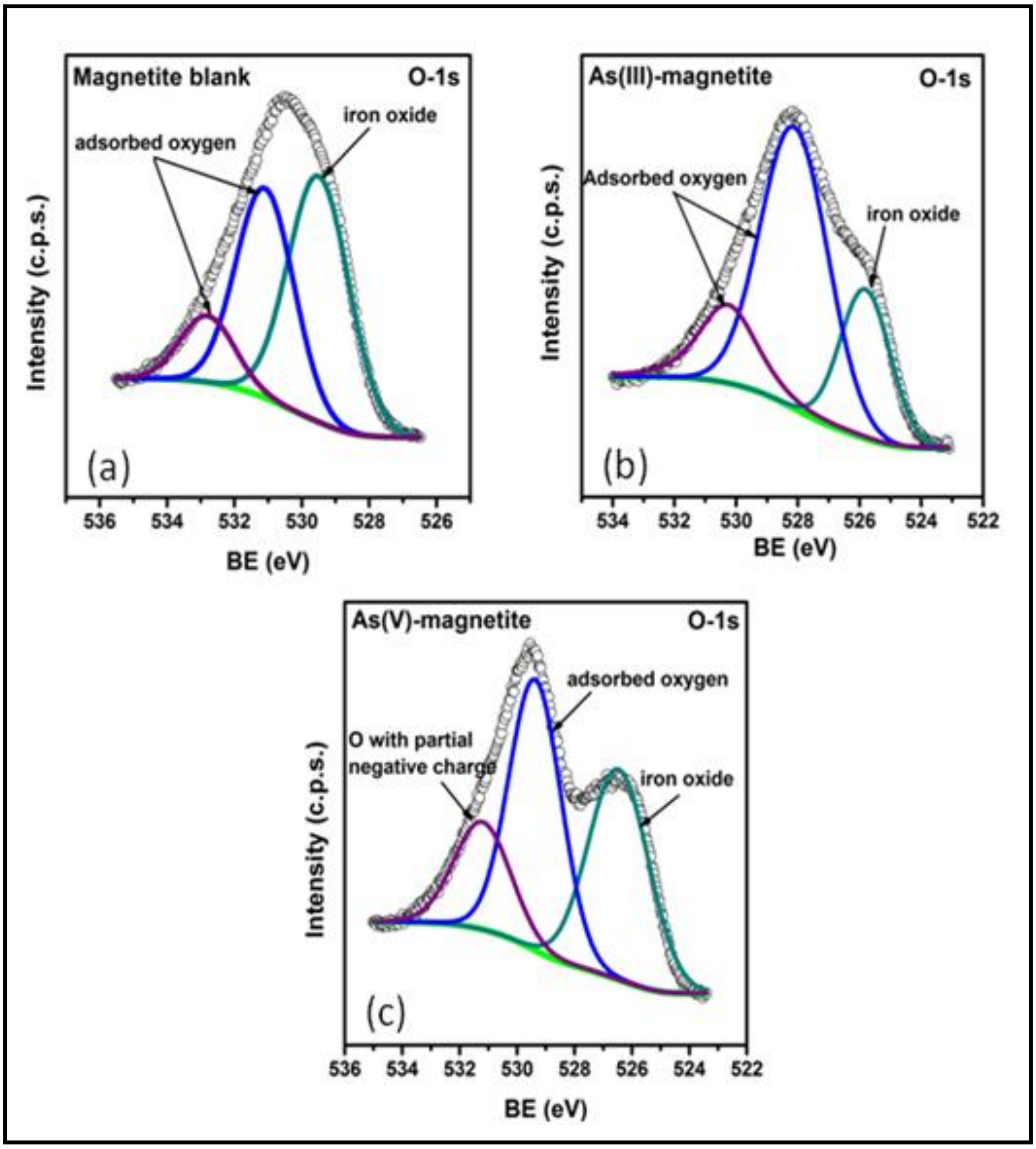

Figure 3.24: Magnetite O 1s XPS plot

3.4.9.2. Electrochemical studies

Cyclic voltammetry (CV) study was carried out on hematite with and without the addition of As(III)/As(V) (Fig. 3.25). From the voltammogram, the redox behavior of hematite modified glassy carbon electrode (GCE) was observed. When As(III) was added (0.5 mg L^{-1}), an oxidation peak was observed at 0.82 V and two reduction peaks were observed at 0.12 and -0.46 V (Fig. 3.25). When As(V) was added, no such peaks were observed. These observations are the clear indication that there exists a strong bonding between As(V) with hematite and the sorption of As(V) on hematite is a non-reversible process.

This also supports our observation that regeneration of hematite was difficult (Section 3.4.5).

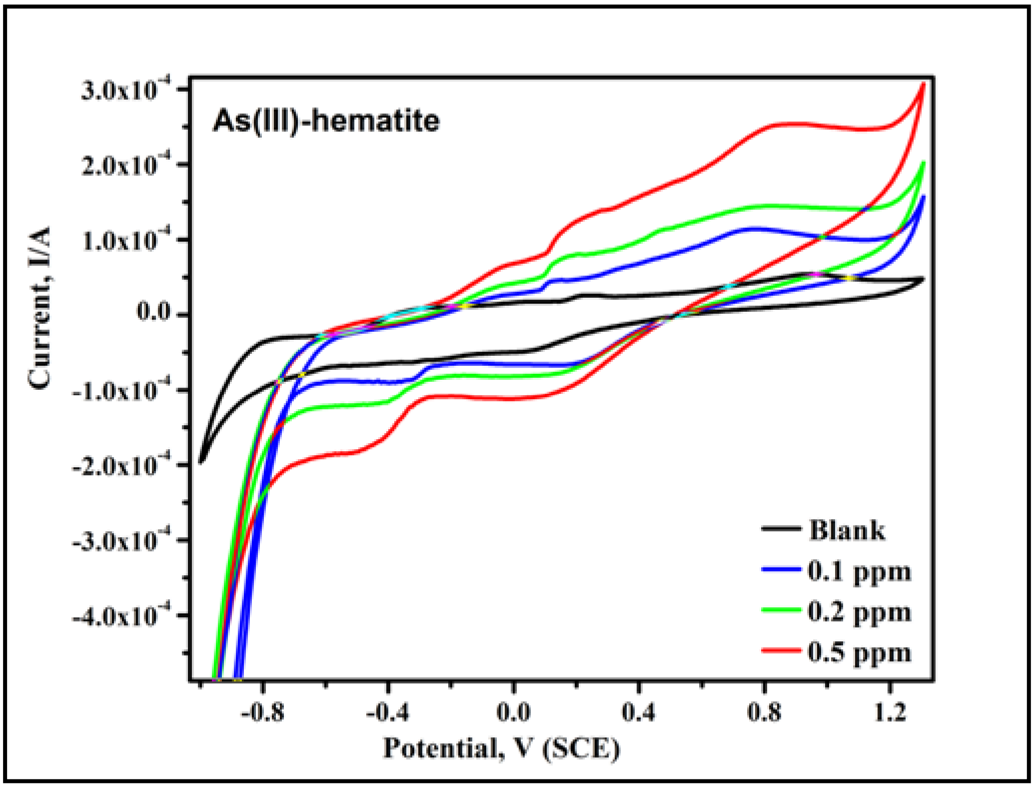

Figure 3.25: CV plot of As(III) - hematite system using hematite modified GCE.

The oxidation behaviour of As(III) was further investigated over the hematite modified GCE in differential pulse voltammetry (DPV) mode (Figs. 3.26 and 3.27). For As(III), the increase in the peak current for the consecutive DPV scans is due to the adsorption of As(III) on the electrode surface and indicates that the species remains redox active on adsorption. In differential pulse mode, the oxidation peak is observed due to the conversion of As(III) to As(V). In this case, the peak current is seen to decrease significantly with the addition of As(V) in the test solution. This decrease in the peak current with the addition of As(V) is due to the occupation of the adsorption sites by As(V) and thus reducing the propensity of As(III) oxidation during subsequent scans.

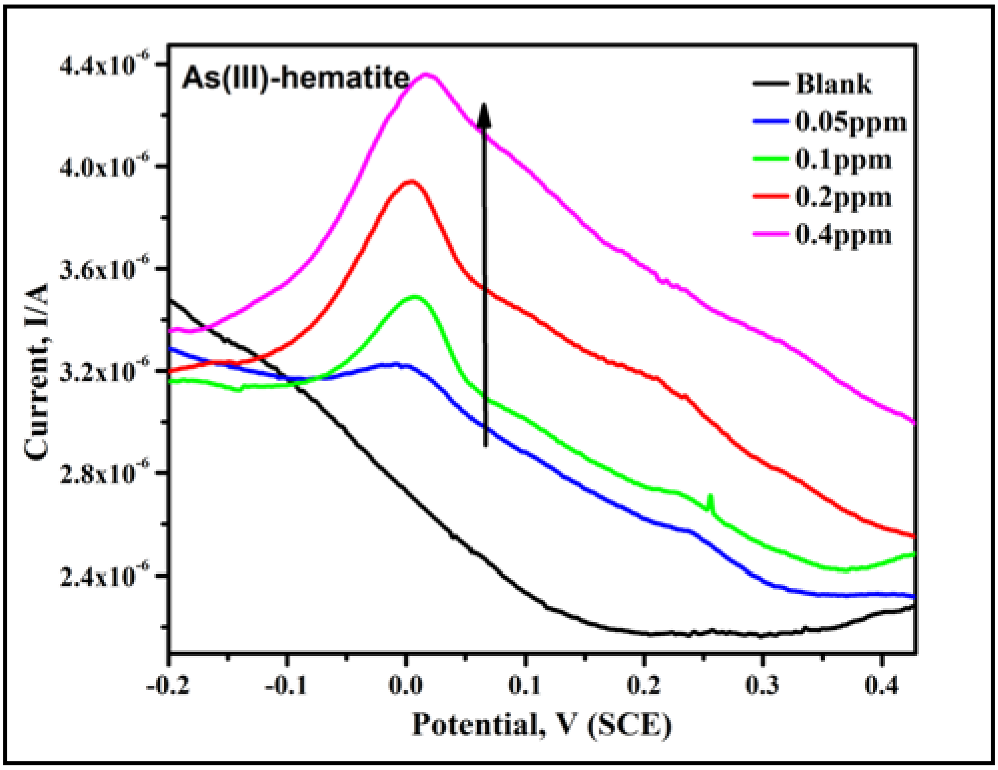

Figure 3.26: DPV plot of As(III) - hematite system.

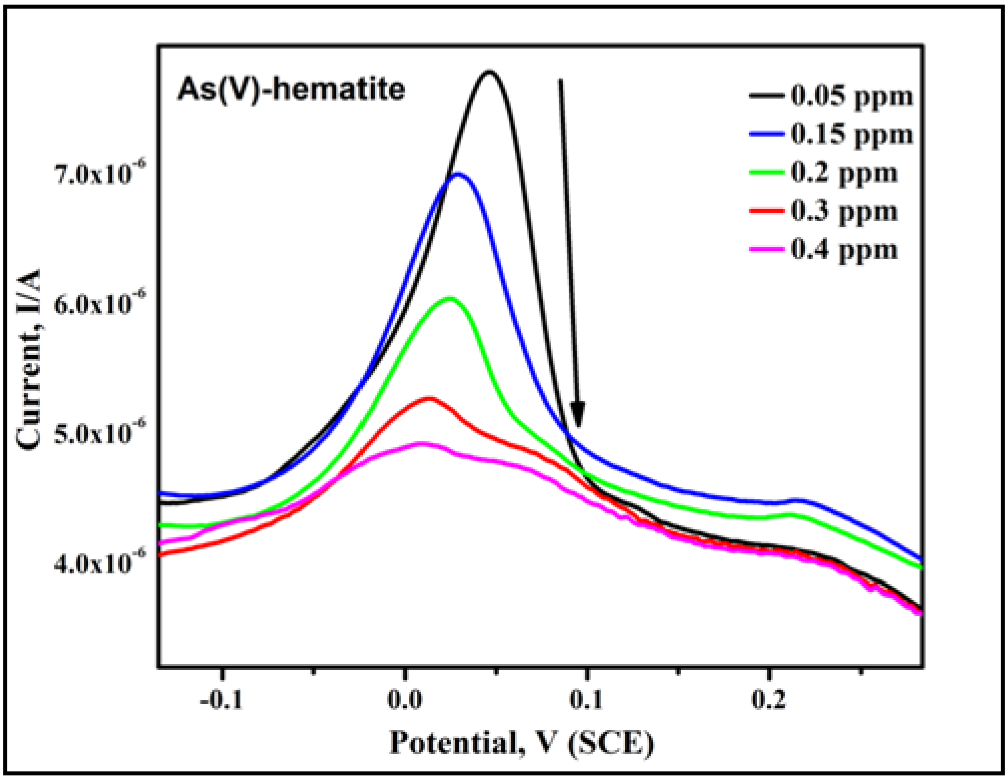

Figure 3.27: DPV plot of As(V) - hematite system.

CV experiments done on As(III) (0.5 mg L^{-1}) solution added to magnetite modified GCE, resulted in two oxidation and two reduction peaks (Fig. 3.28). The plot is an indication of reversibility in the system. The redox property of As(III) remained dynamic even after the uptake over the modified electrode. The result is a confirmation that As(III) is adsorbed as As(III) as such over magnetite.

With As(V) solution, no oxidation peak was observed in the CV measurement. In this case only one reduction peak is observed (Fig. 3.29), corresponding to the reduction of As(V) to As(III) due to the electrochemical reduction. It is evident that As(V) when taken up by magnetite, the uptake becomes irreversible. The redox property of As(V) on magnetite is static in nature. It is indicated that during the electrochemical reduction step, As(V) is reduced to As(III), and the reduced As(III) does not come out from the magnetite matrix as no peak due to the oxidation of As(III) is observed in the oxidation cycle. Therefore, it is suggested that the recovery of magnetite would be difficult following reduction of As(V) to As(III) on the magnetite surface.

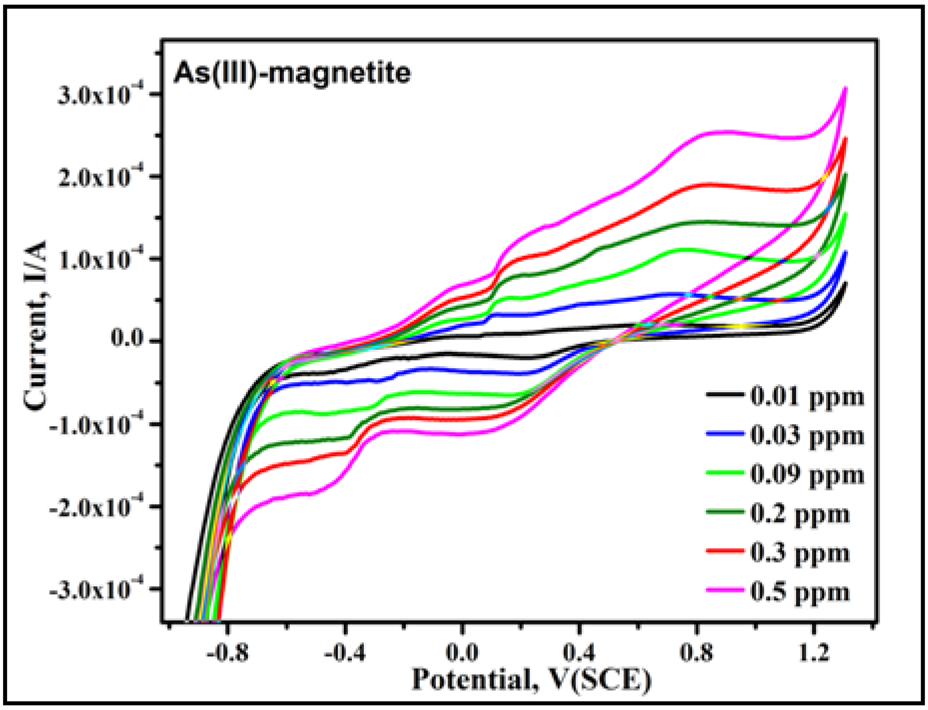

Figure 3.28: CV plot of As(III) - magnetite system using magnetite modified GCE.

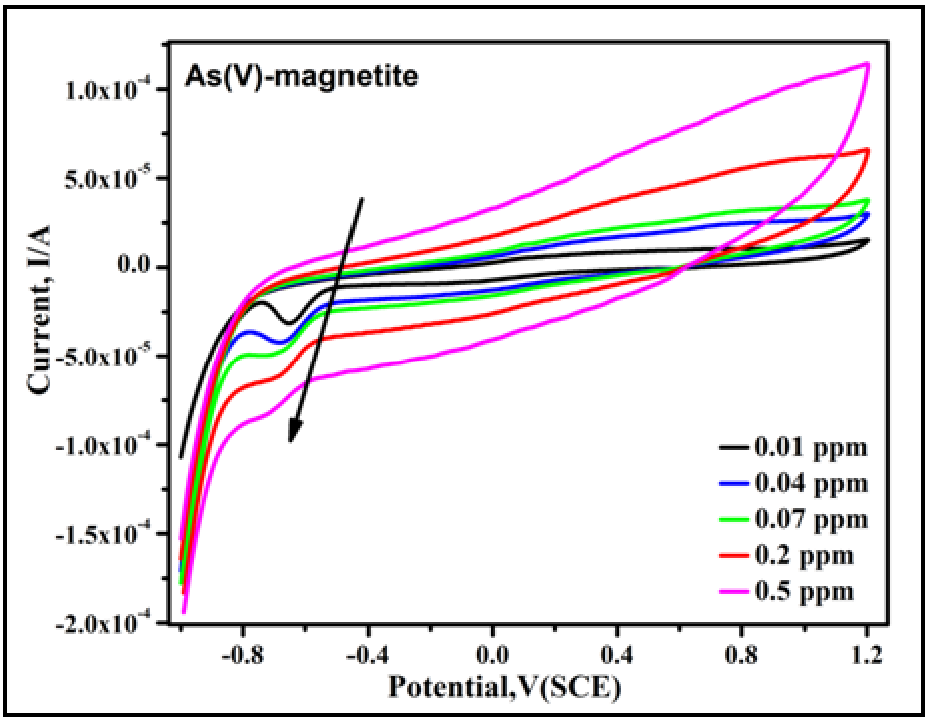

Figure 3.29: CV plot of As(V) - magnetite system using magnetite modified GCE

3.5. Conclusion

The sorption studies for As(III) and As(V) by three different iron oxides confirmed that goethite is having promising sorption properties. The sorption mechanism of arsenic on different iron oxide sorbents has been reported in few literatures [64, 123-126]. Most of the literatures suggest the uptake of arsenic by iron oxides via surface complexation or surface precipitation. In the present study it has been indicated that the sorption of As(III) and As(V) on to goethite and hematite occurs via redox reaction. In these cases while oxidation of As(III) results in As(V) species, the Fe(III) gets reduced to Fe(II). The leaching study of both the oxides confirmed that, there was no increase in the iron concentration in the supernatant. It is thus suggested that the reduction of Fe(III) to Fe(II) results in the formation of surface bound Fe(II) which is subsequently get oxidized to Fe(III). Infact, in the XPS study, only Fe(III) peak could be observed in the present cases. For sorption of As(V), there occurs a Fe(II) oxidation followed by As(V) reduction. In both the iron oxides, the sorption of As(V) resulted in the appearance of a new B.E. peak for Fe. This could be attributed to the arsenic sorption on iron. In the case of mixed iron oxide, i.e. magnetite, there was no redox reaction. Both the arsenic species [As(III) and As(V)] were taken up by magnetite without any change in the oxidation states. The mechanistic schemes for the arsenic uptakes on to goethite/hematite and magnetite sorbents are proposed to be the kinds as shown in the figures below [Figs. 3.30 and 3.31].

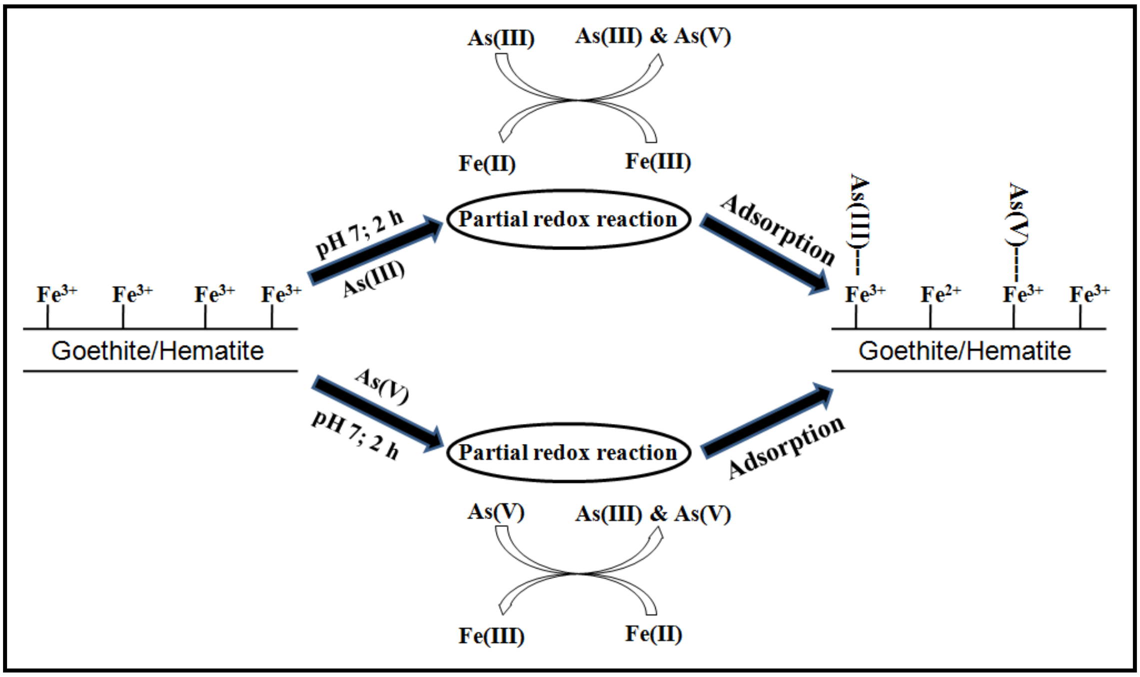

Figure 3.30: Schematic for sorption of arsenic on goethite and hematite

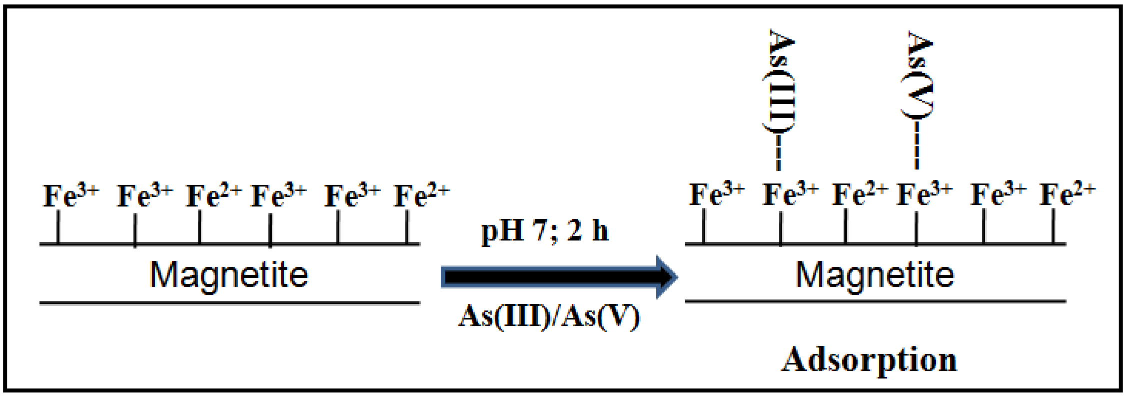

Figure 3.31: Schematic for sorption of arsenic on magnetite

Chapter - IV

Arsenic uptake on manganese dioxides

4.1. Introduction

The toxicity of arsenic and the limit in drinking water has been discussed in literatures [127-129]. In the previous chapter, the sorption using iron oxide has been explained. The main mechanism of removal of arsenic, in sorption technique, is by sorbent-sorbate electrostatic interaction. Hence charge of the arsenic species is important for arsenic removal. Most of the sorbents are successful in removing As(V) - which is negatively charged, but fail in complete removal of As(III) - which is neutral at groundwater pH. An oxidation step prior to adsorption is thus required for removal of As(III), which is more toxic. In this context, a single step of oxidation-sorption mechanism has attracted the interest of the researchers and manganese dioxide (MnO_2), being a well known oxidizing agent, appeared prospective sorbent material in this respect [65, 68, 130-131]. The studies reported on oxidation kinetics of As(III) using iron and manganese oxides, confirmed the fast kinetics of manganese dioxide [71, 132].

In this work, manganese dioxide (MnO_2) has been utilized to understand its arsenic removal prospectives. The sorption behavior of As(III) and As(V) has been studied by using ^{76}As radiotracer in batch equilibration mode. The detailed synthesis and characterization methods have already been discussed in Chapter 2. In the present work, the synthesized MnO_2 has been utilized to study the effect of different solution parameters on the uptake of arsenic. Studies have also been carried out to understand the mechanism of interaction of arsenic with manganese dioxide by using suitable experimental techniques. The sorbent was also applied for removal of arsenic from the arsenic contaminated groundwater samples collected from North 24 parganas, West Bengal, India.

4.2. Materials and methods

4.2.1. Reagents and chemicals

The chemicals used were of analytical reagent (AR) grade and used without further purification. The inorganic salts like, potassium permanganate [$KMnO_4$; molecular weight (MW) - 158.03 g mol^{-1}], manganese sulphate [$MnSO_4.4H_2O$; MW - 223.07 g mol^{-1}], manganese acetate [$Mn(CH_3CO_2)_2.4H_2O$; MW - 245.09 g mol^{-1}], sodium hydroxide pellets (NaOH; MW - 40.00 g mol^{-1}), arsenic trioxide [As_2O_3; MW - 197.84 g mol^{-1}], arsenic pentoxide [As_2O_5; MW - 229.84 g mol^{-1}], sodium chloride [NaCl; MW - 58.44 g mol^{-1}], calcium chloride [$CaCl_2$; MW - 110.98 g mol^{-1}], magnesium chloride [$MgCl_2$; MW - 95.21 g mol^{-1}], sodium bicarbonate [$NaHCO_3$; MW - 84.01 g mol^{-1}] and sodium dihydrogen phosphate [NaH_2PO_4; MW - 119.98 g mol^{-1}] were used in this study to investigate effect on the sorption process. Other AR grade reagents utilized were concentrated hydrochloric acid (HCl), concentrated nitric acid (HNO_3), dilute sodium hydroxide (NaOH) and benzene (C_6H_6). The dissolution of inorganic chemicals as well as the necessary dilutions were carried out using deionised (DI) water (resistivity 18.2 MΩ cm^{-1} and total organic carbon < 10 μg L^{-1}) obtained from Milli-Q water purification system.

4.2.2. Equipments

All the sample weighing was done using a high precision analytical semimicro balance (Mettler - Toledo, dual range, readability - 0.01 mg). pH measurements were carried out in Oakton pH meter employing glass electrode (pH700, USA), with digital display having precision of ± 0.01 unit. A mechanical shaker was utilized for the equilibrations at room temperature. Radioactivity measurements were done using a high purity germanium detector (HPGe) (Canberra, Australia, relative efficiency: 30%, resolution: 1.9 keV at 1332 keV) coupled to 8k channel analyzer. The characterization of the chemical systems were done using X-ray diffraction (XRD), surface area, point of zero charge (PZC), thermogravimetry and transmission electron microscopic (TEM) measurements (Section 2.7). Different techniques used for the studies related to sorption process were inductively coupled plasma optical emission spectrometry (ICP-OES: Horiba JY Activa-500), inductively coupled plasma mass spectrometry (ICPMS: VG PQ ExCell, VG Elemental, UK), neutron activation analysis (NAA), X-ray photoelectron spectrometry (XPS: ESCA and AES System, Surface Nano Analysis, GmbH, Germany) and electrochemical system (potentiostat/galvanostat: CHI 760E from CH Instruments). The basic principles of each of these techniques have been discussed in Section 3.2.2.

4.3. Experimental

4.3.1. Preparation of MnO_2

The manganese dioxide was prepared by two wet chemical methods [Method-1 (M-1) and Method-2 (M-2)] and one dry solid state mixing method [Method-3 (M-3)]. The preparation procedure has already been discussed in Chapter 2, Section 2.4.1. Briefly, in Method-1 [90], $KMnO_4$ (21.3 g L^{-1}) and $MnSO_4$ (71.4 g L^{-1}) solutions were mixed dropwise with constant stirring at 90 ^oC. In Method-2 [68], hot concentrated HCl was added to 0.4 M $KMnO_4$ solution and the resultant solution was heated to 90 ^oC under constant stirring. In Method-3 [91], $KMnO_4$ and manganese acetate salts were mixed together in an agate mortar for 1 h and the mixture taken in DI water was heated at 90 ^oC for 6 h. The MnO_2 samples thus prepared, were air-dried and stored in polypropylene bottles for further use. These synthesized MnO_2 was characterized using X-ray diffraction (XRD), surface area, point of zero charge (PZC), thermogravimetry (TG) and transmission electron microscopic (TEM) measurements (Section 2.7). The details of these measurements have already been discussed in the earlier chapter, Section 2.7.

4.3.2. Sorption studies of arsenic by MnO_2

The arsenic uptake studies were carried out using ^{76}As radiotracer solutions of As(III) and As(V), separately, prepared as per procedure given in Section 2.9. After preparation of arsenic tracer, the oxidation state of the arsenic in the prepared solutions was confirmed by solvent extraction procedure (Section 2.10). The methodology used for the sorption study has been explained in Section 3.3.2. The pH range investigated in the sorption study was 1 – 11 with the sorbent dose of 0.1 g, the arsenic concentration of 2 mg L^{-1} and the optimized equilibration time of 30 min. The studies were done at room temperature and agitation speed maintained as 100 rotations per minute (rpm). Sorption of arsenic was calculated from the initial and final count rates using equation 3.1. These experiments were carried out for As(III) and As(V) solutions, separately, using MnO_2 samples prepared from the three methods.

4.3.3. Kinetic studies for arsenic sorption by MnO_2

The kinetic studies for arsenic sorption on MnO_2 sorbents were done. For these studies, the equilibration time was varied from 0.5 - 60 min. Accurately weighed MnO_2 samples (~ 0.1 g each) were added to the experimental solutions and pH was maintained at 7. The procedure adopted has been explained in detail in Section 3.3.2.

4.3.4. Isotherm studies for arsenic sorption by MnO_2

The adsorption isotherms for As(III) and As(V) sorptions on MnO_2 systems were studied using arsenic radiotracer. The total arsenic was a combination of fixed concentration of arsenic tracer (2 mg L^{-1}) plus varying amounts of inactive arsenic (2 - 400 mg L^{-1}). Experiments were carried out at neutral pH using the optimized parameters, viz. 0.1 g of MnO_2 and 30 min equilibration. The count rate of arsenic in solution was measured, before and after equilibration, and the percentage sorption was calculated using equation 3.1.

4.3.5. Leaching studies on MnO_2

The leaching of manganese from MnO_2, during the sorption of arsenic was systematically studied. The manganese leaching in the absence of arsenic was studied by taking 0.1 g of MnO_2 in 25 mL of DI water (pH = 7) and equilibrating the mixture for 30 min. The similar experiment was also carried out with 25 mL DI water containing 2 mg L^{-1} of arsenic [As(III) or As(V)]. After equilibration, the sorbent was separated by filtration, using whatman 42 filter paper. The supernatant was analysed for manganese, by neutron activation analysis (NAA), using pneumatic carrier facility (PCF) of Dhruva reactor (Mumbai, India). The sample preparation for NAA was as follows: 0.5 mL of each supernatant solution was evaporated on filter paper (1 cm x 1 cm) and triply sealed in clean polyethylene sheets. For Mn standard, Merck ICP manganese standard (1 g L^{-1}) solution was evaporated in similar manner and irradiated along with the samples and polyethylene blank. The quantification of Mn (^{56}Mn, $t_{1/2}$ - 2.58 h, $E\gamma$ - 846.76 and 1810.73 keV) was done by relative method of NAA. The relevant nuclear data of manganese are given in Table 2.3.

4.3.6. Regeneration studies on MnO_2

The desorption study was done on the arsenic sorbed MnO_2. The sorption was done following the procedure used for sorption study (Section 3.3.2). The arsenic sorbed MnO_2 was separated from the suspension by centrifugation and initial counts for ^{76}As was measured. The MnO_2 was then equilibrated with 10 mL each of 0.1, 0.5 and 1 M NaOH for 30 min at room temperature. The suspension then centrifuged, supernatant was discarded and the final activity of ^{76}As remaining on MnO_2 was measured in an identical geometry. Percentage regeneration of arsenic was calculated from the initial and final count rates of ^{76}As on MnO_2.

4.3.7. Reusability studies on MnO_2

The regenerated arsenic sorbed MnO_2 was utilized further on fresh arsenic tracer solutions (2 mg L^{-1}), to see the reusability of the sorbent. The procedure was repeated upto 7 cycles.

4.3.8. Effect of common ions on arsenic sorption by MnO_2

The effect of common ions on the arsenic sorption was studied using Na^+, Ca^{2+}, Mg^{2+}, Cl^-, HCO_3^- and PO_4^{3-} ions. During the study, 0.1 g MnO_2 was taken, the pH was maintained as neutral and arsenic concentration was taken as 2 mg L^{-1}. The concentrations of interfering ions were varied from 5 to 5000 mg L^{-1}.

Sorption experiment was also carried out using two synthetic groundwater samples prepared following the procedure given in the literature [133], one with low ionic strength (SG-1) and other having high ionic strength (SG-2). These synthetic groundwater samples were spiked with As(III)/As(V) radiotracer solutions (containing 2 mg L^{-1} arsenic) for sorption studies.

4.3.9. Application of MnO_2 to arsenic contaminated groundwater

Two real groundwater samples (GW-1 and GW-2) were collected from local tube wells in arsenic contaminated regions of North 24 Parganas, West Bengal, India. Sorption experiments were carried out onsite using 25 mL of groundwater and using 0.1 g MnO_2. After equilibration, the precipitates were filtered, through Whatman 42 filter paper, the filtrates were collected and analyzed for arsenic using ICPMS (VG PQ ExCell, VG Elemental, UK). The concentrations of arsenic were also determined in the groundwater samples before sorption using the same technique. The detailed procedure has been explained in Section 3.3.8.

4.3.10. Study of arsenic sorption mechanism on MnO_2

4.3.10.1. Solvent extraction studies

For studying the oxidation state of arsenic after interaction with MnO_2, a solvent extraction method using benzene was applied. MnO_2 sorbed with As(III) / As(V) radiotracer (procedure of sorption was as per Section 3.3.2), was agitated with 10 mL of 0.1 M NaOH at room temperature for 30 min and centrifuged. The arsenic species got desorbed from MnO_2. The supernatant, containing arsenic, was evaporated to near dryness, 10 mL of concentrated HCl was added and the count rate of ^{76}As was measured (C_{ini}). The solution was transferred to a separating funnel and 10 mL of benzene (pre-equilibrated with concentrated HCl) was added to it. The mixture was agitated for ~10 min and the phases were allowed to separate and the count rate (^{76}As) of aqueous phase was measured (C_{fin}). The percentage of As(V) was calculated using equation 2.22. The detailed scheme is given in Fig. 2.20.

4.3.10.2. XPS measurements

For XPS measurements, sample preparation was done as follows: (1) Blank MnO_2 pellet: 0.25 g MnO_2 was agitated with 25 mL of DI water for 30 min. (2) Arsenic sorbed MnO_2: As(III) or As(V) solution of 5 mg L^{-1} at pH 7 was equilibrated with 0.1 g of MnO_2 for 30 min. MnO_2 was filtered in both the cases, air-dried and pelletized (pellet diameter: 10 mm) using hydraulic press. (3) For standard arsenic pellets: As_2O_3 and As_2O_5 were used as such.

XPS was done utilizing electron spectroscopy for chemical analysis (ESCA) and auger electron spectroscopic (AES) system (Surface Nano Analysis, GmbH, Germany). The measurements were done with Al-Kα (1486.6 eV) as X-ray source and hemispherical analyser (PHOBIOS 150 3D Delayline Energy Analyser). The binding energy scale was calibrated using C-1s peak (284.5 eV) as an internal reference. The peak fitting and deconvolution was done by CASA software. The percentage area coverage in each peak were calculated by taking GL-30 [Gaussian to Lorentzian with Gaussian: 30 %].

4.3.10.3. Electrochemical studies

For understanding the mechanism of arsenic sorption on MnO_2, electrochemical studies were carried out. The studies were done using potentiostat/galvanostat (CHI 760E; from CH Instruments) with three electrode geometry. Modified glassy carbon electrode (GCE), Ag/AgCl and Pt electrodes were used as working, reference and counter electrodes respectively. The experiments were done in quiescent condition and at 298 K. For the experiments, the glassy carbon electrode was modified following the procedure below. Before modification the electrode surface was cleaned by rubbing with 1 μm alumina powder and sonication for 10 min. The MnO_2 suspension was made by 15 min sonication of a mixture of 10 mg MnO_2 in 1 mL DI water containing 0.02 % nafion solution. For modification of electrode surface, 10 μL of solution was drop casted onto the glassy carbon electrode surface. The modified electrode was used in neutral solutions (pH 7) containing 0.005 M of KNO_3. Cyclic voltammetry (CV) and chronopotentiometry (CP) measurements were made without and with the addition of As(III)/As(V) (scan rate: 50 mV s^{-1}).

4.4. Results and discussion

4.4.1. Sorption studies of arsenic by MnO_2

The arsenic sorption studies were done at an arsenic concentration of 2 mg L^{-1} by varying the pH of the solutions from 1 - 11. The equilibration time was fixed as 30 min and done at room temperature. The sorption plots for As(III) and As(V) using all the three MnO_2 samples are given in Figs. 4.1 and 4.2. It is observed that the MnO_2, prepared by solid state mixing method, has promising sorption efficiencies for both As(III) and As(V). The sorption was quantitative up to pH 9. The results are similar to the reported quantitative arsenic sorption by MnO_2 in neutral and acid media [134-135]. But at pH > 9, the sorption efficiency reduced significantly.

The point of zero charge (PZC) of all the three synthesized MnO_2, was found to occur at pH around 4. The surface of MnO_2 is realized to bear a positive charge at pH < PZC. From the arsenic speciation plot given in Figs. 1.3 - 1.4, the As(III) exists as neutral species ($H_3AsO_3^0$) upto pH 9 whereas As(V) species exists as negatively charged ($H_2AsO_4^-$, $HAsO_4^{2-}$) species [54]. Complex formation occurs between the –OH group on the MnO_2 surface as well as the –OH group on the arsenic species is also anticipated for the arsenic-MnO_2 systems (the structure of both the arsenic oxyhydroxide species are given in Fig. 1.2). To be mentioned here that the desorption followed by solvent extraction studies, Section 4.4.9.1, indicated that during sorption of As(III) on MnO_2, the arsenic species is oxidized to As(V). It is thus realized that in all the arsenic-MnO_2 systems, the arsenic is adsorbed on MnO_2 as As(V).

The sorption of As(V) on MnO_2 at pH < 9 was quantitative due to electrostatic interaction. For As(III), due to rapid oxidation in the presence of MnO_2, the sorption remained quantitative upto pH < 9. Thus, the sorption of arsenic on MnO_2 up to pH ~ 9 is understandably due to electrostatic interaction mainly, in addition to some contribution from complexation process, as will be discussed later. When, pH > 9, i.e. at higher alkaline condition, the surface of the sorbents are negatively charged due to the deprotonation of the surface –OH groups. Arsenic also exist as negatively charged species. Due to the electrostatic repulsive force, the sorption efficiency decreases significantly. The results clearly indicate that the initial oxidation state of arsenic does not affect the sorption process any significantly.

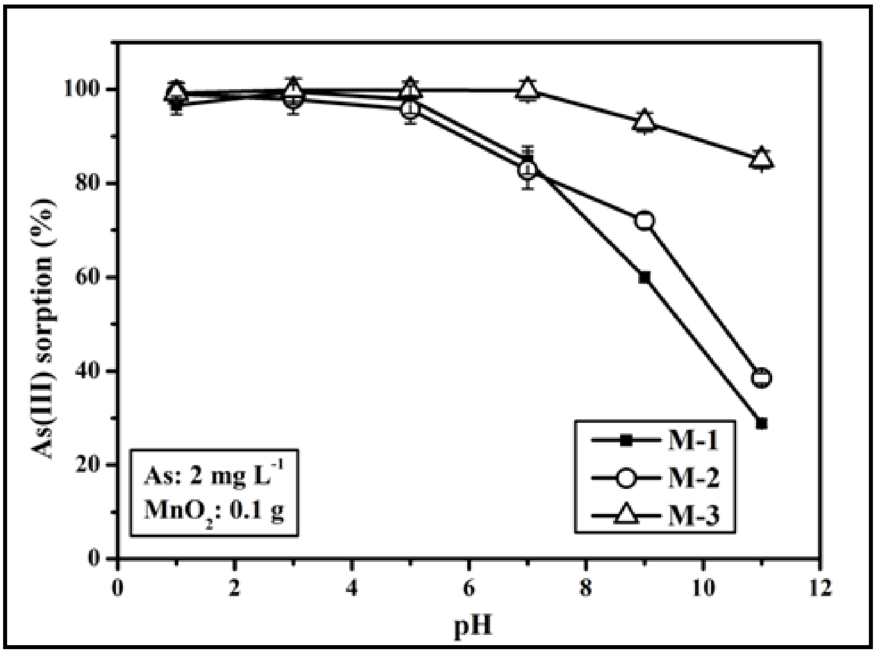

Figure 4.1: Sorption plot of As(III) on MnO_2

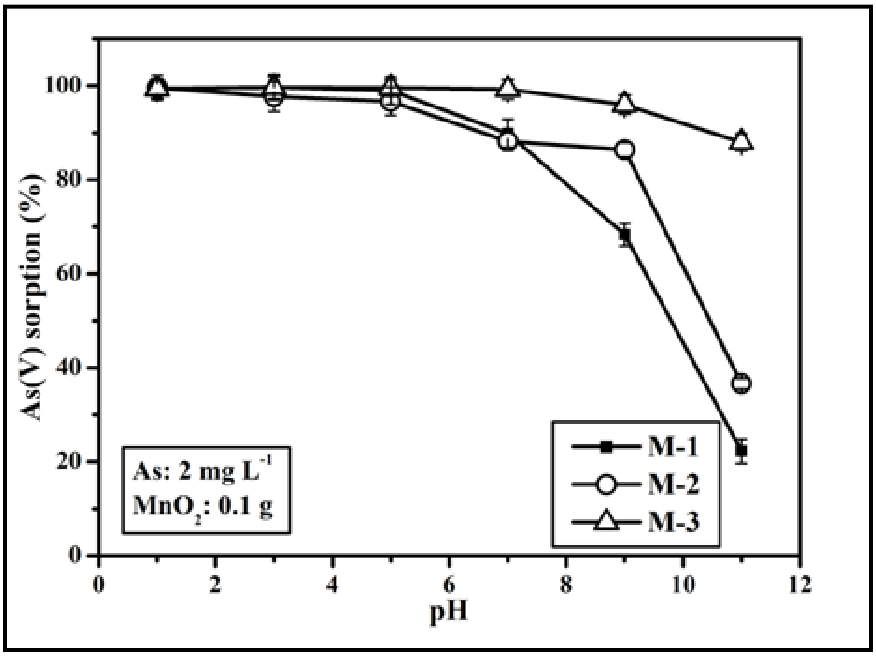

Figure 4.2: Sorption plot of As(V) on MnO_2

4.4.2. Kinetic studies for arsenic sorption by MnO_2

The As(III) and As(V) sorption kinetics at neutral pH for the MnO_2 prepared from solid state mixing method (M-3) are shown in Fig. 4.3. From the kinetic plots, it has been observed that the sorption of both As(III) and As(V) species are very fast (> 98% even for 30 s equilibration time). On further increase in the equilibration time, only marginal increase in the sorption is observed. The equilibration time for all the further studies was thus fixed as 30 min for maximum uptake.

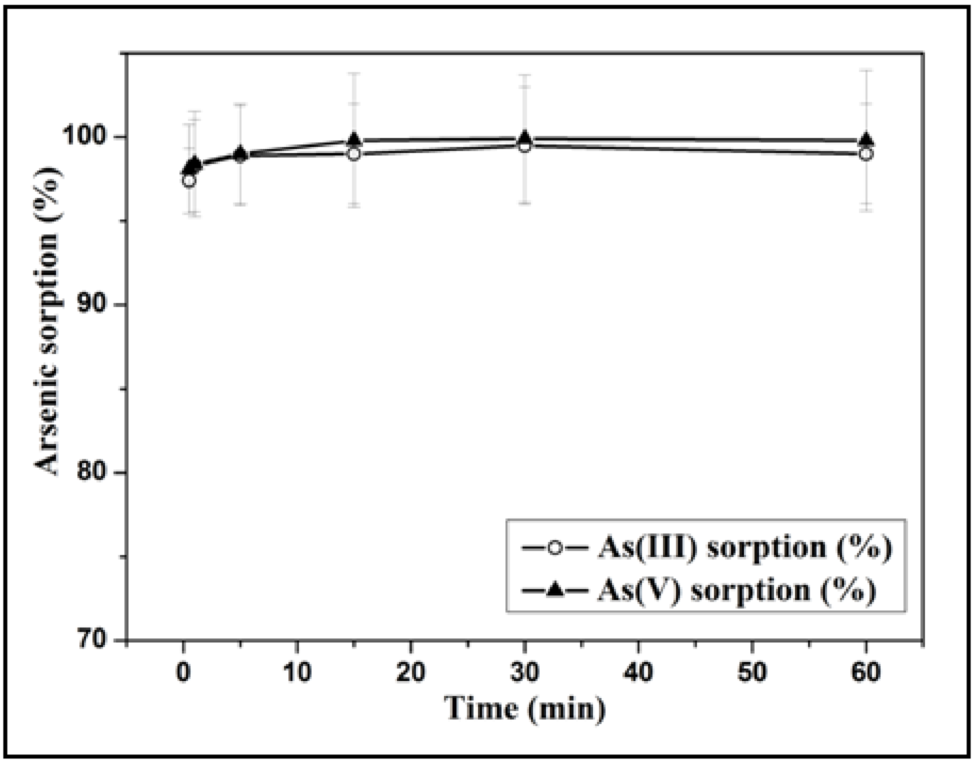

Figure 4.3: Kinetic plot of As(III) and As(V) on MnO_2

The kinetics experimental data for As(III) and As(V) sorption by MnO_2 (prepared by solid state method; M-3) was evaluated by both pseudo first order (PFO) and pseudo second order (PSO) kinetic models (equations 3.2 and 3.3). The data fitted well with pseudo second order (PSO) kinetic equation (equation 3.3). This infers that chemisorption as the predominant mechanism for sorption of As(III) and As(V) by MnO_2. The plot is given in Fig. 4.4. The kinetic parameters obtained from the plots are listed in Table 4.1.

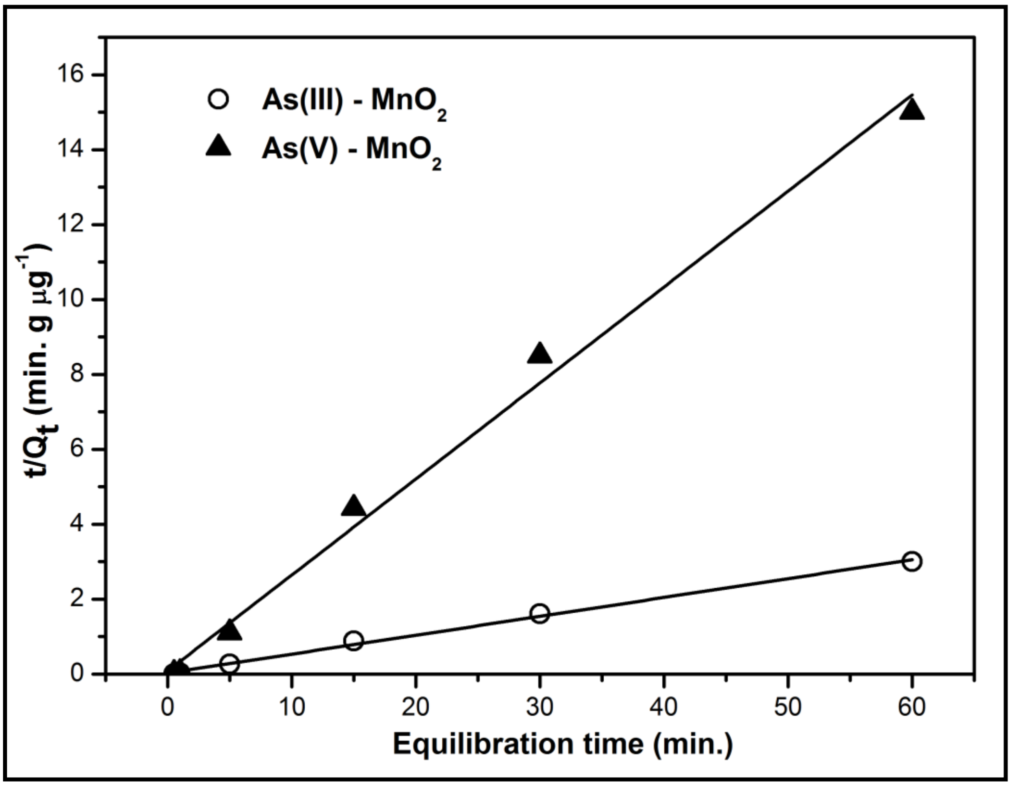

Figure 4.4: Pseudo second order kinetic plot for sorption of As(III) and As(V) on MnO_2 (M-3). (Triangles are the experimental data and the straight lines are the linear fits following equation 3.3).

Table 4.1 A: Kinetic fitting parameters for PSO reaction for As(III) and As(V) adsorption by MnO_2 (M-3)

Sorbent	**Arsenic species**	**Q_e (calculated) mg g^{-1}**	**K_2**	**R^2**
MnO_2	As(III)	0.020	8.1 X 10^{-4}	0.996
	As(V)	0.039	5.1 X 10^{-5}	0.992

4.4.3. Isotherm studies for arsenic sorption by MnO_2

Langmuir and Freundlich isotherms are commonly used to describe the sorption equilibrium [117]. It is observed that the sorption of As(III) and As(V) by MnO_2 follows the Freundlich adsorption isotherm (equation 3.5) [Figs. 4.5 - 4.7]. This sorption model suggests a multilayer sorption on heterogeneous surface sites of MnO_2 [118].

The Freundlich adsorption capacities (K_f) and Freundlich adsorption intensity (n) values obtained for the studied systems are listed in Table 4.2. It is indicated from the Table 4.2 that the 'n' value, $n > 1$ for all the MnO_2 samples, suggesting that, (1) MnO_2 samples have large heterogeneity and (2) the sorption of arsenic by all the MnO_2 samples are very favorable process [119].

From the K_f values as well as the experimental capacities obtained, the arsenic adsorption capacity for MnO_2 prepared from the solid state mixing method (M-3) is found to display the highest value (~60 mg g^{-1}) [85], much higher compared to the capacities displayed by the MnO_2 samples (M-1 and M-2) prepared from the wet chemical methods (~4 mg g^{-1}) [84]. This was explained in terms of the higher surface area (131 m^2 g^{-1}) for the former MnO_2 as compared to the latter. The sorption capacity is found to be almost half for As(III) as compared to As(V). This may be due to the surface modification that occurs due to the oxidation of As(III) while getting adsorbed on the MnO_2 surface.

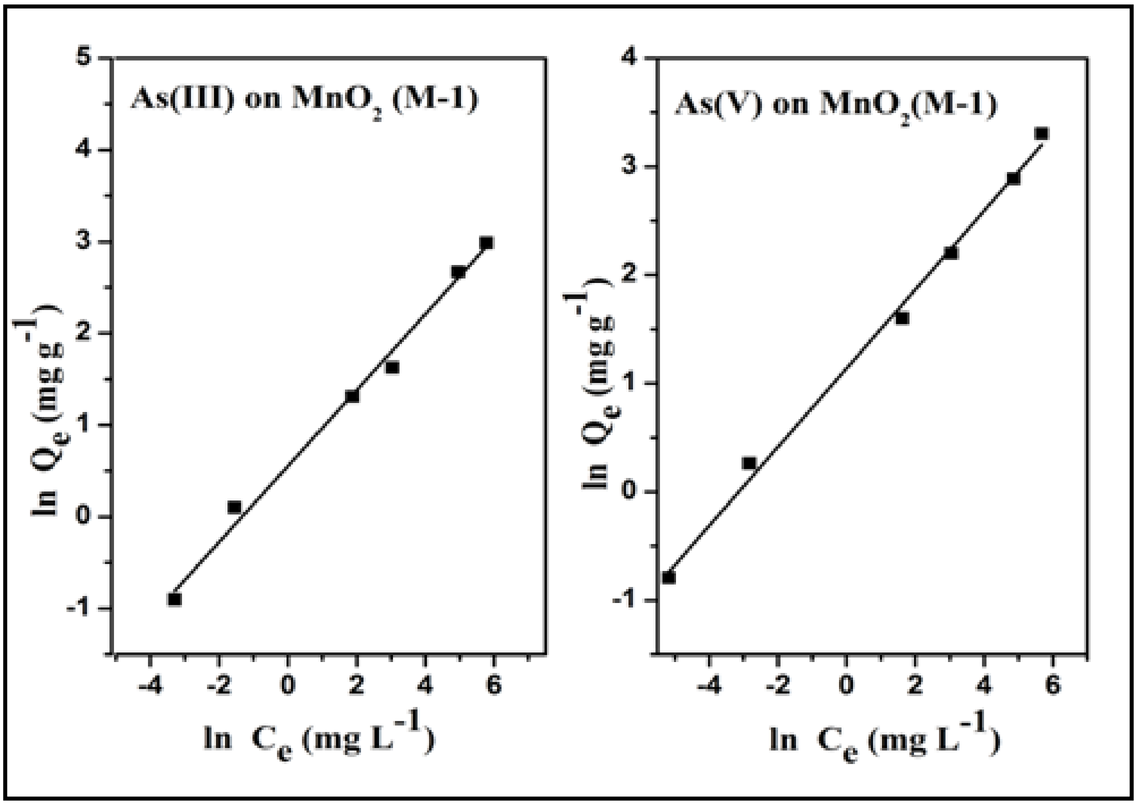

Figure 4.5: Freundlich isotherm for sorption of As(III) and As(V) on MnO_2 (M-1). (Squares are the experimental data and the straight lines are the linear fits following equation 3.5).

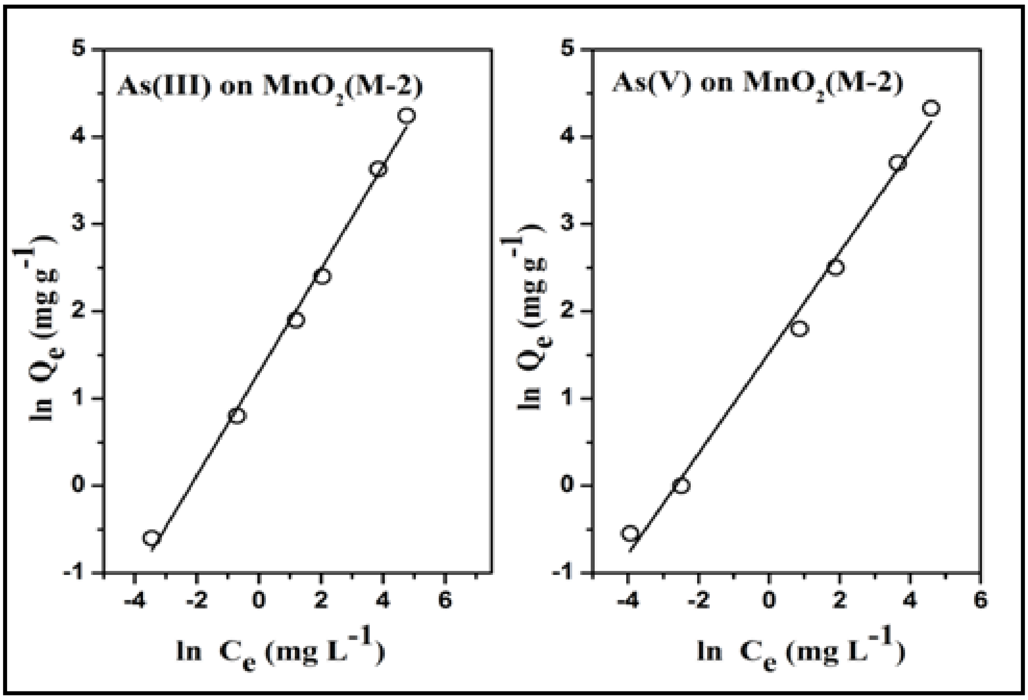

Figure 4.6: Freundlich isotherm for sorption of As(III) and As(V) on MnO_2 (M-2). (Circles are the experimental data and the straight lines are the linear fits following equation 3.5).

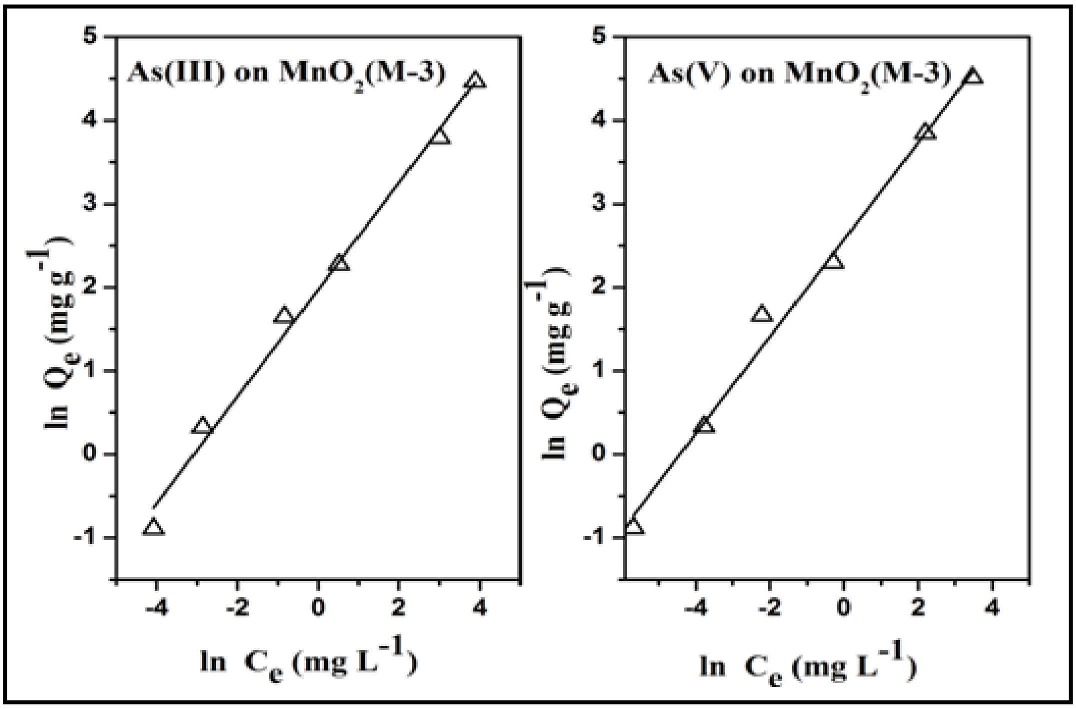

Figure 4.7: Freundlich isotherm for sorption of As(III) and As(V) on MnO_2 (M-3). (Triangles are the experimental data and the straight lines are the linear fits following equation 3.5).

Table 4.2: Fitting parameters for the Freundlich isotherms for As(III) and As(V) adsorption on MnO_2

Sorbent	**Arsenic species**	**R^2**	**K_f (mg g^{-1})**	**n**
MnO_2 (M-1)	As(III)	0.990	1.74	2.42
	As(V)	0.995	3.13	2.75
MnO_2 (M-2)	As(III)	0.995	3.68	1.69
	As(V)	0.991	4.59	1.74
MnO_2 (M-3)	As(III)	0.991	7.19	1.56
	As(V)	0.989	13.09	1.72

4.4.4. Leaching Studies on MnO_2

Manganese is categorized as a secondary contaminant [120], i.e. no direct impact on health but imparts aesthetic changes (includes change in odour, taste etc) to water. The drinking water specification for manganese is 0.05 mg L^{-1}.

For leaching studies, the quantification of Mn was done by neutron activation analysis (NAA) using relative method. The results of quadruplet analyses are listed in Table 4.3. On equilibration of MnO_2 (0.1 g) in 25 mL DI water, the Mn release was quantified as (0.10 ± 0.010) mg L^{-1}. Even though the value is higher compared to the USEPA limit (0.05 mg L^{-1}), it actually corresponds to the solubility of MnO_2 (0.1 mg L^{-1}) at pH 7 [136]. The quantification of Mn in the supernatant in the presence of arsenic showed that sorption of As(III) and As(V) did not cause any increase in the Mn concentration. During the sorption process, the As(III) species undergo oxidation to As(V), while, the Mn(IV) undergoes reduction to Mn(II). Apparently, the so produced Mn(II) binds arsenic species through some complex formation and thus enhancing the arsenic sorption process and reducing the manganese leaching, as indicated from the observed results in the presence of As(III) [66, 71, 121, 137-138].

Table 4.3: Results obtained for Mn leaching from MnO_2

	Mn conc. (mg L^{-1})		
	Without As	**Presence of As(III)**	**Presence of As(V)**
MnO_2	0.110 ± 0.010	0.098 ± 0.010	0.112 ± 0.006

4.4.5. Regeneration Studies on MnO_2

The desorption of arsenic from MnO_2 was studied using different concentrations of NaOH. Desorption using 0.1 M NaOH was most effective; > 95 % desorption was achieved for both As(III) and As(V) at room temperature in two cycles.

4.4.6. Reusability Studies on MnO_2

The regenerated MnO_2 was reused in fresh arsenic [As(III) and As(V)] radiotracer solutions (2 mg L^{-1}) for upto 8 cycles (one cycle comprising of uptake of arsenic from 2 mg L^{-1} solution utilizing 0.1 g of MnO_2) and the results are given in the Fig. 4.8. The results show that the sorption efficiency is always better for the MnO_2 prepared by solid state mixing method. The sorption percentage for both, As(III) and As(V) species remained > 80 % upto the 6th cycle of reuse.

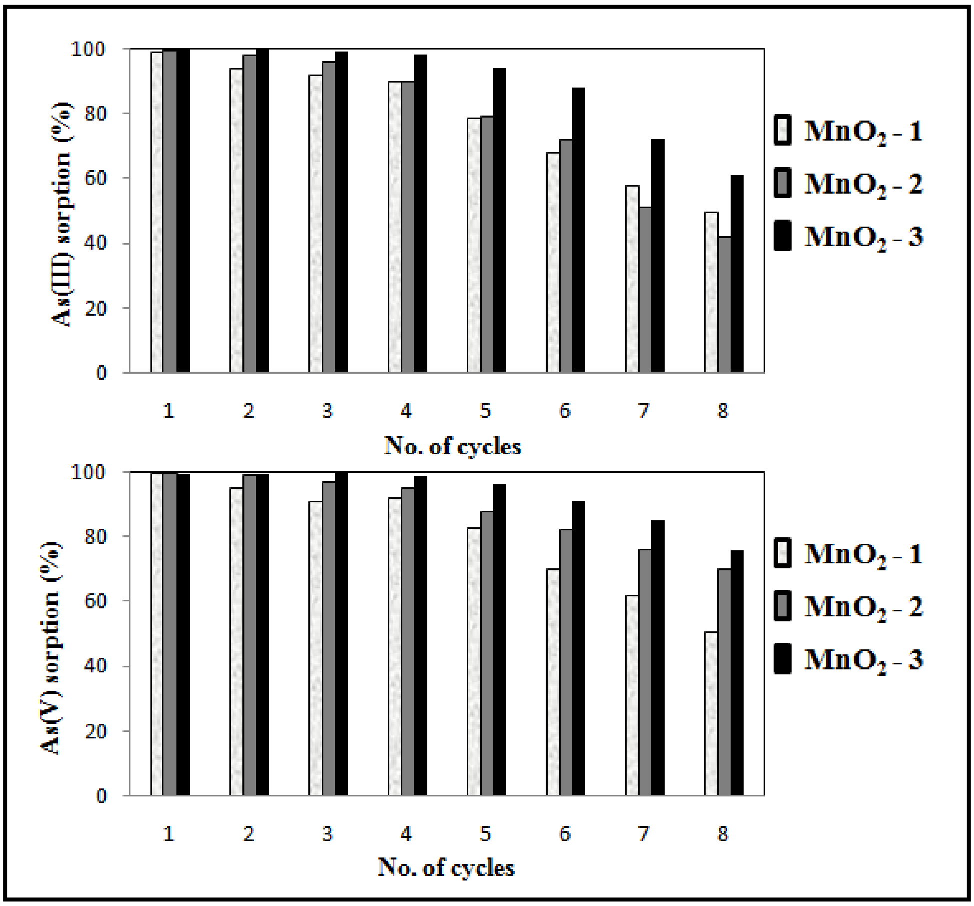

Figure 4.8: Reusability study of MnO_2 for (a) As(III) and (b) As(V)

4.4.7. Effect of common ions on arsenic sorption by MnO_2

The effect of common ions on arsenic sorption was studied using MnO_2 as sorbent. Na^+, Ca^{2+}, Mg^{2+}, Cl^-, HCO_3^- and PO_4^{3-} ions were listed as the commonly occurring ions in ground water [121]. The concentration range of these ions in groundwater is listed in the previous chapter, Table 3.5. The concentrations of these ions were chosen in three different ranges in the current study:

(i) lower range, i.e. ten times lower than the typical concentration in the groundwater,

(ii) in the range of the typical concentration in the groundwater and

(iii) higher range, i.e. ten times more than the typical concentration in the groundwater (Table 4.4).

The presence of HCO_3^- and PO_4^{3-} has a retarding effect on the arsenic sorption [139], but the decrease occurs mostly at very high concentration of these ions, i.e, at > 100 mg L^{-1}. This is possibly due to the structural similarity of these ions with the arsenate group. However, this effect is not a big concern for arsenic removal, because, such a high level of phosphate and bicarbonate are not seen commonly in groundwater samples.

Table 4.4: Effect of interfering ions on sorption of arsenic (2 mg g^{-1}) by MnO_2.

Ion	**Amount taken (mg L^{-1})**	**As(III) sorption (%)**	**As(V) sorption (%)**
Ca^{2+}	5	99.8	99.6
	50	99.4	99.6
	500	99.5	99.3
Mg^{2+}	15	99.5	99.7
	150	99.6	99.5
	1500	99.5	99.6
Na^+	50	99.7	99.8
	500	99.8	99.6
	5000	99.5	99.3
Cl^-	50	99.6	99.5
	500	99.1	99.6
	5000	97.3	98.5
HCO_3^-	60	99.8	99.5
	600	92.1	93.5
	6000	85.2	88.6
PO_4^{3-}	5	99.7	99.6
	50	86.5	83.2
	500	43.2	48.3

To understand the efficacy of MnO_2 as a sorbent, two synthetic groundwater (SG-1 and SG-2) samples were prepared and were spiked with 2 mg L^{-1} of arsenic (as radiotracer). The results of sorption study along with the compositional analysis of these systems are given in Table 4.5. From the table, it is evident that the arsenic sorption efficiency remains quite quantitative inspite of the presence of the other common ions.

Table 4.5: Sorption of arsenic (2 mg L^{-1}) from synthetic groundwater samples

Sorption of arsenic (%)	**SG-1**	**SG-2**
As(III)	97.2 ± 1.6	98.4 ± 1.6
As(V)	99.4 ± 1.8	97.6 ± 1.7
Chemical composition of water (mg L^{-1})		
pH	7.8 ± 0.1	8.4 ± 0.1
Na^+	30.3 ± 0.2	34.9 ± 0.2
K^+	2.7 ± 0.1	9.3 ± 0.1
Mg^{2+}	7.2 ± 0.1	58.4 ± 0.1
Ca^{2+}	16.6 ± 0.3	31.2 ± 0.6
Cl^-	1.7 ± 0.1	176.0 ± 3.5
SO_4^{2-}	35.2 ± 0.7	24.0 ± 0.5
NO_3^-	0.7 ± 0.1	7.5 ± 0.2
TOC	3.4 ± 0.1	1.5 ± 0.1
TIC	16.0 ± 0.3	23.0 ± 0.5

4.4.8. Application of MnO_2 to arsenic contaminated groundwater

Two real groundwater samples (GW-1 and GW-2) were collected directly from North 24 Parganas, West Bengal, India. The characterization of these groundwater samples are shown in Chapter 3, Table 3.7. It has been observed that the removal of arsenic from these real groundwater samples by MnO_2 is very effective to bring the arsenic level below ~ 10 μg L^{-1} (WHO limit). The results obtained for the arsenic concentration in real groundwater samples after equilibration with MnO_2 (M-3) are given in Table 4.6. This study suggests that MnO_2 synthesized via solid state reaction method is very effective for the removal of arsenic from real groundwater samples.

Table 4.6: Concentration of arsenic in groundwater before and after sorption using MnO_2 prepared via solid state reaction method.

Sample	**pH**	**Initial arsenic conc. (μg L^{-1})**	**Conc. after filtration and sorption by MnO_2 (μg L^{-1})**
GW-1	7.3 ±0.2	163 ± 8	1.0 ±0.2
GW-2	7.7 ±0.2	710 ± 35	5.6 ±0.3

4.4.9. Study of arsenic sorption mechanism on MnO_2

4.4.9.1. Solvent extraction studies

A solvent extraction method using benzene was applied for the determination of oxidation of arsenic, after sorption by MnO_2. The adsorbed As(III) or As(V) was desorbed from the surface of MnO_2 following the regeneration procedure elaborated in Section 4.3.5. It is known that the oxidation state of arsenic remained same when desorbed using NaOH solution [140]. The results showed that > 95% of the ^{76}As were retained in the aqueous phase after solvent extraction, for both As(III) and As(V) solutions. As given in the literature, the As(III) forms neutral $AsCl_3$ in strong HCl medium. The neutral species is easily extracted into non-polar solvent benzene, whereas As(V), which forms negatively charged species, is not extracted [106]. The results indicated that MnO_2 completely oxidizes As(III) to As(V). Similar observations are also reported in the literatures [68, 141].

4.4.9.2. XPS measurements

Further, study of the oxidation state of arsenic after the interaction with MnO_2, XPS measurements were carried out. XPS survey scans (Figs. 4.9 and 4.10) show the presence of Mn and O in blank MnO_2 and As, Mn and O in As(III) loaded MnO_2. The XPS plots for arsenic standards ($3p_{3/2}$) are given in Fig. 4.11.

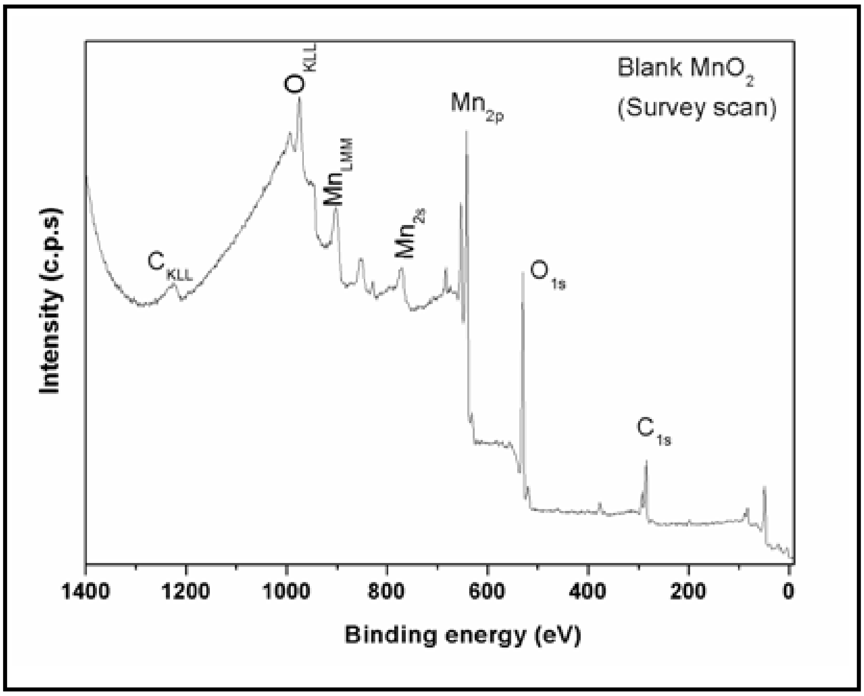

Figure 4.9: XPS survey scan of MnO_2

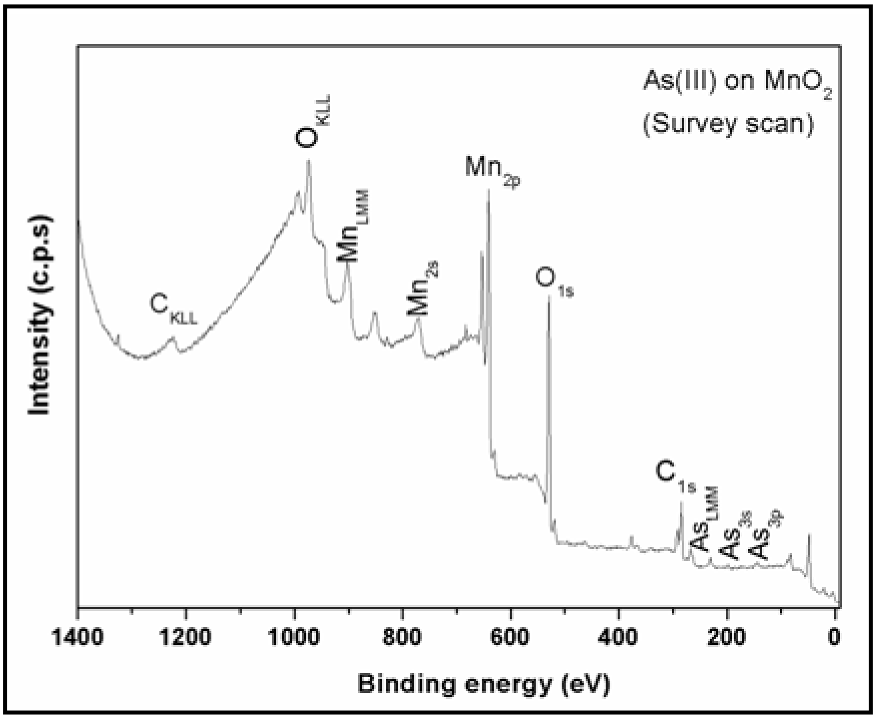

Figure 4.10: XPS survey scan of As(III)-MnO_2

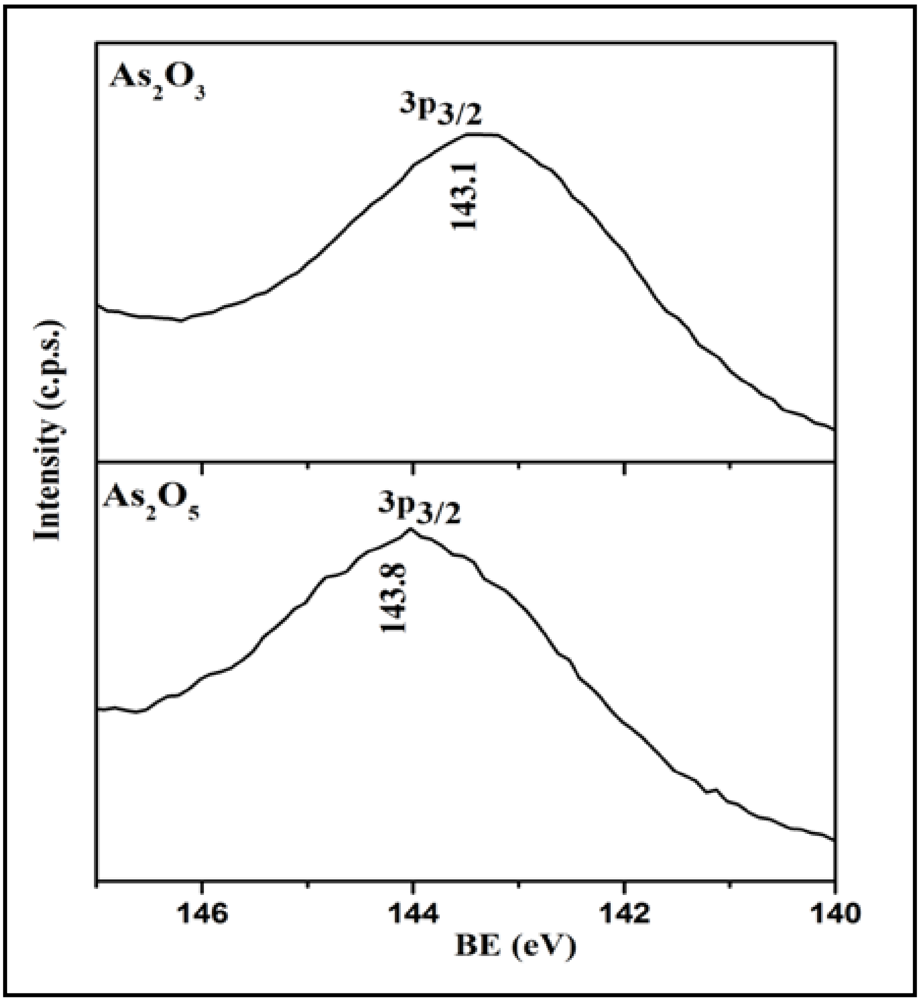

Figure 4.11: XPS plots of arsenic (As $3p_{3/2}$) [As(III) and As(V) standards]

XPS study of MnO_2 system

The XPS *2p* spectrum of MnO_2 is obtained as a doublet, due to spin orbital coupling. The two peaks were (1) Mn $2p_{3/2}$ [binding energy (B. E.) = 641.2 eV] and (2) Mn $2p_{1/2}$ (B.E. = 652.8 eV). The Mn *2p* peaks are characteristics of Mn(IV) in standard MnO_2 [142]. On deconvolution of Mn $2p_{3/2}$ band, two peaks are obtained at B.E. = 640.7 eV and 642.5 eV, respectively, which correspond to Mn(III) and Mn(IV) [Fig. 4.12 (a)]. These results are similar to those reported in the previous literature [143]. The overall results from XPS study are presented in Table 4.7.

Table 4.7: XPS study of MnO_2 - arsenic system (Binding energies in eV)

Sample	**As *3p*$_{3/2}$**	**Mn *2p*$_{3/2}$**	**O *1s***	**Species**
MnO_2	-	640.7	528.9	O^{2-} (Mn - O)
		642.5	530.6	OH^-
As_2O_3: As(III) standard	143.1	-	530.8	O^{2-} (As - O)
As_2O_5: As(V) standard	143.8	-	528.9	O^{2-} (H_2O)
			531.8	O^{2-} (As - O)
As(III)-MnO_2	142.9	639.8	529.5	O^{2-} (Mn - O)
	143.4	641.1	530.1	O^{2-} (Mn - O)
		642.8	530.9	O^{2-} (H_2O)
			531.6	OH^-, H_2O
			532.3	OH^-, H_2O
As(V)-MnO_2	143.5	640.7	530.2	O^{2-} (Mn - O)
		642.5	531.0	O^{2-} (H_2O)
			532.3	OH^-, H_2O
			532.4	OH^-, H_2O

As(III)-MnO_2 system

The arsenic spectrum (As *3p*$_{3/2}$) of As(III) sorbed on MnO_2 is given in Fig. 4.13 (a). On deconvolution of the As *3p*$_{3/2}$ spectrum, two components are observed, indicating the presence of a minor peak of As(III) (B.E. = 142.9 eV) and the major peak of As(V) (B.E. = 143.4 eV). The Mn *2p*$_{3/2}$ spectrum of As(III)-MnO_2 is shown in Fig. 4.12 (b). Deconvolution of Mn *2p*$_{3/2}$ peak, leads to three peaks with B.E. values 639.8, 641.1 and 642.8 eV, attributed to presence of small fraction of Mn(II), Mn(III) and Mn(IV), respectively, present in the MnO_2 (Fig. 4.12 (b) and Table 4.7).

The B.E. of arsenic confirmed the oxidation of As(III) to As(V) on MnO_2 surface, and the B.E. of Mn in As(III) sorbed MnO_2 show the corresponding reduction of Mn(IV) to

Mn(II). This is in accordance with the literature reports [70, 132, 144]. Observations from XPS studies are in agreement with the mechanism that Mn(II) is formed through oxidation of As(III), during the sorption of this arsenic species on MnO_2 surface [85].

As(V)-MnO_2 system

The As $3p_{3/2}$ spectrum of As(V)-MnO_2 system is shown in Fig. 4.13 (b). The spectrum has one peak at 143.5 eV, corresponding to As(V) species only. The Mn $2p_{3/2}$ spectrum of As(V)-MnO_2 is shown in Fig. 4.12 (c). The peak was deconvoluted into two components with B.E. values of 640.7 and 642.5 eV as similar to blank MnO_2. These XPS data confirmed that the As(V) species is sorbed by MnO_2 without any change in the oxidation state.

O 1s spectra

The deconvoluted O *1s* spectra for blank MnO_2, As(III)-MnO_2 and As(V)-MnO_2 are given in Fig. 4.14. The blank MnO_2 [Fig. 4.14 (a)] has two O *1s* peaks at 528.9 and 530.6 eV. The lower peak is attributed to lattice oxygen (O^{2-}) and which could be bonded either to Mn(IV) or Mn(III) in the as prepared MnO_2. The second peak (530.6 eV) is attributed to the OH^-, i.e, oxygen in the adsorbed water layer. The oxygen spectrum of As(III)-MnO_2 [Fig. 4.14 (b)] shows five O *1s* peaks at 529.5, 530.1, 530.9, 531.6 and 532.3 eV respectively. The peaks at the lower binding energies 529.5, 530.1 and 530.9 eV are assigned to O^{2-} linked with Mn in MnO_2 lattice whereas peaks at 531.6 and 532.3 eV are attributed to hydroxide oxygen from the chemically or physically adsorbed water. The oxygen peaks obtained for As(V)-MnO_2 [Fig. 4.14 (c)] are also similar to that of As(III)-MnO_2, suggesting that the sorption of both the arsenic species are similar (i.e. as As(V)) irrespective of their initial oxidation states.

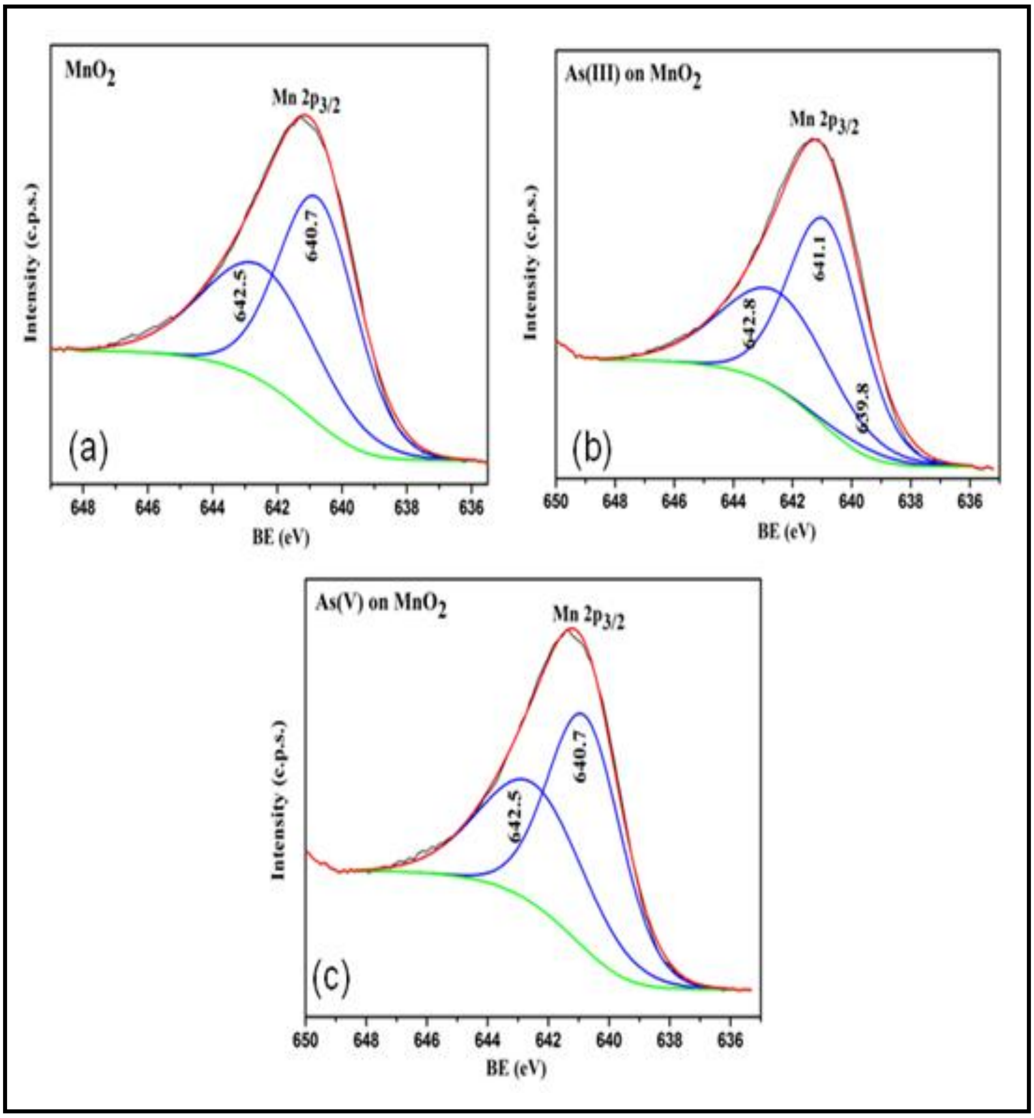

Figure 4.12: Mn *2p$_{3/2}$* XPS plot of MnO$_2$

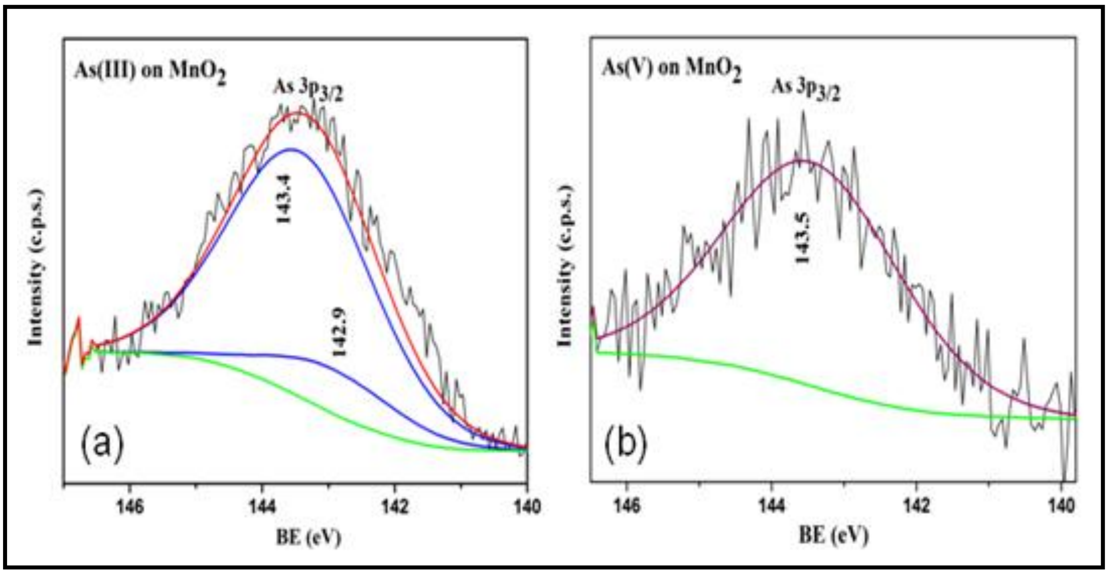

Figure 4.13: As *3p$_{3/2}$* XPS plot of MnO$_2$

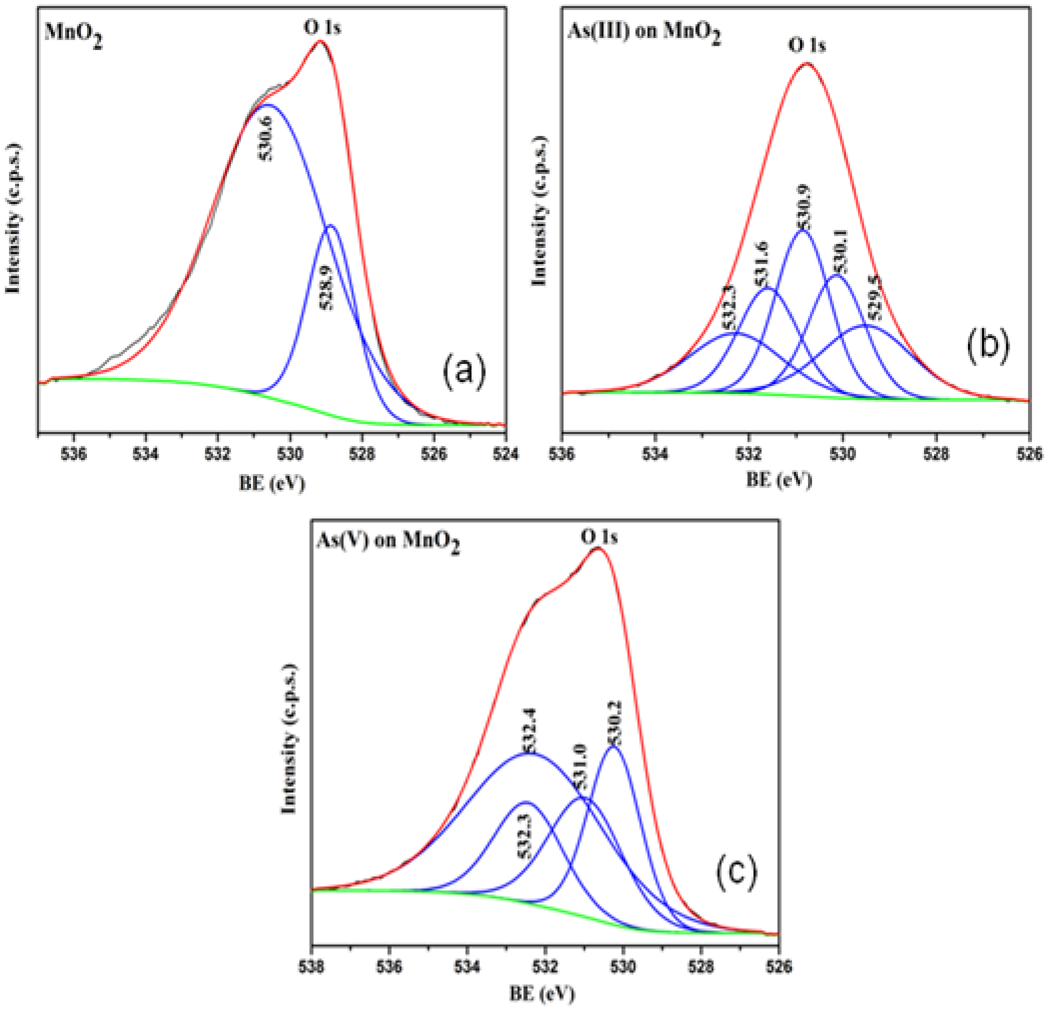

Figure 4.14: O *1s* XPS plot of MnO_2

4.4.9.3. Electrochemical studies

The arsenic - MnO_2 sorption mechanism was further investigated by electrochemical measurements. Cyclic voltammetry (CV) studies were done on MnO_2 (using MnO_2 modified glassy carbon electrode (GCE)), with and without the presence of As(III)/As(V) [Fig. 4.15]. With the addition of As(III) (0.5 mg L^{-1}), two oxidation peaks (0.57 and 1.34 V) and three reduction peaks are observed (0.91, 0.61 and -0.33 V) [Fig. 4.15 (a)]. The CV measurements carried out with increasing concentration of As(III) show that the oxidation peak at 0.57 V is shifted towards positive direction and the peak current is gradually decreased. For oxidation peak at 1.34 V, there is a drastic decrease in the peak current but no shift in the peak position. All the reduction peaks show a negative shifting. The peak current at 0.91 V show a drastic decrease, whereas for peaks at 0.61 and -0.33 V are decreased slowly. Following the dissolution and the solvent extraction studies (Section 4.4.4 and 4.4.9.1), it is realized that the As(III) undergoes oxidation to As(V) by the presence of MnO_2 and adsorbed over the electrode surface. As a result, the electrode surface gain electrons and acts as a reduction center and further oxidation of arsenic becomes difficult causing a decrease in oxidation current. This also results in the shifting of the reduction peak [Mn(II) to Mn(0)] towards negative direction.

When As(V) is used, two oxidation peaks and three reduction peaks are observed in the cyclic voltammogram [Fig. 4.15 (b)], similar to the case of As(III) discussed above. Thus, on addition of As(V), the behavior of the oxidation peak at 0.57 V remains similar to that of As(III). Interestingly, however, for the peak at 1.34 V, there is a negative shifting along with a decrease in the peak current. For the reduction peaks at 0.91 and -0.33 V, the peak current decreased but no shift was observed in the peak positions. Since As(V) in the solution do not undergo any redox reaction during adsorption over the MnO_2 surface, the peak positions remained the same. For the reduction peak at 0.61 V, the peak position showed a negative shifting along with a marginal increase in peak current up to 6 mg L^{-1} concentration.

The CV measurements were also carried out in the simultaneous presence of both As(III) and As(V) species in equal concentrations [Fig. 4.15 (c)]. There was no significant synergistic or antagonistic effect. The responses are very similar to that obtained for the species when they are used individually. The CV responses show that the arsenic - MnO_2 systems are reversible. Due to the availability of redox centers on MnO_2 surface, the intermediate states are easily formed in the presence of As(III)/As(V) species. This result in a strong interaction between both As(III) and As(V) with the MnO_2 modified GCE.

For comparison of the observed CV responses, substantial reports are not available in the literature. The study by Mishra et al, an electrochemical investigation on iron oxide graphene composite for sorption of arsenic [145] revealed that the two reduction peaks observed in the case of As(III) sorption could be attributed to two step reduction of the arsenic sorbed species, i.e As(V) to As(III) followed by reduction to As(0). These can be correlated with the results obtained by our study.

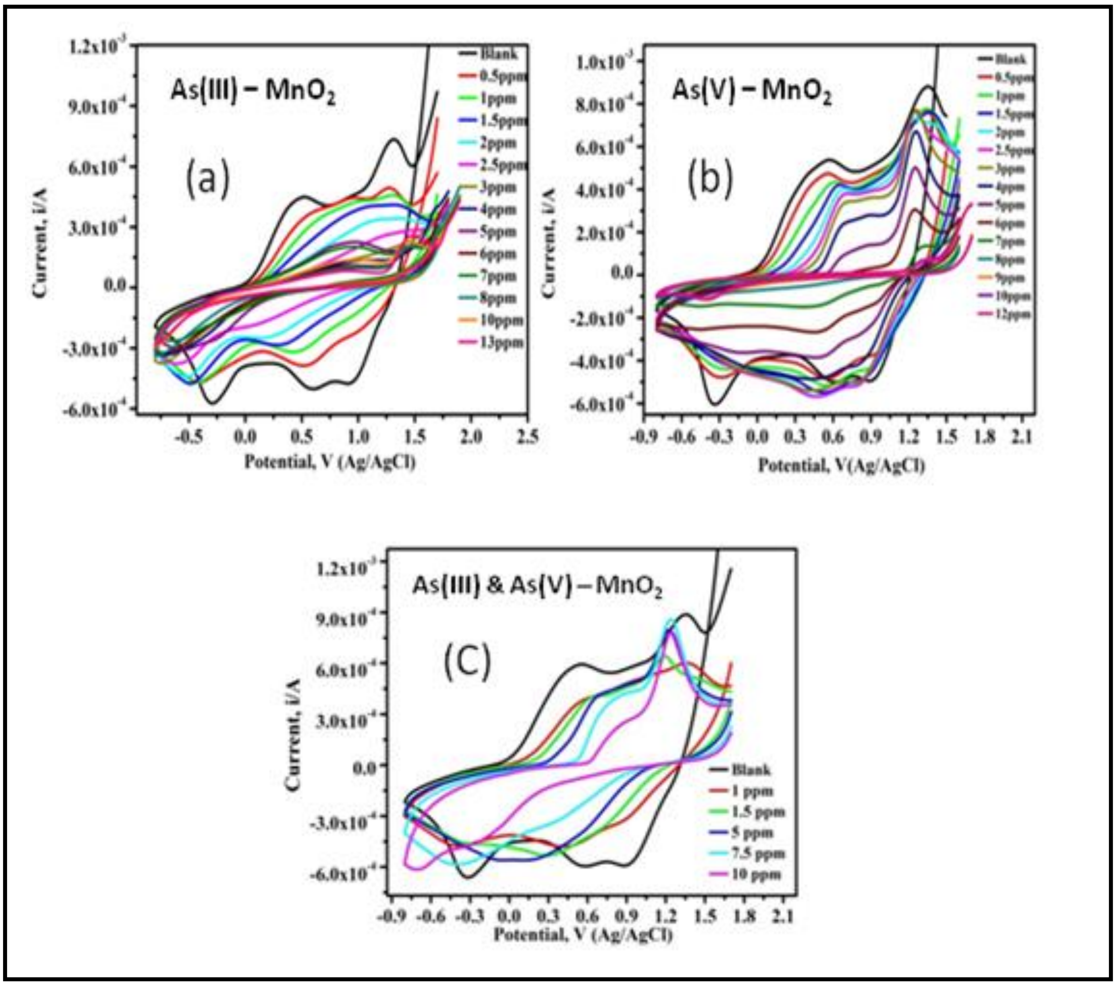

Figure 4.15: CV plots of (a) As(III)-MnO_2 (b) As(V)-MnO_2 and (c) As(III) and As(V)-MnO_2

The chronopotentiometric (CP) measurements were carried out at open circuit conditions to study the interaction of As(III) and As(V) with MnO_2 [Fig. 4.16]. The open circuit potential (OCP) of the modified GCE was measured with time, with and without the addition of As(III) and As(V) (0.5 mg L^{-1}). For the solution without arsenic, the OCP measured for GCE showed a steady change with time. When As(III) was added to solution the OCP underwent an instantaneous negative shifting, whereas when As(V) was added, the OCP showed an instantaneous positive shifting. During the interaction of As(III) on MnO_2, the electrons released by the arsenic was gained by the GCE resulting in a negative shifting of OCP. Thus the As(III) uptake by MnO_2 is realized to be assisted by the oxidation of As(III) to As(V) over the MnO_2 modified electrode. But for As(V)-MnO_2 interaction, there is no redox reaction anticipated. Thus, the CP and CV measurements support the mechanism of uptake for As(III) as the oxidative adsorption process and As(V) undergo adsorption straightaway without any redox reaction.

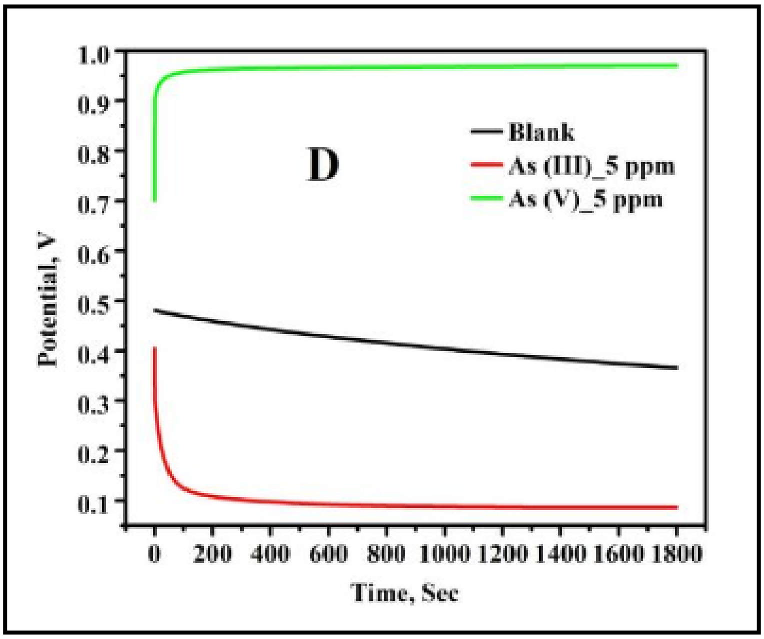

Figure 4.16: CP plot of arsenic - MnO_2 system.

4.5. Conclusion

The studies on MnO_2 prepared by the three different methods confirmed that the MnO_2 prepared by solid state method is having better sorption properties. The mechanism of arsenic and MnO_2 was investigated. The preliminary studies of oxidation state of arsenic after sorption on MnO_2 was done by solvent extraction. From the results, it was evident that the arsenic species after sorption remained as As(V) only, irrespective of the initial oxidation state. The XPS studies on the As(III) and As(V) sorbed MnO_2, elucidated the arsenic removal mechanism as sorption on MnO_2 by forming As(V). The CV and CP studies confirmed that interaction of both As(III) and As(V) with MnO_2 were different. The results obtained from the studies confirmed that a redox reaction was responsible for the uptake of arsenic by MnO_2.

On MnO_2 surface, the As(III) species got oxidized and adsorbed, whereas the As(V) species adsorbed on the surface as such. During the oxidation of As(III), the Mn(IV) got reduced to Mn(II) [69]. The Mn leaching studies revealed that there was no increase in the Mn content in supernatant after arsenic uptake [85]. Thus confirmed that, the Mn(II) is adsorbed on the MnO_2 surface facilitating the sorption further. From these data as well as the literatures, a mechanism for the sorption of As(III) and As(V) on MnO_2 was proposed [Fig. 4.17].

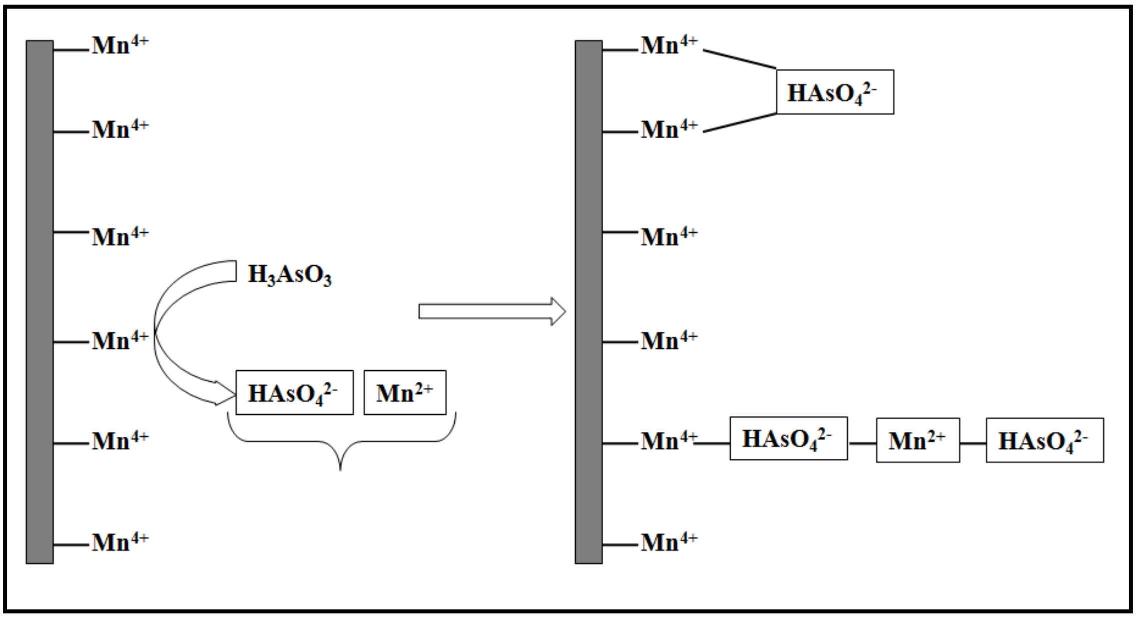

Figure 4.17: Schematic for sorption of arsenic on MnO_2 [141]

Chapter - V

Modified sorbent for arsenic removal from groundwater

5.1. Introduction

Adsorption is a highly utilized method in arsenic contaminated areas. For the removal of arsenic, it is inevitable that the material should be of low cost, easy to operate, easily regenerable and reproducible. There is practical limitation for the use of synthetic sorbents, in powder form. The direct use in column application results in choking up of the column, resulting in high resistance to the feed water flow. Therefore, researchers have tried to modify the well known arsenic sorbents, as a coating on solid inert supports for easy utilization in column mode [46, 146-147].

Among various polymeric sorbents, amberlite XAD resins has been studied by many researchers for the preconcentration or/and removal of heavy metal ions from water [148-150]. The widespread application of thee resin is due to the high surface area and excellent physical, chemical and thermal stability.

Various wet chemical methods are available [151-154] for coating a suitable sorbent onto an inert support materials. Among them, the in-situ coating by applying ultrasound is a clean technology. There are literatures available on ultrasound assisted synthesis of nanomaterials [155-158]. In this method, a very high temperature and pressure is generated for few microseconds, resulting in the free radical formation, which eventually leads to the chemical reaction responsible for the coating of sorbents on the solid supports. Among various resins, the amberlite resin XAD-4 is well known polymeric support material with good sorption properties, thermal stability and easily modifiable [159-160].

From the previous studies (Chapter 3 and 4), manganese dioxide (MnO_2) was found to be very efficient sorbent for arsenic sorption, much better than the iron oxide sorbents. The favorable factors with MnO_2 are: high arsenic sorption efficiency, fast kinetics, tolerance to the co-occurring ions and easy regeneration capability. Hence, MnO_2 was chosen as the sorbent of interest for coating the surface of XAD-4 beads.

MnO_2 was prepared by a sono-chemical reduction method. In-situ coating of MnO_2 was done on XAD-4 resin beads. The detailed procedure of synthesis and characterization methods have already been discussed in Chapter 2. In the present chapter, optimization of the sorbent preparation parameters for MnO_2 coated XAD-4 resin beads as the sorbent, and the application of this sorbent for arsenic removal studies in batch mode utilizing ^{76}As as the radiotracer have been discussed. Various parameters like effect of pH on sorption of arsenic, sorption isotherm, regeneration of the sorbent and application of the sorbent material to real groundwater sample have been evaluated.

5.2. Materials and methods

5.2.1. Reagents and chemicals

The chemicals, potassium permanganate [$KMnO_4$; molecular weight (MW) - 158.03 g mol^{-1}], arsenic trioxide (As_2O_3; MW - 197.84 g mol^{-1}), arsenic pentoxide (As_2O_5; MW - 229.84 g mol^{-1}] and sodium hydroxide pellets (NaOH; MW - 40.00 g mol^{-1}) were of analytical reagent (AR) grade and used as purchased. As the inert support material for MnO_2, amberlite XAD-4 resin beads (20 - 60 mesh size), was used. Before application, these beads were washed thoroughly with deionised water (DI) for removing the impurities. The reagents: concentrated hydrochloric acid (HCl), concentrated nitric acid (HNO_3) and benzene (C_6H_6) were of AR grade and used without further purification. All the necessary dilutions were done using DI water (resistivity 18.2 MΩ cm^{-1} and total organic carbon < 10 μg L^{-1}) obtained from Milli-Q water purification system.

5.2.2. Equipments

All the weighing was done using a high precision analytical semimicro balance (Mettler - Toledo, dual range, readability - 0.01 mg). pH measurements were carried out in Oakton pH meter employing glass electrode (pH700, USA), with digital display having an precision of ± 0.01 unit. A mechanical shaker was utilized for equilibrations at room temperature. Radioactivity measurements were done using a high purity germanium (HPGe) detector (Canberra, Australia, relative efficiency: 30 %, resolution: 1.9 keV at 1332 keV) coupled to 8k channel analyzer. For ultrasound applications, Retsch UR-1 ultrasonic bath (35 kHz, 240 W) was used. For characterization of the sorbent, Fourier-transform infrared spectroscopy (FTIR) analysis, scanning electron microscopy (SEM), neutron activation analysis (NAA) and point of zero charge (PZC) measurements were utilized.

5.3. Experimental

5.3.1. Preparation of modified sorbent

The XAD-4 resin beads, were taken in $KMnO_4$ solution and ultrasound irradiation, using Retsch UR-1 ultrasonic bath (35 kHz, 240 W), was done for 15 min. A sonochemical assisted reduction reaction occurs due to the formation of free radicals. The product, nanosized MnO_2 [92], got coated onto XAD-4 resin. The detailed mechanism has been discussed in Chapter 2, Section 2.5. Henceforth, the manganese dioxide coated XAD-4 beads are designated as MX-4. The images of XAD-4 and MX-4 resin beads are shown given in Chapter 2, Fig. 2.4. The characterization of MX-4 was done using Fourier-transform infrared spectroscopy (FTIR) analysis, scanning electron microscopy (SEM), neutron activation analysis (NAA) and point of zero charge (PZC) measurements. The details of these techniques are given in Chapter 2, Section 2.8.

The optimization of different parameters for preparation of MX-4 beads was systematically carried out. Studies include the effect of (1) reagent concentration, i.e. $KMnO_4$ concentration, on the MnO_2 coating formed, (2) sonication frequency, (3) time of sonication and (4) adsorbent dose. The studies have been carried out by measuring the percentage of arsenic sorption using As(V) radiotracer solution (2 mg L^{-1}). To study the effect of $KMnO_4$ concentration, the beads were prepared by varying the concentration of $KMnO_4$ from 0.001 - 1 M. For selecting the sonication frequency, two frequencies were studied, 25 and 35 kHz. The effect of time of sonication, on the arsenic sorption efficiency, was studied by varying the sonication time from 1 to 60 min. To study the adsorbent dose, the amount of the MX-4 beads, taken for the experiments, was varied from 0.1 - 10 g. The MX-4 prepared were subjected to sorption studies using As(V) radiotracer solution of concentration 2 mg L^{-1}, following the procedure of sorption explained in Section 5.3.2.

5.3.2. Sorption studies of arsenic by MX-4 beads

The synthesized beads were utilized for the sorption of arsenic. The sorption studies were carried out using As(III) and As(V) radiotracer solutions (2 mg L^{-1}) separately in batch equilibration mode. The procedure of preparation of tracer solutions has been given in Section 2.9. After preparation of arsenic tracer solutions, the oxidation state of the arsenic in the prepared solution was confirmed by solvent extraction procedure (Section 2.10.). For sorption, the pH range was chosen as 3 - 11. The sorbent dose used for sorption studies were ~2 g of MX-4 beads and equilibration time was 30 min. The detailed procedure of sorption study has been explained in Section 3.3.2. Sorption of arsenic was calculated from the initial and final count rates using equation 3.1.

5.3.3. Kinetic studies for arsenic sorption by MX-4 beads

Arsenic sorption kinetic studies using MX-4 beads are carried out as follows. In these studies, the equilibration time was varied from 5 - 60 min. ~ 2 g of MX-4 beads were added to each of the solutions and pH was kept at 7. The procedure adopted has been explained in detail in Section 3.3.2.

5.3.4. Isotherm studies for arsenic sorption by MX-4 beads

The adsorption isotherms for arsenic uptake by MX-4 beads were obtained using arsenic tracer solutions. The method was similar to the sorption study given in Section 5.3.2. The studies were done at neutral pH and arsenic concentrations were varied from 2 to 400 mg L^{-1}. The arsenic in solutions was taken as a combination of fixed concentration of radioactive arsenic (2 mg L^{-1}) and varying amounts of inactive arsenic. The time of equilibration was fixed as 30 min. The count rates of arsenic were measured, before and after equilibration, and the percentage sorption was calculated using equation 3.1.

5.3.5. Leaching studies on MX-4 beads

The manganese leaching from MX-4 beads, with and without the presence of arsenic, was studied. For Mn leaching in the absence of arsenic, 2 g of MX-4 was equilibrated with 25 mL of DI water (pH 7) for 30 min. Similar experiment was repeated with 25 mL DI water containing 2 mg L^{-1} of arsenic [As(III) and As(V) separately] and 2 g of MX-4 resin. After equilibration, the sorbent was separated by filtration, using whatman 42 filter paper. The supernatant was analysed for manganese, by neutron activation analysis (NAA) using pneumatic carrier facility (PCF) of Dhruva reactor (Mumbai, India). The sample preparation for NAA was the same as mentioned in Chapter 4, Section 4.3.5. The quantification of Mn (^{56}Mn, $t_{1/2}$ - 26.24 h, $E\gamma$ - 846.76 and 1810.73 keV) was done using relative method of NAA. The relevant nuclear data of manganese has been given in Chapter 2, Table 2.3.

5.3.6. Regeneration studies on MX-4 beads

Regeneration of MX-4 beads was carried out using different NaOH concentrations. The study was done on arsenic sorbed MX-4. The sorption was done following the procedure used for sorption study (Section 5.3.2). The arsenic sorbed MX-4 was separated by filtration and an initial count rate for ^{76}As was recorded. The beads were then equilibrated with 10 mL each of 0.1, 0.5 and 1 M NaOH for 30 minutes at room temperature. The suspension then centrifuged, supernatant was discarded and the final activity of ^{76}As remaining on MX-4 was measured in an identical geometry. Percentage regeneration of arsenic was calculated from the initial and final count rates of ^{76}As on MX-4.

5.3.7. Reusability studies on MX-4 beads

The synthesized MX-4 beads were studied for their reusability in the arsenic sorption. This study was carried out for 4 cycles (one cycle involves one sorption and desorption). The sorption procedure remained the same as in Section 5.3.2.

5.3.8. Application of MX-4 beads to arsenic contaminated groundwater

Two groundwater samples (GW-1 and GW-2) were collected from local tube wells in arsenic contaminated regions of North 24 Parganas, West Bengal, India. Sorption experiments utilizing the modified sorbent, MX-4 beads, were carried out uilizing 25 mL of groundwater and using 2 g MX-4. After equilibration for 30 min, the beads were separated and the solution was analyzed for arsenic using ICPMS (VG PQ ExCell, VG Elemental, UK). The concentrations of arsenic were also determined in the groundwater samples before sorption using the same technique. The detailed procedure has been explained in Section 3.3.8.

5.4. Results and discussion

5.4.1. Preparation of MX-4 beads: Optimization of different parameters

5.4.1.1. Effect of $KMnO_4$ concentration

Studies were done to find out the effect of reagent concentration, i.e. $KMnO_4$ concentration, on the MnO_2 coating formed. The effect was studied by measuring the percentage of arsenic sorption using, As(V) radiotracer solution (2 mg L^{-1}). The MX-4 beads were prepared by varying the concentration of $KMnO_4$ from 0.001 - 1 M. The experiments were done at room temperature and pH used was neutral. Figure 5.1 shows the percentage sorption of arsenic on the MX-4 beads prepared from different $KMnO_4$ concentration. Each point shows the average of triplicate measurements, with standard deviation shown as an error bar. The plot shows that the sorption was maximum at 0.1 M $KMnO_4$. The less sorption, at < 0.1 M $KMnO_4$ concentration, was due to the insufficient MnO_2 formation on the surface of beads. At > 0.1 M $KMnO_4$ concentration, the sorption again decreases due to the precipitation of MnO_2 on the surface of beads resulting in the clogging of pores so that the arsenic species got hindered from exchange reactions. Thus the $KMnO_4$ concentration was optimized to be 0.1 M.

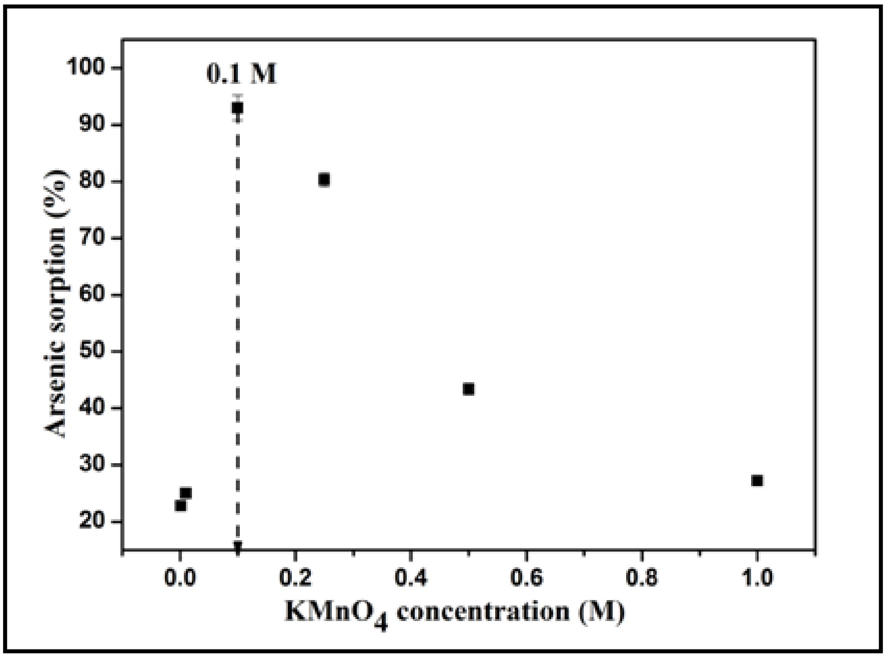

Figure 5.1: Effect of $KMnO_4$ concentration on sorption efficiency of As(V) by MX-4

5.4.1.2. Effect of sonication frequency

To study the effect of frequency of sonication on the preparation of MX-4 resin, two frequencies, i.e, 25 and 35 kHz, were used. The coating was done by taking the 0.1 M $KMnO_4$ solution in separate stoppered flasks with equal amount of XAD-4 beads and irradiated for 10 min using an ultrasound of 25 and 35 kHz frequency. The optimization of the sonication frequency was evaluated by As(V) sorption efficiency. The coated beads thus obtained were applied for arsenic sorption using 2 mg L^{-1} As(V) radiotracer solution. The sorption efficiency remained higher (96 %) for the MX-4 prepared using 35 kHz frequency. The amount of MnO_2 formed on the beads was quantified for both the cases using NAA, as explained in Section 2.8.3. The results are shown in Table 5.1. The lower sorption on the MX-4 produced at lower frequency can be explained clearly by the amount of MnO_2 present on the beads as indicated from Table 5.1. Thus, for further studies, the frequency of sonication was fixed as 35 kHz for the preparation of MX-4 sorbents.

Table 5.1: Concentration of MnO_2 on MX-4 resin beads

Sonication frequency (kHz)	**As(V) sorption (%)**	**Concentration of MnO_2 (%)**
25	63 ± 4	0.98 ± 0.33
35	96 ± 2	2.65 ± 0.21

5.4.1.3. Effect of sonication time

The effect of the time of sonication on the arsenic sorption efficiency was carried out by varying the sonication time of $KMnO_4$ from 1 to 60 min. The coating was done by taking the 0.1 M $KMnO_4$ solution in different stoppered flasks with equal amount of XAD-4 beads and irradiating them for different times using an ultrasound of 35 kHz frequency. The coated beads so obtained in different cases were used for arsenic sorption from aqueous solutions of 2 mg L^{-1} arsenic concentrations. The plot obtained for the sonication time and arsenic removal efficiency is given in Fig. 5.2. Each point on the graph, shows an average of triplicate measurements, with standard deviation shown as an error bar. The sorption of arsenic was maximum for the MX-4 beads prepared with 10 min sonication time, which indicated that an optimum MnO_2 coating was obtained at 10 min. When the sonication was done for < 10 min, the sorption of arsenic is less, this is because of the incomplete reduction of MnO_4^- to Mn(IV). But when the sonication time was increased > 10 min, then the subsequent reduction of Mn(IV) to Mn(II) occurs and the Mn^{2+} ions dissolve into the solution. This causes a less amount of MnO_2 coating on the resin beads leading to a decrease in the arsenic sorption. Hence, 10 min of sonication was considered as the optimum time for the preparation of the MX-4 sorbent beads.

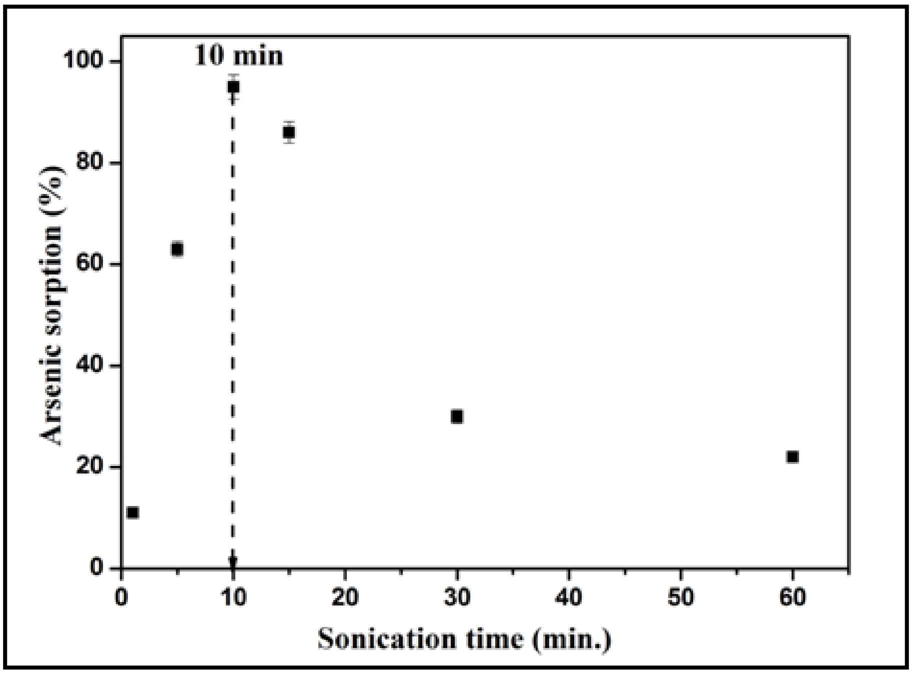

Figure 5.2: Effect of sonication time on sorption efficiency of As(V) by MX-4

5.4.1.4. Effect of amount of adsorbent

For the optimization of the adsorbent dose, i.e. the amount of MX-4 sorbent required for maximum arsenic sorption, was investigated following the sorption study. These sorption studies were carried out using arsenic radiotracer solutions (2 mg L^{-1}) at neutral pH. The amount of MX-4 beads, taken for the experiments, was varied from 0.1 - 10 g. The equilibration time was kept as 30 min at 100 rpm and the results are shown in Fig. 5.3. It is indicated from this figure that the sorption of arsenic is increased from ~20 % to ~95 % on increasing the amount of MX-4. With the increasing adsorbent dose, the extent of the surface active groups also increases accordingly, resulting an increase in the arsenic sorption, most prominently upto ~ 2 g of the sorbent. Further increase in the adsorbent dose, however, shows only a little effect in the percentage sorption of arsenic. Following the results, all the sorption experiments were carried out using an adsorbent dose of 2 g.

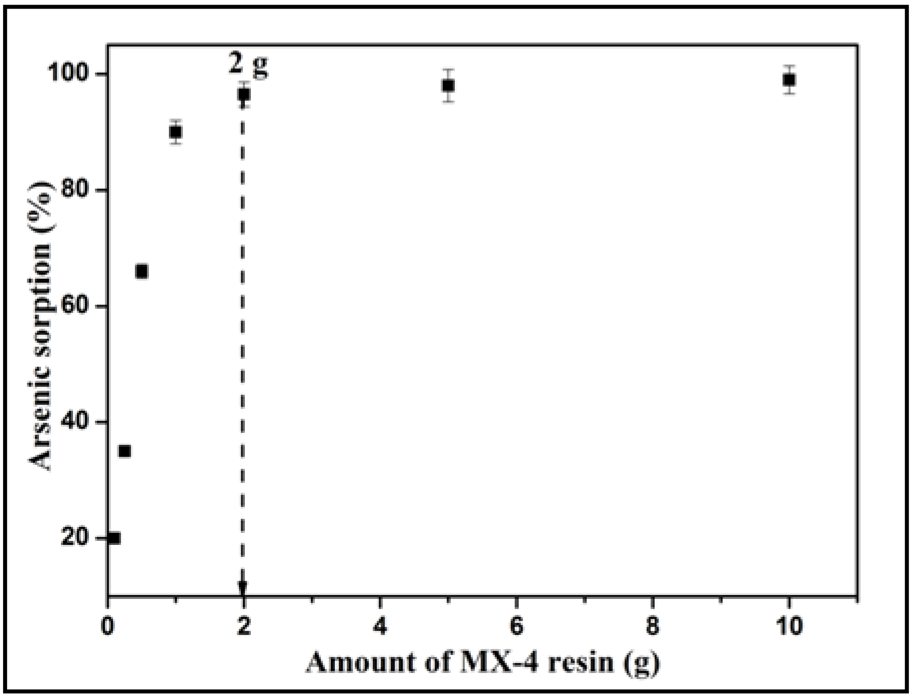

Figure 5.3: Effect of adsorbent dose on sorption efficiency of As(V) by MX-4

5.4.2. Sorption studies of arsenic by MX-4 beads

The results of the pH dependent arsenic sorption studies on MX-4 beads are shown in Fig. 5.4. The studies were done by varying the pH from 3-11. Very low pH (< 3) was avoided in this study due to the dissolution of the coated MnO_2. The MX-4 resin taken was 2 g. The NAA results, during characterization (Chapter 2, Section 2.8), showed that the MnO_2 concentration was 2.6 %, ie, MnO_2 on the sorbent was ~15 mg, in each experiment.

The sorption plots obtained for both arsenic species, As(III) and As(V) show similar behavior, i.e. the sorption efficiency increased with increasing pH, and after reaching a maximum for the pH range of about 7 to 9, the sorption efficiency decreases again on increasing the pH further.

The sorption trend can be explained using point of zero charge (PZC) of MX-4. The PZC for MX-4 obtained was 8.7 ± 0.2 (Chapter 2, Section 2.8.4). In Fig. 5.4, the arsenic sorption efficiency for both species was maximum around PZC. At pH < PZC, the arsenic species are negatively charged and the MX-4 surface are positively charged. Hence due to electrostatic attraction between the analyte and sorbent, the sorption efficiency is found to be quite high. When the pH > PZC, the net surface charge of sorbent became negative and the arsenic species becomes neutral, and thus the sorption efficiency decreases significantly.

For As(III), the sorption efficiency is maximum (70.6 %) at pH ~9, whereas for As(V), the sorption efficiency is maximum (96.5 %) at pH ~7. Further, the sorption efficiency for As(III) is in general less as compared to As(V). As discussed in Chapter 4, during the sorption of As(III) on MnO_2, oxidation occurs for As(III) and reduction for Mn(IV). Thus the surface of MX-4 gets modified, resulting in a decrease of number of adsorption sites available. Hence the sorption efficiency of As(III) is less. On the contrary, As(V) is adsorbed as such by the resin without involving any redox reaction. Therefore, the efficiency for As(V) sorption by MX-4 is much higher.

The sorption efficiency of XAD-4 was also evaluated in the same way as that of MX-4. The results show that the sorption efficiency is only about 16.5 % for As(III) and about 19 % for As(V) at pH 7. Thus the MnO_2 coating on XAD-4 beads largely improved the sorption efficiency, making the system useful for arsenic removal.

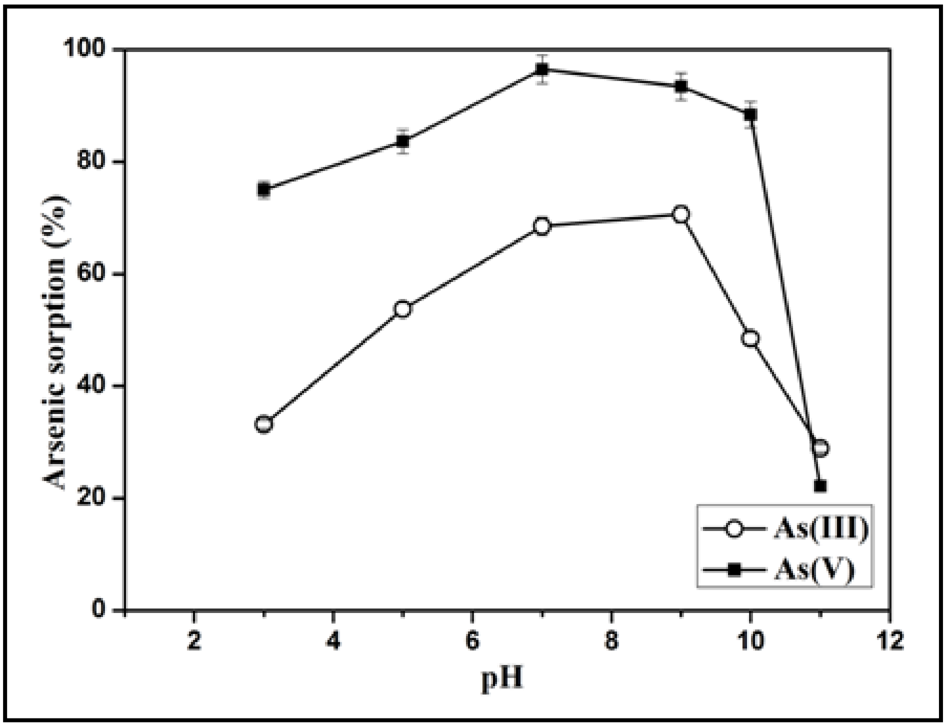

Figure 5.4: Sorption plot of As(III) and As(V) on MX-4

5.4.3. Kinetic studies for arsenic sorption by MX-4 beads

The kinetic studies for the sorption of As(III) and As(V) on the MX-4 beads were carried out at neutral pH and the results are shown in Fig. 5.5. From the observed plots, it is observed that the sorption kinetics of As(III) and As(V) species by MX-4 are quite similar to that of simple MnO_2 sorbent (> 98% even for 30 s equilibration time) as given in Chapter 4, Section 4.4.2. Following the results in Fig. 5.5, the equilibration time for all the further studies was fixed as 30 min, to ensure complete equilibrium.

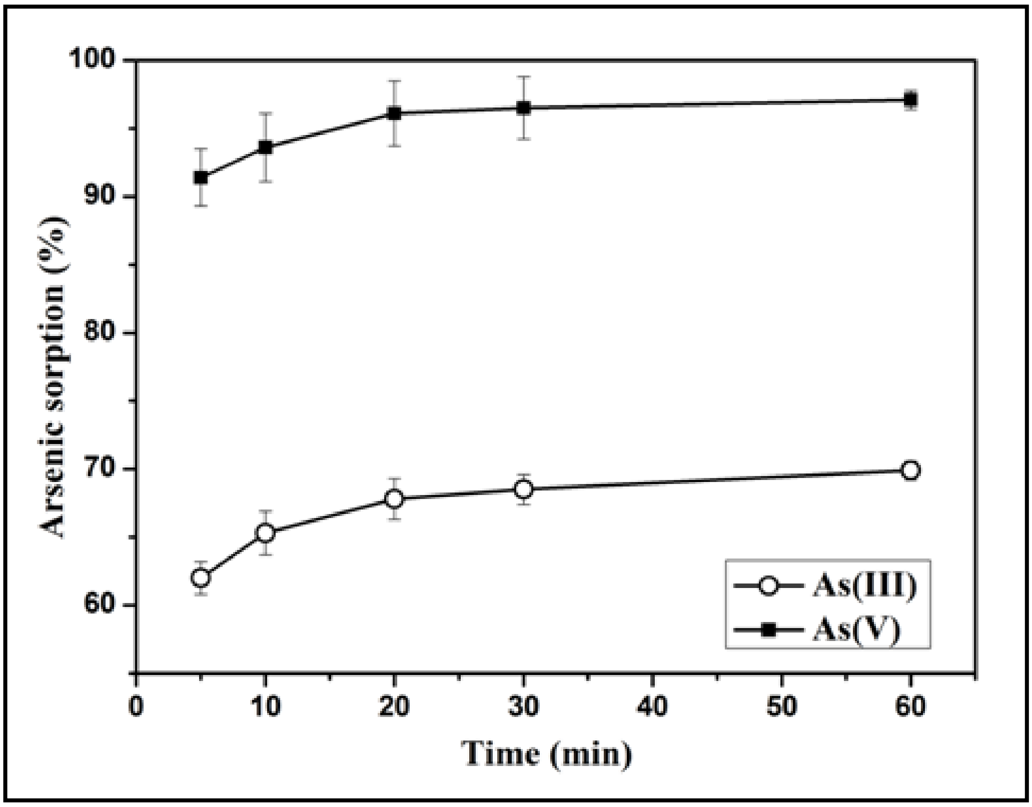

Figure 5.5: Kinetic plot of As(III) and As(V) on MX-4 beads

The kinetics experimental data for As(III) and As(V) sorption by MX-4 beads was evaluated by both pseudo first order (PFO) and pseudo second order (PSO) kinetic models (equations 3.2 and 3.3). The data fitted well with pseudo second order (PSO) kinetic equation (equation 3.3). This infers that chemisorption as the predominant mechanism for sorption of As(III) and As(V) by MX-4 beads. The plot is given in Fig. 5.6 A. The kinetic parameters obtained from the plots are listed in Table 5.2.

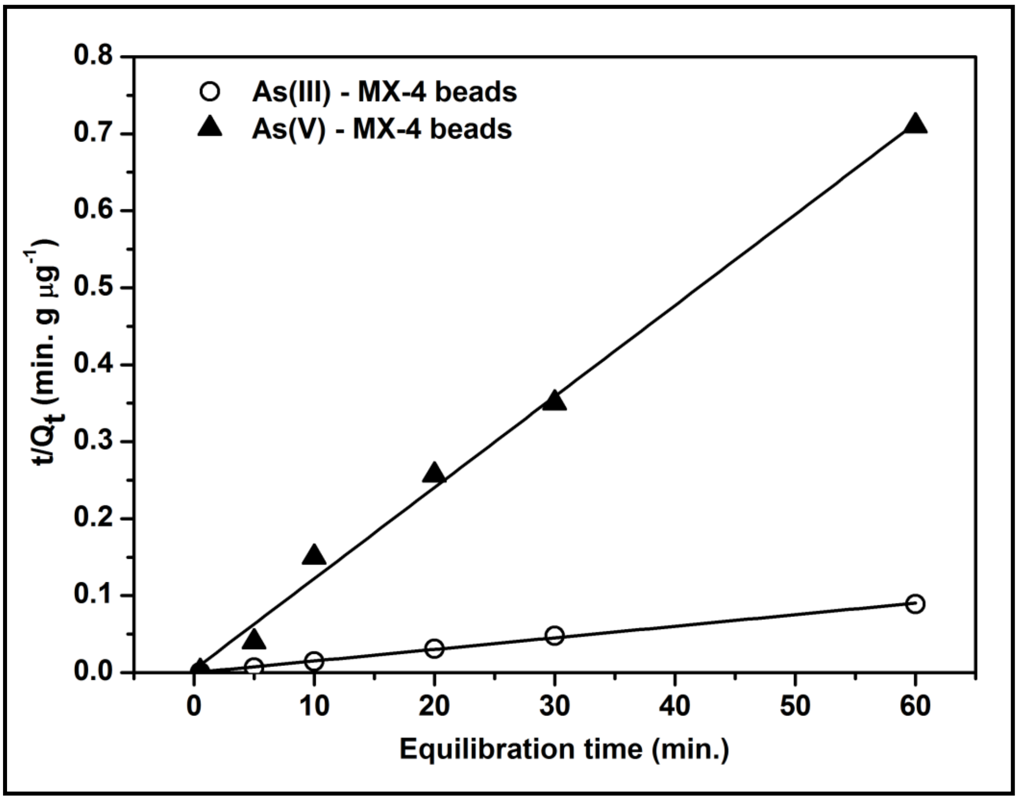

Figure 5.6: Pseudo second order kinetic plot for sorption of As(III) and As(V) on MX-4 beads. (Points are the experimental data and the straight lines are the linear fits following equation 3.3).

Table 5.2: Kinetic fitting parameters for PSO reaction for As(III) and As(V) adsorption by MX-4 beads.

Sorbent	**Arsenic species**	**Q_e (calculated) mg g^{-1}**	**K_2**	**R^2**
MX-4 beads	As(III)	0.667	2.0×10^{-10}	0.998
	As(V)	0.085	5.0×10^{-7}	0.994

5.4.4. Isotherm studies for arsenic sorption by MX-4 beads

The sorption mechanism as well as the sorption capacity was investigated following adsorption isotherm studies. Generally, Langmuir and Freundlich isotherms are commonly used in describing the sorption equilibrium in various environmental applications [117]. The adsorption isotherm for the arsenic uptake by MX-4 is seen to follow the Langmuir adsorption model [Fig. 5.7]. The assumptions of Langmuir model are: (i) adsorbent surface has finite number of active sites, (ii) they are homogeneously distributed, (iii) monolayer adsorption of analyte on the sorbent and (iv) no interaction between adsorbed molecules [161].

The Langmuir isotherm is represented by the following equation:

$$Q_e = \frac{Q_m\, C_e}{K_d + C_e} \tag{5.1}$$

The above equation 5.1, can be written in the linearized form as below,

$$\left(\frac{C_e}{Q_e}\right) = \frac{1}{Q_m\, K_d} + \frac{C_e}{Q_m} \tag{5.2}$$

The feasibility of reaction is defined by the dimensionless quantity as,

$$R_L = \frac{1}{1 + K_d\, C_e} \tag{5.3}$$

Where C_e = the equilibrium arsenic concentration (mg L^{-1}) and Q_e = the amount of arsenic adsorbed per gram of the MX-4 resin at equilibrium (mg g^{-1}), Q_m = the maximum amount of arsenic taken up per unit mass of MX-4 resin (mg g^{-1}) and K_d = Langmuir adsorption constant related to stability of the active sites (mg L^{-1}). The slope and intercept gives the information about the adsorption capacity (mg g^{-1}) and energy of the reaction (L mg^{-1}). The dimensionless factor, R_L, indicates the feasibility of reaction (equation 5.3). The R_L values indicate the reaction as:

- $R_L = 0$, irreversible
- $0 < R_L < 1$, favorable
- $R_L > 1$, unfavorable
- $R_L = 1$, linear

For the isotherm studies, time was kept at 30 min and ~ 1 g MX-4 resin was used. The As(III) and As(V) adsorption capacities (Q_m) were calculated from the slope ($1/Q_m$) and found to be 5.5 and 7.6 mg g^{-1} respectively, as given in Table 5.3. The K_d values were determined from the intercept ($1/K_d \cdot Q_m$) and listed in Table 5.3. The R_L values calculated for 2 - 400 mg L^{-1} of arsenic were in between 0 and 1, indicating the sorption to be favorable.

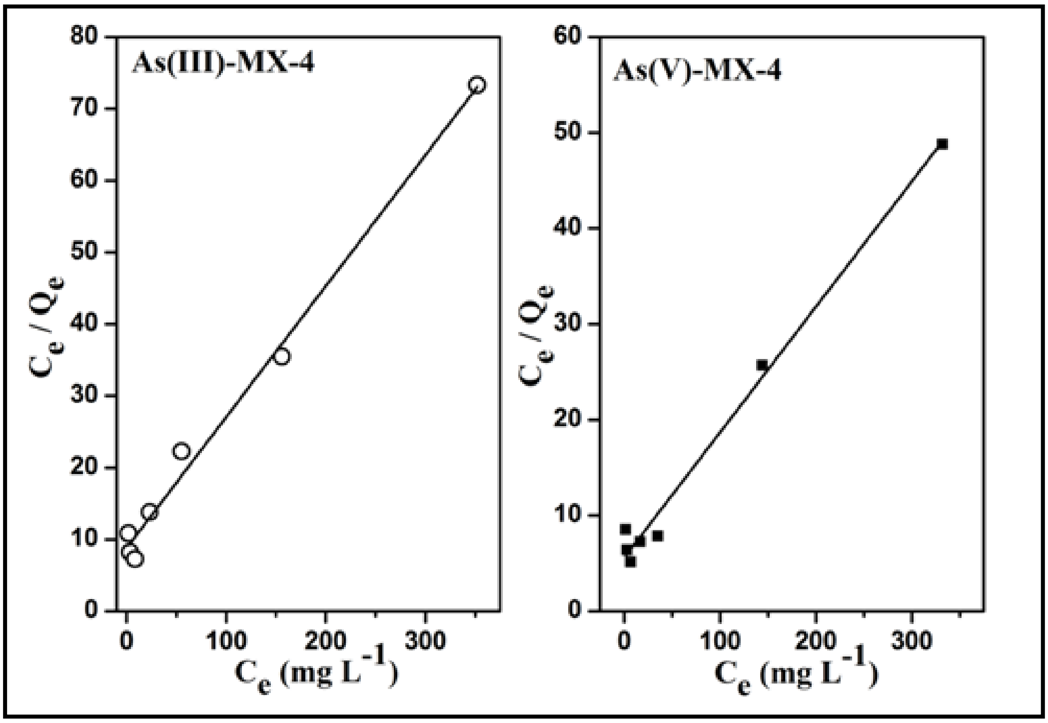

Figure 5.7: Langmuir isotherm for sorption of As(III) and As(V) on MX-4. (Points are the experimental data and the straight lines are the linear fits following equation 5.2).

Table 5.3: Fitting parameters for the Langmuir isotherms for As(III) and As(V) adsorption on MX-4.

Sorbent	**Arsenic species**	**R^2**	**Q_m (mg g^{-1})**	**K_d (L mg^{-1})**	**R_L (for 50 mg As / L)**
MX-4	As(III)	0.990	5.48	0.021	0.466
	As(V)	0.987	7.63	0.024	0.546

5.4.5. Regeneration studies on MX-4 beads

The regeneration studies were done using different concentrations of NaOH solutions by 30 min equilibration at 100 rpm speed. The results show that 0.1 M NaOH is able to regenerate the used MX-4 resin. The regeneration efficiency for As(III) and As(V) species in single step was ~ 77 % and 81 %, respectively.

5.4.6. Reusability studies on MX-4 beads

The MX-4 beads were reused in fresh arsenic [As(III) and As(V)] radiotracer solutions (2 mg L^{-1}) for upto 4 cycles (one cycle comprising of uptake of arsenic from 2 mg L^{-1} solution utilizing 0.1 g of MnO_2) and the results are given in the Fig. 5.8. The results indicate that the MX-4 beads are atleast reusable upto 4 cycles.

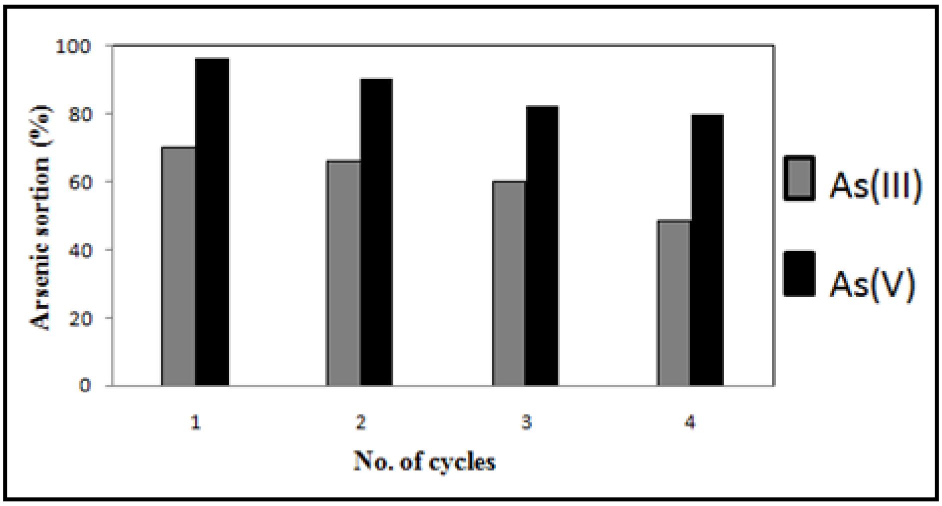

Figure 5.8: Reusability study of MX-4 for (a) As(III) and (b) As(V)

5.4.7. Application of MX-4 beads to arsenic contaminated groundwater

The MX-4 beads were applied for total arsenic remediation from two real groundwater samples (GW-1 and GW-2) collected directly from North 24 Parganas, West Bengal, India having pH of 7.3 and 7.7, respectively. The characterizations of these groundwater samples are shown in Chapter 3, Table 3.7. The concentration of total arsenic was determined using inductively coupled plasma mass spectrometer (ICPMS: VG PQ ExCell, VG Elemental, UK). It is seen that using MX-4 beads the removal of arsenic is possible to below about 10 μg L^{-1} (WHO limit) following 3 - 4 successive equilibrations. The results obtained for the arsenic concentration in groundwater before and after equilibration with MX-4 are given in Table 5.4.

Table 5.4: Concentration of arsenic in groundwater before and after sorption using MX-4 resin beads

Sample	**pH**	**Initial conc. (μg L^{-1})**	**Conc. after filtration and sorption by MX-4 (μg L^{-1})**
GW-1	7.3 ± 0.2	163 ± 8	4.1 ± 0.2*
GW-2	7.7 ± 0.2	710 ± 35	5.9 ± 0.5#

* Arsenic removal achieved in 3 cycles; # Arsenic removal achieved in 4 cycles

5.5. Conclusion

The study on sorption of arsenic on MnO_2, in Chapter 4, Section 4.5, revealed the detailed mechanism of sorption. The MnO_2 takes up As(III) after oxidizing to As(V). At the same time, the Mn(IV) gets reduced to Mn(II) and instead of getting released to the solution, these formed Mn(II) remains adsorbed on to the MnO_2 surface. Thus, making the MnO_2 surface positive, beyond the PZC. These results have been reported in the literature [131, 137, 141, 162-163], indicating the chemisorption as the mechanism of sorption by MnO_2. For the As(V) sorption by MnO_2, however, does not involve any redox reaction.

Similar to pure MnO_2 sorbent, on the surface of MX-4 beads, also, the As(III) species gets sorbed through redox reaction and attached possibly either as a mono-dentate or a bi-dentate complex. Though during sorption, As(III) is oxidized to As(V) and the released electrons are taken up by Mn(IV) to get it reduced to Mn(II), the so formed Mn(II) does not get released to the solution, but remains adsorbed on the surface of the MX-4 bead. Unlike As(III), sorption of As(V) by MX- does not involve any redox reaction and thus sorption efficiency is significantly higher. In this case, As(V) possibly bind to MX-4 as a bidentate binuclear complex [69-70, 144]. Observed results are the basis of proposing the mechanism of sorption of arsenic [As(III) and As(V)] on to the MX-4 beads as given in Fig. 5.9.

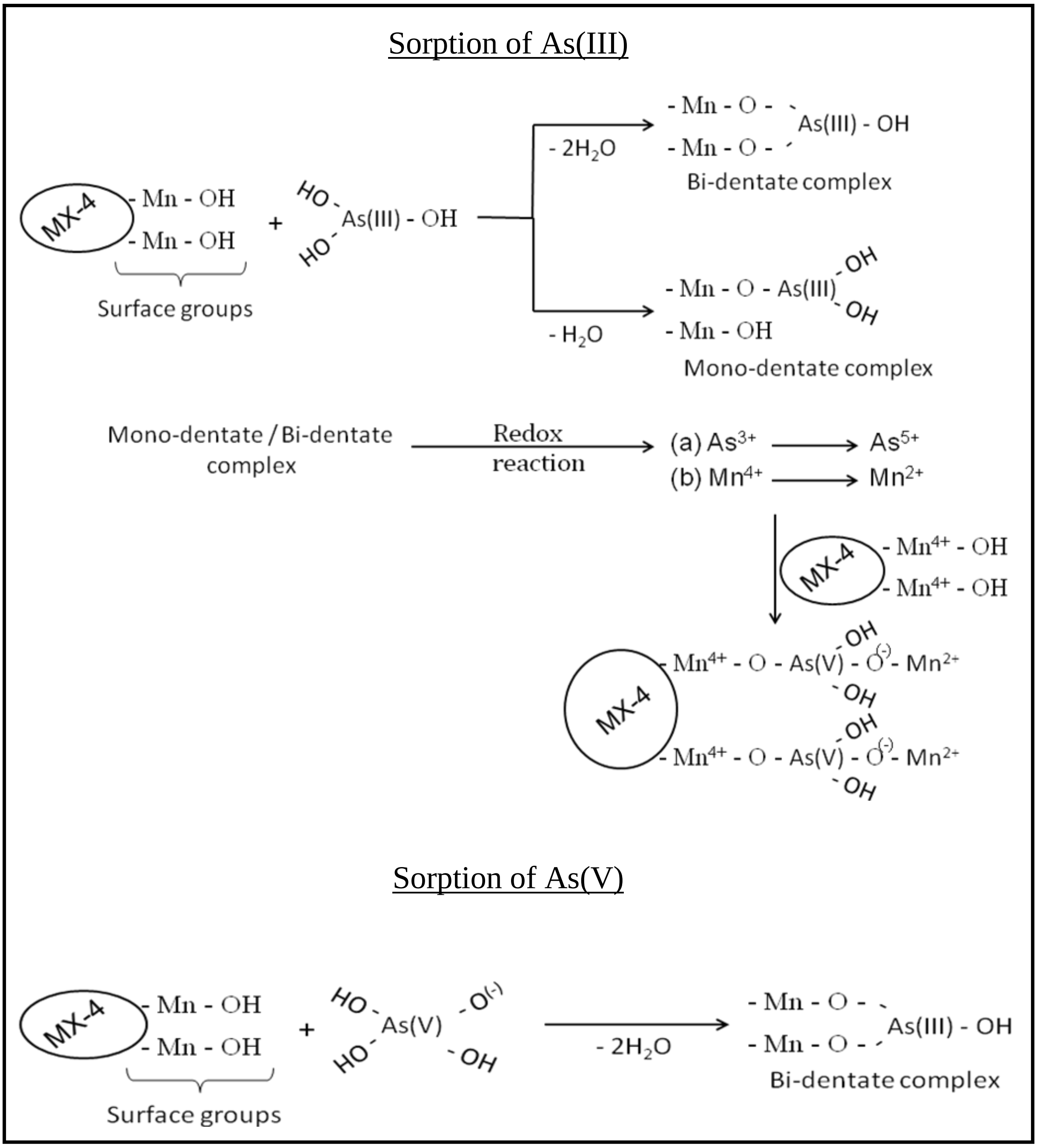

Figure 5.9: Schematic for sorption of arsenic on MX-4 [86]

Chapter - VI

Summary, Conclusions and Future work

6.1. Summary

The arsenic contamination in groundwater is currently a major problem in many parts of the world, which needs to be addressed adequately to meet the demand of the safe potable water. Many researchers in different parts of the world are in search for an easy, fast and economical remedy. This thesis explores synthesis, characterization and efficacy of different sorbents, based on iron and manganese oxides for arsenic uptake and possible arsenic remediation from water. The studies include the effect of pH, kinetics, isotherm evaluation, effect of co-occurring ions on the sorption behavior of the studied sorbent materials and also evaluate their applicability in removing arsenic from real groundwater samples. The sorbents have been studied for the leaching property in groundwater pH and also for their regeneration and reusability. The studies have been carried out using ^{76}As radiotracer in batch equilibration mode. With the knowledge gained, a sorbent, MnO_2, has been identified successfully, which has also been modified in the form of coating on resin beads and applied for arsenic removal studies. The conclusions derived from this research have been summarized in this chapter, along with the future perspectives.

Results of the studies are summarized as follows.

6.1.1. Arsenic uptake on iron oxides

Arsenic mobilization studies have revealed that iron oxides present in the soil play a vital role and accordingly different theories have been predicted for arsenic mobilization in water. The arsenic usually remains adsorbed onto the iron oxide surface; however it can get solubilized into water depending on various conditions prevailing in the environment, which in-turn results in the arsenic contamination in water. This has been the basis of the idea that since iron oxide has a strong binding property with arsenic; it must also be having the potential to be utilized for arsenic removal as well!! With this perspective, in the present study, three different iron oxide sorbents: (a) goethite (α-FeOOH),

(b) hematite (α-Fe_2O_3) and (c) magnetite (Fe_3O_4) were synthesized to investigate their arsenic sorption characteristics. X-ray diffraction (XRD) measurements have been used to confirm the structures of the oxides. Surface area, particle size and point of zero charge (PZC) measurements have been carried out for the characterization of the synthesized oxides. The PZC values for iron oxides are found to be in the range of 6.8 - 8.0, which lies in the range of the normal groundwater pH, and is a suitable characteristic for their application in the groundwater treatment.

To study the effect of pH on the sorption efficiency of arsenic by iron oxides, pH range of 3 - 11 was chosen in the present study. The sorption experiments were carried out at an arsenic concentration of 2 mg L^{-1} using ^{76}As radiotracer. Observed results indicated that, the percentage sorption of As(III) and As(V) is almost quantitative in the $pH < 9$ for all the three iron oxide sorbents, indicating the participation of electrostatic interaction, in addition to some complexation process in the arsenic sorption by the studied sorbents. The kinetics and efficiency of the sorption process by the studied iron oxides follows the order, goethite (> 98 %) > magnetite (> 90 %) > hematite (> 78 %) at 2 h equilibration. The sorption data fitted well with Freundlich isotherm model. The arsenic adsorption capacity for goethite (~4 mg g^{-1}) is found to be better as compared to other two iron oxides. The results are listed in table 6.1. The leaching studies of the iron oxides in the presence and absence of arsenic show that, except for magnetite, the iron release was within the acceptable limit in drinking water (1 mg L^{-1}). The results of the regeneration studies were, however, found to be not very encouraging. In spite of insufficient regeneration, the reusability study was also carried out and the results show that the sorption efficiency remains > 90 % for both magnetite and goethite till 5th cycle, but for hematite the efficiency is decreased just in 2 cycles. The effect of common ions on the arsenic sorption efficiency was also studied using goethite as the selective sorbent. The sorption studies were carried out in the presence of commonly occurring ions in groundwater such as Na^+, Ca^{2+}, Mg^{2+}, Cl^-, HCO_3^- and PO_4^{3-}. It is found that there is no significant effect of these ions on sorption of arsenic by the iron oxide sorbent except for PO_4^{3-} ion. This predictably happens due to the similarity in the chemical structure of both phosphate and arsenate ions, which results in the competitive adsorption of these ions on to the iron oxide sorbent. But this interfering effect is found to be prominent only at very high concentration of PO_4^{3-} (0.5 g L^{-1}), and importantly, such a high value of phosphate is generally not seen in normal environmental conditions in groundwater. Since the sorption efficiency is not affected by the presence of common ions, goethite, hematite and magnetite were also applied for total arsenic removal from real groundwater samples. Two groundwater samples were collected from North 24 Parganas, West Bengal, India and chemical characterization of these samples was carried out thoroughly. It is seen that the removal of arsenic is effective enough to bring its level below 10 μg L^{-1} (WHO limit) just in one equilibration using magnetite as the sorbent, though with goethite and hematite, it took at least two and more equilibrations to reach similar level of arsenic removal.

The mechanism of arsenic sorption by iron oxide sorbents was also investigated thoroughly using X-ray photoelectron spectroscopy (XPS) and electrochemical methods like cyclic voltammetry (CV) and differential pulse voltammetry (DPV). For goethite and hematite, sorption of As(III) and As(V) is observed to be associated with a redox reaction. During oxidation of As(III), the Fe(III) gets reduced to Fe(II). This results in the formation of surface bound Fe(II) which eventually gets oxidized again to Fe(III). In the case of As(V) sorption, the reaction associated is the oxidation of Fe(II) assisted by the reduction of As(V). In the case of mixed iron oxide, i.e. magnetite, there is no redox reaction indicated in the arsenic sorption process. Thus, both the arsenic species [As(III) and As(V)] are taken up by magnetite without any change in the oxidation states. The mechanisms of arsenic uptake by goethite/hematite and magnetite, as proposed in the present study, have been conceptually shown in Figs. 3.30 and 3.31.

6.1.2. Arsenic uptake on manganese dioxide

The manganese containing minerals are also reported as natural sorbent for arsenic removal. In the present study, manganese dioxide (MnO_2) samples were prepared by different methods: two wet chemical methods and one solid state mixing method. The characterization of the synthesized manganese dioxides was carried out using XRD, surface area, thermogravimetry (TG) and PZC measurements. The PZC values of the MnO_2 samples were found to be in the range of 3.8 - 4.1, and the surface of these sorbents remained positively charged only in the acidic pH range (Table 6.1). The surface morphology of the MnO_2 samples was studied by using transmission electron microscopic imaging.

Sorption of arsenic by MnO_2 was studied in the pH range of 1 - 11. Sorption of both As(III) and As(V) was quantitative in this pH range. Sorption kinetics is found to be quite fast and more than 98 % of arsenic was sorbed within 30 s. The sorption follows Freundlich isotherm model. Studies have shown that the amount of Mn released is not affected by arsenic uptake. Desorption process is found to be most effective on using 0.1 M NaOH, whereby > 95 % desorption was achieved for both As(III) and As(V) at room temperature in two cycles. The MnO_2 was also reused with fresh arsenic [As(III) and As(V)] radiotracer solutions (2 mg L^{-1}) for up to 8 cycles (one cycle comprising of uptake of arsenic from 2 mg L^{-1} solution utilizing 0.1 g of MnO_2) and the results indicated that the sorption efficiency is better for the MnO_2 prepared by solid state mixing method. The sorption percentage for both As(III) and As(V) species remained > 80 % up to 6th cycles of reuse. The sorption studies were carried out in the presence of commonly occurring ions in groundwater such as Na^+, Ca^{2+}, Mg^{2+}, Cl^-, HCO_3^- and PO_4^{3-}. The presence of HCO_3^- and PO_4^{3-} has a retarding effect on arsenic sorption, but the decrease was substantial only at a very high concentration, i.e., at > 0.1 g L^{-1}. Studies using arsenic spiked synthetic groundwater samples and real groundwater samples from arsenic affected areas of West Bengal showed that the concentration of arsenic can be reduced below 10 μg L^{-1}, the WHO limit simply in a single step of equilibration with MnO_2. Promising results have been observed especially for the MnO_2 sample prepared by the solid state mixing route.

The mechanism of sorption was studied by solvent extraction, XPS measurements and electrochemical study. Results of solvent extraction, viz. oxidation of As(III) by MnO_2 followed by sorption, were confirmed by XPS. Electrochemical study revealed the clear difference in the sorption mechanism of As(III) and As(V). On MnO_2 surface, the As(III) species gets oxidized and adsorbed, whereas the As(V) species are adsorbed on the surface as such. Also during the oxidation of As(III), the Mn(IV) gets reduced to Mn(II) and adsorbed on the MnO_2 surface facilitating further sorption. These results helped us in proposing a mechanism for the sorption of As(III) and As(V) on MnO_2, as conceptually shown in Fig. 4.17.

6.1.3. Modified sorbent for arsenic removal from groundwater

From the above studies, it was confirmed that MnO_2 is a promising sorbent for arsenic uptake from groundwater. But the direct field application of MnO_2 was limited due to the difficulty in the separation step because of powdered nature of the sorbent. Thus the aim was to modify the sorbent such that it can even be utilized effectively in column mode with ease. Various matrices like silica, charcoal, glass, anion exchanger resin and XAD were studied for MnO_2 incorporation/coating. The XAD-4 was chosen, in our study, since it was well known for chemical as well as surface modifications. As reported in the literature, after modification, XAD can be used as an easy and economical choice for the separation and preconcentration of heavy metal ions from aqueous samples.

In the present study, a sonochemical reduction method was applied for modification of XAD resin with MnO_2, for arsenic removal application. The MnO_2 modified XAD beads (MX-4) were characterized using Fourier-transform infrared spectroscopy (FTIR), scanning electron microscopy (SEM) imaging, neutron activation analysis (NAA) and PZC measurements. From the NAA results, the average concentration of MnO_2 was calculated to be (2.65 ± 0.21) %. The PZC values for XAD-4 and MX-4 resin were found to be 7.6 ± 0.3 and 8.7 ± 0.2, (given in table 6.1) respectively, which are quite similar to the groundwater pH. The different parameters like, sonication time, sonication frequency, reagent concentration and adsorbent dose were optimized to obtain reproducible coating and maximum arsenic removal efficiency.

These MX-4 beads were applied successfully for the removal of As(III) and As(V) from aqueous solutions. The sorption efficiency obtained for As(III) and As(V) was 70.6 % (pH ~9) and 96.5 % (pH ~7), respectively. The less sorption for As(III) compared to As(V) was explained as follows. During the interaction of As(III) and MnO_2, a redox reaction occurs, resulting in the oxidation of As(III) to As(V) and reduction of Mn(IV) to Mn(II). The surface of MX-4 got modified by the presence of so produced Mn(II) and number of adsorption sites available gets reduced. Hence the sorption efficiency for As(III) is less. As(V) was taken as such by the resin, so the efficiency was high. The arsenic uptake by MX-4 followed Langmuir isotherm indicating monolayer formation. Capacity studies of the coated resin were done for both As(III) and As(V) and found to be 5.5 and 7.6 mg g^{-1}, respectively. Regeneration of the resin using 0.1 M NaOH solution for As(III) and As(V) species in single step was ~ 77 % and 81 %, respectively. After exhaustion of the MX-4, i.e., after 4 cycles, the entire coating was dissolved in 1 M HNO_3

and the beads could be used for fresh coatings. The modified resin was applied for removal of arsenic from two groundwater samples collected from arsenic contaminated regions of North 24 Parganas, West Bengal, India. It was seen that the removal of arsenic could be achieved quite effectively to take the arsenic level below 10 μg L^{-1} (WHO limit) following 3 - 4 successive equilibrations. The mechanism of arsenic uptake by MX-4 beads, as proposed in the present study, has been shown in detail in Fig. 5.8.

Table 6.1: Summary of sorbents

Sorbents	**Surface area (m^2g^{-1})**	**PZC**	**Sorption pH**	**Eqbn. time (min.)**	**Arsenic sorption capacity (mg g^{-1})**	**Isotherm**	**Literature arsenic sorption capacity (mg g^{-1})**
Goethite	51	8.0	5 - 7	120	4.0	Freundlich	0.5 [53] 1.2 [64]
Hematite	18	7.2	5 - 7	120	1.3	Freundlich	0.8 [53] 0.4 [64]
Magnetite	35	6.8	5 - 7	120	3.4	Freundlich	0.3 [53] 0.9 [64]
MnO_2 (M-1)	77	3.8	3 - 5	30	3.1	Freundlich	0.2 [76] 2.3 [164]
MnO_2 (M-2)	67	3.9	3 - 5	30	4.6	Freundlich	-
MnO_2 (M-3)	131	4.1	5 - 7	30	13.0	Freundlich	-
MX-4 beads	750	8.7	7 - 9	30	7.6	Langmuir	-

6.2. Conclusions

The conclusions drawn in this study are:

1) MnO_2, prepared from solid state mixing method, is a promising sorbent for arsenic removal.

2) The difference in the interaction of arsenic with iron oxide and manganese dioxide is studied in detail. The mechanism study reveals (i) in the case of iron oxides, oxidation of As(III) occurs in the case of goethite and hematite, whereas for magnetite there is no redox reaction occurring; (ii) for MnO_2, As(III) gets oxidized on MnO_2 followed by sorption whereas As(V) is adsorbed as such.

3) MnO_2 completely oxidises the As(III) species to less toxic As(V) during the sorption process.

4) MnO_2 could successfully be applied to real groundwater from West Bengal and the arsenic level was reduced to below WHO limit in single equilibration.

5) An electrochemical method was designed for the in-situ sorption mechanism investigation.

6) A simple sonochemical method has been optimized for modification of XAD resin coated with MnO_2 for arsenic removal application.

7) The results obtained from the present work will form literature database on:

- Sorption of arsenic on sorbents – iron oxides and manganese dioxides
- Effect of various parameters on sorption of arsenic
- Mechanism of sorption
- Inputs for large scale water purification applications

The above work has produced five publications in peer reviewed journals and four symposia presentations.

6.3. Future work

The future studies need to be carried out on the following areas:

1) Iron and manganese oxides have good arsenic sorption properties. Study needs to be done on understanding the synergistic effects of both the oxides, by mixing them in variable proportions.

2) A binary oxide, of iron oxide and MnO_2, needs to be synthesized and study the arsenic sorption mechanism.

3) A detailed thermodynamic investigation needs to be done for the arsenic uptake by metal oxides.

4) The MX-4 resin is found to be having good arsenic removal capability, hence a thorough investigation of interaction mechanism of arsenic and MX-4 resin needs to be carried out.

5) EXAFS study on arsenic and MnO_2 system can provide more information regarding the molecular level of bond formation, bond length and coordination number during the sorption process.

6) More studies needs to be done on preparation of modified materials with high arsenic sorption efficiency for direct field applications.

LIST OF ABBREVIATIONS

World Health Organization	WHO
United States Environmental Protection Agency	USEPA
Bureau of Indian Standards	BIS
Maximum Permissible Limit	MPL
Critical Facility	CF
Pneumatic Carrier Facility	PCF
High Purity Germanium Detector	HPGe
X-Ray Diffraction	XRD
Brunauer-Emmett-Teller	BET
Point of Zero Charge	PZC
Neutron Activation Analysis	NAA
Scanning Electronic Microscopy	SEM
Transmission Electron Microscopy	TEM
Thermo-Gravimetry	TG
Fourier Transform Infrared Spectroscopy	FTIR
Inductively Coupled Plasma Optical Emission Spectrometry	ICPOES
Inductively Coupled Plasma Mass Spectrometry	ICPMS
X-Ray Photoelectron Spectroscopy	XPS
Binding Energy	BE
Cyclic Voltammetry	CV
Differential Pulse Voltammetry	DPV
Chrono-Potentiometry	CP
Glassy Carbon Electrode	GCE
Open Circuit Potential	OCP

SYNOPSIS

Arsenic is considered as a major groundwater pollutant [1 - 4] due to its potential harmfulness to human health. Arsenic comes into groundwater by natural processes as well as anthropogenic activities. The natural processes include (i) leaching from rocks and minerals, (ii) from volcanic activities. The anthropogenic activities are (i) excessive use of pesticides and wood preservatives, (ii) by excessive usage of groundwater [5]. Generally arsenic exists as inorganic and organic species in groundwater. Inorganic arsenic is considered to be more toxic [1, 5]. World Health Organization (WHO) has kept the provisional guideline value as 10 $\mu g\ L^{-1}$ for arsenic in groundwater [6].

In literature, many arsenic removal technologies like oxidation, co-precipitation, adsorptive removal, ion exchange and membrane based techniques have been reported [7 - 13]. Among these removal processes, adsorption is superior due to the high removal efficiency, high capacity for adsorbate and reusability. Since the process under consideration for removal of arsenic in this thesis work is adsorption, it is important to study the adsorbent - adsorbate interaction. For the complete understanding of arsenic removal by an adsorbent, these studies should include the effect of pH, adsorbent dose, regeneration method and the elucidation of interaction mechanism of arsenic with the sorbent. A detailed understanding of the chemistry / interactions is inevitable for the optimum, efficient and economical usage of existing as well as modified adsorbents. It was noted that a comprehensive literature on such studies was scarce. Naturally occurring metal oxides such as iron oxide and manganese dioxide are extensively used as sorbents for arsenic removal from groundwater. Hence, the main aim of this work is to explain the sorption process of arsenic on to iron oxide and manganese dioxide using appropriate analytical techniques.

The present thesis work, performed on sorption of arsenic and the study of mechanism investigated, has been described in six chapters. Chapter-1 explains the extensive literature survey on arsenic removal using different adsorbents and their interactions. Chapter-2 comprehends the synthesis of adsorbents for arsenic uptake studies, and their characterization. The techniques used for this work have been presented in brief. Chapter-3 gives the discussion on the studies carried out on different iron oxides and the interactions of arsenic with iron oxides have been investigated using solvent extraction, X-ray photoelectron spectroscopy (XPS) and electrochemical studies. Similarly, the studies using manganese dioxide as adsorbent have been explained in Chapter-4. The studies on the changes of oxidation states of arsenic and manganese during sorption have also been explained in this chapter. In Chapter-5, the studies on MnO_2 coated resin for arsenic removal have been discussed in detail. The conclusions and future studies have been listed out in the last chapter, Chapter-6.

Chapter - 1: Introduction

In this chapter, an extensive literature review has been presented on the subject area of removal of arsenic from groundwater. The first section of this chapter deals with the general discussion on arsenic, remediation methods currently in use and their shortcomings. This deal with reports on adsorption of arsenic using variety of adsorbents like charcoal, sand, zeolites, polymeric materials and naturally occurring metal oxides/hydroxides [14-18].

The second section describes the review on arsenic removal by adsorbents like iron oxide and manganese dioxide. In these context, iron oxide and manganese dioxide (MnO_2) [19-27] have been reported as the promising sorbents for total arsenic removal due to the strong adsorption properties. But before selecting the best adsorbent, it is necessary to understand in detail the various parameters which affect the sorption efficiency involving these sorbent materials.

The available literature compilation, on mechanism of arsenic interaction with these adsorbents, forms the third section of this chapter. Even though a large number of literature reports the aspect of arsenic removal, a detailed study on the mechanisms involved in these processes are not fully explored. There are only few literatures available on the speciation of the arsenic species after sorption [28-36]. In general, the literatures indicate that the changes in arsenic species occur at the surface of the adsorbents only after the adsorption process. To study the changes in the oxidation state during the interaction of the arsenite and arsenate species with the adsorbents, one has to depend up on the highly sophisticated spectroscopic techniques like X-ray photoelectron spectroscopy (XPS), X-ray absorption near edge structure (XANES) and extended X-ray absorption fine structure (EXAFS). These studies require a lot of expertise especially during data interpretation.

The main objective of this work has been to study the changes occurring to the oxidation states of both the adsorbent and adsorbate during their interaction. The study has been aimed to explore the mechanism of these changes following the classical method like solvent extraction and an electrochemical method. These results from the studies are compared with the results obtained from the well-established XPS measurements. The most promising adsorbent with favourable properties, like high arsenic sorption efficiency, fast kinetics, tolerance to the co-occurring ions and easy regeneration capability has been chosen to prepare a modified material for easy and efficient arsenic removal. The synthetic adsorbents in their powder form, pose problem of column clogging when applied for removal of toxicants from groundwater in the form of fixed bed column. Thus a modified sorbent was synthesized and the properties were evaluated so that it can be applicable in the form of column bed for purification of groundwater.

Chapter - 2: Synthesis of adsorbents and Characterization

Three different iron oxides, namely magnetite, goethite and hematite, were synthesized by chemical methods. The magnetite was prepared from Mohr's salt [$(NH_4)_2SO_4.FeSO_4.6H_2O$] and $Fe(NO_3)_3.9H_2O$ following the literature procedure [36]. The brown colored precipitate of iron hydroxide, obtained on mixing the above two reactants, was heated for the conversion of hydroxides to oxides. The final powder obtained was black in color, indicating the color of magnetite (Fe_3O_4). Goethite (α-FeOOH) was prepared by heating alkaline ferric nitrate solution under constant stirring. The dark red precipitate obtained was changed to yellowish in color, indicating the conversion of ferrihydrite to goethite [37]. For the preparation of hematite (α-Fe_2O_3), the procedure was similar to that of goethite. The dark red precipitate obtained was heated in a muffle furnace. The final product was reddish brown colored hematite [37]. The structures of the synthesized oxides were revealed by X-ray powder diffraction (XRD) analysis. The particle size, surface area and point of zero charge (PZC) of the synthesized iron oxides were estimated and results were compared with those reported in the literature.

Manganese dioxide (MnO_2) was prepared by two chemical routes and a solid state mixing route. The chemical methods used were: (1) manganese dioxide was prepared by mixing potassium permanganate and manganese sulphate solutions followed by heating the resultant solution [38] and (2) mixing potassium permanganate solution with concentrated HCl [30]. In the solid state mixing method, manganese dioxide was prepared via solid-state reaction of manganese acetate and potassium permanganate [39]. The mixture was heated in water for 6 h. XRD, surface area, PZC, transmission electron microscope (TEM) images and thermo-gravimetric measurements (TG) were carried out for the characterization of the prepared MnO_2 samples. The XRD spectrum identified the prepared sorbents to be ramsdellite and α-MnO_2. Transmission electron microscopic (TEM) measurement (magnification: 50 k) showed that most of the MnO_2 particles were needle shaped and were of 100 - 200 nm range.

Sonochemical reduction of permanganate (MnO_4^-) was used for the preparation of MnO_2 nanoparticles [40] and was used for coating on XAD-4 resin. Characterization of the modified MnO_2 coated XAD-4 resin (MX-4) was done by attenuated total reflection Fourier transform infrared spectrometry (ATR-FTIR), scanning electron microscopy (SEM), neutron activation analysis (NAA) and PZC measurements.

The characterization techniques, their working principles and the optimized parameters for these measurements have been described briefly in this chapter. The methods of preparation of the arsenic tracer solutions and the other working solutions have also been described in this chapter.

Chapter - 3: Arsenic uptake on iron oxides

Sorption studies of As(III) and As(V) on chemically synthesized iron oxides like magnetite (Fe_3O_4), goethite (α-FeOOH) and hematite (Fe_2O_3) have been described in this chapter. The studies were performed using ^{76}As radiotracer in batch equilibration mode. To study the effect of pH on the sorption efficiency of arsenic by iron oxides, a pH range of 3 - 11 was chosen. The sorption experiments were carried out at an arsenic concentration of 2 mg L^{-1} using radiotracer. In the batch sorption studies, it was observed that, the percentage sorption of As(III) and As(V) was almost quantitative in the pH range of 3 - 9 for all the three iron oxide sorbents. The kinetics of sorption for arsenic by these iron oxides are in the order, goethite (> 98 %) > magnetite (> 90 %) > hematite (> 65 %) at 2 h equilibration. The kinetics data fitted well with pseudo second order kinetic equation. The adsorption data fitted well with Freundlich isotherm model. The arsenic adsorption capacity for goethite (4 mg g^{-1}) was found to be higher among the three iron oxides studied.

The final application of the iron oxide was to use it as a sorbent for arsenic removal from groundwater. In this context interferences of other ions on sorption efficiency of the iron oxides for arsenic in water were also studied. The tolerance studies were carried out in the presence of commonly occurring ions in groundwater such as Ca^{2+}, Mg^{2+}, Na^{+}, Cl^{-}, HCO_3^{-} and PO_4^{3-}. It was found that there is no significant effect of these ions on the sorption of arsenic by iron oxides except for PO_4^{3-} ion. This happened due to the similarity in the chemical structure of both phosphate and arsenate ions which resulted in the competitive adsorption of both the ions on the iron oxide sorbents. But the decrease was prominent only at very high concentration of PO_4^{3-} (500 mg L^{-1}), which is generally not seen in normal environmental conditions.

Since the presence of common ions had little impact on the sorption efficiency, these sorbents were subsequently applied on real groundwater samples, which were collected directly from North 24 Parganas, West Bengal, India. It was seen that the removal of arsenic by the studied iron oxide sorbents is very effective to reduce the toxicant below the WHO limit. The arsenic desorption and thus regeneration of the sorbents was also carried out using 1 M NaOH. For water purification application, the leaching studies of the sorbents were also done as a function of pH.

The sorption mechanism of the studied iron oxides for arsenic was studied initially by solvent extraction method applying benzene as the organic phase [41]. However due to incomplete regeneration of the adsorbents, these studies could not enlighten the sorption mechanism fully. Hence an electrochemical investigation was carried out using cyclic voltammetry (CV) and differential pulse voltammetry (DPV) methods. The results showed that in magnetite, the As(III) and As(V) were taken up as such. For hematite, however the As(III) got oxidized and As(V) got reduced partially. Thus, the mechanism of uptake of As(III) and As(V) with hematite was found to be redox type of interaction. For goethite also there was a redox reaction happening in the presence of both As(III) and As(V). Observed CV results were corroborated nicely from the XPS study. The XPS results revealed that for hematite and goethite, the As(III) got oxidized partially and correspondingly the Fe(III) got reduced to Fe(II). For As(V) we observed an extra peak at lower binding energy which can be attributed to the complex formation of arsenic with iron, which could again be ascertained by the observation of a peak at higher binding energy for iron. Based on these studies, the sorption mechanism of the iron oxides for arsenic could be established satisfactorily [42].

Chapter - 4: Arsenic uptake on manganese dioxides

The manganese dioxide samples prepared by chemical methods (i.e, by two solution methods) and solid state mixing method were characterized as explained in Chapter-2. The studies on sorption of arsenic (both As(III) & As(V)) by MnO_2 was studied by batch equilibration method using ^{76}As radiotracer in the pH range of 1 to 11. For sorption experiments, concentration of arsenic was selected as 2 mg L^{-1} based on the maximum reported concentration of arsenic in the affected region of West Bengal, India. Sorption of both As(III) and As(V) were > 99 % up to pH 9. The experimental results were very promising especially in regard to the sorption efficiency shown by MnO_2 prepared from solid state mixing method. Kinetics was faster for the MnO_2 prepared by solid state method, i.e. ~ 98 % within 30 s of equilibration. The sorption data followed Freundlich isotherm model and the arsenic removal capacity obtained for MnO_2 was 70 mg g^{-1}, which was a higher value as compared to the natural oxides.

The effect of commonly occurring ions such as Ca^{2+}, Mg^{2+}, Cl^-, SO_4^{2-}, HCO_3^- and PO_4^{3-} on the extent of arsenic uptake was investigated separately. It was found that Ca^{2+}, Mg^{2+}, Cl^- and SO_4^{2-} did not affect the sorption of arsenic. It was observed that the extent of sorption of arsenic was quantitative at lower concentrations of HCO_3^- and PO_4^{3-}. But decreased at higher concentrations of these ions, where the effect of PO_4^{3-} was more severe than that of HCO_3^-. However it is important to note that the groundwater usually does not contain such high concentrations of HCO_3^- and PO_4^{3-} ions. The MnO_2 regeneration was done using different concentrations of NaOH. Results showed that about 90 % of the sorbed arsenic can be removed in a single equilibration with 0.1 M NaOH with only 30 min contact time. The MnO_2 leaching study in the presence and in the absence of arsenic was also carried out in detail as a function of pH and the leaching of the sorbent was found to be significantly small.

MnO_2 was applied as a sorbent to purify two synthetic groundwater samples spiked with 2 mg L^{-1} of arsenic (as radiotracer). The sorption of As(III) and As(V) on manganese dioxide from both the water samples was > 97 %. Arsenic sorption study was also carried out on two groundwater samples collected from arsenic contaminated areas of West Bengal, India. The results of sorption indicated that the concentrations of arsenic can be reduced below WHO permissible limit of 10 μg L^{-1} even with single equilibration with MnO_2 as sorbent. This study suggests that the manganese dioxide synthesized via solid state reaction method is very effective for removal of arsenic from groundwater [43, 44].

The interaction of arsenic and manganese was also investigated in detail. The aim was to study (i) the changes occurring on MnO_2 during sorption of arsenic and (ii) to study the interaction of manganese and arsenic, by following the changes in the oxidation states.

Solvent extraction study [41] was done as a preliminary investigation method for elucidation of the oxidation state of sorbed arsenic. Solvent extraction study using benzene as solvent was done using arsenic radiotracer. The ^{76}As activity was retained in the aqueous phase irrespective of the initial oxidation state of the As radiotracer. This clearly indicated the oxidation of As(III) to As(V) during sorption on manganese dioxide.

An electrochemical method was developed for explaining the arsenic - manganese interactions. Chronopotentiometry (CP) and cyclic voltammetry (CV) were recorded using the MnO_2 modified glassy carbon (GC) electrode without and with addition of arsenic in the solution. The CV measurements support the CP measurements with mechanism of uptake for As(III) as the oxidative adsorption process and As(V) undergo adsorption without any redox modification.

For the confirmation of the above observations and to investigate the oxidation states with a well established technique, XPS measurements were carried out. Observed results indicated reduction of Mn(IV) to Mn(II) during the sorption of As(III) and also confirmed the sorption of Mn(II) on the surface of the sorbent. From these data, a detailed mechanism of sorption of arsenic onto MnO_2 could be proposed [45].

Chapter - 5: Modified sorbent for arsenic removal from groundwater

The extensive investigation of the interaction of manganese dioxide (MnO_2) and arsenic resulted in establishing MnO_2 as one of the promising sorbent for removal of arsenic. However the application becomes limited due to difficulty of packing it into a column for direct field use. Therefore coating of MnO_2 on inert solid support was studied as described in Chapter-5 [8, 46]. The MnO_2 was prepared by reduction of $KMnO_4$ using ultrasound and in-situ coating on XAD-4 was done. Optimization of various parameters like $KMnO_4$ (reagent) concentration, sonication time and amount of MX-4 resin used were done for obtaining reproducible coating of MnO_2. These MX-4 beads were applied for the removal of As(III) and As(V) from aqueous solutions. Batch sorption studies were done using arsenic (^{76}As) radiotracer. For the sorption studies, pH was varied from 3 to

11. The data obtained by the adsorption studies followed the Langmuir isotherm indicating monolayer adsorption. The regeneration of the sorbent was done by 0.1 M NaOH solution. The modified resin was applied for quantitative removal of arsenic from two groundwater samples collected from arsenic contaminated regions of North 24 Parganas, West Bengal, India, and found to be quite effective. A schematic mechanism for the removal of arsenic by MX-4 beads could be proposed from the results obtained from the present study [47].

Chapter - 6: Summary, Conclusions and future work

This chapter gives the highlights of the entire work along with the future arenas to be explored.

The highlights of this work are:

1) MnO_2 prepared by solid state mixing method is found to be a promising material for arsenic removal from groundwater.

2) Elaborate studies have been carried out with both iron and manganese oxides and the results are compared with the reported data.

3) Application of the adsorbent to real groundwater from West Bengal has been demonstrated.

4) Sorption mechanism of arsenic using iron and manganese oxides has been established.

5) An electrochemical method was designed for the in-situ sorption mechanism investigation.

6) A simple sonochemical method has been optimized for modification of XAD resin coated with MnO_2 for arsenic removal application.

The study reveals (i) during uptake of arsenic on iron oxides, oxidation of As(III) occurs in the case of goethite and hematite, whereas for magnetite there is no change in the oxidation state of both As(III) and As(V) species; (ii) during uptake on manganese dioxide, there is a clear difference in the sorption of As(III) and As(V). As(III) gets oxidized on MnO_2 followed by sorption whereas As(V) is adsorbed as such.

In future, following studies will be done for complete understanding of the adsorbent-adsorbate interaction.

1) Investigation of interaction mechanism of arsenic and MX-4 resin.

2) Study the synergistic effects of iron and manganese binary / combination oxides on arsenic sorption and study their sorption mechanisms.

3) EXAFS study to confirm the bond length and the coordination number in regard to the sorption of arsenic on the metal oxides.

4) Preparation of modified materials with high arsenic sorption efficiency for direct field applications.

References

1. Shankar S., Shanker U. and Shikha, Arsenic contamination of groundwater: A review of sources, prevalence, health risks, and strategies for mitigation, The Scientific World Journal, Article ID 304524, (2014) 1-18.

2. Ghosh N. C. and Singh R. D, Groundwater arsenic contamination in India: Vulnerability and scope for remedy, National Institute of Hydrology, Roorkee, 2010.

3. Wang S. and Mulligan C.N., Occurrence of arsenic contamination in Canada: Sources, behavior and distribution, Sci. Total Environ., 366/2–3 (2006) 701-721.

4. Mandal B.K. and Suzuki K.T., Arsenic round the world: A review, Talanta, 58 (2002) 201-235.

5. Smedley P. L. and Kinniburgh D.G., A review of the source, behaviour and distribution of arsenic in natural waters, Applied Geochemistry, 17 (2002) 517-568.

6. World Health Organization, Arsenic in the drinking water fact sheet 210. World Health Organization, Geneva, Switzerland, 2006.

7. Nur T., Loganathan P., Ahmed M. B., Johir M. A. H., Nguyen T. V. and Vigneswaran S., Removing arsenic from water by coprecipitation with iron: Effect of arsenic and iron concentrations and adsorbent incorporation, Chemosphere, 226 (2019) 431-438.

8. Dinesh M. and Pittman C.U.Jr., Arsenic removal from water/wastewater using adsorbents - A critical review, J. Hazard. Mater., 142/1-2 (2007) 1-53.

9. Singh R., Singh S., Parihar P., Singh V. P. and Prasad S. M., Arsenic contamination, consequences and remediation techniques: a review, Ecotoxicol Environ Saf., 112 (2015) 247-270.

10. Nicomel N. R., Leus K., Folens K., Van Der Voort P. and Du Laing G., Technologies for arsenic removal from water: Current status and future perspectives, International journal of environmental research and public health, 13/1 (2016) 62-85.

11. Mondal P., Bhowmick S., Chatterjee D., Figoli A. and Vander Bruggen B., Remediation of inorganic arsenic in groundwater for safe water supply: A critical assessment of technological solutions, Chemosphere, 92 (2013) 157-170.

12. Vaclavikova M., Gallios G.P., Hredzak S. and Jakabsky S., Removal of arsenic from water streams: an overview of available techniques, Clean Technol. Environ. Policy, 10 (2008) 89-95.

13. Wang S. and Mulligan C. N., Speciation and surface structure of inorganic arsenic in solid phases: A review, Environment International, 34/6 (2008) 867-879.

14. Pattanayak J., Mondal K., Mathew S. and Lalvani S.B., A parametric evaluation of the removal of As(V) and As(III) by carbon based adsorbents, Carbon, 38/4 (2000) 589-596.

15. Chutia P., Kato S., Kojima T. and Satokawa S., Adsorption of As(V) on surfactant-modified natural zeolites, Journal of Hazardous Materials, 162/1 (2009) 204-211.

16. Lenoble V., Chabroulle, C., Shukry R., Serpaud B., Deluchat V. and Bollinger J.C., Dynamic arsenic removal on a MnO_2-loaded resin, J. Coll. Interf. Sci., 280 (2004) 62-67.

17. Kim J. and Benjamin M. M., Modeling a novel ion exchange process for arsenic and nitrate removal, Water Research, 38/8 (2004) 2053-2062.

18. Asere T. G., Stevens C.V. and Laing G.D., Use of (modified) natural adsorbents for arsenic remediation: a review, Sci. Total Environ., 676 (2019) 706-720.

19. Polowczyk I., Cyganowski P., Ulatowska, J., Sawiński J. and Bastrzyk A., Synthetic iron oxides for adsorptive removal of arsenic, Water Air Soil Pollut., 229 (2018) 203.

20. Mamindy-Pajany Y., Hurel C., Marmier N. and Romeo M., Arsenic(V) adsorption from aqueous solution onto goethite, hematite, magnetite and zero-valent iron: Effects of pH, concentration and reversibility, Desalination, 281 (2011) 93-99.

21. Garcia M. G., Muñiz K. R. and Song S., Arsenic removal from water by adsorption using iron oxide minerals as adsorbents: A review, Mineral Processing & Extractive Metall. Rev., 33 (2012) 301-315.

22. Gimenez J., Pablo J. De, Rovira M. and Duro L., Arsenic sorption onto natural hematite, magnetite, and goethite, Journal of Hazardous Materials, 141 (2007) 575-580.

23. Tuutijarvi T., Lu J., Sillanpaa M. and Chen G., As(V) adsorption on maghemite nano-particles, J. Hazard. Mater., 166 (2009) 1415-1420.

24. Deliyanni E. A., Bakoyannakis D. N., Zouboulis A. I. and Matis K. A., Sorption of As(V) ions by akaganéite-type nanocrystals, Chemosphere, 50/1 (2003) 155-163.

25. Dixit S. and Hering J., Comparison of arsenic(V) and arsenic(III) sorption onto iron oxide minerals, Environmental Science and Technology, 37/18 (2003) 4182-4189.

26. Kong S. Q., Wang Y. X., Huang X. W. and Wang C., As(III) and As(V) removal on manganese dioxide, Advanced Materials Research, 573-574 (2012) 39-42.

27. Feng X. H., Zu y. Q., Tan W. F. and Liu F., Arsenite oxidation by three types of manganese oxides, Journal of Environmental Sciences, 18/2 (2006) 292-298.

28. Wu K., Liu R.P., Li T., Liu H.J., Peng J.M. and Qu J.H., Removal of arsenic(III) from aqueous solution using a low-cost by-product in Fe-removal plants-Fe-based backwashing sludge, Chem. Eng. J., 226 (2013) 393-401.

29. Manning B. A., Fendorf S. E. and Goldberg S., Surface structures and stability of arsenic(III) on goethite: Spectroscopic evidence for inner-sphere complexes, Environ. Sci. Technol., 32 (1998) 2383-2388.

30. Manning B. A., Fendorf S. E., Bostick B. and Suare, D. L., Arsenic(III) oxidation and arsenic(V) adsorption reactions on synthetic birnessite, Environ. Sci. Technol., 36 (2002) 976-981.

31. Hou J., Luo J., Song S., Li Y. and Li Q., The remarkable effect of the coexisting arsenite and arsenate species ratios on arsenic removal by manganese oxide, Chem. Eng. J., 315 (2017) 159-166.

32. Saleh T. A., Agarwal S. and Gupta, V. K., Synthesis of MWCNT/MnO_2 and their application for simultaneous oxidation of arsenite and sorption of arsenate, Applied Catalysis B: Environmental, 106/1 (2011) 46-53.

33. Foster A. L., Brown G. E. and Parks G. A., X-ray absorption fine structure study of As(V) and Se(IV) sorption complexes on hydrous Mn oxides, Geochim. Cosmochim. Acta., 67 (2003) 1937-1953.

34. Tournassat C., Charlet L., Bosbach D. and Manceau A., Arsenic(III) oxidation by birnessite and precipitation of manganese(II) arsenate, Environ. Sci. Technol., 36 (2002) 493-500.

35. Nesbitt H. W., Canning G. W. and Bancroft G. M., XPS study of reductive dissolution of 7A-birnessite by H_3AsO_3, with constraints on reaction mechanism, Geochim. Cosmochim. Acta., 62 (1998) 2097-2110.

36. Schwertmann U. and Cornell R. M., The iron oxides: Iron oxides in the laboratory-preparation and characterization, Encyclopedia of Earth Sciences Series, (2007) 5-18.

37. Abdulkadir I. and Abubakar B. A., Some wet routes for synthesis of hematite nanostructures, African Journal of Pure and Applied Chemistry, 7/3 (2013) 114-121.

38. Bigliocca C., Girardi F., Pauly J., Sabbioni E., Meloni S. and Provasoli A., Radiochemical separations by adsorption on manganese dioxide, Anal. Chem., 39/13 (1967) 1634-1639.

39. Li Q., Luo G., Li J. and Xi X., Preparation of ultra fine MnO_2 powders by the solid state method reaction of $KMnO_4$ with Mn(II) salts at room temperature, J. Mater. Proc. Technol., 137 (2003) 25-29.

40. Fujimoto T., Mizukoshi Y., Nagata Y., Maeda Y. and Oshima R., Sonolytical preparation of various types of metal nanoparticles in aqueous solution, Scripta Materialia, 44/8–9 (2001) 2183.

41. Sandell E.B. and Onishi H., Photometric determination of traces of metals, 4th Edition, John Wiley and Sons: New York, (1978) 829-830.

42. Nicy Ajith and K.K. Swain, Study on the performance and interaction of different synthetic iron oxides for arsenic uptake using ^{76}As radiotracer, Applied Radiation and Isotopes, 153 (2019) 108807.

43. Aditi A. Dalvi, Nicy Ajith, Kallola K. Swain and Rakesh Verma, Sorption of arsenic on manganese dioxide synthesized by solid state reaction, Journal of Environmental Science and Health, Part A, 50/8 (2015) 866-873.

44. Nicy Ajith, Aditi A. Dalvi, Kallola K. Swain, P.S. Remya Devi, Bhupesh B. Kalekar, Rakesh Verma and A.V.R. Reddy, Sorption of As(III) and As(V) on chemically synthesized manganese dioxide, Journal of Environmental Science and Health, Part A, 48/4 (2013) 422-428.

45. Nicy Ajith, Kaustava Bhattacharyya, Priyanka R. Ipte, Ashis K. Satpati, Arvind K. Tripathi, Rakesh Verma and Kallola K. Swain, Interaction of arsenic(III) and arsenic(V) on manganese dioxide: XPS and electrochemical investigations, Journal of Environmental Science and Health, Part A, 54/4 (2019) 277-285.

46. Criscuoli A., Majumdar S., Figoli A., Sahoo G.C., Bafaro P., Bandyopadhyay S. and Drioli E., As(III) oxidation by MnO_2 coated PEEK-WC nanostructured capsules, Journal of Hazardous Materials, 211–212 (2012) 281-287.

47. Nicy Ajith and K. K. Swain, An ultrasound assisted reductive method for preparation of MnO_2: Modification of XAD and application in removal of arsenic, Separation Science and Technology, (2019) https://doi.org/10.1080/01496395.2019.1604756.

References

1. https://www.koshland-science-museum.org/water/html/en/Sources/Where-is-the-Earths-Water.html Accessed on 4th December 2019.

2. http://www .healthgoods. com/blog/national-primary-and-secondary- drinking- water-regulations / Accessed on 4th December 2019.

3. Indian Standard Drinking Water Quality Specifications, ISO-10500: **2012**.

4. Carelton J., Final Report: Biogeochemistry of Arsenic in Contaminated Soils of Super-fund Sites, EPA, *United States Environmental Protection Agency*, **2007**.

5. https://monographs.iarc.fr/list-of-classifications Accessed on 4th December 2019.

6. Smedley P. L and Kinniburgh D. G., A review of the source, behaviour and distribution of arsenic in natural waters, *Applied Geochemistry*, **2002**, 17, 517-568.

7. Al-Abed S. R., Jegadeesan G., Purandare J. and Allen D., Arsenic release from iron rich mineral processing waste: Influence of pH and redox potential, *Chemosphere*, **2007**, 66/4, 775-782.

8. Bhattacharya P., Frisbie S. H., Smith E., Naidu R., Jacks G. and Sarkar B., Arsenic in the environment: A global perspective, *Handbook of heavy metals in the environment*, New York, Marcell Dekker, **2002**, 147-215.

9. Mandal B. K. and Suzuki K. T., Arsenic around the world: A review, *Talanta*, **2002**, 58, 201-235.

10. Mukherjee A., Sengupta M. K., Hossain M. A., Ahamed S., Das B., Nayak B., Lodh D., Rahman M. M. and Chakraborti D., Arsenic contamination in groundwater: A global perspective with emphasis on the asian scenario, *Journal of Health, Population and Nutrition*, **2006**, 24/2, 142-163.

11. Bundschuh J., Litter M. I., Parvez F., Román-Ross G., Nicolli H. B., Jean J. S., Liu C.W., López D., Armienta M. A., Guilherme L. R., Cuevas A. G., Cornejo L., Cumbal L.

and Toujaguez R., One century of arsenic exposure in Latin America: A review of history and occurrence from 14 countries, *Science of the Total Environment*, **2012**, 429, 2-35.

12. Chakraborty M., Mukherjee A. and Ahmed K. M., A review of groundwater arsenic in the Bengal Basin, Bangladesh and India: From source to sink, *Current Pollution Reports*, **2015**, 1, 220-247.

13. Nickson R. T., McArthur J. M., Ravenscroft P., Burgess W. B. and Ahmed K. M., Mechanism of As poisoning of groundwater in Bangladesh and West Bengal, *Applied Geochemistry*, **2000**, 15, 403-413.

14. Ghosh N. C. and Singh R. D., *Groundwater arsenic contamination in India: Vulnerability and scope of remedy*, **2009**, http://cgwb.gov.in/documents/papers/incidpapers/Paper%208%20-%20Ghosh.pdf.

15. Smith A. H., Lingas E. O. and Rahman M., Contamination of drinking-water by arsenic in Bangladesh: A public health emergency, *Bulletin of the World Health Organization*, **2000**, 78/9, 1093-1103.

16. https:// www.indiatoday.in/ education- today / gk- current- affairs/ story/ 1-47-crore-indians-at-high-risk-of-cancer-due-to-arsenic-contaminated-water-1368198-2018-10-15 Accessed on 4th December 2019.

17. *The Hindu* (Mumbai edition), published on 19th May **2018**.

18. Mondal P., Bhowmick S., Chatterjee D., Figoli A. and Van der Bruggen B., Remediation of inorganic arsenic in groundwater for safe water supply: A critical assessment of technological solutions, *Chemosphere*, **2013**, 92/2, 157-170.

19. Sonia Aredes, Arsenic removal by iron oxides, *PhD Thesis*, **2005**.

20. Bose U., Rahman M. and Alamgir M., Arsenic toxicity and speciation analysis in groundwater samples: A review of some techniques, *International Journal of Chemical Technology*, **2011**, 3, 14-25.

21. Hung Q. D., Nekrassova O. and Compton R. G., Analytical methods for inorganic arsenic in water: A review, *Talanta*, **2004**, 64/ 2, 269-277.

22. Panagiotaras D., Papoulis D., Panagopoulos G. and Avramidis P., Arsenic geochemistry in groundwater system, Open access peer-reviewed chapter-2, *Intech Open Access Publisher,* **2012**.

23. Pal P., Groundwater arsenic remediation: Treatment technology and scale up, *Elsevier*, Oxford, **2015**.

24. Manning B. A. and Goldberg S., Arsenic(III) and arsenic(V) absorption on three California soils, *Soil Science,* **1997**, 162, 886-895.

25. Wang S. and Mulligan C. N., Occurrence of arsenic contamination in Canada: Sources, behaviour and distribution, *Science of the Total Environment*, **2005**, 366/2-3, 701-721.

26. Vaclavikova M., Gallios G. P., Hredzak S. and Jakabsky S., Removal of arsenic from water streams: an overview of available techniques, *Clean Technologies and Environmental Policy*, **2008**, 10, 89-95.

27. Thomas D. J., Styblo M. and Lin S. The cellular metabolism and systemic toxicity of arsenic, *Toxicology and Applied Pharmacology,* **2001**, 176, 127-144.

28. Saha J. C., Dikshit A. K., Bandyopadhyay M. and Saha K. C., A review of arsenic poisoning and its effects on human health, https://www.epa.gov/sites/production/files/2014-03/documents/a_review_of_arsenic_poisoning_and_its_effects_on_human_health_3v.pdf.

29. Arsenic: Medical and biological effects of environmental pollutants, Washington D. C., *National Academies Press (US),* **1977**.

30. Abernathy C. O. and Ohanian E. V., Health effects of inorganic arsenic in drinking water, *Proc. AWWA WQTC,* Miami, Fla., **1993**.

31. McKinney J. D., Metabolism and disposition of inorganic arsenic in laboratory animals and humans, *Environmental Geochemistry and Health*, **1992**, 14, 43-48.

32. Thompson D. J., A chemical hypothesis for arsenic methylation in mammals, *Chemico-Biological Interactions*, **1993**, 88, 89-114.

33. Nakamuro K. and Sayato T., Comparative studies of chromosomal aberration induced by trivalent and pentavalent arsenic, *Mutation Research*, **1981**, 88, 73-80.

34. SOS arsenic poisoning in Bangladesh/India. http://www.sos-arsenic.net/ Accessed on 2nd December 2019.

35. Guha Mazumder D. N., Ghosh N., De B. K., Santra A., Das S., Lahiri S., Haque R., Smith A. H. and Chakraborti D., Epidemiological study on various non-carcinomatous manifestations of chronic arsenic toxicity in a District of West Bengal, *Book Title: Arsenic Exposure and Health Effects*, Edited by: Chappell W. R., Abernathy C. O. and Calderon R. L., Elsevier science, Amsterdam, **2001**, 153-164.

36. Rahman M. M., Chowdhury U. K., Mukherjee S. C., Mondal B. K., Paul K., Lodh D., Biswas B. K., Chanda C. R., Basu G. K., Saha K. C., Roy S., Das R., Palit S. K., Zaman Q. Q. and Chakraborti D., Chronic arsenic toxicity in Bangladesh and West Bengal- India - A review and commentary, *Journal of Toxicology: Clinical Toxicology*, **2001**, 39/7, 683-700.

37. Arsenic treatment technologies for soil, waste and water U.S.EPA., *EPA-542-R-02 004,* **2002**, http://clu in.org/download/remed/542r02004/arsenic_report.pdf.

38. National primary drinking water regulations: Arsenic and clarifications to compliance and new source contaminants monitoring, final rule, *U.S.EPA, Federal Register*, **2001**, 66/14, 6975-7066. http://www.epa.gov/sbrefa/documents/pnl14f.pdf.

39. Drinking water specification, Second revision of IS 10500, *Doc: FAD 25(2047) C, Bureau of Indian Standards (BIS),* Government of India: New Delhi, India, **2009**.

40. Chakraborti D., Singh S. K., Rahman M. M., Dutta R. N., Mukherjee S. C., Pati S. and Kar P. B., Groundwater arsenic contamination in the Ganga river basin: A future health danger, *International Journal of Environmental Research and Public Health*, **2018**, 15/2, 180-199.

41. Singh R., Singh R., Parihar P., Singh V. P. and Prasad S. M., Arsenic contamination, consequences and remediation techniques: A review, *Ecotoxicology and Environmental Safety*, **2015**, 112, 247-270.

42. Zakhar R., Derco J. and Cacho F., An overview of main arsenic removal technologies, *Acta Chimica Slovaca*, **2018**, 11/2, 107-113.

43. Sanjrani M. A., Zhou B., Zhao H., Bhutto S. A., Muneer A. S. and Xia S. B, Arsenic contaminated groundwater in china and Its treatment options: A review, *Applied Ecology and Environmental Research*, **2019**, 17/2, 1655-1683.

44. Nicomel N. R., Leus K., Folens K., Van Der Voort P. and Du Laing G., Technologies for arsenic removal from water: Current status and future perspectives, *International Journal of Environmental Research and Public Health*, **2015**, 13/1, 62, 1-24.

45. Sposito G., The chemistry of soils, Oxford university press, New York, **1989**.

46. Mohan D. and Pittman Jr. C. U., Arsenic removal from water/wastewater using adsorbents - A critical review, *Journal of Hazardous Materials*, **2007**, 142, 1-53.

1.47. Ma L. Q., Komar K. M., Tu C., Zhang W., Cai Y. and Kennelley E. D., A fern that hyperaccumulates arsenic, *Nature*, **2001**, 409, 579.

48. Behera K. K., Phytoremediation, transgenic plants and microbes, *Sustainable Agriculture Reviews*, **2014**, 13, 65-85.

49. Ike M., Miyazaki T., Yamamoto N., Sei K. and Soda S., Removal of arsenic from groundwater by arsenite-oxidizing bacteria, *Water Science and Technology*, **2008**, 58, 1095-1100.

50. Yamamura S., Ike M. and Fujita M., Dissimilatory arsenate reduction by a facultative anaerobe, Bacillus sp. strain SF-1, *Journal of Bioscience and Bioengineering*, **2003**, 96, 454-460.

51. Alvarado S., Guédez M., Lué-Merú M. P., Nelson G., Alvaro A., Jesús A. C. and Gyula Z., Arsenic removal from water by bioremediation with the aquatic plants Water Hyacinth (Eichornia crassipes) and Lesser Duckweed (Lemna minor), *Bioresource Technology*, **2008**, 99, 8436-8440.

52. Kumar M., Das N., Goswami R., Sarma K. P., Bhattacharya P. and Ramanathan A. L., Coupling fractionation and batch desorption to understand arsenic and fluoride co-contamination in the aquifer system, *Chemosphere,* **2016**, 164, 657-667.

53. Mamindy-Pajany Y., Hurel C., Marmier N. and Romeo M., Arsenic(V) adsorption from aqueous solution onto goethite, hematite, magnetite and zero-valent iron: Effects of pH, concentration and reversibility, *Desalination*, **2011**, 281, 93-99.

54. Garcia M. G., Muñiz K. R. and Song S., Arsenic removal from water by adsorption using iron oxide minerals as adsorbents: A review, *Minerals processing and extractive metallurgy review*, **2012**, 33, 301-315.

55. Gimenez J., Pablo J. De, Rovira M. and Duro L., Arsenic sorption onto natural hematite, magnetite, and goethite, *Journal of Hazardous Materials,* **2007**, 141, 575-580.

56. Tuutijarvi T., Lu J., Sillanpaa M. and Chen G., As(V) adsorption on maghemite nano-particles, *Journal of Hazardous Materials,* **2009**, 166, 1415-1420.

57. Deliyanni E. A., Bakoyannakis D. N., Zouboulis A. I. and Matis K. A., Sorption of As(V) ions by akaganéite-type nanocrystals, *Chemosphere*, **2003**, 50/1, 155-163.

58. Dixit S. and Hering J., Comparison of arsenic(V) and arsenic(III) sorption onto iron oxide minerals, *Environmental Science and Technology,* **2003**, 37/18, 4182-4189.

59. Wu K., Liu R. P., Li T., Liu H. J., Peng J. M. and Qu J. H., Removal of arsenic(III) from aqueous solution using a low-cost by-product in Fe-removal plants-Fe-based backwashing sludge, *Chemical Engineering Journal*, **2013**, 226, 393-401.

60. Manning B. A., Fendorf S. E. and Goldberg S., Surface structures and stability of arsenic(III) on goethite: Spectroscopic evidence for inner-sphere complexes, *Environmental Science and Technology*, **1998**, 32, 2383-2388.

61. Sun X. and Doner H. E., Adsorption and oxidation of arsenite on goethite, *Soil Science*, **1998**, 163, 278-287.

62. Sherman D. M. and Randall S. R., Surface complexation of arsenic(V) to iron(III) (hydr)oxides: Structural mechanism from ab initio molecular geometries and EXAFS spectroscopy, *Geochimica et Cosmochimica Acta*, **2003**, 67, 4223-4230.

63. Hubbard A. T., *Encyclopedia of Surface and Colloid Science*, Vol 1, New York: Dekker, **2002**, 388-390.

64. Mamindy P. Y., Hurel Ch., Marmier N. and Romeo M., Arsenic adsorption onto hematite and goethite, *Comptes Rendus Chimie*, **2009**, 12, 876-881.

65. Kong S. Q., Wang Y. X., Huang X. W. and Wang C., As(III) and As(V) removal on manganese dioxide, *Advanced Materials Research*, **2012**, 573-574, 39-42.

66. Driehaus W., Seith R. and Jekel M., Oxidation of arsenate(III) with manganese oxides in water treatment, *Water Research*, **1995**, 29/1, 297 – 305.

67. Contreras R. and Lapidus G. T., Combined water and ion exchange characteristics of manganese dioxide production by ozonation, *Journal of colloid and interface science*, **1999**, 213, 251-257.

68. Manning B. A., Fendorf S. E., Bostick B. and Suare D. L., Arsenic(III) oxidation and arsenic(V) adsorption reactions on synthetic birnessite, *Environmental Science and Technology*, **2002**, 36, 976-981.

69. Tournassat C., Charlet L., Bosbach D. and Manceau A., Arsenic(III) oxidation by birnessite and precipitation of manganese(II) arsenate, *Environmental Science and Technology*, **2002**, 36, 493-500.

70. Nesbitt H. W., Canning G. W. and Bancroft G. M., XPS study of reductive dissolution of 7A-birnessite by H_3AsO_3, with constraints on reaction mechanism, *Geochimica et Cosmochimica Acta*, **1998**, 62, 2097-2110.

71. Scott M. J. and Morgan J. J., Reactions at Oxide Surfaces. 1. Oxidation of As(III) by synthetic birnessite, *Environmental Science and Technology*, **1995**, 29/8, 1898-1905.

72. Foster A. L., Brown G. E. and Parks G. A., X-ray absorption fine structure study of As(V) and Se(IV) sorption complexes on hydrous Mn oxides, *Geochimica et Cosmochimica Acta*, **2003**, 67, 1937-1953.

73. Guo H., Stuben D. and Berner Z., Removal of arsenic from aqueous solution by natural siderite and hematite, *Applied Geochemistry,* **2007**, 22, 1039-1051.

74. Singh D. B., Prasad G. and Rupainwar D. C., Adsorption technique for the treatment of As(V)-rich effluents, *Colloids and Surfaces A: Physicochemical and Engineering Aspects*, **1996**, 111, 49-56.

75. Asta P. M., Cama J., Martinez M. and Gimenez J., Arsenic removal by goethite and jarosite in acidic conditions and its environmental implications, *Journal of Hazardous Materials*, **2009**, 171, 965-972.

76. Ouvrard S., Simonnot M. O. and Sardin M., Reactive behavior of natural manganese oxides toward the adsorption of phosphate and arsenate, *Industrial and Engineering Chemistry Research*, **2002**, 41, 2785-2791.

77. Chakravarty S., Dureja V., Bhattacharyya G., Maity S. and Bhattacharjee S., Removal of arsenic from groundwater using low cost ferruginous manganese ore, *Water Research*, **2002**, 36/3, 625-632.

78. Pattanayak J., Mondal K., Mathew S. and Lalvani S.B., A parametric evaluation of the removal of As(V) and As(III) by carbon based adsorbents, *Carbon*, **2000**, 38/4, 589-596.

79. Chutia P., Kato S., Kojima T. and Satokawa S., Adsorption of As(V) on surfactant-modified natural zeolites, *Journal of Hazardous Materials*, **2009**, 162/1, 204-211.

80. Lenoble V., Chabroulle C., Shukry R., Serpaud B., Deluchat V. and Bollinger J.C., Dynamic arsenic removal on a MnO_2-loaded resin, *Journal of Colloid and Interface Science*, **2004**, 280, 62-67.

81. Kim J. and Benjamin M. M., Modeling a novel ion exchange process for arsenic and nitrate removal, *Water Research*, **2004**, 38/8, 2053-2062.

82. Asere T. G., Stevens C.V. and Laing G.D., Use of (modified) natural adsorbents for arsenic remediation: A review, *Science of the Total Environment*, **2019**, 676, 706-720.

83. Ajith N. and Swain K. K., Study on the performance and interaction of different synthetic iron oxides for arsenic uptake using ^{76}As radiotracer, *Applied Radiation and Isotopes*, **2019**, 153, 108807.

84. Ajith N., Dalvi A. A., Swain K. K., Devi P. S. R., Kalekar B. B., Verma R. and Reddy A. V. R., Sorption of As(III) and As(V) on chemically synthesized manganese dioxide, *Journal of Environmental Science and Health Part A*, **2013**, 48/4, 422-428.

85. Dalvi A. A., Ajith N., Swain K. K. and Verma R., Sorption of arsenic on manganese dioxide synthesized by solid state reaction, *Journal of Environmental Science and Health Part A*, **2015**, 50/8, 866-873.

86. Ajith N. and Swain K. K., An ultrasound assisted reductive method for preparation of MnO_2: Modification of XAD and application in removal of arsenic, *Separation Science and Technology*, **2020**, 55(9), 1715-1723.

87. Schwertmann U. and Cornell R. M., The iron oxides: Iron oxides in the laboratory-preparation and characterization, *Encyclopedia of Earth Sciences Series*, **2007**, 5-18.

88. Abdulkadir I. and Abubakar B. A., Some wet routes for synthesis of hematite nanostructures, *African Journal of Pure and Applied Chemistry*, **2013**, 7/3, 114-121.

89. Iwasaki T., Mizutani N., Watano S., Yanagida T. and Kawai T., Size control of magnetite nanoparticles by organic solvent-free chemical coprecipitation at room temperature, *Journal of Experimental Nanoscience*, **2010**, 5/3, 251-262.

90. Bigliocca C., Girardi F., Pauly J., Sabbioni E., Meloni S. and Provasoli A., Radiochemical separations by adsorption on manganese dioxide, *Analytical Chemistry*, **1967**, 39/13, 1634-1639.

91. Li Q., Luo G., Li J. and Xi X., Preparation of ultra fine MnO_2 powders by the solid state method reaction of $KMnO_4$ with Mn(II) salts at room temperature, *Journal of Materials Processing Technology*, **2003**, 137, 25-29.

92. Fujimoto T., Mizukoshi Y., Nagata Y., Maeda Y. and Oshima R., Sonolytical preparation of various types of metal nanoparticles in aqueous solution, *Scripta Materialia*, **2001**, 44/8-9, 2183-2186.

93. https:// www.lenntech.com/ Data-sheets/Amberlite-XAD4-L.pdf Accessed on 08th November 2019.

94. Okitsu K., Iwatani M., Nanzai B., Nishimura R. and Maeda Y., Sonochemical reduction of permanganate to manganese dioxide: The effects of H_2O_2 formed in the sonolysis of water on the rates of reduction, *Ultrasonics Sonochemistry*, **2009**, 16/3, 387-391.

95. Abulizi A., Yang G.H., Okitsu K. and Zhu J.J., Synthesis of MnO_2 nanoparticles from sonochemical reduction of MnO_4^- in water under different pH conditions, *Ultrasonics Sonochemistry*, **2014**, 21/5, 1629-1634.

96. Baral S., Pereira C.L., Janata E. and Henglein A., Chemistry of colloidal manganese dioxide. 2. Reaction with superoxide anion (0^{2-}) and hydrogen peroxide (pulse radiolysis and stop flow studies), *The Journal of Physical Chemistry*, **1985**, 89/26 5779-5783.

97. Eby G. N., Principles of Environmental Geochemistry, *Brooks/Cole-Thomson Learning*, **2004**, 212-214.

98. Brunauer S., Emmett P. H. and Teller E., Adsorption of gases in multimolecular layers, *Journal of the American Chemical Society*, **1938**, 60, 309-319.

99. Xu R., Particle characterization: Light scattering methods, Chapter 6, *Dordrecht: Kluwer*, **2000**, 299-343.

100. https:// nanocomposix.com/ pages/chr6-zeta-potential-measurements, Accessed on 20th October 2019.

101. Particle Size Analysis – Dynamic Light Scattering (DLS). *International Organization for Standardization*, **2017**, ISO 22412:2017.

102. Liu B., Thomas P. S., Willams R. P. and Donne S. W., Thermal characterization of chemically reduced electrolytic manganese dioxide, *Journal of Thermal Analysis and Calorimetry*, **2005**, 80, 625-629.

103. Kolta G. A., Kerim F. M. A. and Azim A. A. A., Infrared absorption spectra of some manganese dioxide modifications and their thermal products, *Zeitschrift für anorganische und allgemeine Chemie*, **1971**, 384, 260.

104. https:// www-nds.iaea.org/ relnsd/ vcharthtml/VChartHTML.html, Accessed on 1st November 2019.

105. Leon C. A. L. Y., Solar J. M., Calemma V. and Radovic L. R., Evidence for the protonation of basal plane sites on carbon, *Carbon*, **1992**, 30/5, 797.

106. Sandell E. B. and Onishi H., Photometric determination of traces of metals, 4th Edition, *JohnWiley and Sons:NewYork*, **1978**, 829-830.

107. Pattanayak J., Mondal K., Mathew S. and Lalvani S.B., A parametric evaluation of the removal of As(V) and As(III) by carbon based adsorbents, *Carbon*, **2000**, 38/4, 589-596.

108. Chutia P., Kato S., Kojima T. and Satokawa S., Adsorption of As(V) on surfactant-modified natural zeolites, *Journal of Hazardous Materials*, **2009**, 162/1, 204-211.

109. Lenoble V., Chabroulle C., Shukry R., Serpaud B., Deluchat V. and Bollinger J.C., Dynamic arsenic removal on a MnO_2-loaded resin, *Journal of Colloid and Interface Science*, **2004**, 280, 62-67.

110. Kim J. and Benjamin M. M., Modeling a novel ion exchange process for arsenic and nitrate removal, *Water Research*, **2004**, 38/8, 2053-2062.

111. Asere T. G., Stevens C.V. and Laing G.D., Use of (modified) natural adsorbents for arsenic remediation: A review, *Science of the Total Environment*, **2019**, 676, 706-720.

112. Shankar S., Shanker U. and Shikha, Arsenic contamination of groundwater: A review of sources, prevalence, health risks, and strategies for mitigation, *The Scientific World Journal*, **2014**, Article ID 304524, 1-18.

113. Polowczyk I., Cyganowski P., Ulatowska, J., Sawiński J. and Bastrzyk A., Synthetic iron oxides for adsorptive removal of arsenic, *Water Air and Soil Pollution*, **2018**, 229, 203.

114. Singh P., Sharma S., Chauhan K. and Singhal R. K., Fabrication of economical thiol-tethered bifunctional iron composite as potential commercial applicant for arsenic sorption application, *ACS Industrial and Engineering Chemistry Research*, **2018**, 57/39, 12959-12972.

115. Couture R. M., Rose J., Kumar N., Mitchell K., Wallschläger D. and Van Cappellen P., Sorption of arsenite, arsenate and thioarsenates to iron oxides and iron sulfides: A

kinetic and spectroscopic investigation, *Environmental Science and Technology*, **2013**, 47/11, 5652-5659.

116. Kempahanumakkagari S., Deep A., Kim K. H., Kumar Kailasa S. and Yoon H. O., Nanomaterial-based electrochemical sensors for arsenic - A review, *Biosensors and Bioelectronics*, **2017**, 95, 106-116.

117. Limousin G., Gaudet J. P., Charlet L., Szenknect S., Barthes V. and Krimissa M., Sorption isotherms: A review on physical bases, modeling and measurement, *Applied Geochemistry*, **2007**, 22/2, 249-275.

118. Freundlich H. M. F., Over the adsorption in solution, *The Journal of Physical Chemistry*, **1906**, 57/4, 385-470.

119. Dada A. O., Olalekan A. P., Olatunya A. M. and Dada O., Langmuir, Freundlich, Temkin and Dubinin–Radushkevich isotherms studies of equilibrium sorption of Zn^{2+} unto phosphoric acid modified rice husk, *IOSR Journal of Applied Chemistry*, **2012**, 3/1, 38-45.

120. https://www.epa.gov/dwstandardsregulations/secondary-drinking-water-standards-guidance-nuisance-chemicals Accessed on 28th October 2019.

121. https://pubs.usgs.gov/wri/wri024045/htms/report2.htm Accessed on 28th October 2019.

122. Bhandari N., Reeder R. J. and Strongin D. R., Photoinduced oxidation of arsenite to arsenate in the presence of goethite, *Environmental Science and Technology*, **2012**, 46/15, 8044-8051.

123. Hao L., Liu M., Wang N. and Li G., A critical review on arsenic removal from water using iron-based adsorbents, *RSC Advances*, **2018**, 8, 39545-39560.

124. Lafferty B. J. and Loeppert R. H., Methyl arsenic adsorption and desorption behavior on iron oxides, *Environmental Science and Technology*, **2005**, 39/7, 2120-2127.

125. Sonia A., Bern K. and Marek P., The removal of arsenic from water using natural iron oxide minerals, *Journal of Cleaner Production*, **2012**, 29-30, 208-213.

126. Xiuli J., Changjun P., Dun F., Zheng C., Liang S., Qingbiao L., Tong O. and Yuanpeng W., Removal of arsenate by ferrihydrite via surface complexation and surface precipitation, *Applied Surface Science*, **2015**, 353, 1087-1094.

127. Guidelines for drinking water quality, 4th edition, *World Health Organization*, **2011**.

128. https://www.who.int/ipcs/features/arsenic.pdf Accessed on 06th November 2019.

129. Ratnaike R. N., Acute and chronic arsenic toxicity, *Postgraduate Medical Journal*, **2003**, 79, 391-396.

130. Feng X. H., Zu Y. Q., Tan W. F. and Liu F., Arsenite oxidation by three types of manganese oxides, *Journal of Environmental Sciences*, **2006**, 18/2, 292-298.

131. Hou J., Luo J., Song S., Li Y. and Li Q., The remarkable effect of the coexisting arsenite and arsenate species ratios on arsenic removal by manganese oxide, *Chemical Engineering Journal*, **2017**, 315, 159-166.

132. Oscarson D. W., Huang P. M., Defosse C. and Herbillon A., Oxidative power of Mn(IV) and Fe(III) oxides with respect to As(III) in terrestrial and aquatic environments, *Nature*, **1981**, 291, 50-51.

133. Methods for measuring the acute toxicity of effluents and receiving waters to freshwater and marine organisms, *EPA 821-R-020-013*, 5th Edition, October **2002**, 31-32.

134. Girardi F., Pietra R. and Sabbioni J., Radiochemical separations by retention of ionic precipitate adsorption tests on 11 materials, *Journal of Radio-analytical and Nuclear Chemistry*, **1970**, 5, 141-171.

135. Thanabalasingham P. and Pickering W. F., Effect of pH on interaction between As (III) or As(V) and manganese(IV) oxide, *Water, Air and Soil Pollution*, **1986**, 29, 205-216.

136. Swain H.A., Lee C. and Rozelle R. B., Determination of the solubility of manganese hydroxide and manganese dioxide at 25°C by atomic absorption spectrometry, *Analytical Chemistry*, **1975**, 47/7, 1135-1137.

137. Lenoble V., Laclautre C., Serpaud B., Deluchat V. and Bollinger J. C., As(V) retention and As(III) simultaneous oxidation and removal on a MnO_2-loaded polystyrene resin, *Science of the Total Environment*, **2004**, 326/1-3, 197-207.

138. Oscarson D.W., Huang P. M., Liaw W. K. and Hammer U. T., Kinetics of oxidation of arsenite by various manganese dioxides, *Soil Science Society of America Journal*, **1983**, 47, 644-648.

139. Issa N. B., Vladana N. R. O., Branislava M. J. and Ljubinka V. R., Determination of inorganic arsenic species in natural waters - Benefits of separation and preconcentration on ion exchange and hybrid resins, *Analytica Chimica Acta*, **2010**, 673, 185-193.

140. Mendham J., Denney R. C., Barnes J. D. and Thomas M. J. K., *Vogel's textbook of quantitative chemical analysis*, 6th edition, Pearson Education Limited, London, **2000**, 664-665.

141. Ajith N., Bhattacharyya K., Ipte P. R., Satpati A. K., Tripathi A. K., Verma R. and Swain K. K., Interaction of arsenic(III) and arsenic(V) on manganese dioxide: XPS and electrochemical investigations, *Journal of Environmental Science and Health Part A*, **2019**, 54/4, 277-285.

142. NIST X-ray Photoelectron Spectroscopy Database; *NIST Standard Reference Database 20*, Version 4.1, **2012**.

143. Feng Q., Kanoh H. and Ooi K., Manganese oxide porous crystals, *Journal of Materials Chemistry*, **1999**, 9, 319-333.

144. Shubina V., Gaillet L., Girard S. A., Gaudefroy V., Chaussadent T., Farcas F., Meylheuc T., Dagbert C. and Creus J., The influence of biosurfactant adsorption on the

physicochemical behaviour of carbon steel surfaces using contact angle measurements and X-ray photoelectron spectroscopy, *Applied Surface Science*, **2015**, 351, 1174-1183.

145. Mishra A. K. and Ramaprabhu S., Ultrahigh arsenic sorption using iron oxide-graphene nanocomposite supercapacitor assembly, *Journal of Applied Physics*, **2012**, 112, 104315.

146. Mohanty D., Conventional as well as emerging arsenic removal technologies - A critical review, *Water Air and Soil Pollution*, **2017**, 228/10, 381.

147. Criscuoli A., Majumdar S., Figoli A., Sahoo G. C., Bafaro P., Bandyopadhyay S. and Drioli E., As(III) oxidation by MnO_2 coated PEEK-WC nanostructured capsules, *Journal of Hazardous Materials*, **2012**, 211-212, 281-287.

148. Kabay N., Demiraoglu M., Ekinci H., Yuksel M., Saglam M. and Streat M., Extraction of Cd(II) and Cu(II) from phosphoric acid solutions by solvent-impregnated resins (SIR) containing Cyanex 302, *Reactive and Functional Polymers*, **1998**, 38, 219.

149. Rajesh N. , Krishna Kumar A. S., Kalidhasan S. and Vidya Rajesh, Trialkylamine Impregnated Macroporous Polymeric Sorbent for the Effective Removal of Chromium from Industrial Wastewater, *Journal of Chemical and Engineering Data*, **2011**, 56, 5, 2295-2304.

150. Santhana Krishna Kumar A., Development of novel and suitably tailored adsorbents for chromium and mercury detoxification, *PhD Thesis*, **2013**, BITS - Pilani.

151. Ahmad A., Siddique J. A., Laskar M. A., Kumar R., Mohd-Setapar S. H., Khatoon A. and Shiekh R.A., New generation Amberlite XAD resin for the removal of metal ions: A review, *Journal of Environmental Sciences-China*, **2015**, 31, 104-123.

152. Feiz Bakhsh A. R., Panahi H. R., Nezhati M. N., Amrollahi M. and Mahmoudi F., Synthesis, characterization, and application of m -Phenylendiamine-modified Amberlite

XAD-4 Resin for preconcentration and determination of metal ions in water samples, *Water Environment Research*, **2009**, 81/5, 532-539.

153. Hosseini M. S., Bandegharaei A. H. and Hosseini M., Column-mode separation and pre-concentration of some heavy metal ions by solvent-impregnated resins containing quinizarin before the determination by flame atomic absorption spectrometry, *International Journal of Environmental Analytical Chemistry*, **2009**, 89/1, 35-48.

154. Hoshi S., Fujisawa H., Nakamura K., Nakata S., Uto M. and Akatsuka K., Preparation of Amberlite XAD resins coated with dithiosemicarbazone compounds and preconcentration of some metal ions, *Talanta*, **1994**, 41/4, 503-507.

155. Suslick K. S. and Price G. J., Applications of ultrasound to materials chemistry, *Annual Review of Materials Research*, **1999**, 29/1, 295-326.

156. Gedanken A., Doping nanoparticles into polymers and ceramics using ultrasound radiation. *Ultrasonics Sonochemistry*, **2007**, 14/4, 418-430.

157. Manoiu V. S. and Aloman A., Obtaining silver nanoparticles by sonochemical methods, *UPB Scientific Bulletin, Series B: Chemistry and Materials Science*, **2010**, 72/2, 179-186.

158. Okitsu K., Bandow H., Maeda Y. and Nagata Y., Sonochemical preparation of ultrafine palladium particles, *Chemistry of Materials*, **1996**, 8/2, 315-317.

159. Uzun A., Soylak M. and Elci L., Preconcentration and separation with Amberlite XAD-4 resin; Determination of Cu, Fe, Pb, Ni, Cd and Bi at trace levels in waste water samples by flame atomic absorption spectrometry, *Talanta*, **2001**, 54, 197-202.

160. Soylak M., Elci L. and Dogan M., Solid phase extraction of trace metal ions with Amberlite XAD resins prior to atomic absorption spectrometric analysis, *Journal of Trace and Microprobe Techniques*, **2001**, 19, 329-344.

161. Langmuir I., The adsorption of gases on plane surface of glass, mica and platinum, *Journal of the American Chemical Society*, **1916**, 40, 1361-1403.

162. Babaeivelni, K. and Khodadoust A.P., Removal of arsenic from water using manganese (III) oxide: Adsorption of As(III) and As(V), *Journal of Environmental Science and Health Part A*, **2016**, 51/4, 277-288.

163. Ocinsky D., Irena J.S. and Elzbieta K.B., Oxidation and adsorption of arsenic species by means of hybrid polymer containing manganese oxides, *Journal of Applied Polymer Science*, **2014**, 131/3, 39489 (1-11).

164. Yong J. J. and Yuki K., Arsenic removal properties by electrolyzed and calcined manganese dioxide, *Environmental Engineering Research*, **2020**, 25(5), 735-741.